

Structure and Reactivity of α,β -Unsaturated Ethers. VIII. Cationic Copolymerizations and Acetal Additions of Propenyl and Isobutenyl Ethyl Ethers

T. OKUYAMA and T. FUENO, *Faculty of Engineering Science, Osaka University, Toyonaka, Osaka, Japan*, and J. FURUKAWA, *Department of Synthetic Chemistry, Kyoto University, Kyoto, Japan*

Synopsis

Cationic copolymerizations of *cis*- and *trans*-propenyl ethyl ethers (PEE) with isobutenyl ethyl ether (IBEE) were carried out in methylene chloride at -78°C with the use of boron trifluoride etherate as catalyst. Monomer reactivity ratios were $r_1 = 24.0 \pm 2.4$ and $r_2 = 0.02 \pm 0.02$ for the *cis*-PEE (M_1)-IBEE (M_2) system and $r_1 = 19.1 \pm 1.8$ and $r_2 = 0.04 \pm 0.02$ for the *trans*-PEE (M_1)-IBEE (M_2) system, indicative of the reactivity order: *cis*-PEE > *trans*-PEE \gg IBEE. In separate experiments, these β -methyl-substituted vinyl ethers were allowed to react with various acetals in the presence of boron trifluoride etherate. The relative reactivities of these ethers were generally found to decrease in the order: *cis*- β -monomethylvinyl > vinyl > *trans*- β -monomethylvinyl > β,β -dimethylvinyl. Comparisons of these results with previously published copolymerization data have permitted the conclusion that, in both the copolymerizations and acetal additions, the single β -methyl substitution on vinyl ethers exerts little steric effect against their additions toward any alkoxy-carbonium ion, whereas the β,β -dimethyl substitution results in a large adverse steric effect toward both β -monomethyl- and β,β -dimethyl-substituted alkoxy-carbonium ions.

INTRODUCTION

In previous papers,^{1,2} of this series, the cationic polymerizations of various alkenyl alkyl ethers have been investigated with particular attention to the effects of β -substituents as well as geometrical structure. It has been shown that a β -methyl group enhances the cationic polymerizability of vinyl alkyl ethers in homogeneous media and exhibits little adverse steric effect. A similar observation was also reported by Higashimura et al.^{3,4} These observations were interpreted⁵ in terms of the electronic effect of the methyl group as calculated by the extended Hückel molecular orbital theory.

Nonetheless, we have found, in addition, that β,β -dimethyl substitution reduces the polymerizability of vinyl ethers considerably and that this retarding effect is largely dependent on the nature of the attacking chain-end carbonium ions.² Conceptionally, this is a reflection of the steric effect involved in reactions of this particular type of unsaturated ethers.

It is known, on the other hand, that acetals react with α,β -unsaturated

ethers in the presence of a small amount of acid to give addition products.⁶ Since this reaction is essentially an addition of the alkoxy-carbonium ion formed from an acetal to the double bond of unsaturated ethers, it should closely resemble the propagation step of the cationic polymerization of the ethers. Thus, it seems interesting to compare the ether reactivities in both reactions, and thereby to look into the type of the steric effect involved.

In the present study, mutual copolymerizations of propenyl and isobutenyl ethyl ethers have been conducted on one hand, and the relative reactivities of these unsaturated ethers toward various acetals have been kinetically evaluated on the other. On the basis of the results obtained, the steric effects of the β -methyl substitution on the addition reactions in question have been analyzed from both sides of unsaturated ethers and attacking alkoxy-carbonium ions.

EXPERIMENTAL

Materials

Vinyl (VEE), propenyl (PEE), and isobutenyl (IBEE) ethyl ethers were obtained and purified as described previously.² 1,1-Diethoxyethane (I) and 1,1-diethoxypropane (II) were prepared from appropriate aldehydes and ethanol.⁷ 1,1,3-Triethoxybutane (III), 1,1,3-triethoxy-2-methylbutane (IV), and 1,1,3-triethoxy-2,2-dimethylbutane (V) were obtained by the reaction of I with VEE, PEE and IBEE, respectively,⁶ where one mole of unsaturated ethers and 3-4 moles of I were used in the presence of boron trifluoride etherate. Boiling points and refractive indices of the acetals obtained are summarized in Table I. Purities of the compounds were checked by vapor-phase chromatography. Diethyl ether was distilled from metallic sodium. Methylene chloride, *n*-heptane, and boron trifluoride etherate were purified as before.¹

TABLE I
Boiling Point and Refractive Index Data of Various Acetals

No.	Acetal	Bp, °C/mm Hg		n_D^{25} (obsd.)	n_D^{20} (lit.)
		Obsd.	Lit.		
I	CH ₃ CH(OC ₂ H ₅) ₂ ^a	103/760	104.2/760	1.3801	1.3805
II	C ₂ H ₅ CH(OC ₂ H ₅) ₂ ^b	124/760	124/760	1.3885	1.3892
III	CH ₃ CH(OC ₂ H ₅)CH ₂ CH(OC ₂ H ₅) ₂ ^c	77/12	68/10	1.4065	1.4069
IV	CH ₃ CH(OC ₂ H ₅)CH(CH ₃)CH(OC ₂ H ₅) ₂ ^c	66/5	69/5	1.4125	1.4115
V	CH ₃ CH(OC ₂ H ₅)C(CH ₃) ₂ CH(OC ₂ H ₅) ₂	87/10	—	1.4184	—

^a Data from *Kagaku Binran*.⁸

^b Data of Farina et al.⁹

^c Data of Hoaglin et al.⁶

Copolymerization

The methods of copolymerization and of the monomer reactivity ratio calculations are identical to those described previously.¹

Acetal Addition

In a glass-stoppered flask with a side-arm for nitrogen inlet were placed a 10-ml portion of an acetal and 0.8 ml of unsaturated ether mixture. After the mixture was thermostatted at 0°C, a solution of $\text{BF}_3 \cdot \text{OEt}_2$ in 0.2 ml diethyl ether was introduced under magnetic stirring and the reaction started. At specified intervals of time, small portions of the reaction mixture were sampled out with a syringe, and the reaction was stopped by the addition of methanolic potassium hydroxide. All the courses were traced under dry nitrogen. The residual ethers were determined by use of a Shimadzu Model GC-2C gas chromatograph. Diethyl ether was used as an internal standard for the ether determinations.

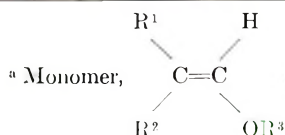
RESULTS

Copolymerizations

Copolymerization was carried out in methylene chloride at -78°C . with the use of $\text{BF}_3 \cdot \text{OEt}_2$ as catalyst. Monomer reactivity ratios were calculated by use of the integral form of the Mayo-Lewis copolymerization equation and are given in Table II together with related data obtained

TABLE II
Summary of the Monomer Reactivity Ratios

M_1^a			M_2^a			r_1^b	r_2^b	Ref.
R^1	R^2	R^3	R^1	R^2	R^3			
H	CH_3	C_2H_5	CH_3	CH_3	C_2H_5	24.0 ± 2.4	0.02 ± 0.02	This work
CH_3	H	C_2H_5	CH_3	CH_3	C_2H_5	19.1 ± 1.8	0.04 ± 0.02	This work
H	H	<i>i</i> - C_4H_9	H	CH_3	C_2H_5	0.23 ± 0.07	2.25 ± 0.10	2
H	H	<i>i</i> - C_4H_9	CH_3	H	C_2H_5	0.56 ± 0.03	1.44 ± 0.02	2
H	H	<i>i</i> - C_4H_9	CH_3	CH_3	C_2H_5	1.48 ± 0.03	0.00 ± 0.01	2

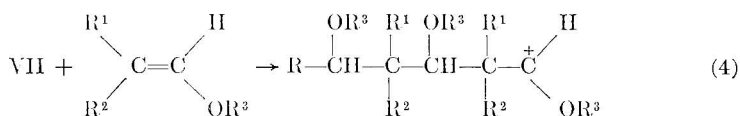
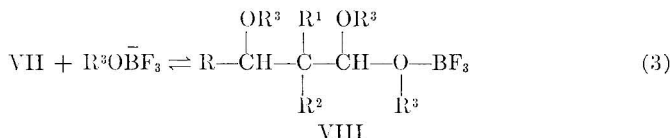
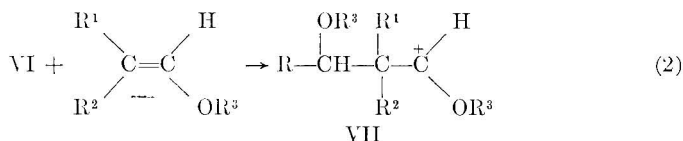
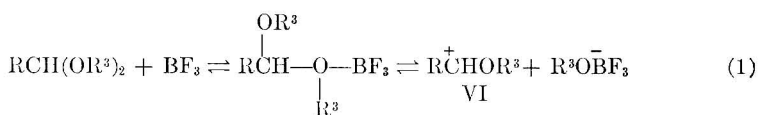


^b Uncertainties are the probable errors.

previously.² The β,β -disubstituted ether, IBEE, is considerably lower in reactivity toward both the IBEE and PEE cations. This result seems to be in contrast with the previous result that the deactivation of IBEE toward an unsubstituted vinyl ether cation is moderate.²

Acetal Addition

An addition of an acetal to an α,β -unsaturated ether catalyzed by an acid is considered to proceed through the attack of alkoxy-carbonium ion toward the β -carbon of the ether.⁵



Since a first product VIII is also an acetal, the produced acetal can undergo further addition to produce dimer acetal [eq. (4)] and so on. However, it was confirmed, in the synthetic reaction of acetals III–V that a 1:1 addition product forms in over 90% yield by the reaction of a large excess of an acetal with an unsaturated ether. In the present kinetic conditions, the main reaction is no doubt the 1:1 reaction as is shown in eqs. (1)–(3).

It was found that the acetal addition to an α,β -unsaturated ether proceeds with a short induction period and following first-order decay in almost all cases. Typical examples of the reaction course are seen in Figures 1 and 2. The induction period was shortened by the increasing concentration of catalyst but was independent of the order of addition of an ether and catalyst. The course of reaction with a mixture of ethers seems to be essentially the same as that with a pure ether. Each ether component of the mixture was consumed according to the same kinetic law separately.

TABLE III
Effect of β -Methyl Substitution on the Reactivity of Vinyl Ethyl Ether toward Various Alkoxy-carbonium Ions by Acetal Additions^a

No.	Carbonium ion	β -Substituent		
		<i>cis</i> -CH ₃	<i>trans</i> -CH ₃	(CH ₃) ₂
I	$\text{CH}_3\text{CH}^+(\text{OC}_2\text{H}_5)$	2.97	0.83	0.41
II	$\text{C}_2\text{H}_5\text{CH}^+(\text{OC}_2\text{H}_5)$	2.24	0.69	0.22
III	$\text{CH}_3\text{CH}^+(\text{OC}_2\text{H}_5)\text{CH}_2\text{CH}^+(\text{OC}_2\text{H}_5)$	1.33	0.67	0.21
IV	$\text{CH}_3\text{CH}^+(\text{OC}_2\text{H}_5)\text{CH}(\text{CH}_3)\text{CH}^+(\text{OC}_2\text{H}_5)$	1.25	0.57	0.04
V	$\text{CH}_3\text{CH}^+(\text{OC}_2\text{H}_5)\text{C}(\text{CH}_3)_2\text{CH}^+(\text{OC}_2\text{H}_5)$	1.3	0.4	0.01

^a Reactivities are shown by the relative values to the reactivity of vinyl ethyl ether (= 1.00) in each line.

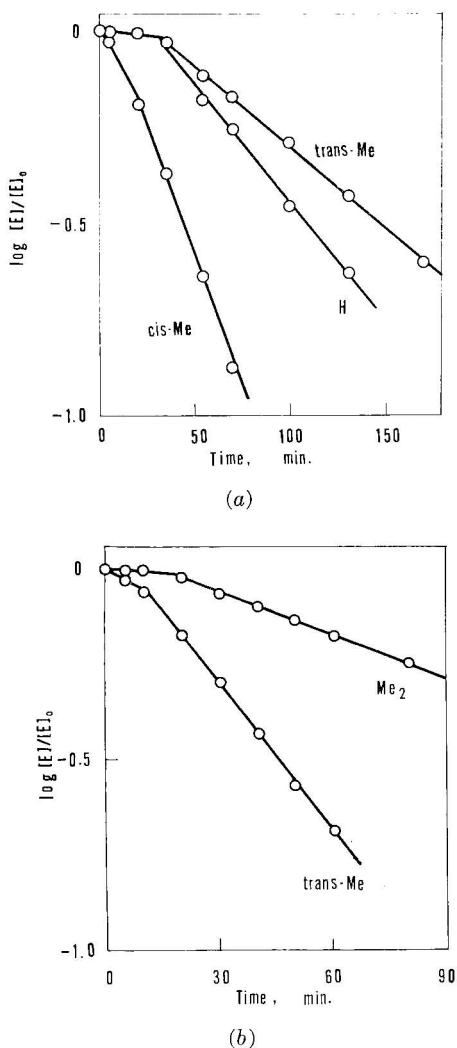
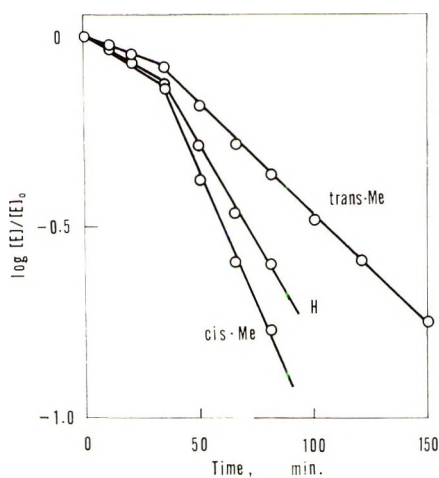


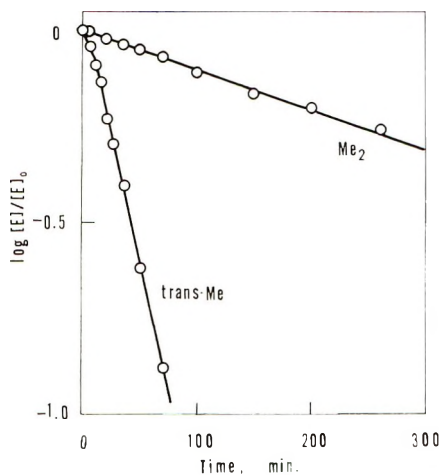
Fig. 1. Ether consumption curves in the reaction of 1,1-diethoxypropane with β -methyl-substituted vinyl ethyl ethers at 0°C at concentrations of $\text{BF}_3 \cdot \text{OEt}_2$ of (a) 4 mmole/l. and (b) 10 mmole/l. Symbols show β -substituents, where Me refers to a methyl group.

Thus, the relative reactivities of ethers were compared by the reaction with a mixture of ethers, the competitive reaction, and estimated from the relative slopes of the first-order decay part of the reaction. Since strict control of the amount of catalyst seems to be difficult, it is not only easier but also more reliable to compare the relative reactivities by competitive reactions.

Listed in Table III are the relative reactivities of ethers obtained toward various acetals. Ethyl vinyl ether (VEE) is taken as a standard. Therefore, the magnitude of the reactivity shown in Table III is relative to



(a)



(b)

Fig. 2. Ether consumption curves in the reaction of 1,1,3-triethoxy-2-methylbutane with β -methyl-substituted vinyl ethyl ethers at 0°C at concentrations of $\text{BF}_3 \cdot \text{OEt}_2$ of (a) 10 mmole/l. and (b) 20 mmole/l. Symbols show β -substituents, where Me refers to a methyl group.

that of VEE in each line or should be taken as a magnitude of substituent effect on the reactivity of VEE toward respective alkoxy-carbonium ions.

The reactivities decrease in the order *cis*-PEE > VEE > *trans*-PEE > IBEE. Although the effect of β -monomethyl substitution on the vinyl ether reactivity varies slightly, depending on the structure of attacking carbonium ions, that of β,β -dimethyl substitution is largely dependent on the structure of carbonium ions. That is, β -methyl substitution on the attacking alkoxy-carbonium ion reduces the reactivity of IBEE more prominently than that of PEE.

DISCUSSION

As has been described above, relative reactivities of the various unsaturated ethers toward given acetals were evaluated from their competitive rates of addition reaction. Probably, the overall rate of reaction is dependent on the equilibrium constant of the ionization of an acetal (1) as well as the rate of addition of the carbonium ion (2). In order to obtain more significant kinetic data, it will be necessary to disentangle the reaction mechanism and calculate pertinent rate constants of the elementary reactions. However, we had to be satisfied at this stage merely with the comparisons of the relative reactivities obtained by the competitive method. An induction period was observed in every case studied. The situation is very similar to that found in the cationic polymerization.

Table III shows that, for all the acetals studied here, the relative reactivities of β -methyl-substituted vinyl ethyl ethers decreases in the order: *cis*-CH₃ > H > *trans*-CH₃ > (CH₃)₂. A remarkable adverse effect of β,β -dimethyl substitution was observed toward β -monomethyl and β,β -dimethyl-carbonium ions (IV and V). On the contrary, an effect of β -monomethyl substitution is rather independent of the attacking carbonium ions. Thus, although β,β -dimethylvinyl ethyl ether showed a very small reactivity toward β -monomethylcarbonium ion (IV), β -monomethylvinyl ethyl ethers exhibited a moderate reactivity, even toward β,β -dimethylcarbonium ion (V). The *cis*- β -monomethyl substitution even enhances the reactivity of vinyl ether toward β,β -dimethylcarbonium ion (V).

In the copolymerizations of PEE with IBEE, the reactivity of IBEE is markedly smaller than those of PEE toward both PEE and IBEE chain ends, as can be seen in Table II. Contrasting results were obtained previously² in the copolymerization of vinyl isobutyl ether and IBEE, where the reactivity of IBEE was only slightly smaller than that of vinyl ether toward vinyl ether chain end. These results are consistent with those of acetal additions that an adverse steric effect is remarkable for IBEE- β -methyl-substituted acetal pairs while moderate effect is observed for IBEE-simple acetal pairs.

TABLE IV
Relative Reactivities of β -Methyl-Substituted Vinyl Ethyl Ethers
toward Polymer Chain Ends in the Cationic Copolymerizations^a

Chain end	β -Substituent			
	H	<i>cis</i> -CH ₃	<i>trans</i> -CH ₃	(CH ₃) ₂
$\sim\text{CH}_2\text{CH}^+(\text{O}-i\text{-C}_4\text{H}_9)$	(1.00)	3.99	1.64	0.62
$\sim\text{CH}(\text{CH}_3)\text{CH}^+(\text{OC}_2\text{H}_5)$	(1.00) ^b	2.25	1.44	0.07-0.09
$\sim\text{C}(\text{CH}_3)_2\text{CH}^+(\text{OC}_2\text{H}_5)$	[very large]	(1.00)	0.5	0.02

^a Figures in parentheses show the reference reactivity of each line.

^b A reference monomer is vinyl isobutyl ether.

In Table IV, polymerization results are summarized for the sake of easier comparison with the data shown in Table III. Results shown in Tables III and IV closely resemble each other. However, it must be remembered here that the copolymerizations were carried out in methylene chloride at -78°C while the acetal additions were in excess acetals at 0°C . Thus, some differences seen in these two tables may partly be ascribed to the solvent and temperature effects. The effect of *trans*- β -methyl substitution is an example of such differences.

Furthermore, the PEE chain ends in copolymerizations proved to be different depending on the geometrical configurations of precursor monomers, *cis* or *trans*. Because the last line of Table IV was estimated from the copolymerization results with IBEE where r_2 values are extremely small, it seems to be less reliable.

With these limitations in mind, the following general conclusions may be drawn concerning common behaviors of the reactant ethers in cationic polymerization and acetal addition.

(1) β -Monomethyl substitution enhances the reactivity of vinyl ethyl ether toward alkoxy-carbonium ions and shows little adverse steric effect toward any alkoxy-carbonium ions studied.

(2) β,β -Dimethyl substitution reduces the reactivity of vinyl ethyl ether toward β -unsubstituted alkoxy-carbonium ions only moderately but exhibits a large adverse steric effect against the addition of β -monomethyl- and β,β -dimethyl-substituted alkoxy-carbonium ions.

The latter conclusion is consistent with the low homopolymerizability of β,β -disubstituted monomers, an observation which was previously noted for isobutenyl ethyl ether.²

References

1. T. Okuyama, T. Fueno, and J. Furukawa, *J. Polym. Sci. A-1*, **6**, 993 (1968).
2. T. Okuyama, T. Fueno, J. Furukawa, and K. Uyeo, *J. Polym. Sci. A-1*, **6**, 1001 (1968).
3. A. Mizote, S. Kusudo, T. Higashimura, and S. Okamura, *J. Polym. Sci. A-1*, **5**, 1727 (1967).
4. T. Higashimura, S. Kusudo, Y. Ohsumi, and S. Okamura, *J. Polym. Sci. A-1*, **6**, 2523 (1968).
5. T. Fueno, T. Okuyama, and J. Furukawa, *J. Polymer Sci. A-1*, in press.
6. T. I. Hoaglin and D. H. Hirsh, *J. Amer. Chem. Soc.*, **71**, 3468 (1949).
7. H. Adkins and B. H. Nissen, *Organic Syntheses, Vol. I*, Wiley, New York, 1932, p. 1.
8. S. Iwamura et al., *Kagaku Binran, Ed.*, Chemical Society of Japan, Ed., Maruzen, Tokyo, 1966, p. 168.
9. M. Farina, M. Peraldo, and G. Bressan, *Ind. Chim. (Milan)*, **42**, 967 (1960).

Received February 28, 1969

Effect of Polymer Crystallinity on the Wetting Properties of Certain Fluoroalkyl Acrylates

ALLEN G. PITTMAN and BARBARA A. LUDWIG,
*Western Regional Research Laboratory, Agricultural Research Service,
U. S. Department of Agriculture, Albany, California 94710*

Synopsis

The wetting properties of a series of polyacrylates containing the fluoroalkyl group $(\text{CF}_2)_n\text{CF}_2\text{H}$ have been studied. Where n is 7 and 9, the polyacrylates are highly crystalline at room temperature. Since the polymers were prepared under atactic free-radical conditions and the polyacrylates with shorter alkyl groups (where n is 3 or 5) were not crystalline at room temperature, the crystallinity is presumed to occur as a result of side-chain packing and not involve the backbone. The polymers become more wettable (higher γ_c) as polymer crystallinity was reduced by quenching or heating past T_m . Correlations have been made between the work of Zisman and co-workers on the wetting properties of various fluorinated acid monolayers and the wetting properties of these fluoroalkyl acrylates. The results obtained in this study concerning the influence of polymer crystallinity on surface wetting are discussed in relation to the findings of Schonhorn and Ryan on the wettability of polyethylene single crystal aggregates.

INTRODUCTION

The wetting behavior of polymers as determined by liquid-solid contact angle measurements and the critical surface tension of wetting γ_c for solid polymer surfaces has received an increasing amount of attention in recent years owing partly to the interrelation between wetting, adhesion, and frictional properties.¹⁻⁴ Zisman and co-workers have shown that the wetting properties of a given organic solid are controlled by the nature and packing of the outermost atoms or groups of atoms at the air/solid interface.^{1,2} As a result of extensive studies on the wetting properties of oriented monolayers and various polymers, γ_c values have been tabulated which are associated with the wetting behavior of a variety of groups which can occur at the air/solid interface of a solid material.³

The influence of crystallinity (or chain packing) on γ_c was first demonstrated by Fox and Zisman⁶ in a comparison of the γ_c for a monolayer of octadecylamine and a crystal of hexatriacontane. The lower γ_c associated with the crystal (20-22 dyne/cm compared to 22-24 dyne/cm) was attributed to a tighter packing of the alkyl chains with a concomitant greater concentration of $-\text{CH}_2$ groups at the air/solid interface. Until recently, the question of the influence of polymer crystallinity on wetting behavior had been largely ignored. Schonhorn and Ryan⁷ examined the wettability

of a compressed aggregate of polyethylene crystals and found a γ_c value of 53.6 dyne/cm, which is considerably higher than that for ordinary melt-crystallized polyethylene (31 dyne/cm).² Schonhorn has also reported γ_c values for bulk polyethylene, nylon 66, polychlorotrifluoroethylene, and isotactic polypropylene which are considerably higher than previously reported values.³ These higher values were obtained after a slow melt crystallization of the polymers against a thin gold film. Subsequent dissolution of the film reportedly left a surface region of high crystallinity. In the case of polyethylene, the wetting properties of the slow melt-crystallized polymer against gold were similar to those of the compressed single-crystal aggregates.^{3,9}

This work has raised a question as to the effect of increasing or decreasing the surface density of particular groups on surface wettability. The decrease in γ_c previously found in comparing single crystals of *n*-hexatriacontane to an adsorbed monolayer of octadecylamine would suggest that increased packing or density of $-\text{CH}_3$ groups at the air/solid interface causes a lowering of surface wettability.⁶ However, the increase in γ_c found when comparing a polyethylene single-crystal mat to ordinary bulk polyethylene⁷ suggests the opposite effect for the methylene ($-\text{CH}_2-$) group.

Schonhorn and Ryan suggested that an increased γ_c would be expected for polyethylene with increasing surface density, since γ_c was previously shown to be proportional to the fourth power of the amorphous density of polyethylene,⁷ and they have developed equations relating γ_c to polymer density.

The effect of crystallinity on the wetting properties has not been reported for polymers containing pendant groups capable of orientation and packing. Wetting properties of a number of atactic, noncrystalline fluoroalkyl acrylates and methacrylates have been reported in which the fluoroalkyl group was either linear or branched.¹⁰⁻¹² In several cases where polymers were examined which carried pendant $\text{CF}_3(\text{CF}_2)_n$ groups, the γ_c values were always higher than for values given for fluorocarbon acid monolayers with comparable fluoroalkyl side chains. The higher γ_c associated with these polymers was attributed to a poorer packing of the alkyl group than was possible in a monolayer as well as surface exposure of the nonfluorinated polymer backbone.¹² In order to increase our understanding of the influence of polymer crystallinity on wettability we have examined the surface wetting properties of some crystalline and noncrystalline fluoroalkyl acrylates containing the alkyl group $\text{HCF}_2(\text{CF}_2)_n\text{CH}_2-$, where *n* is 1, 3, 5, 7, and 9. Of this series, the acrylates with *n* = 7 and 9 form polymers which are partially crystalline at room temperature, presumably by orientation and packing of the alkyl side chains. In order to simplify identification of the acrylate polymers employed in this study, we will refer to the acrylates in terms of the number of carbon atoms present in the alkyl side chain. For example, the acrylate polymer derived from the monomer $\text{HCF}_2(\text{CF}_2)_9\text{CH}_2\text{OOCCH}=\text{CH}_2$ will be referred to as the C-11 acrylate (eleven carbon atoms in the alkyl side chain).

We have examined contact angle variations, primarily with hexadecane, on these crystalline polymers after altering crystallinity by annealing, quenching, and by heating past the crystalline melting point (T_m).

EXPERIMENTAL

The fluoroalcohols employed in this study had the structure: $\text{HCF}_2(\text{CF}_2)_n\text{CH}_2\text{OH}$, where n is 3, 5, 7, and 9. These alcohols were obtained through the courtesy of the E. I. du Pont de Nemours and Company. Preparation of these alcohols involves a telomerization reaction between methanol and tetrafluoroethylene.¹³

The fluoroalkyl acrylates were either synthesized by reaction of the appropriate fluoroalcohol with acryloyl chloride¹⁴ or were obtained as research samples through the courtesy of the E. I. du Pont de Nemours and Company. The acrylates were redistilled under vacuum before use and had physical properties consistent with those previously reported. (See Table I).¹⁵

TABLE I
Physical Properties of Fluoroalkyl Acrylates, $\text{CH}_2=\text{CHCOOCH}_2(\text{CF}_2)_n\text{CF}_2\text{H}$

n	Bp, °C/mm	Refractive index (at T)
3	69-70/21 ^a	1.3431 ^a
5	41.5-42.5/0.5	1.3393 (26.5°C)
7	87-88/1	1.3359 (26.5°C)
9	45-47 (mp)	

^a Data of Bittles.¹⁵

Polymer Preparation

Polymers were obtained by free-radical polymerization of the monomers with the use of α, α' -azobisisobutyronitrile as the initiator. Monomers were dissolved in an equal volume of freshly distilled 1,3-bis(trifluoromethyl)benzene in screw-cap vials, the catalyst was added (0.5-1 mole-%) and the vials flushed with nitrogen before closing and placing in an oil-bath held at 75-80°C. After 5-6 hr, the vials were removed from the oil bath and polymer was obtained by the addition of heptane to the hexafluoroxylenepolymer solution. The precipitated polymer was collected, redissolved in a small amount of tetrahydrofuran or acetone, and reprecipitated with benzene. Reprecipitation with benzene was repeated one more time to assure removal of monomer. The polymers were then placed in a vacuum oven held at 80°C/0.1 mm pressure for 24 hr. The polymers having the 5-carbon and 7-carbon side chains were rubbery solids which were clear or slightly opaque. The polymer having the 9-carbon side chain was a hard, white solid with a waxlike feel, while the C-11 acrylate consisted of a white powder. All of the polymers had appreciable solubility in tetrahydrofuran and acetone with the exception of the C-11 acrylate. This acrylate could also be completely dissolved, however, if the solvents were warmed to 40-

50°C. The molecular weight of the C-9 acrylate was determined on a Mechrolab membrane osmometer with the use of 1,3-bis(trifluoromethyl)benzene as solvent, \bar{M}_n 101 620.

Measurement of Critical Surface Tension of Wetting (γ_c) for the Fluoroalkyl Acrylates

Polymer-coated glass slides were prepared by immersing clean glass microslides in a solution of the polymer (2–5 wt-%). The slides were slowly withdrawn from the solution in a vertical position, air-dried for several hours, then heated in an oven at 110°C for 15 min. After the slides were removed from the oven, they were conditioned at 45% RH, 23.5°C for a period of about 2 hr before use. Measurements of contact angle were obtained by projecting profiles of the drops onto a screen and drawing tangent lines as described in a previous article.^{11,12} The test liquids were a homologous series of *n*-alkanes with the purity and surface tensions given previously.^{11,12}

Examination of Changes in the Contact Angle of Hexadecane and Heptane on the C-9 and C-11 Acrylate Polymers with Changes in Crystallinity

This series of contact angle measurements was made by direct observation of the drops by using an NRL contact-angle goniometer purchased from Ramé-Hart, Inc., and an environmental chamber (model B-100) attachment which allows for controlled heating of the polymer specimen as well as control of the atmosphere.

Powdered polymer was placed in a limited area on 22 × 50 mm. Corning cover glass. The cover glass was then placed in a 150°C oven for about 1 min and removed. In the case of the C-9 acrylate, this usually resulted in a thick polymer film (ca. 1–2 mm thick) with a smooth surface. Additional time in the 150°C oven was employed if the surface appeared uneven.

Quenching of the polymer films was carried out by immersing the films in ice water immediately after removal from the 150°C oven. After removal of excess water from the slide by shaking, the slides were placed in a vacuum oven held at 23°C/0.1 mm for 3–4 hr before use. Quenching of the polymers resulted in clear films which became opaque after annealing slightly below the T_m for the polymer. It was difficult to obtain good films with the C-11 acrylate, since the polymer contracted greatly on cooling and tended to develop numerous fissures along the surface. We had to select areas in the film which seemed free of cracks when measuring the contact angles for this particular polymer.

Annealing of the polymer to induce maximum orientation and crystallization of the side chain was carried out by heating the slides in the environmental chamber in a nitrogen atmosphere to about 5°C past the T_m , then allowing the polymer to cool back to a temperature slightly below the temperature where the onset of melting occurred (37°C for the C-9 acrylate, 97°C for the C-11 acrylate).

Observations of the contact angle of hexadecane on the polymer films

from 23°C through the polymer crystalline melting were carried out by using the NRL contact angle goniometer and the environmental chamber. Polymer films used in this case were either obtained by dipping glass cover slides in a 2–5% polymer solution or by preparing a thick (1–2 mm) film as described above. Drops of hexadecane were placed on the polymer film at 23°C and contact angles taken at various intervals as the polymer was heated to above the T_m . Heating rates of Ca. 1°C/min and 5°C/min were employed. When a change in contact angle was observed, a new drop of hexadecane was placed on the polymer surface and the temperature held constant for 5 min. Readings of the new drop were taken initially and at the end of the 5-min period.

Observations on the Melting Behavior of the C-9 Acrylate and C-11 Acrylate Polymers

A Perkin-Elmer differential scanning calorimeter (DSC-1) was used to follow the melting characteristics of the C-9 and C-11 acrylate polymers. Heating rates of 5°C/min and 10°C/min were used on sample sizes ranging from 10 to 20 mg. The melting range was recorded as the temperature at which deflection from the base line first occurred to the temperature at which the peak maximum occurred. Effects of annealing and quenching on polymer melting were also studied with the scanning calorimeter. Quenching was carried out by surrounding the aluminum housing which covers the sample wells of the DSC-1 with dry ice. The polymer sample was then heated to about 5°C past its melting point and then allowed to cool as rapidly as possible to 0°C. Another quenching technique was also utilized which involved heating the polymer in a sample pan supplied for use with the DSC-1 to a temperature of 150°C in an air oven, removing the sample pan from the oven, and immediately placing it on Dry Ice.

DISCUSSION

γ_c Values for Various Acrylate Polymers with the $\text{HCF}_2(\text{CF}_2)_n\text{CH}_2$ —Side Chain

Figure 1 illustrates a Zisman type γ_c plot for a series of fluoroalkyl acrylate polymers in which the size of the fluoroalkyl chain has been varied. Contact angles θ in these cases were obtained on glass slides which had been coated with a polymer by immersion in a 2–5% polymer solution (see Experimental). The contact angles for the γ_c plot of the C-3 methacrylate (where $n = 1$) were reported by Tamaribuchi.¹⁶ The C-3 methacrylate and the C-5 and C-7 acrylates (where n is 1, 3, and 5, respectively) gave γ_c plots which displayed definite curvature. Initially, we assumed that this curvature was due to solubility of the alkanes in the polymer film. Two variables were examined in order to assess possible solubility effects. In one case, we preconditioned the test alkanes by placing them in contact with the C-5 acrylate polymer at room temperature for a period of 5 days. The contact angles of the preconditioned alkanes on the C-5 acrylate film

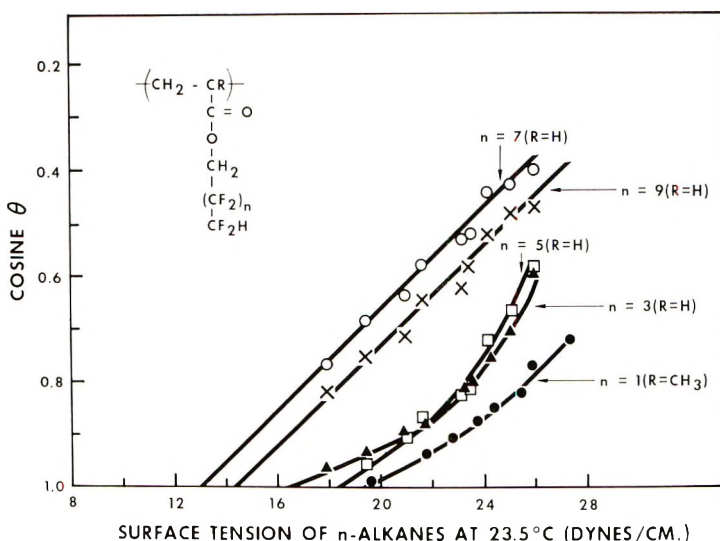


Fig. 1. γ_c Plots for fluoroalkyl acrylate polymers (cosine of contact angle θ , vs. surface tension).

were then compared with angles obtained with the unconditioned alkanes. No essential differences were noted with these two sets of alkanes. In another case, we examined the contact angles of hexadecane and tetradecane as a function of time. The drops did not creep during a 2-hr period and the contact angles remained constant. If the drops were allowed to remain for a sufficient length of time (overnight) evaporation occurred, and the drops decreased in size, occasionally giving lower (receding) angles. As a result of these tests, we do not feel the curvature displayed by the smaller-chained acrylate polymers is a result of alkane-polymer solubility; however, we are unable to provide an alternate explanation for this behavior.

The γ_c values obtained for the C-9 and C-11 acrylate polymers were 13 and 15 dyne/cm, respectively. It is of interest to compare the contact angle values for these polymers with the values reported for an acid monolayer of ω -hydroperfluoroundecenoic acid.¹⁷ The contact angle data are presented in Table II and the γ_c plots given in Figure 2. It can be seen that values for θ for ω -hydroperfluoroundecenoic acid are nearly the same as the values for the C-11 acrylate (Table II) and that a γ_c plot gives a value of 15 dyne/cm for both acid monolayer and polymer (Fig. 2). Table III gives a comparison of the γ_c values for several fluorinated acid monolayers and fluoroalkyl acrylate polymer films. In the first two cases, where the fluoroalkyl chain is $\text{CF}_3(\text{CF}_2)_2-$ and $\text{CF}_3(\text{CF}_2)_6-$, we can see that the acid monolayer gives lower γ_c values than the acrylates. These two fluoroalkyl acrylate polymers were both atactic, noncrystalline polymers,¹² and higher γ_c values would be expected owing to poor side-chain alignment and surface exposure of polymer backbone. A different situation obviously

TABLE II
Comparisons of Contact Angle θ for C-9 and C-11 Acrylate Polymer
and ω -Hydroperfluoroundecenoic Acid Monolayer

	θ		
	Acid monolayer ^a	C-11 acrylate ^b	C-9 acrylate ^b
Hexadecane	67	62	66
Tetradecane	65	61	64
Dodecane	59	58	63
Decane	53	51	57
Octane	50	44	51
Hexane	35	35	40

^a Data of Ellison et al.;¹⁷ angles and surface tensions reported at 20°C.

^b Angles and surface tensions at 23.5°C. The surface tensions we have obtained^{11,21} are slightly lower than those used by Ellison et al.¹⁷

occurs with the C-9 and C-11 acrylates containing the HCF₂-terminated alkyl chains. For these two polymers, the C-11 acrylate has the same γ_c as the corresponding acid monolayer, and the C-9 acrylate has an even lower γ_c than the longer-chained C-11 acrylate and/or acid monolayer. We believe the low γ_c values displayed by the C-9 and C-11 acrylates result from polymer crystallinity which gives improved packing of the fluoroalkyl side chain. In the C-9 acrylate, we assume that the packing is greater than in the C-11 acrylate or the C-11 acid monolayer and that a higher concentration of HCF₂— occurs at the air/solid interface. This phenomenon would, of course, be analogous to Zisman's observation that a lower γ_c can be obtained with a crystal of hexatriacontane than a monolayer of octadecylamine.⁶

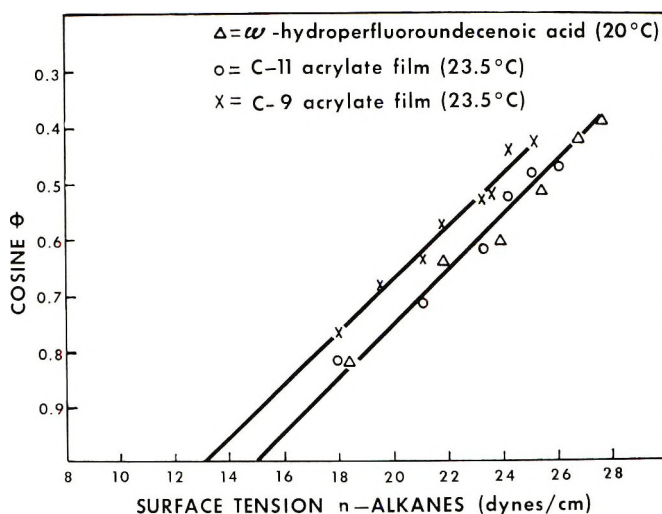


Fig. 2. Comparative γ_c plots for (Δ) C-11 acid monolayer, (O) C-11 acrylate polymer, and (\times) C-9 acrylate polymer.

TABLE III
Wetting Properties of Acid Monolayers and Comparable Acrylate Films

Fluorocarbon chain	γ_c , dyne/cm	
	Monolayer acid	Acrylate film
$\text{CF}_3(\text{CF}_2)_2$	9.2 ^a	15.5 ^b
$\text{CF}_3(\text{CF}_2)_6$	7.9 ^a	10.3 ^b
$\text{HCF}_2(\text{CF}_2)_7$	—	13
$\text{HCF}_2(\text{CF}_2)_9$	15 ^c	15

^a Data of Hare et al.²³

^b Data of Pittman et al.¹²

^c Data of Ellison et al.¹⁷

Crystallinity of the C-9 and C-11 acrylate polymers was confirmed by an examination of the x-ray diffraction patterns of powders of these two polymers at room temperature. The x-ray diffraction analysis of the C-5 and C-7 acrylate polymers, which were rubbery materials at room temperature, did not give evidence for a significant amount of crystallinity. Since these polymers were prepared under conditions in which stereoregularity would not be expected to develop, we assume that the crystallinity arises from alignment and packing of the fluoroalkyl side chains. Stereoregular polymers containing long unbranched side chains (e.g., polyoctadecene-1) have been reported in which crystallization can involve both the side chain and the main chain.^{18,19}

Melting Characteristics of the C-9 and C-11 Acrylates

We observed the thermal changes which occurred on heating these polymers using a Perkin-Elmer differential scanning calorimeter. The energy-temperature profile for the C-9 acrylate polymer is shown in Figure 3. The polymer obtained by precipitation as described in the Experimental section gave a broad endotherm beginning at ca. 42°C and peaking at 51°C (curve 1, Fig. 3). We attribute this endotherm to crystalline melting since, in this temperature range, we observed the disappearance of birefringence on examination with crossed optical polarizers. In addition, the polymer changed from an opaque solid to a clear melt in this temperature range when examined with a melting hot-stage. Annealing the polymer below its melting point caused a shift in the melting endotherm with a peak at 56°C (Fig. 3, curve 2). Quenching the polymer melt lowered the melting endotherm and gave rise to a rather broad melting range centered at 44°C. Quenching the C-9 acrylate also tended to reduce the overall per cent crystallinity. In one case, the area under the curve was reduced by 40% from the annealed polymer. In another case, no endothermic peak was observed after quenching.

The C-11 acrylate produced an endotherm between 97 and 113°C (Fig. 4). This temperature range is assumed to be the temperature range of crystalline melting as we observed the disappearance of optical birefringence

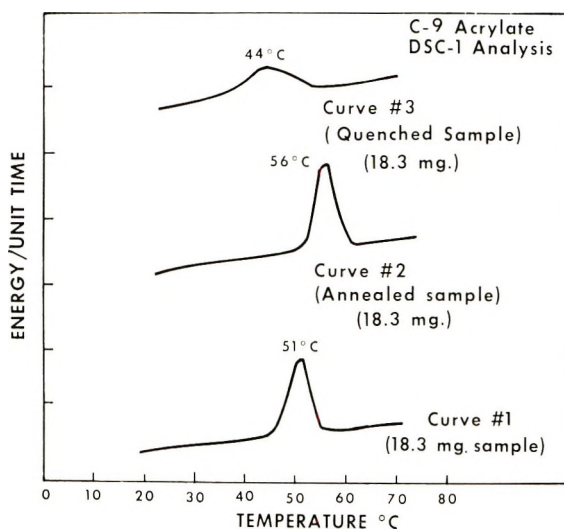


Fig. 3. Differential scanning calorimeter results for C-9 acrylate polymer.

and the transformation from a white powder to a clear melt in this temperature range. The polymer obtained by precipitation gave several distinct peaks at 105, 109, and 113°C (Fig. 4, curve 1). Annealing overnight at 97°C resulted in a polymer which gave only one sharp endothermic peak (peak temperature 113°C). Quenching the C-11 acrylate polymer resulted in two distinct endothermic peaks at 105 and 113°C. The occurrence of multiple endothermic peaks in the melting curve for C-11 polymer samples which had not been annealed could represent the melting of different

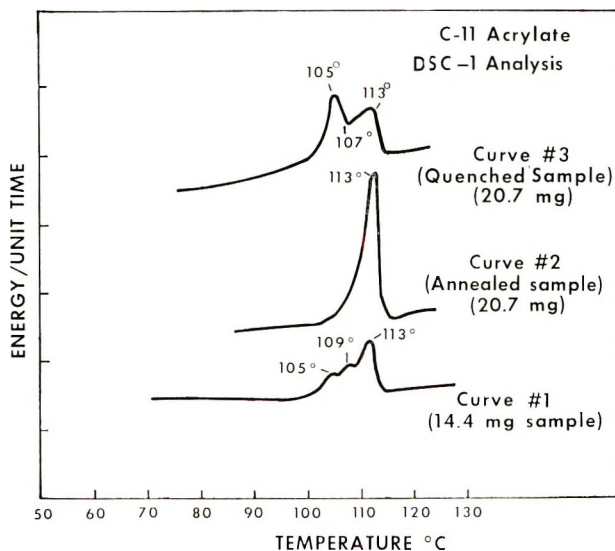


Fig. 4. Differential scanning calorimeter results for C-11 acrylate polymer.

crystalline forms or could simply be an artifact. It is possible that the curve for the quenched polymer (Fig. 3, curve 3) represents a broad endotherm with an exothermic crystallization (peak temperature 107°C) taking place before final melting. There have been a number of reports in the literature of multiple endothermic peaks occurring in crystalline polymers.²⁰ We have previously mentioned the two crystalline forms which occur in isotactic polyoctadecene-1.^{18,19}

Wetting Changes With Crystalline Modification

Contact angles for hexadecane and heptane were observed on a C-9 acrylate polymer film 1–2 mm thick. The quenched film gave contact angles of 50° and 17° for hexadecane and heptane, respectively. It is interesting to note that these angles are quite close to the angles given for the —CF₂— surface of polytetrafluoroethylene (hexadecane 46°, heptane 21°).²¹ Annealing the polymer overnight at 37°C resulted in increased contact angles for both hexadecane and heptane (61° and 45°, respectively). As discussed in the preceding section, thermal analysis of this polymer showed that after annealing the quenched polymer, there was an increase in the overall energy absorbed during melting and a narrowing of the melting range. These phenomena indicate, as one would expect for an annealing process, an increase in overall crystalline content and fewer crystalline defects. Since these polymers were formed under atactic free-radical conditions, the crystallinity is assumed to occur as a result of fluoroalkyl side-chain packing. Packing of the fluoroalkyl sidechains should also result in a greater concentration of HCF₂— end groups at the air/solid interface than occurs in the quenched polymer. The fact that the crystalline C-9 polymer gave a γ_c value of 13 dyne/cm (Fig. 1) indicates that the HCF₂—

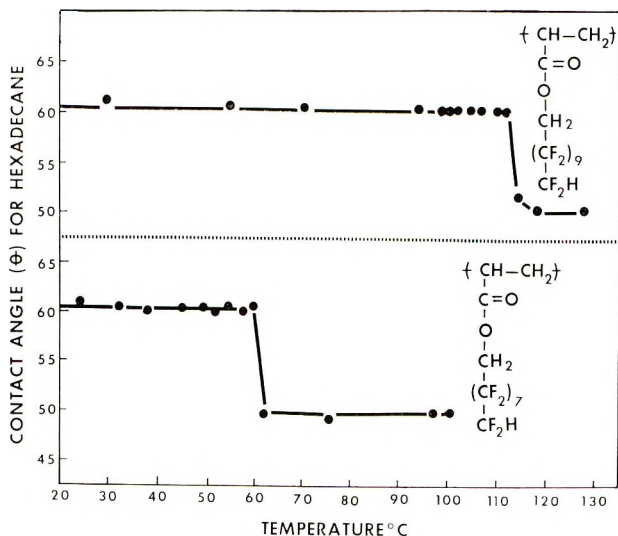


Fig. 5. Effect of temperature on θ for C-9 and C-11 acrylate polymers.

function, when closely packed at the air/solid interface, reduces surface wettability to greater extent than originally found for a long-chained HCF_2 -terminated acid monolayer.¹⁷ This finding is in accordance with Zisman's observation on the differences in wetting for CH_3 -terminated materials.⁶

The C-11 acrylate polymer showed a similar reduction in the contact angle of hexadecane on quenching followed by an increase in contact angle after annealing (quenched 55° , annealed 64°).

From the preceding observation, one would anticipate increased wetting properties of these polymers above their crystalline melting points. As indicated in Figure 5, a substantial decrease in θ did in fact occur for hexadecane above the melting ranges for these polymers. The angles observed above T_m are approximately the same as those found for the quenched polymers. It is possible that some of the decrease above T_m is due to slight solubility of the polymer in the alkane or a gravitational effect of the alkane on the molten polymer since we noted a ring or shallow crater on the polymer surface after removal of the drops from the molten polymer.

It should be noted that other polymers, notably polyhexafluoropropylene, have not exhibited changes in the advancing contact angle over a rather wide temperature range.²²

Aspects of Polymer Crystallinity and Wettability

Earlier research on the wetting behavior of specific groups has indicated the variability which can occur depending on the concentration of these groups at the air/solid interface. For example, research on acid monolayers has shown that γ_c values of from 6 to 9 dyne/cm can be obtained with perfluorocarbon acid monolayers of different chain lengths.²³ The value of 6 dyne/cm has been accepted as representative of the CF_3 group in its closest packing at the air/solid interface. Variations in wettability have also been noted for CH_3 -terminated hydrocarbon materials. As previously mentioned the value of 20–22 dyne/cm is presumed to represent the lowest γ_c possible for CH_3 -groups concentrated at the air/solid interface since this value was obtained from a single crystal of hexatriacontane and should represent the optimum in packing for an alkyl chain terminated by the methyl group.⁶

Similarly, we have found that polymers containing fluoroalkyl side chains terminated by HCF_2 display a range of γ_c values depending on such factors as fluoroalkyl chain length and side-chain crystallization. Both of these factors influence the packing or density of terminal HCF_2 groups at the air/solid interface. As would be predicted from the work of Zisman et al.²³ on acid monolayers, increasing the length of the fluoroalkyl side-chain tends to decrease the wettability (or lower γ_c). Where crystallinity occurs in the fluoroalkyl side chain, as with the C-9 and C-11 polyacrylates, γ_c can be even lower than reported for an HCF_2 -terminated acid monolayer. As crystallinity is reduced by quenching or by heating past T_m , the wettability of these polymers is increased and the wetting properties approach

those found for a $-\text{CF}_2-$ surface of poly(tetrafluoroethylene). It should be emphasized that the presence of polymer crystallinity as determined by x-ray diffraction does not necessarily imply crystallinity in the surface region. However, the results obtained in this study are understandable on the basis of a crystalline packing of fluoroalkyl side groups at the air/solid interface.

The findings of Zisman² and those presented here, as opposed to the findings of Schonhorn and Ryan,⁷ would at first seem contradictory. That is, γ_c has been found to decrease with substances presenting either CH_3 -⁶ or HCF_2 - at the air/solid interface as a closer packed more crystalline arrangement is achieved; however, Schonhorn and Ryan have found that γ_c increases as the crystallinity of polyethylene is increased.

With a methyl (CH_3-) surface, an increase in the number of methyl groups at the air/solid interface should result in a lower γ_c as a result of the decrease in $-\text{CH}_2-$ exposure. A surface comprised of methylene groups is known to have a higher γ_c than one comprised of methyl groups. The same argument can apply to perfluoroalkyl chains terminated by $-\text{CF}_2\text{H}$. That is, as the concentration of $-\text{CF}_2\text{H}$ increases at the air/solid interface as a result of side-chain packing during crystallization, an attendant decrease in the $-\text{CF}_2-$ groups will occur which should cause an overall decrease in γ_c .

In the case of polymers whose chains are comprised only of secondary carbon atoms, such as polyethylene, different considerations are obviously involved. Although the relation between the specific surface free energy γ_s and γ_c is not entirely clear, γ_s will be given by the product of the number of molecules per unit surface area and the molecular free surface energy. Therefore, one might expect an increase in γ_s (and hence also in γ_c) with increasing surface packing in a polymer such as polyethylene, where there is only the possibility of methylene groups occurring at the air/solid interface. As noted in the introductory remarks, Schonhorn and Ryan have developed equations relating γ_c to polymer density which predict an increase in γ_c with increasing surface density. Although a higher γ_c was found for a crystalline mat of polyethylene than for bulk crystallized polyethylene, it is not clear whether or not the increase in γ_c is in this case the result of increased surface packing of the methylene groups. It would seem that the alternate possibility exists; that of decreased methylene packing at the surface of a crystalline polyethylene mat.

It is well established that the lamellae surface of polymer single crystals consists of some type of folded chain in which the polymer chains exit from the crystal lattice, fold, and re-enter the crystal lattice.^{24,25} The exact nature of the fold surface is controversial and a number of models have been proposed.²⁶⁻²⁹

However, regardless of the model one favors to describe the exit and re-entry of the polymer chains into the crystal lattice, there is considerable evidence which indicates that there is an amorphous component associated with the surface region which amounts to ca. 10-20% of the total weight.^{30,31}

The amorphicity present at the fold or crystal surface together with the increased internal energy associated with sharp folds may be sufficient to account for the increased wettability (higher γ_c) found for the polyethylene single-crystal aggregate. In any case, a liquid in contact with a polyethylene single-crystal aggregate would have minimum exposure to a close-packed array of minimum energy planar zigzag methylene groups. Instead the wetting liquid would presumably be exposed to a disordered, loosely packed methylene surface and/or a sharp folded methylene surface in a higher energy state than found in the planar zigzag conformation. In order to assess the wetting behavior of close-packed methylene groups in a state of low internal energy, it will be necessary to examine a surface composed of methylene groups in the extended chain planar zigzag conformation. We hope to examine such a surface since, in certain cases, extended chain crystals reportedly occur in polyethylene after special melt crystallization techniques,^{32,33} and special techniques involving simultaneous polymerization and crystallization.³⁴

CONCLUSIONS

The wetting properties of polymers containing side chains can be markedly influenced by packing of the side chains resulting from crystallization. Polymers containing crystalline segments involving a fluoroalkyl side chain terminated by HCF_2- can give rise to γ_c values lower than the γ_c value previously found for a long chain HCF_2- terminated acid monolayer. That implies that the minimum γ_c value for a CF_3- surface could be less than the 6 dyne/cm reported for a long-chain CF_3 -terminated acid monolayer.

The findings presented here support the view that, where primary carbon atoms make up the surface layer (e.g., CH_3- , CF_3- , HCF_2- , etc.), the constitution of the surface group and the packing or concentration of this group at the air/solid interface control the wetting properties of the solid surface. We suggest that, where the surface is made up of groups comprised of secondary carbon atoms (e.g., $-\text{CH}_2-$, $-\text{CHF}-$, $-\text{CHCl}-$, etc.), account must also be taken of the conformational arrangements of these groups and the packing which results.

The authors wish to thank Mrs. Kay Lee for x-ray diffraction analyses and Dr. F. Jones for microscopic examinations. The authors also wish to thank Dr. E. Menefee of this laboratory and Dr. P. Ingram of the Camille Dreyfus Laboratory, Research Triangle Institute, for helpful discussions on polymer morphology.

Reference to a company or product name does not imply approval or recommendation of the product by the U. S. Department of Agriculture to the exclusion of others that may be suitable.

References

1. W. A. Zisman, *Record Chem. Progr.*, **26**, 13 (1965).
2. W. A. Zisman, in *Advances in Chemistry*, No. 43, American Chemical Society, Washington, D. C., 1964, p. 1.
3. J. R. Huntsberger, in *Treatise on Adhesion and Adhesives*, R. L. Patrick, Ed., Vol. I, Dekker, New York, 1967, p. 119.

4. L. H. Sharp and H. Schonhorn, Adhesion in *Advances in Chemistry*, No. 43, American Chemical Society, Washington, D. C., 1964, p. 189.
5. E. G. Shafrin and W. A. Zisman, *J. Phys. Chem.*, **64**, 519 (1960).
6. H. W. Fox and W. A. Zisman, *J. Colloid Sci.*, **7**, 428 (1952).
7. H. Schonhorn and F. W. Ryan, *J. Phys. Chem.*, **70**, 3811 (1966).
8. H. Schonhorn, *J. Polym. Sci. B*, **5**, 919 (1967).
9. H. Schonhorn and F. W. Ryan, *J. Polymer. Sci. A-2*, **6**, 231 (1968).
10. M. K. Bernett and W. A. Zisman, *J. Phys. Chem.*, **66**, 1207 (1962).
11. A. G. Pittman, D. L. Sharp, and B. A. Ludwig, paper presented at American Chemical Society Meeting, New York, Sept., 1968; *Polymer Preprints*, **7** (2), 1093 (1966).
12. A. G. Pittman, D. L. Sharp, and B. A. Ludwig, *J. Polymer. Sci. A-1*, **6**, 1729 (1968).
13. R. M. Joyce, U. S. Pat. 2,559,628 (1951).
14. D. W. Coddling, T. S. Reid, A. H. Ahlbrecht, G. H. Smith, Jr., and D. R. Husted, *J. Polymer Sci.*, **15**, 515 (1955).
15. J. A. Bittles, Jr., U. S. Pat. 2,628,958 (1953).
16. K. Tamaribuchi, paper presented at American Chemical Society Meeting, Miami Beach, April, 1967; *Polymer Preprints*, **8** (1), 631 (1967).
17. A. H. Ellison, H. W. Fox, and W. A. Zisman, *J. Phys. Chem.*, **57**, 622 (1953).
18. A. T. Jones, *Makromol. Chem.*, **71**, 1 (1964).
19. D. W. Aubrey and A. Barnatt, *J. Polym. Sci. A-2*, **6**, 241 (1968).
20. B. Ke, in *Newer Methods of Polymer Characterization* (Polymer Reviews, Vol. 6), Interscience, New York, 1964, p. 347.
21. H. W. Fox and W. A. Zisman, *J. Colloid Sci.*, **5**, 514 (1950).
22. R. E. Johnson, Jr. and R. H. Dettre, *J. Colloid Sci.*, **20**, 173 (1965).
23. E. F. Hare, E. G. Shafrin, and W. A. Zisman, *J. Phys. Chem.*, **58**, 236 (1954).
24. P. H. Geil, *Polymer Single Crystals*, Interscience, New York, 1963.
25. D. H. Reneker and P. H. Geil, *J. Appl. Phys.*, **31**, 1916 (1960).
26. A. Keller, *Polymer*, **3**, 393 (1962).
27. P. J. Flory, *J. Amer. Chem. Soc.*, **84**, 2857 (1962).
28. E. W. Fischer and R. Lorenz, *Kolloid-Z.*, **189**, 97 (1963).
29. D. J. Blundell, A. Keller, and T. M. Connor, *J. Polym. Sci. A-2*, **5**, 991 (1967).
30. P. Ingram and A. Peterlin, in *Encyclopedia of Polymer Science and Technology*, Interscience, New York, Vol. 9, 1968, p. 204.
31. A. Keller, paper presented at Conference on Crystallization of Polymers, Garmisch-Partenkirchen, Germany, Sept. 27-29, 1967; *Kolloid-Z.*, in press.
32. P. H. Geil, F. R. Anderson, B. Wunderlich, and T. Arakawa, *J. Polym. Sci. A*, **2**, 3707 (1964).
33. F. R. Anderson, *J. Appl. Phys.*, **35**, 64 (1964).
34. H. Chanzy, A. Day, and R. H. Marchessault, *Polymer*, **8**, 567 (1967).

Received November 15, 1968

Revised March 5, 1969

Thermal Degradation of Poly(methyl α -Phenylacrylate)

G. G. CAMERON* and G. P. KERR,* *Department of Chemistry, The University of St. Andrews, St. Andrews, Fife, Scotland*

Synopsis

Volatile products, molecular weight changes, and rates of volatilization have been examined during the thermal decomposition of poly(methyl α -phenylacrylate) in vacuum at 210–280°C. In the early stages of the decomposition, initiation occurs at random within the polymer backbone to give radicals which unzip exclusively to monomer, with a kinetic chain length of about 500. Later in the reaction, chain-end initiation becomes important and predominates beyond about 45% conversion. There is no evidence that transfer reactions occur during the degradation.

INTRODUCTION

Poly(methyl α -phenylacrylate) (PMPA) represents a structural link between poly(methyl methacrylate) (PMMA) and polystyrene (PS). Since the thermal decomposition mechanisms of these two polymers fall into two distinct classes it is of interest to discover into which group the decomposition of PMPA fits. According to current generalizations on the relationship between degradation behavior and polymer structure one would predict that PMPA would closely resemble PMMA. This investigation therefore provides an interesting test of these generalizations and could throw some light on the controversy which still persists over the mechanism of PS degradation.¹ Methyl α -phenylacrylate monomer, however, is unreactive in free-radical polymerization,² and it is only comparatively recently that it has been shown to yield high polymers in "living" anionic syntheses.^{2,3}

EXPERIMENTAL

The PMPA sample employed in this study was kindly gifted by Professor K. Chikanishi of Kyoto University, Japan. (This polymer is PMPA 5 of ref. 4.) It was prepared by CaZnEt_4 initiation in THF at -78°C , and possessed the following molecular weight averages:

$$\begin{aligned}\bar{M}_n &= 140\,000 \\ \bar{M}_v &= 366\,000 \\ \bar{M}_v/\bar{M}_n &= 2.61\end{aligned}$$

* Present address: Department of Chemistry, The University of Aberdeen, Old Aberdeen, Scotland.

The number-average molecular weight was measured by osmometry in benzene at 25°C using a Mechrolab model 501 osmometer fitted with Ultra-cella filter membranes, "allerfeinst" grade. Osmometry on the degraded samples was not possible because of diffusion of low molecular weight material through the membrane. Consequently all molecular weight measurements on degraded polymers were done by viscometry in benzene at 24.5°C, by using the published Mark-Houwink constants K and a , 2.9×10^{-4} and 0.593, respectively.³

Rates of volatilization and molecular weight changes were studied by pyrolyzing 100 mg samples of polymer isothermally in a molecular still under a vacuum of 10^{-5} mm Hg. Further isothermal rates of volatilization were obtained by degrading 10-mg samples using a Cahn R.G. electro-balance in the installation described elsewhere.⁴

The volatile pyrolysis products from PMPA were collected by degrading samples in a closed inverted U-tube. One limb, containing polymer, was immersed in a Wood's metal bath, controlled thermostatically at the degradation temperature (250°C), and the other was cooled in liquid nitrogen. The volatiles which condensed in the cold limb were analysed by gas-liquid chromatography (GLC) and infrared and NMR spectroscopy.

RESULTS AND DISCUSSION

Analysis of the Volatile Fraction from Pyrolyzed PMPA

GLC, infrared and NMR analyses proved that the sole volatile product of degradation was monomer; there was no evidence of higher molecular weight material, such as dimer etc. Subsequent gravimetric analysis proved that the recovery of volatile material was quantitative. These results confirm the preliminary observation of Hopff, Lussi, and Borla³ that unzipping of the macromolecules to monomer is the predominant reaction in the pyrolysis of PMPA. The absence in the volatiles of detectable quantities of species larger than monomer proves that transfer reactions play a negligible role in the degradation mechanism.

Molecular Weight Changes in Pyrolyzed PMPA

Molecular weight changes as a function of conversion to volatiles are shown in Figure 1. The curves are very similar to analogous ones for poly-(α -methylstyrene) (PMS),^{5,6} and closely resemble theoretical curves^{7,8} based on a mechanism comprising random initiation followed by unzipping of the primary radicals to monomer. Intermolecular transfer reactions, which would cause a more precipitous fall in molecular weight, appear to be absent, a conclusion which is supported by the analysis of the volatile products of pyrolysis. The degradation mechanism is therefore the same as that which occurs in PMS^{5,6} and ionically synthesized PMMA,⁹ an observation which reinforces the generalization that the predominant reaction in the decomposition of polymers of α,α -disubstituted olefins is unzipping to

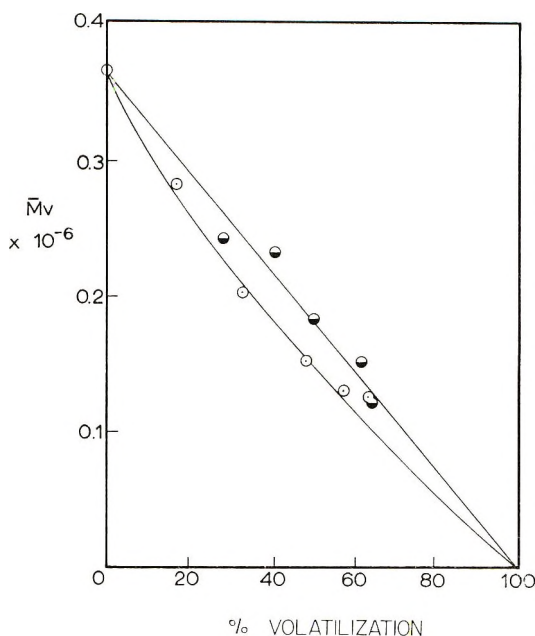


Fig. 1. Viscosity-average molecular weight \bar{M}_v for PMPA as a function of conversion to monomer: (●) 220°C; (○) 210°C.

monomer. Only when α -hydrogen atoms are present, as in polystyrene¹ and poly(methyl acrylate) (PMA),¹⁰ do transfer reactions become significant, resulting in a different—and generally more complex—pattern of decomposition.

The comparatively low temperatures at which PMPA decomposes are noteworthy. Ionically polymerized PMS and PMMA, which like the present PMPA sample contain no terminal unsaturation, are much more thermostable and do not show appreciable decomposition below 270°C.^{5,8} This relative instability in PMPA is probably due to the greater steric strain induced in the polymer backbone by the bulky substituents.

In the early stages of a randomly initiated degradation the number of macromolecules in the residue is given by $(1 - x)/\bar{M}_n$, where x is the fractional conversion to monomer and \bar{M}_n is the number-average molecular weight at time t .¹¹ In the present instance it was not possible to obtain accurate values of \bar{M}_n and the less precise viscosity averages \bar{M}_v were used instead. Thus variations in molecular population with time were followed by determining the value of the expression $[(1 - x)/\bar{M}_v] - (1/\bar{M}_v)$, where \bar{M}_v and \bar{M}_v are viscosity-average molecular weights at zero time and time t , respectively. A plot of this quantity (Fig. 2) shows an increase up to ca. 45% conversion, followed by a gradual decay. This maximum signifies that up to 45% conversion a large proportion of the primary macroradicals formed by random scission are terminated before complete unzipping to monomer, whereas beyond 45% conversion most acts

of initiation result in complete unzipping of the polymer chains. The degree of polymerization, DP , at the maximum should therefore be approximately equal to the average zip length. In Figure 2 viscosity-average molecular weights are employed, but since it has been shown that polymers undergoing random degradation rapidly tend to a "most probable" distribution of molecular weights,¹² the number-average DP is given by:¹³

$$DP_n = DP_v / [\Gamma(a + 2)]^{1/a}$$

where a is the exponent in the Mark-Houwink viscosity relationship, and Γ is the gamma function. Thus, the average zip length is 525 monomer units

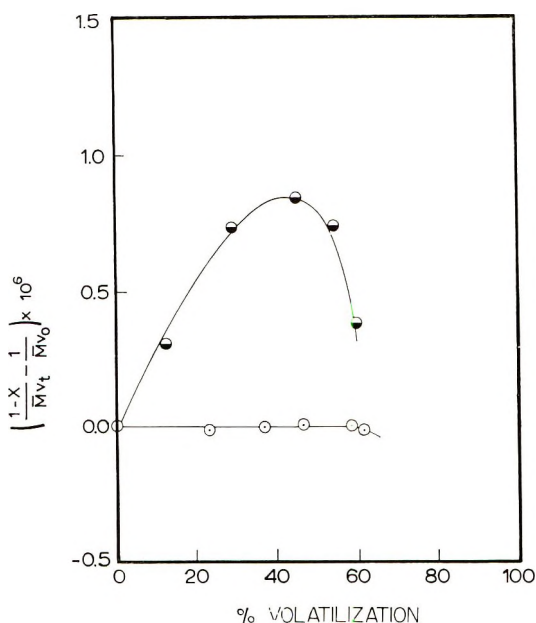


Fig. 2. Variation in molecular population of PMPA as a function of conversion to monomer. Plot of $[(1-x)/M_v] - (1/M_{v0})$ as a function of conversion to monomer: (●) 210°C; (○) 220°C.

per polymer molecule initiated at 210–220°C. This value compares with 460–900 monomer units at 300°C for ionically prepared PMMA⁹ and 1340 monomer units at 282.5°C for PMS.⁵

During the degradation of high molecular weight PMMA it has been shown¹⁴ that the occurrence of a termination step following randomly initiated depropagation leads to an element of chain-end initiated decomposition, which probably occurs at the unsaturated terminal units formed by disproportionation termination. This situation may also arise in the case of PMPA, since some termination occurs in the early stages of the decomposition and may be detected in the rate of volatilization data which will now be considered.

Rates of Volatilization of PMPA

The rates of volatilization R_2 (as a percentage of the residual weight of polymer) are shown as a function of conversion in Figures 3 and 4. These plots again show a strong resemblance to analogous rate curves for PMS.^{5,6}

It has been shown¹⁴ that for random initiation and unzipping to monomer, the rate R_2 should be invariant with molecular weight (and conversion)

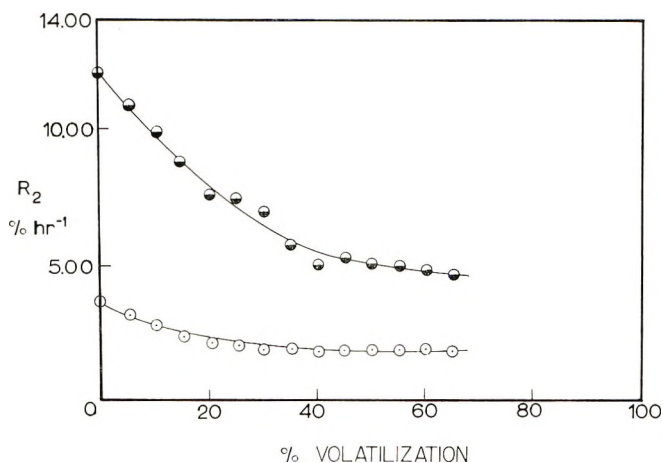


Fig. 3. Rate of volatilization R_2 (per cent residue weight per hour) as a function of conversion to monomer for degradations in the molecular still: (●) 220°C; (○) 210°C.

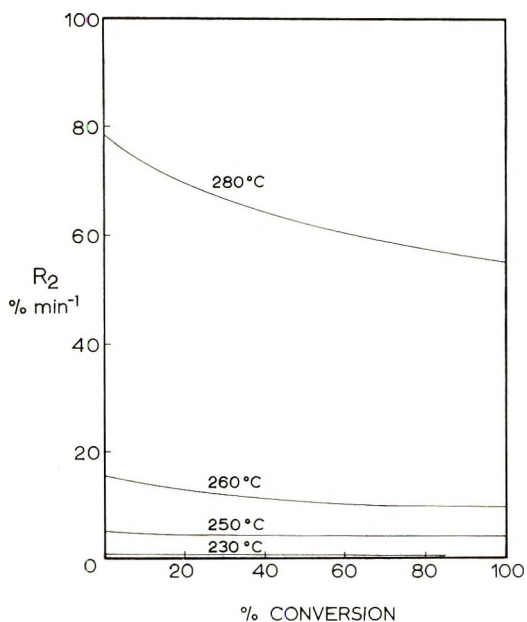


Fig. 4. Rate of volatilization R_2 (per cent residue weight per minute) as a function of conversion to monomer for degradations in the electrobalance.

when the zip length is less than the average DP, but proportional to the molecular weight for a zip length greater than the DP. For chain-end initiation, R_2^2 is inversely proportional to the molecular weight when termination is second-order and the zip length is less than the DP, but when the zip length exceeds the DP R_2 (and R_2^2) is invariant with molecular weight. Plots of R_2 and R_2^2 versus reciprocal DP are shown in Figure 5. Initially, where R_2 decreases with increasing reciprocal DP, the degradation mechanism appears to comprise complete unzipping following random initiation. Later, however, where R_2 is almost invariant with DP, decomposition appears to become initiated predominantly at chain ends, with

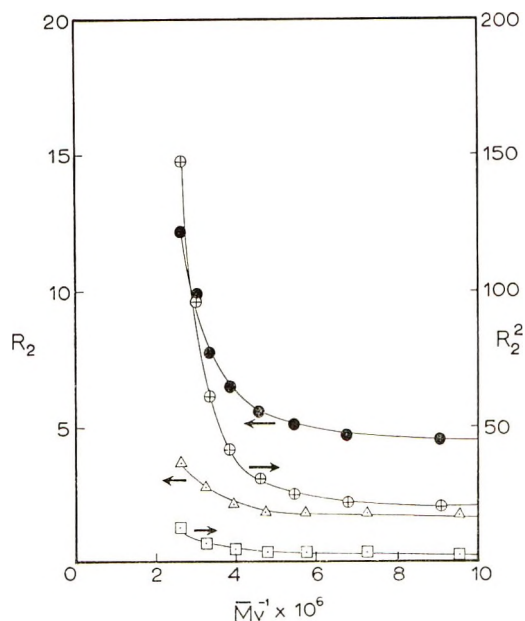


Fig. 5. Rate of volatilization R_2 (per cent residue weight per hour) and R_2^2 as functions of reciprocal viscosity-average molecular weight: (●) R_2 vs. \bar{M}_v^{-1} , 220°C; (⊕) R_2^2 vs. \bar{M}_v^{-1} , 220°C; (△) R_2 vs. \bar{M}_v^{-1} , 210°C; (⊞) R_2^2 vs. \bar{M}_v^{-1} , 210°C.

a small residual component of random scission. Again, the zip length is greater than the DP. This change in the mode of initiation probably reflects the increasing contribution of decomposition initiated at the labile—possibly unsaturated—chain ends which are formed in the early part of the degradation by termination before complete unzipping of the macroradicals. The conclusion drawn from the R_2 data—that the zip length exceeds the DP even in the initial stages of the decomposition—appears to contradict that drawn from the molecular weight data in Figure 2, i.e., that a measure of termination occurs up to 45% conversion. However, it must be remembered that in the present sample, with its relatively wide distribution of molecular weights, some of the chains will decompose completely, while

others will not. It is probable that the rate data reflects the effect of the chains which decompose completely, while the molecular weight changes show the effect of those which do not. The important observation, however, is that in the later phase of decomposition initiation appears to occur predominantly at chain ends.

The extrapolated initial rates in Figures 3 and 4 give activation energies E_a of 56 and 57 kcal/mole, respectively. Since in the initial polymer some chains unzip completely and others do not, these figures have no kinetic significance. E_a for random initiation and complete unzipping is given¹³ by:

$$E_a = E_i \quad (1)$$

but when a second-order termination step occurs before unzipping is complete, E_a is given by:

$$E_a = 1/2E_i + E_d - 1/2E_t \quad (2)$$

where E_i , E_d , and E_t are activation energies for initiation, depropagation (unzipping), and termination, respectively. The value of 56–57 kcal/mole therefore represents an unknown combination of these two situations and should be viewed accordingly. It has been shown⁴ that for low molecular weight PMPA which conforms to eq. (1) E_i is approximately 80 kcal/mole, which agrees closely with the corresponding values¹³ for PMMA and PMS. There are insufficient data available at present to estimate E_d and E_t for this polymer, and indeed E_t is a difficult parameter to measure in any degrading polymer since it is almost certainly diffusion-controlled.

SUMMARY AND CONCLUSIONS

The preceding results show that PMPA degrades thermally with a long zip length to give monomer exclusively. Transfer reactions appear to be absent. The molecular weight and rate of volatilization data are consistent with a mechanism which at first comprises initiation by random scission, depropagation by unzipping to monomer, and termination, probably by radical disproportionation. At higher conversions an element of terminal scission gains significance, and eventually predominates beyond 45% conversion. Because of the relatively low molecular weight and wide molecular weight distribution, the kinetics over the first 45% conversion are complicated, but it seems that there is a considerable measure of complete unzipping following random initiation. Beyond 45% conversion, decomposition is initiated primarily at chain ends, and the macroradicals depropagate completely to monomer.

We wish to record our appreciation to the Science Research Council for a Research Studentship (to G. P. K.), and for a grant to purchase the electrobalance.

References

1. G. G. Cameron and J. R. MacCallum, *J. Macromol. Sci.*, **C1**, 327 (1967).
2. K. Chikanishi and T. Tsuruta, *Makromol. Chem.*, **73**, 23 (1964); *ibid.*, **81**, 198 (1965).
3. H. Hopff, H. Lussi, and L. Borla, *Makromol. Chem.*, **61**, 268 (1965).
4. G. G. Cameron and G. P. Kerr, *Vacuum Microbalance Techniques*, Vol. 7, Plenum Press, New York, in press.
5. D. W. Brown and L. A. Wall, *J. Phys. Chem.*, **62**, 848 (1958).
6. H. H. G. Jellinek and H. Kachi, in *Macromolecular Chemistry, Tokyo-Kyoto, 1966* (*J. Polym. Sci. C*, **23**), I. Sakurada and S. Okamura, Eds., Interscience, New York, 1968, p. 97.
7. R. Simha and L. A. Wall, *J. Phys. Chem.*, **58**, 707 (1952).
8. R. H. Boyd, *J. Polym. Sci. A-1*, **5**, 1573 (1967).
9. H. H. G. Jellinek and M. D. Luh, *J. Phys. Chem.*, **70**, 3672 (1966).
10. G. G. Cameron and D. R. Kane, *Makromol. Chem.*, **109**, 194 (1967).
11. N. Grassie and E. M. Grant, *Europ. Polym. J.*, **2**, 255 (1966).
12. R. H. Boyd and T.-P. Lin, *J. Chem. Phys.*, **45**, 778 (1966).
13. J. Rehner, *Ind. Eng. Chem.*, **38**, 118 (1944).
14. G. G. Cameron and G. P. Kerr, *Makromol. Chem.*, **115**, 268 (1968).
15. L. A. Wall and J. H. Flynn, *Rubber Chem. Technol.*, **35**, 1157 (1962).

Received December 30, 1968

Revised March 14, 1969

Polythiazolines

YOSHIO IWAKURA, KEISUKE KURITA, and FUSAKAZU HAYANO,

Department of Synthetic Chemistry, Faculty of Engineering,

University of Tokyo, Tokyo, Japan

Synopsis

Polythioureas having pendant hydroxyl groups were prepared by the polyaddition reaction of bisaminoalcohols and diisothiocyanates. The polythioureas had inherent viscosities in the range of 0.22–1.08 dl/g and gave transparent films by solution casting. These polythioureas were converted to polythiazolines by treatment with poly(phosphoric acid) or to poly(thiazoline-oxazolines) by treatment with a mixture of poly(phosphoric acid) and a polar solvent.

INTRODUCTION

Synthesis of polymers having pendant functional groups and their derived polymers with heterocycles in the main chain is of interest in connection with improving the reactivity, thermal stability, and crystallinity of the resulting polymers.

In a preceding paper,¹ it was shown that polyamides having hydroxyl groups were prepared from bisaminoalcohols and diacid chlorides and then these polyamides were converted to polyoxazolines by dehydration. However, polyoxazolines were obtained only as hydrochlorides, and dehydrochlorination to free polyoxazolines did not succeed, since the oxazoline ring was very sensitive to alkaline hydrolysis, which changed the polyoxazolines to the starting polyamides.

In continuation of the study of polymer synthesis, 2-aminothiazoline, which was more stable than oxazoline toward alkaline hydrolysis, was chosen to prepare new polymers containing heterocycles in the main chain.

RESULTS AND DISCUSSION

Polythioureas

The bisaminoalcohols, reported previously,¹ were subjected to polyaddition reaction with *p*- and *m*-phenylene diisothiocyanates to form polythioureas having hydroxyl groups [eq. (1)].*

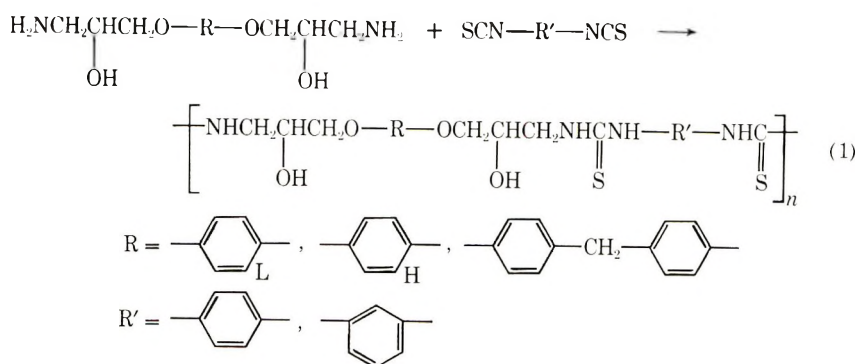
* We use subscripts H and L for the higher melting bisaminoalcohol and its derivatives and the lower melting one and its derivatives, respectively, as used in the preceding paper.¹

TABLE I
 Polythioureas

$\left[\text{NHCH}_2\text{CH}(\text{OH})\text{CHO} \rightarrow \text{R} \rightarrow \text{OCH}_2\text{CH}(\text{OH})\text{CH}_2\text{NHCNH} \rightarrow \text{R}' \rightarrow \text{NHC} \right]_n$		Yield, %	η_{inh}^a dl/g	PMT, °C ^b	Nitrogen content, %		
R	R'				Calcd	Found	
I			98	1.08	173	12.49	12.25
II			88	0.81	184	12.49	12.03
III			93	0.25	75	10.40	10.73
IV			92	0.62	80	12.49	12.87
V			91	0.57	94	12.49	12.61
VI			96	0.22	75	10.40	10.34

^a Determined at a concentration of 0.5 g/100 ml in dimethylformamide at 30°C.

^b Polymer melt temperature.

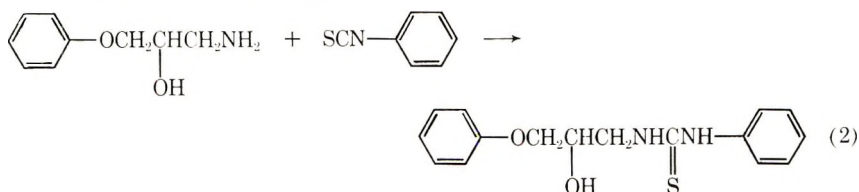


The polyaddition reaction was carried out in the usual manner of low-temperature solution polymerization with dimethyl sulfoxide as a solvent. Table I summarizes the yields, the inherent viscosities, the melting points and the analytical data of the resulting polythioureas. These polythioureas were soluble in dimethylformamide, dimethyl sulfoxide, *m*-cresol, and dichloroacetic acid and insoluble in formic acid, dioxane, toluene, and acetone. Transparent films were obtained by solution casting.

Thermogravimetric analysis of these polymers in nitrogen at a heating rate of 5°C/min showed that weight loss began at around 200°C.

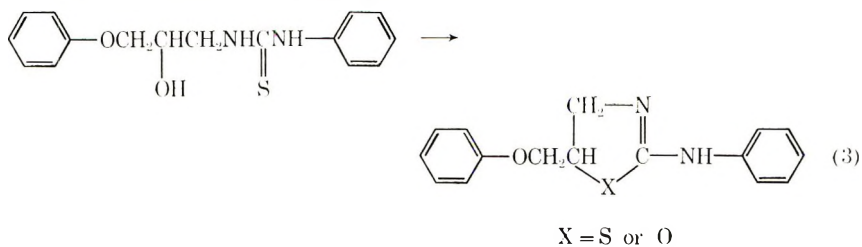
Model Compounds

To confirm the structure of the polymers and investigate the cyclization reaction of the polymers, 1-(3-phenoxy-2-hydroxypropyl)-3-phenyl-2-thiourea was prepared [eq. (2)].



Infrared spectra of both the thiourea and the polythioureas obtained above were essentially the same, and the most characteristic absorption bands were found at 3250–3300 cm⁻¹ (NH and OH stretching) and 1550–1575 cm⁻¹ (NH deformation).

By treating this thiourea with various acids, not only thiazoline but also oxazoline or a thiazoline–oxazoline mixture was formed, depending on the character of the acids used [eq. (3)].



As an authentic sample, oxazoline was prepared according to eq. (4).

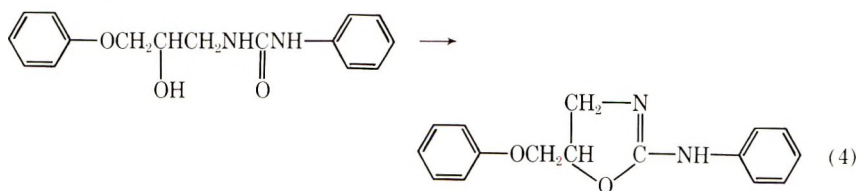
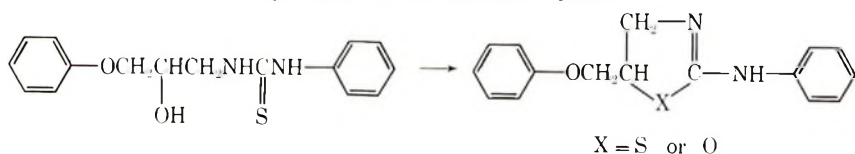


Table II summarizes the results of the cyclization of the thiourea by various acids. Infrared spectra of some of the resulting products taken in a Nujol mull or in a chloroform solution showed two characteristic absorption bands at 1635 and 1685 cm^{-1} , assignable to C=N stretching vibration of thiazoline and oxazoline, respectively, as shown in Figure 1. The picrate of this mixture also showed two bands at 1635 and 1695 cm^{-1} , characteristic of the picrates of authentic thiazoline and oxazoline, respectively. Moreover,

TABLE II
Cyclization of the Model Compound



Reaction medium ^a	Solvent ^b	Reaction temp, °C	Reaction time, hr	Yield, g ^c	Product composition, C/C ^d	
					Thia- zoline	Oxazo- line
HBr	W	130	9	0.70	98	2
HCl	W	110	5	0.75	94	6
<i>p</i> -CH ₃ C ₆ H ₄ SO ₃ H	T or D	Reflux	37	0.73	92	8
Picric acid	T, D or W	Reflux	38	0.80	0	100
BF ₃ ·OEt ₂		Reflux	7	0.75	0	100
<i>p</i> -CH ₃ C ₆ H ₄ SO ₂ Cl	P	Room temp	48	1.20	0	100
PPA		120	2	0.75	100	0
PPA-dioxane		80	8	0.89	100	0
PPA-DMAc		70	12	0.81	98	2
PPA-HMPA		80	12	0.83	95	5
PPA-NMP		75	6	0.82	85	15
PPA-DMF		70	7	0.82	73	27
PPA-pyridine		90	10	0.65	66	34

^a PPA, poly(phosphoric acid); DMAc, dimethylacetamide; HMPA, hexamethylphosphoramide; NMP, *N*-methylpyrrolidone; DMF, dimethylformamide.

^b W, water; T, toluene; D, dioxane; P, pyridine.

^c From 1.0 g of thiourea except in the case of *p*-CH₃C₆H₄SO₂Cl, where a 1.5 g sample was used.

^d Determined by a calibration curve.

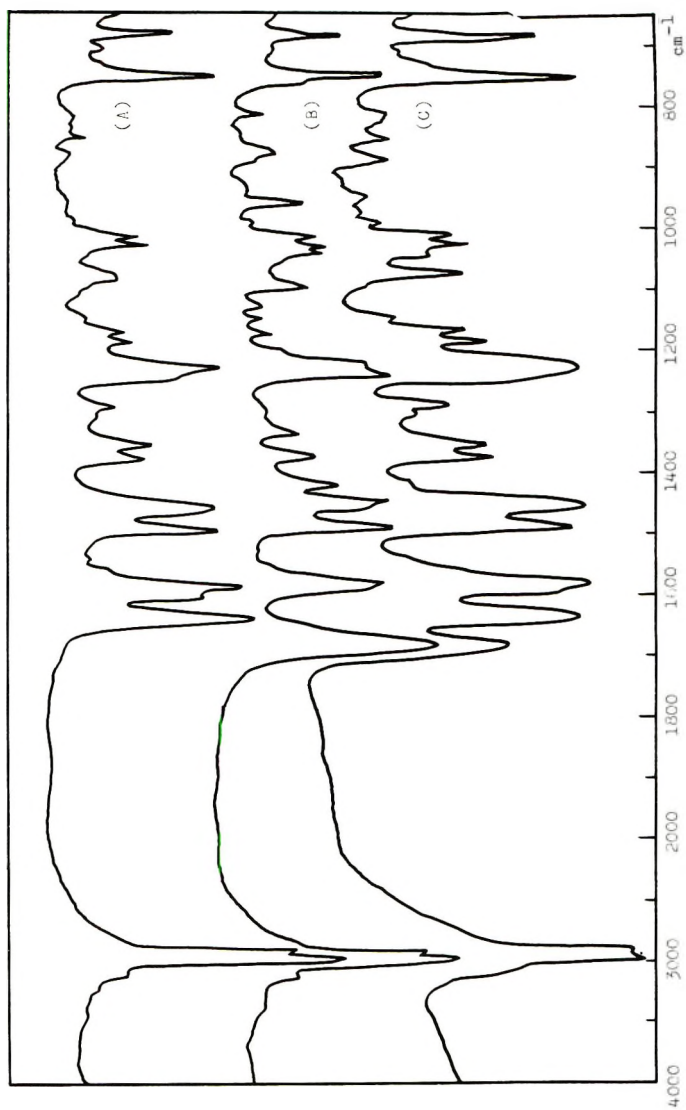


Fig. 1. Infrared spectra of the cyclization products of model compounds: (A) 5-phenoxyethyl-2-anilino-2-thiazoline; (B) 5-phenoxyethyl-2-anilino-2-oxazoline; (C) cyclization product of thiourea obtained with the use of a mixture of poly(phosphoric acid) and dimethylformamide.

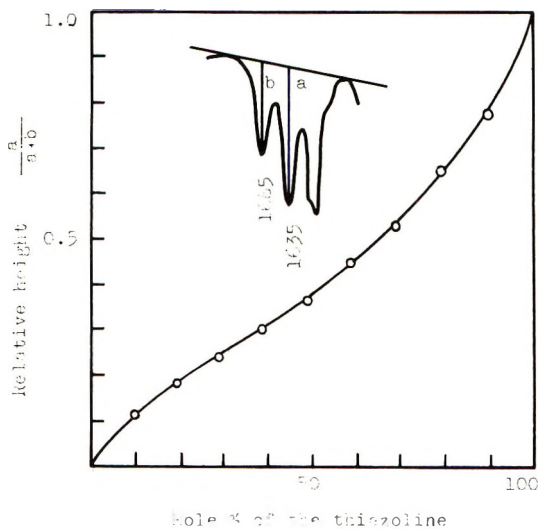


Fig. 2. Calibration curve for determining the product composition (proportion of thiazoline and oxazoline).

thiazoline was obtained pure from this mixture by fractional recrystallization from ethanol and acetone. As mentioned above, it was concluded from the infrared spectra and from fractional recrystallization that the resulting mixture contains both thiazoline and oxazoline.

The ratio of thiazoline and oxazoline products was determined by comparison of the relative height of the absorption bands at 1635 cm^{-1} of the thiazoline and at 1685 cm^{-1} of the oxazoline with a calibration curve (Fig. 2) for a mixture of authentic thiazoline and oxazoline of known composition.

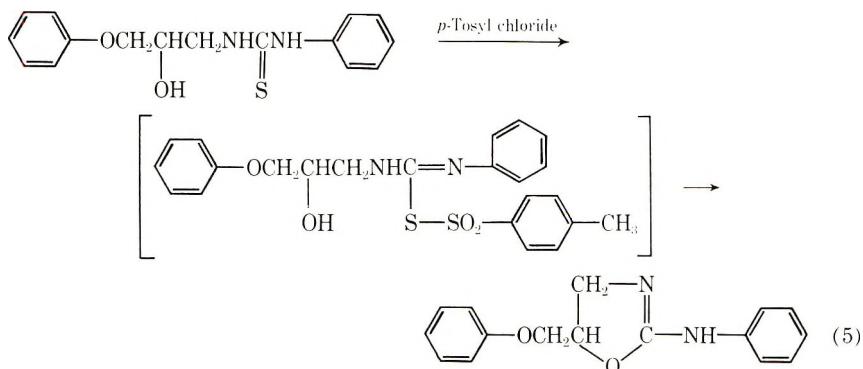
As shown in Table II, cyclization by hydrobromic or hydrochloric acid yielded the thiazoline as a major product. On the other hand, cyclization by picric acid or boron trifluoride etherate gave oxazoline as the sole product. This phenomenon seemed to be attributed to the difference in the nucleophilicity of the conjugated bases of the cyclization reagents.

With hydrobromic or hydrochloric acid, the conjugate base of which is thought to be strongly nucleophilic, nucleophilic substitution at C_2 seemed to take place, expelling the hydroxyl group; subsequently the sulfur atom of the thiourea linkage attacked the same position to give the thiazoline. However, when picric acid or a Lewis acid such as boron trifluoride etherate was used, on account of the lack in nucleophilicity, the proton or boron trifluoride probably formed a stronger complex through the sulfur atom of the thiourea linkage than through the oxygen atom of the hydroxyl group, and so cyclization might occur by attack of the oxygen atom of the hydroxyl group on the carbon atom of the thiourea linkage to give oxazoline.

This assumption was supported by another fact, namely, that cyclization by the more nucleophilic acid, hydrobromic acid, yielded a greater ratio of thiazoline than by the less nucleophilic acid, hydrochloric acid.

It is considered that cyclization by *p*-tosyl chloride presumably proceeded

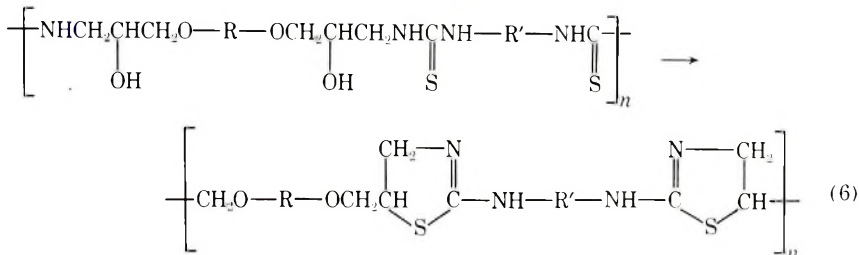
through the isothiuronium structure [eq. (5)], a route suggested by Adcock, et al.,² who prepared 2-anilino-2-oxazoline from 1-(2-hydroxyethyl)-3-phenyl-2-thiourea and methyl iodide.



The mechanism of cyclization by a mixture of poly(phosphoric acid) and a polar solvent, shown in Table II is not clear at present.

Polythiazolines

By treating the polythioureas obtained above with a mixture of poly(phosphoric acid) and dioxane, polythiazolines were obtained [eq. (6)].



Results are listed in Table III.

These polythioureas have two linkages, ether and thiourea, which are well known to undergo scission by acid. The thiourea linkage is especially apt to dissociate to amine and isothiocyanate in acid.³ However, on taking account of the inherent viscosities of the resulting polythiazolines in Table III, reduction of the values was not so great; therefore scission of the polymer main chain by acid appeared to occur only to a small extent under such a mild cyclization condition.

Cyclization by other reagents produced polymers containing both thiazoline and oxazoline rings in the main chain (Table IV):

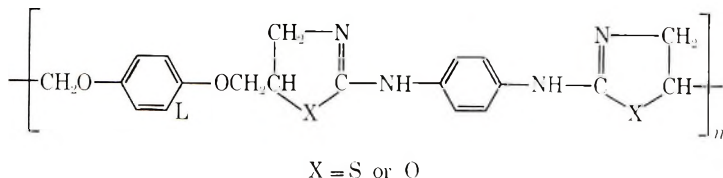


TABLE III
 Polythiazolines

$\left[\text{CH}_2\text{O}-\text{R}-\text{OCH}_2\text{CH}(\text{CH}_2-\text{N}=\text{C}(\text{NH}-\text{R}'-\text{NH})-\text{S}) \right]_n$		Reaction temp, °C	Reaction time, hr	Yield, %	$\eta_{\text{inh}}^{\text{b}}$ dl/g ^a	PMT, °C ^b	TGA, °C ^c	WR, % ^d
I		70	11	100	0.64	181	290 (250)	69
II		70	19	82	0.33	177	285 (258)	59
III		70	13	89	0.28	170	274 (258)	64
IV		70	17	74	0.28	170	265 (246)	43
V		70	17	93	0.36	173	264 (246)	52
VI		70	13	67	0.26	168	275 (252)	63

^a Determined at a concentration of 0.5 g/100 ml in dichloroacetic acid at 30°C.

^b Polymer melt temperature.

^c Temperature at which rapid weight loss was observed (at which weight loss began) in thermogravimetric analysis (5°C/min, in N₂).

^d Weight residue at 500°C in thermogravimetric analysis (5°C/min, in N₂).

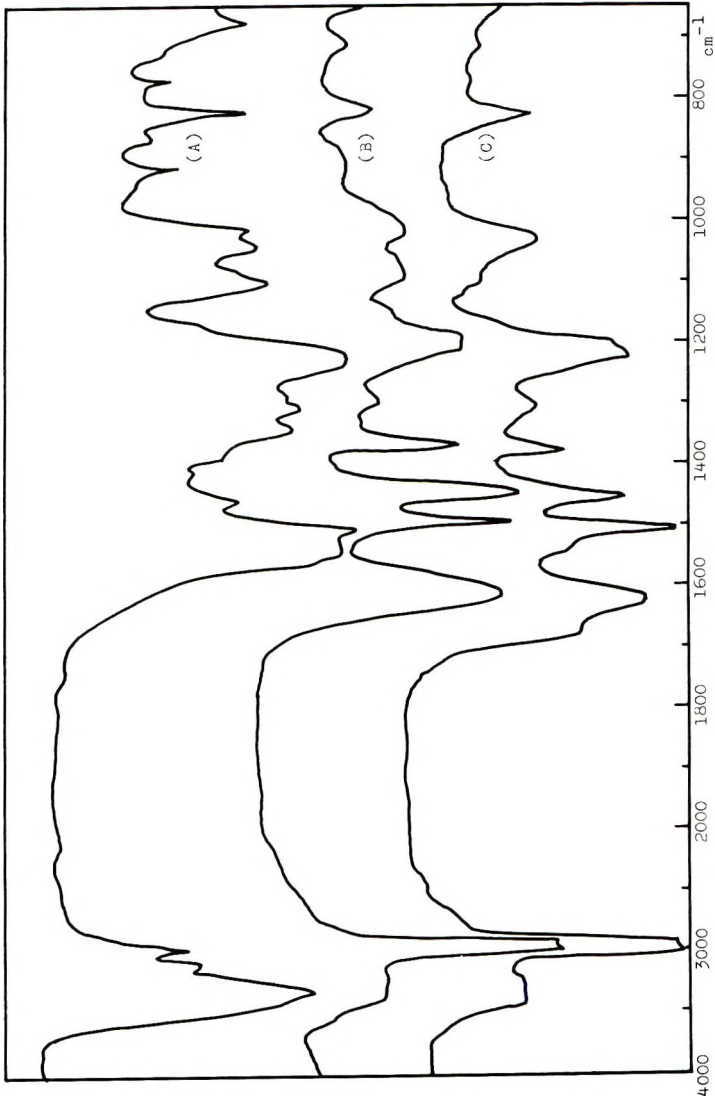
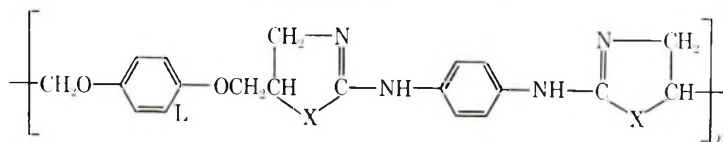


Fig. 3. Infrared spectra of the polymers: (A) polythiourea I (film); (B) polythiazoline I (Nujol mull); (C) poly(thiazoline-oxazoline) cyclized by a mixture of poly(phosphoric acid) and dimethylformamide (Nujol mull).

TABLE IV
 Poly(thiazoline-oxazoline)


X = S or O

Reaction medium	Poly-thiourea, g	Reaction temp, °C	Reaction time, hr	Yield, g	η_{inh} , dl/g ^a	Infrared absorption, cm ⁻¹ ^b
PPA	1.0	85	32	0.72	0.27	1625 (s)
PPA-dioxane	1.0	70	11	0.92	0.64	1625 (s)
PPA-DMAc	1.0	80	10	0.85	0.37	1625 (s), 1670 (w)
PPA-NMP	1.0	100	6	0.78	0.27	1625 (s), 1670 (w)
PPA-DMF	1.0	50	6	0.87	0.69	1625 (s), 1670 (m)
PPEt ^c -DMF	1.0	80	6	0.52	0.17	1625 (s), 1670 (m)
HCl (aq)	1.0	110	2	0.66	0.22	1625 (s), 1670 (m)
HCl(aq)-dioxane	1.0	110	4	0.50	0.30	1625 (s), 1670 (m)

^a Determined at a concentration of 0.5 g/100 ml in dichloroacetic acid at 30°C.

^b In a Nujol mull; (s) strong, (m) middle, (w) weak.

^c Ethyl ester of poly(phosphoric acid) prepared from phosphorus pentoxide and ethyl ether.

Figure 3 shows the infrared spectra of polythiazoline and poly(thiazoline-oxazoline). An absorption band at 1625 cm⁻¹ appearing in both spectra is the most characteristic of the polythiazoline, and an additional band at 1670 cm⁻¹ indicates the presence of oxazoline ring as well as thiazoline ring in the main chain.

The polythiazolines and poly(thiazoline-oxazolines) obtained here were soluble only in dichloroacetic acid and insoluble in other usual organic solvents. Films were cast from dichloroacetic acid solution; however, they were rather brittle.

Thermogravimetric analysis of these polythiazolines examined in nitrogen at the heating rate of 5°C/min showed that the initial weight loss occurred at about 250°C, and the weight residue at 500°C was about 60%.

The x-ray diffraction diagrams obtained by the powder method with the use of nickel-filtered CuK α radiation showed that all the polythioureas, polythiazolines, and poly(thiazoline-oxazolines) were amorphous.

EXPERIMENTAL

Polythiourea I

To a solution of 10.0 g (0.039 mole) of 1,1'-*p*-phenylenedioxybis(3-amino-2-propanol) (L) in 100 ml of dimethyl sulfoxide was added a solution of 7.5 g (0.039 mole) of *p*-phenylene diisothiocyanate in 20 ml of tetrahydro-

furan at 10°C. After stirring the mixture for 1 hr at room temperature, the product was precipitated by pouring the viscous solution into 3 l. of chloroform. The polymer was obtained as white fibrous material and weighed 17.1 g (98%). The inherent viscosity was 1.08 dl/g, determined at a concentration of 0.5 g/100 ml in dimethylformamide at 30°C.

1-(3-Phenoxy-2-hydroxypropyl)-3-phenyl-2-thiourea

To a solution of 3.34 g (0.02 mole) of 1-amino-3-phenoxy-2-propanol in 20 ml of methanol was added 2.70 g (0.02 mole) of phenyl isothiocyanate dropwise over a period of 3 min. The mixture was stirred at room temperature for 1 hr and the solvent was evaporated under reduced pressure. The residual white solid was recrystallized from 200 ml of toluene to give 5.4 g (90%) of the product, mp 142–143.5°C.

ANAL. Calcd for $C_{16}H_{18}O_2N_2S$: C, 63.55%; H, 6.00%; N, 9.26%; S, 10.60%. Found: C, 63.46%; H, 5.96%; N, 9.10%; S, 10.60%.

1-(3-Phenoxy-2-hydroxypropyl)-3-phenylurea

This compound was prepared by the same method described in a preparation of the thiourea.

From 6.68 g (0.04 mole) of 1-amino-3-phenoxy-2-propanol in 60 ml of dry dioxane and 4.76 g (0.04 mole) of phenyl isocyanate was obtained an almost quantitative yield of the crude urea, which after recrystallization from 500 ml of toluene yielded 8.0 g (70%) of the product, mp 146–147°C.

ANAL. Calcd for $C_{16}H_{18}N_2O_3$: C, 67.11%; H, 6.34%; N, 9.78%. Found: C, 67.01%; H, 6.12%; N, 9.82%.

Cyclization of the Thiourea

By a Mixture of Poly(phosphoric Acid) and Dioxane. To 1.0 g (0.0033 mole) of the thiourea was added 7 ml of dioxane and 7 g of poly(phosphoric acid) (P_2O_5 content, 84%). After stirring for 8 hr at 80°C, the mixture was poured into 100 ml of 2*N* sodium hydroxide at 0°C. The precipitated oil soon solidified. The product was collected by filtration and weighed 0.89 g (95%). Recrystallization from a mixture of toluene and *n*-hexane gave white crystals, mp 129–131°C.

ANAL. Calcd for $C_{16}H_{16}N_2SO$: C, 67.58%; H, 5.67%; N, 9.85%; S, 11.27%. Found: C, 67.30%; H, 5.77%; N, 9.55%; S, 11.02%.

By a Mixture of Poly(phosphoric Acid) and Dimethylformamide. The thiourea, 1 g (0.0033 mole), was treated with a mixture of 7 ml of dimethylformamide and 7 g of poly(phosphoric acid) at 70°C for 7 hr. The product was isolated as described above and weighed 0.82 g. This product consisted of 73% of thiazoline and 27% of oxazoline, determined by the calibration curve. Fractional recrystallization from a mixture of ethanol and acetone gave 0.29 g of pure thiazoline and 0.35 g of a mixture containing 45% of thiazoline and 55% of oxazoline.

By Picric Acid. A solution of 1 g (0.0033 mole) of the thiourea and 1 g (0.0044 mole) of picric acid in 10 ml of dioxane was refluxed for 30 hr. The solvent was removed mostly under reduced pressure and the residual viscous oil was poured into 200 ml of 2*N* sodium hydroxide and extracted with toluene. The extract was dried over sodium sulfate and concentrated under reduced pressure to give 0.80 g (90%) of 5-phenoxyethyl-2-anilino-2-oxazoline.

By Boron Trifluoride Etherate. The thiourea, 1 g (0.0033 mole), was refluxed with 10 ml of freshly distilled boron trifluoride etherate for 7 hr. After cooling to room temperature, the solution was added gradually to 200 ml of 2*N* sodium hydroxide at 0°C. Extraction with toluene, drying, and removal of solvent under reduced pressure gave 0.75 g (85%) of the oxazoline.

By *p*-Tosyl Chloride. To a solution of 1.5 g (0.005 mole) of the thiourea in 7 ml of dry pyridine was added 0.95 g (0.005 mole) of *p*-tosyl chloride. The mixture was allowed to stand at room temperature for 2 days and poured into 200 ml of 2*N* sodium hydroxide and extracted with chloroform. The dried chloroform extract, on evaporation under reduced pressure, gave 1.20 g (90%) of the oxazoline.

5-Phenoxyethyl-2-anilino-2-oxazoline

This compound was obtained by treating 1-(3-phenoxy-2-hydroxypropyl)-3-phenylurea with a mixture of poly(phosphoric acid) and dioxane according to the same procedure as used to prepare the thiazoline from the thiourea. The yield was 73%. Recrystallization from cyclohexane gave white crystals, mp 111–113°C.

ANAL. Calcd for $C_{16}H_{16}N_2O_2$: C, 71.62%; H, 6.01%; N, 10.44%. Found: C, 71.90%; H, 6.09%; N, 10.57%.

Polythiazoline II

To 1 g of polythiourea II was added 10 ml of dioxane and 10 g of poly(phosphoric acid) and by stirring the mixture at 70°C, the polythiourea went into solution gradually. The stirring was continued for 19 hr; after the solution was cooled to room temperature, it was poured into 200 ml of ice-cooled 2*N* sodium hydroxide. The polythiazoline was precipitated as fine fibrous or powdery material and was collected by filtration after centrifugation and washed well with water. A white polymer was obtained in a 82% yield. The inherent viscosity was 0.33 dl/g, determined at a concentration of 0.5 g/100 ml in dichloroacetic acid at 30°C.

The experimental value of the elemental analysis of polythiazoline was not in good agreement with the calculated value, since a residue was apt to remain at higher temperature.

ANAL. Calcd for $(C_{20}H_{20}N_4S_2O_2)_n$: C, 58.23%; H, 4.89%; N, 13.58%. Found: C, 56.47%; H, 5.43%; N, 11.62%.

Poly(thiazoline-oxazoline)

An example of the synthesis of a poly(thiazoline-oxazoline) was as follows. Treating 1 g of polythiourea I with a mixture of 10 g of poly(phosphoric acid) and 10 ml of dimethylformamide gave 0.87 g of poly(thiazoline-oxazoline). The inherent viscosity was 0.69 dl/g, determined at a concentration of 0.5 g/100 ml in dichloroacetic acid at 30°C.

References

1. Y. Iwakura, S. Izawa, F. Hayano, and K. Kurita, *Makromol. Chem.*, **104**, 66 (1967).
2. B. Adcock, A. Lawson, and D. H. Miles, *J. Chem. Soc.*, **1961**, 5120.
3. S. J. Assony, in *Organic Sulfur Compounds*, Vol. 1, N. Kharasch, Ed., Pergamon Press, Oxford, 1961, p. 330.

Received February 25, 1969

Revised March 25, 1969

Relation of the Chemical Structure of Polycyanurates to Thermal and Mechanical Properties

YOSHIRO NAKAMURA, KUNIO MORI,
KOSAKU TAMURA, and YOSHIKO SAITO,

Department of Applied Chemistry, Iwate University, Morioka, Japan

Synopsis

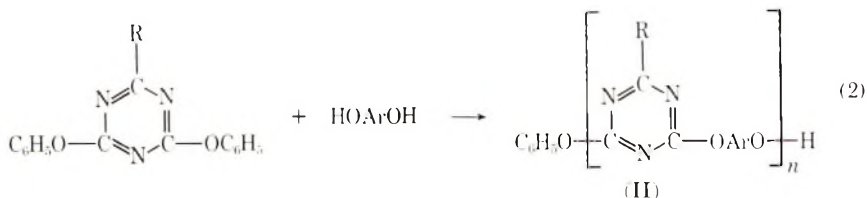
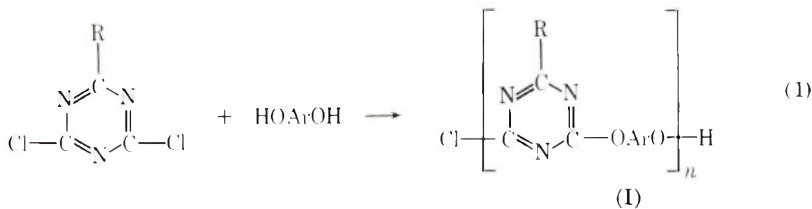
Forty polycyanurates were prepared by the interfacial polycondensation of 2-substituted 4,6-dichloro-*s*-triazines with various aromatic diols. Nitrobenzene was used as a solvent, aqueous sodium hydroxide as an acid acceptor, and a cationic emulsifier as an accelerator. The rate of reaction was largely increased by ultrasonic irradiation. The polymer yield was in the range 57–91%, and the reduced viscosity was 0.41–3.5. The polymers were soluble in chloroform, nitrobenzene, and *o*-dichlorobenzene but insoluble in common organic solvents such as alcohol, acetone, and hydrocarbons. A clear film was obtained from the chloroform-soluble polymers after evaporation of the solvent. The softening temperature and the thermal stability of each polycyanurate was significantly related to the substituent on the *s*-triazine nucleus as well as to the diol component in the molecular chain. Polymers of favorable properties were derived from 2-substituted 4,6-dichloro-*s*-triazines with R = $-\text{C}_6\text{H}_5$, $-\text{N}(\text{C}_6\text{H}_5)_2$, $-\text{N}(\text{C}_6\text{H}_{11})_2$, $-\text{N}(\text{C}_6\text{H}_5)(\text{SO}_2\text{C}_6\text{H}_4\text{CH}_3)$, or carbazyl and aromatic diols such as 4,4'-dihydroxybenzophenone, Bisphenol A, or phenolphthalein. These polymers showed tensile strength of 500–670 kg/cm², elongation at break of 2.9–6.0%, and a minor weight loss at 300–350°C.

INTRODUCTION

Attempts have been made in recent years by several investigators to prepare polycyanurates having the structure I or II by differing methods of preparation.

Audebert^{1,2} reported the synthesis of polycyanurates of structure I from 2-piperidyl-, 2-phenyl-, or 2-methoxy-4,6-dichloro-*s*-triazine and Bisphenol A in Decalin by heating at 150–200°C for 90 hr in the presence of sodium carbonate as a hydrogen chloride acceptor. Polycyanurates of low molecular weight were prepared by Korshak³ and Murave'ov⁴ from cyanuric chloride or 2-diphenylamino-4,6-dichloro-*s*-triazine and Bisphenol A or its derivatives in ditolylmethane by heating in the presence of tin at 180–240°C for 12–24 hr in an inert atmosphere. Preparation of insoluble polycyanurates was reported by Saunders⁵ from cyanuric chloride or 2-phenyl-4,6-dichloro-*s*-triazine and resorcinol, hydroquinone, 4,4'-dihydroxybiphenyl, or Bisphenol A. In this case, the interfacial polycondensation procedure was followed, with benzene, chloroform, chlorobenzene,

trichloroethane, or diphenyl ether as the solvent and aqueous sodium hydroxide as the acid acceptor.



In our continuing work⁶ on the preparation of polycyanurates according to the eqs. (1) and (2) by interfacial polycondensation with stirring or by a high-temperature ester exchange method, polycyanurates of high molecular weight were synthesized which can serve for the study of thermal and mechanical properties. The best results were obtained in the system consisting of nitrobenzene, aqueous sodium hydroxide, and cationic emulsifier.

In this paper, syntheses and properties of forty polycyanurates so far prepared are reported, and the relation of chemical structure to the thermal and mechanical properties of the polycyanurates are discussed.

EXPERIMENTAL

2-Substituted 4,6-Dichloro-*s*-triazines

N-Substituted 2-amino-4,6-dichloro-*s*-triazines, 2-alkoxy-4,6-dichloro-*s*-triazines, and 2-alkyl or 2-phenyl-4,6-dichloro-*s*-triazines were prepared by the modification of the methods of Thurston,⁷ Lundberg⁸ and Hirt,⁹ respectively. Details of dichloro-*s*-triazines used are listed in Tables I and II.

Polycondensation

Procedure A. Into a 100-ml three-necked flask equipped with a stirrer, a condenser, and a thermometer, was taken 0.001 mole 2-substituted 4,6-dichloro-*s*-triazine and nitrobenzene. Aromatic diol (0.001 mole) in sodium hydroxide solution (0.002 mole) and a cationic emulsifier (Cation AB, Nihonyushi Co., Japan) were rapidly added to the dichloride solution at the indicated temperature with vigorous stirring. The mixture was stirred for the period indicated and was then neutralized with dilute hydrochloric acid. After decanting the aqueous phase, the polymer solution

was poured into excess acetone. The polymer was collected by filtration, washed well with water and acetone, and dried.

Procedure B. A solution of 2-R-4,6-dichloro-*s*-triazine (0.001 mole) and aromatic diol (0.001 mole) in nitrobenzene was placed in a 100-ml. three-necked flask, and held at the first temperature of each pair as indicated in Table I. Sodium hydroxide solution (0.001 mole) saturated with sodium chloride and the cationic emulsifier were rapidly added to the solution with vigorous stirring. The mixture was then stirred at the same temperature until the pH dropped to about 7. The temperature was then raised as indicated in Table I (second temperature of pair), and sodium hydroxide solution (0.001 mole) saturated with sodium chloride was added. The mixture was stirred until the pH dropped to about 7. The reaction time required is listed in Table I. The polymer was collected by the same procedure as in A.

Procedure C. The procedure was similar to procedure B but sodium chloride was not used.

Analysis and Measurement

The softening temperature of the polymers was measured on a copper block. Viscosity was measured in an Ostwald viscometer at 30°C with the polymer solution in chloroform; in the case of chloroform-insoluble polymers, *o*-dichlorobenzene or nitrobenzene was used as the solvent.

Tensile strength and elongation at break were determined with a recording Autograph P-100 at a drawing rate of 5 mm/min at 20°C. Zero-strength temperature and elongation were measured with Toyoseiki tensile heat distortion apparatus (ASTM D1637-59T) under the specified stress of 100 kg/cm² at a heating rate of 2°C/min. Thermogravimetric analysis (TGA) was performed for 100 mg of powdered polymers at a heating rate of 5°C/min in the air.

RESULTS AND DISCUSSION

Optimum Conditions of Interfacial Polycondensation

In our earlier papers,⁶ factors influencing the synthesis of polycyanurates of high molecular weight were studied. The variables examined were reaction temperature, concentration and equivalence of reactants, variation of acid acceptors, accelerators (emulsifiers), and solvents, and the method of reactant addition. Most of the variables also tested in the preparation of new polycyanurates are listed in Table I, which illustrates the optimum conditions for the interfacial polycondensation of typical polycyanurates of favorable properties.

Influence of Ultrasonic Irradiation on Interfacial Polycondensation

Figure 1 shows the influence of ultrasonic irradiation on the rate of polycondensation of 2-diphenylamino-4,6-dichloro-*s*-triazine and Bisphenol

TABLE I
Optimum Conditions of Polycondensation of Typical 2-Substituted 4,6-dichloro-s-triazines and Bisphenol A^a

R	2-R-4,6-dichloro-s-triazine		Solvent (nitro- benzene), ml	Aqueous NaOH		Emulsifier (Cation AB), ml	Temp, °C	Time, hr	Pro- cedure	Yield, %	η_{sp}/c^b
	Bp, °C/mm.Hg or mp, °C	Vol, ml		Vol, ml	%						
Cl	144-145	10.0 ^b	6.5	2.5	0.1	7	5	A	92	0.73	
CH ₃	96-98 ^c	3	3 ^d	2.7	0.2	15	5	A	66	0.60	
C ₂ H ₅	92/13	4.5	3	1.8	0.3	17	5	A	64	0.41	
n-C ₄ H ₉	110/13	3	3	2.7	0.3	17	5	A	75	0.96	
n-C ₈ H ₁₇	106/0.07	3	3	2.7	0.3	7	5	A	77	0.40	
C ₆ H ₅	120	{ 10.0 ^b 1.25	13	1.25	0.3	6	0.5	B	72	2.58 ^e	
O(n-C ₈ H ₁₇)	66/0.1	3	2	10.0	0.2	15	4	A	79	0.59	
O(i-C ₃ H ₇)	45/0.07	3	2	2.7	0.5	7	5	A	57	0.58	
O(CH ₂ CH=CH ₂)	75/0.2	10.0 ^b	6.5	2.5	0.2	6	7	A	84	1.29	
OCH ₂ C≡CH	40-41	4.5	3	1.8	0.3	15	5	A	81	0.49 ^o	
OCH ₂ CHClCH ₂	62-63	9 ^c	6	1.8	0.6	6	2	A	71	1.91	
O(CH ₂ CH ₂ OEt)	101/0.15	3	3	2.7	0.2	17	5	A	68	1.45	
O(CH ₂ CH ₂ OBu)	118/0.03	3	3	2.7	0.2	17	5	A	71	1.55	
O(CH ₂ CH ₂ OC ₆ H ₅)	155/0.16	3	3	2.7	0.3	17	6	A	74	0.75	
O(CH ₂ CH ₂ O) ₂ Et	120/0.1	3	3	2.7	0.2	7	5	A	80	1.15	
O(CH ₂ CH ₂ O) ₂ Bu	125/0.12	3	2	2.7	0.2	7	5	A	68	1.13	
O(CH ₂ CH ₂ O) ₂ Bu	131/0.16	3	3	2.7	0.3	7	5	A	67	0.40	

N ₃ (C ₆ H ₅) ₃ ^a	61-62	2	8	1	0.4	7	5	A	78	1.73
N(C ₆ H ₅) ₃ ^b	77-78	7.5	7.5 ^b	3.3	0.2	80	5	A	70	1.03
N(<i>m</i> -C ₆ H ₇) ₂	57-59	3	6 ^c	2.7	1	70	5	A	89	1.09
N(CH ₂ CH=CH ₂) ₂	43-44	6	{ 5.0 ^b 1.3	2.5	0.2	50	0.5	B	78	1.54
			{ 1.3	10.0		80				
N(CH ₂ CH ₂ CN) ₂	212-215	3	3	2.7	0.3	70	5	A	80	0.74 ^c
N(CH ₂) ₅	91-92	8	{ 8.0 ^b 2.5	1.6	0.3	40	1.5	C	81	0.83
			{ 9 ^b 4.5	5.0		80	4			
N(C ₆ H ₅) ₂	172-173	9	9 ^b	2.8	0.3	50	5	A	91	1.17
N(C ₆ H ₁₁) ₂	173-174	3	4.5	1.8	0.3	95	3	A	91	0.56
N(C ₆ H ₅)(CH ₂ C ₆ H ₅)	99-100	2	3	2.7	0.3	50	5	A	86	1.30
N(CH ₂ C ₆ H ₅) ₂	116-118	3	{ 2.23 0.77	1.8	0.3	40	1	C	90	0.70
			{ 16.0 0.4	5.0	0.2	70	4			
Carbazyl-N	238	16	{ 16.0 3.0	0.25	0.4	50	0.25	B	82	Insol.
			{ 0.4 1.33	10.0		80	4			
N(C ₆ H ₅)(SO ₂ C ₆ H ₄ CH ₃)	223	4	3.0	1.33	0.2	7	0.5	B	85	3.52
			0.4	10.0		35	5			
N(C ₆ H ₅)(C ₁₂ H ₂₅)	45-46	3	{ 3.0 1.5	1.35	0.3	35	0.5	C	89	0.15
			{ 1.5	2.5	0.15	70	5			
N(C ₆ H ₅)(β-naphthyl)	152-153	3	4.5	1.8	0.45	50	6	A	78	0.24

^a 0.001 mole of 2-substituted 4,6-dichloro-s-triazine and bisphenol A were taken.

^b In this run, 0.003 mole of each reactant.

^c In sealed tube.

^d CH₂Cl₂ solvent.

^e In *o*-Cl₂C₆H₄.

^f In this run, 0.002 mole of each reactant.

^g In NO₂C₆H₅.

^h = 0.5 g/100 ml.

TABLE II
 Properties of Polycyanurates

No.	R	Bisphenol A	η_{sp}/c	Softening temp, °C	T_g , °C ^a	T_g , °C ^b	T_g , °C ^c	E_{10} , % ^d	Tensile strength, kg/cm ²	Elongation at break, %
1	Cl	HOArOH	0.54	140-200	140	95	95	0	432	3.5
2	CH ₃	"	0.60	255	330	128	160	130	480	4.0
3	C ₂ H ₅	"	0.41	225	340	129	129	36	520	5.3
4	<i>n</i> -C ₄ H ₉	"	0.96	154	310	e	e	e	e	e
5	<i>n</i> -C ₈ H ₁₇	"	0.40	106	280	e	180	60	500	5.5
6	C ₆ H ₅	"	2.58 ^f	300	365	179	85	30	495	3.6
7	OCH ₃	"	1.58	250	290	e	85	30	495	3.6
8	O(<i>n</i> -C ₃ H ₇)	"	0.59	240	305	e	100	33	682	7.5
9	O(<i>t</i> -C ₃ H ₇)	"	0.58	220	230	100	100	33	682	7.5
10	OCH ₂ CH=CH ₂	"	1.29	280	280	120	235	300	437	5.0
11	OCH ₂ C≡CH	"	0.49 ^f	230	260	e	e	e	e	e
12	OCH ₂ CHCH ₃	"	1.91	260	260	87	102	400	722	6.1
13	OCH ₂ CH ₂ OEt	"	1.45	158	270	97	110	390	567	11.5
14	OCH ₂ CH ₂ OBu	"	1.55	144	270	62	78	365	465	17.0
15	OCH ₂ CH ₂ OPh	"	0.75	154	280	66	70	118	560	6.8
16	O(CH ₂ CH ₂ O) ₂ Et	"	1.15	110	260	60	83	578	485	15.3
17	O(CH ₂ CH ₂ O) ₂ Bu	"	1.13	105	260	33	41	165	397	17.8
18	O(CH ₂ CH ₂ O) ₃ Bu	"	0.40	89	260	e	e	e	e	e
19	OC ₆ H ₅	"	0.80	180	175	e	e	e	e	e
20	N ₃	"	1.73	g	155	e	e	e	e	e
21	N(C ₂ H ₅) ₂	"	1.03	248	320	105	110	45	506	4.1
22	N(<i>n</i> -C ₃ H ₇) ₂	"	1.09	228	330	118	132	188	644	5.0
23	N(<i>i</i> -C ₃ H ₇) ₂	"	0.40	245	320	e	e	e	e	e
24	N(CH ₂ CH=CH ₂) ₂	"	1.54	247	230	149	210	473	542	2.3
25	N(CH ₂ CH ₂ CN) ₂	"	0.74 ^h	248	295	125	152	276	538	3.3
26	N(CH ₂) ₅	"	0.83	268	240	123	130	597	597	4.2
27	N(C ₆ H ₅) ₂	"	1.17	275	360	205	207	55	595	6.0
28	N(C ₆ H ₁₁) ₂	"	0.56	290	330	180	190	80	425	4.7

29	$\text{N} \begin{array}{l} \diagup \text{C}_6\text{H}_5 \\ \diagdown \end{array}$	1.30	252	310	130	144	263	487	4.5
30	$\text{N} \begin{array}{l} \diagup \text{CH}_2\text{C}_6\text{H}_5 \\ \diagdown \text{C}_6\text{H}_5 \end{array}$	0.70	173	330	100	105	31.5	556	5.5
31	$\text{N} \begin{array}{l} \diagup \beta\text{-naphthyl} \\ \diagdown \text{N}(\text{C}_6\text{H}_5)(\text{C}_{12}\text{H}_{25}) \end{array}$	0.24	225	390	e				
32	$\text{N}(\text{C}_6\text{H}_5)(\text{C}_{12}\text{H}_{25})$	0.15	85	370	e				
33	Carbazyl-N C_6H_5	i	340	375	e				
34	$\text{N} \begin{array}{l} \diagup \text{SO}_2\text{C}_6\text{H}_4\text{CH}_3 \\ \diagdown \end{array}$	3.52	275	275	140	180	420	560	3.8
35	Hydroquinone	1.09 ^h	>360	360	e				
36	4,4'-Dihydroxy-diphenyl	0.80 ^h	310-320	180	e				
37	4,4'-Dihydroxy-diphenylmethane	0.78	255	350	175	180	30	518	4.5
38	4,4'-Dihydroxy-benzophenone	0.83	340	330	180	205	43	480	2.9
39	4,4'-Dihydroxy-diphenylsulfone	0.37 ^f	303	320	e				
40	Phenolphthalein	0.68	325	330	>250	>250	>18	669	5.8

^a Temperature at which weight loss begins.

^b Temperature at which heat-distortion begins under the specified stress of 100 kg/cm².

^c Temperature at which breaking occurs under the specified stress of 100 kg/cm².

^d Elongation at T_0 .

^e Film could not be obtained.

^f In $o\text{-Cl}_2\text{C}_6\text{H}_4$.

^g Infusible.

^h In $\text{NO}_2\text{C}_6\text{H}_5$.

ⁱ Insoluble.

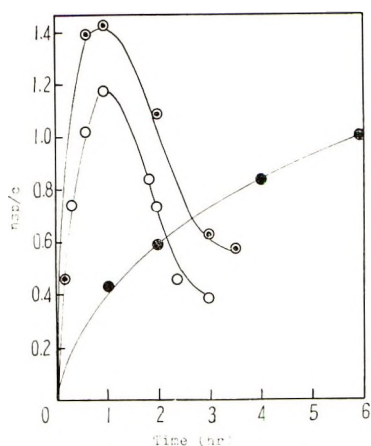


Fig. 1. Effect of ultrasonic irradiation on the polycondensation of 2-diphenylamino-4,6-dichloro-*s*-triazine and Bisphenol A: (●) no irradiation, 0.2 ml cationic emulsifier; (⊙) 1.2 Mcps irradiation, 0.08 ml cationic emulsifier; (○) 400 kcps irradiation, 0.08 ml cationic emulsifier. Procedure A was followed, with the use of 0.001 mole reactants, 3 ml nitrobenzene, 3 ml aqueous NaOH (0.002 mole) and the indicated volume of cationic emulsifier at 60°C.

A by procedure A. The rate is increased in the presence of a smaller amount of emulsifier than that required in the method without irradiation. Ultrasonic waves of the frequency of 400 kcps and 1.2 Mcps are both effective. However, a longer reaction time depresses the molecular weight of polycyanurates by the shearing force of the ultrasonic wave. No attempts to obtain the polycyanurate in the absence of emulsifier by using the ultrasonic irradiation have been successful.

Properties of Polycyanurates

Table II summarizes the properties of the forty polycyanurates. The polymers are white powders soluble in chloroform, nitrobenzene, and *o*-dichlorobenzene, but insoluble in common organic solvents such as alcohol, acetone, and hydrocarbons. The chloroform-soluble polymers form clear films after evaporation of the solvent. Elemental analyses and infrared spectra⁶ show that the process of polycondensation and the structure of polymers are as proposed before.

From the data in Table II, the relation of the chemical structure of substituent R or aromatic nucleus in the molecular chain to the thermal and mechanical properties of polycyanurates can be discussed.

Softening Temperature. The softening temperature of polycyanurates of lower molecular weight is closely related to molecular weight. However, after a certain size of molecule is reached, there is very little increase in the softening temperature with the increase in the size of the molecule (Fig. 2).

The structure of the aromatic nucleus in the molecular chain and of the substituent R on the *s*-triazine nucleus greatly affects the softening temper-

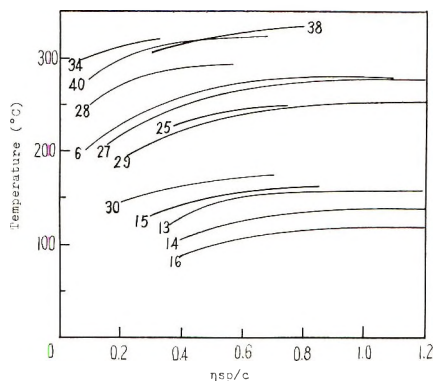


Fig. 2. Relation between η_{sp}/c and the softening temperature of polycyanurates. Numbers refer to polymers in Table II.

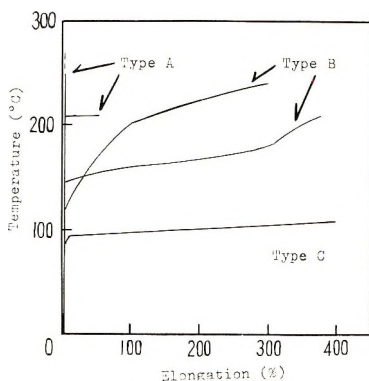


Fig. 3. Tension-heat distortion curves for polycyanurates heated at a heating rate of $2^{\circ}\text{C}/\text{min}$ under a stress of $100\text{ kg}/\text{cm}^2$ in air.

ature. The high softening temperature of polycyanurates from Bisphenol A is apparently related to the rigid aromatic nucleus or to polar substituents such as nitrile group. Substituents which cause a marked increase in the softening temperature are $-\text{C}_6\text{H}_5$, $-\text{N}(\text{C}_6\text{H}_5)_2$, $-\text{N}(\text{C}_6\text{H}_{11})_2$, $-\text{N}(\text{C}_6\text{H}_5)$ ($\text{SO}_2\text{C}_6\text{H}_4\text{CH}_3$), or carbazyl. Polycyanurates obtained from polar aromatic diols as 4,4'-dihydroxydiphenylsulfone, 4,4'-dihydroxybenzophenone, or phenolphthalein also have higher softening temperature than those from Bisphenol A. On the other hand, polycyanurates having flexible side chains such as $-\text{CH}_2(\text{CH}_2\text{OCH}_2)_n\text{CH}_2\text{OC}_m\text{H}_{2m+1}$ show a considerable decrease in the softening temperature with the increase in n and m as illustrated in Figure 2.

Tension-Heat Distortion Curve. Tension-distortion curves from the various polycyanurates are classified into three types A, B, and C as shown in Figure 3.

Type A shows considerably high zero-strength temperature and low distortion. Polycyanurates having a rigid aromatic nucleus in the molec-

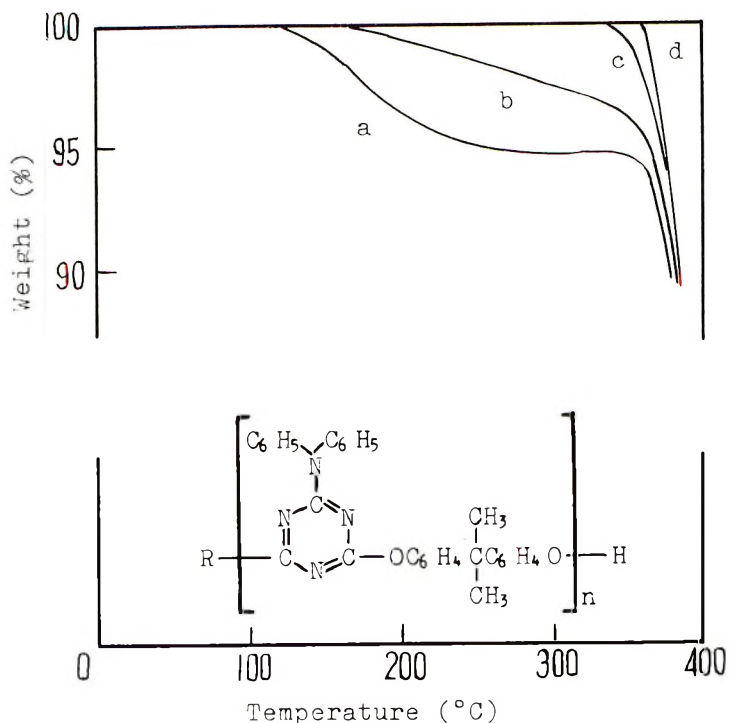


Fig. 4. Effect of the end group R of polycyanurates on the temperature at which weight loss begins: (a) $\eta_{sp}/c = 0.53$, R = Cl; (b) $\eta_{sp}/c = 0.60$, R = $\text{OC}_6\text{H}_4\text{—C}(\text{CH}_3)_2\text{C}_6\text{H}_4\text{OH}$; (c) $\eta_{sp}/c = 0.63$, R = $\text{N}(\text{C}_6\text{H}_5)_2$; (d) $\eta_{sp}/c = 1.53$, R = Cl.

ular chain such as 4,4'-dihydroxybenzophenone and phenolphthalein and such side chains as $\text{—C}_6\text{H}_5$, $\text{—N}(\text{C}_6\text{H}_5)_2$, and $\text{—N}(\text{C}_6\text{H}_{11})_2$ belong to this. Type B shows the beginning of heat distortion at a low temperature but an excellent thermal stability to break at elevated temperature due to the thermal crosslinking or to the presence of polar substituents. Examples are

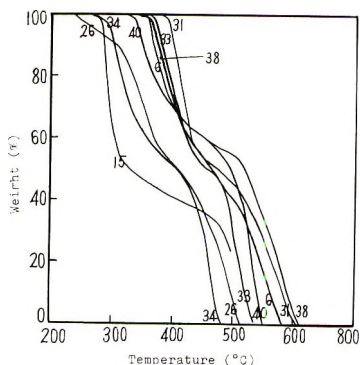


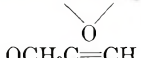
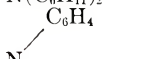

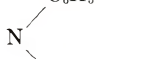
Fig. 5. TGA curves of typical polycyanurates heated in air. Heating rate, $5^\circ\text{C}/\text{min}$; 100 mg powdered sample was used in each run. Numbers refer to polymers in Table II.

the polycyanurates having allyloxy, diallylamino, or *p*-toluenesulfonamide groups on the side chain. Type C polymers show the beginning of heat distortion and a high degree of distortion at break at quite low temperatures. To this group belong the polycyanurates having flexible ether linkages in the side chain.

Thermal Stability. The thermal stabilities of polycyanurates determined by TGA or by heat treatment at 200°C for 1 hr are shown in Figure 4 and Table III.

Figure 4 shows that the thermal stability of polycyanurates of lower molecular weight greatly depends on the endgroups; the thermal stability increases in the order $-\text{Cl} < -\text{OC}_6\text{H}_4\text{C}(\text{CH}_3)_2\text{C}_6\text{H}_4\text{OH} < -\text{N}(\text{C}_6\text{H}_5)_2$.

TABLE III
Effect of Heat Treatment on Typical Polycyanurates

R in polymer	η_{sp}/c		Insoluble in CHCl_3 , %	
	Untreated	Heat-treated ^a	Untreated	Heat-treated ^a
OCH_3	1.15	0.28	0	5.0
$\text{O}(i\text{-Pr})$	0.46	0.25	0	0
$\text{OCH}_2\text{CH}=\text{CH}$	1.15	0.77	0	3.8
$\text{OCH}_2\text{CH}_2\text{OEt}$	1.45	0.83	0	35.8
$\text{O}(\text{CH}_2\text{CH}_2\text{O})_2\text{Et}$	1.15	0.86	0	60.8
$\text{OCH}_2\text{CH}_2\text{OBu}$	0.81	0.73	0	18.3
$\text{OCH}_2\text{CH}_2\text{OC}_6\text{H}_5$	0.75	0.90	0	0
$\text{OCH}_2\text{CHCH}_2$	0.42	—	0	90.6 ^b
				
$\text{OCH}_2\text{C}\equiv\text{CH}$	0.68	—	0	46.0 ^{c,d}
OC_6H_5	0.66	—	0	73.6
Cl	0.71	—	0.6	54.8
N_3	0.30	—	0	98.2 ^e
$\text{N}(\text{CH}_2)_5$	0.83	—	0	94.3
$\text{N}(\text{C}_6\text{H}_5)_2$	1.17	1.17	0	0
$\text{N}(\text{C}_6\text{H}_{11})_2$	0.43	0.44	0	0
				
N	0.76	0.77	0	0
				
$\text{N}(\text{CH}_2\text{C}_6\text{H}_5)_2$	0.62	0.75	0	0
				
N	3.62	3.55	0	0
$\text{N}(\text{C}_2\text{H}_5)_2$	1.03	1.03	0	0
$\text{N}(\text{CH}_2\text{CH}_2\text{CN})_2$	0.74	0.50	0 ^f	0
$\text{N}(\text{CH}_2\text{CH}=\text{CH}_2)_2$	1.54	—	0	95.2
CH_3	0.35	0.34	0	2.0
C_2H_5	0.41	—	0	68.4
<i>n</i> -Bu	0.67	0.84	0	16.8
C_6H_5	2.58	2.58	0 ^d	0

^a Heat treatment at 200°C for 60 min unless otherwise noted.

^b Heat treatment at 150°C for 10 min.

^c Heat treatment at 150°C for 60 min in the presence of dicumyl peroxide.

^d In *o*-Cl₂C₆H₄.

^e Heat treatment at 170°C for 50 min.

^f In NO₂C₆H₅.

Polycyanurates of higher molecular weight prepared from equivalent reactants are found to show excellent stability. Thermal degradation or crosslinking of the molecular chain is observed with the polycyanurates having an alkoxy (except $-\text{OCH}_2\text{CH}_2\text{OC}_6\text{H}_5$), piperidyl, chloro, or phenoxy substituent in the *s*-triazine nucleus (Table III). Such a substituent has an effect on weight loss on heating. Polycyanurates having $-\text{C}_6\text{H}_5$, $-\text{N}(\text{C}_6\text{H}_5)_2$, or carbazyl substituent show excellent thermal stability for TGA (Fig. 5). The initial weight loss occurs mostly at about 360–375°C in the air. Polycyanurates having phenolphthalein, dihydroxybenzophenone, or a diphenyl sulfone nucleus in the molecular chain show a smaller weight loss in the temperature range 350–400°C than does a polycyanurate having a bisphenol nucleus.

Tensile Strength. The mechanical properties of the various polycyanurates of different molecular weight may not be compared, but Table II indicates that most polycyanurates have tensile strength in the range of 450–600 kg/cm² and an elongation at break of 2–7%, and some polycyanurates with a substituent having the flexible ether structure have a higher elongation (about 15%).

Thanks are given to K. Tazima, K. Sawada, and K. Masuda for their assistance in the experimental work.

References

1. R. Audebert and J. Néel, *C. R. Acad. Sci. Paris*, **T258**, 4749 (1964).
2. R. Audebert in *Macromolecular Chemistry, Prague 1965* (*J. Polym. Sci. C*, **16**), O. Wichterle and B. Sedláček, Eds., Interscience, New York, 1967, p. 3245.
3. V. V. Korshak, *Soobshch. Akad. Nauk. Gruz. SSR*, **46**, 353 (1967).
4. Y. A. Murave'ov, *Tr. Mosk. Khim. Tekhnol. Inst.* **No. 52**, 159 (1967).
5. T. F. Saunders and L. G. Picklesimer, *J. Polymer Sci. A-1*, **3**, 2673 (1965).
6. Y. Nakamura, *Kogyo Kagaku Zasshi*, **68**, 1626 (1965); *ibid.*, **70**, 784, 2066 (1967).
7. J. T. Thurston and J. R. Dudley, *J. Amer. Chem. Soc.*, **73**, 2981 (1951).
8. L. A. Lundberg, U. S. Pat. 3,127,399 (1964).
9. R. Hirt and N. Nidecker, *Helv. Chim. Acta*, **33**, 1365 (1950).

Received March 4, 1969

Revised March 27, 1969

Kinetics of Anionic Polymerization of α -Methylstyrene in Tetrahydrofuran

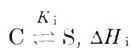
K. M. HUI and T. L. NG, *Department of Chemistry,
University of Singapore, Singapore, 10*

Synopsis

The kinetics of anionic polymerization of α -methylstyrene have been studied in tetrahydrofuran at -30 to 10°C with Na^+ and K^+ as cations. In the Na^+ system, a negative activation energy of -2 kcal/mole was observed in the temperature range -10 to $+10^\circ\text{C}$. The results were analyzed in terms of propagation by both contact and solvent-separated ion-pairs. The relative proportions of the two types of ion-pair were estimated by making use of our data and those of Dainton et al. for the same system at -60 to -30°C . The rate constants of solvent-separated ion-pairs, k_s , were estimated as 4.2 and 0.64 l./mole-sec at -31°C and -59°C , respectively. The discrepancy between our values of k_s and Dainton's was discussed. It is concluded that poly- α -methylstyryl sodium has a higher tendency than polystyryl sodium to form solvent-separated ion pairs. In the K^+ system, our data at -30 to 10°C and those of Dainton et al. at -60 to -40°C fit well into a straight line in the same Arrhenius plot from which an activation energy of 5.2 kcal/mole and $\log A = 3.4$ (l./mole-sec) were obtained.

INTRODUCTION

The kinetics of anionic polymerization of α -methylstyrene in tetrahydrofuran (THF) have been studied by Dainton et al.¹ at -60 to -30°C with Na^+ and K^+ as cations. They found that the rate constants for the propagation of α -methylstyrene by ion-pairs with Na^+ as cation were abnormally high compared with those with K^+ as cation. Furthermore, the activation energy of ion-pair propagation for the Na^+ system was abnormally low, 0.7 kcal/mole. These results were interpreted in terms of propagation at different rates by two types of ion-pair: contact ion-pairs, C, and solvent-separated ion-pairs, S, in equilibrium with each other, the latter being more reactive than the former:



When two types of ion-pair are involved, the kinetic behavior is complex. There may be a transition from propagation entirely by solvent-separated ion-pairs at low temperatures (rate constant k_s) to propagation entirely by contact ion-pairs at high temperatures (rate constant k_c), as discussed by Barnikol and Schulz.² The behavior in the intermediate temperature range depends on the magnitude of the heat of interconversion, ΔH_i ,

of the two types of ion-pair as compared to the activation energies of the two ion-pairs. It may be shown that if $k_s K_i \gg k_c$ and K_i is small (contact ion-pairs dominant, but propagation via solvent-separated ion-pairs) the activation energy of ion-pair propagation, $E_{(\pm)}$, is given by³

$$E_{(\pm)} \approx E_s + \Delta H_i / (1 + K_i) \approx E_s + \Delta H_i$$

where E_s is the activation energy of the solvent-separated ion-pairs propagation. As ΔH_i is negative, $E_{(\pm)}$ may be negative, depending on the relative magnitude of E_s and ΔH_i . However, negative activation energy has not been observed by Dainton et al.¹ in the Na^+ - α -methylstyrene-THF system.

We have now extended their study to the higher temperature range -30 to $+10^\circ\text{C}$. In the present paper, we report the kinetic data in this temperature range and discuss the significance of the difference between the Arrhenius plot in this temperature range and that between -60 and -30°C studied by Dainton et al.¹

EXPERIMENTAL

As air and moisture react very rapidly with poly- α -methylstyryl anions and render them unreactive towards the monomer, it is necessary to carry out the final stages of purification of the monomer and the solvent and the filling of the dilatometer on a vacuum line. Break-seals were used in place of taps to facilitate transfer of solution in vacuum and to avoid contaminating the solutions with grease.

The materials used were purified as described below.

α -Methylstyrene (Fluka) was dried with anhydrous MgSO_4 , filtered, and then fractionally distilled; the fraction distilled over at 164 – 165°C was collected. It was then dried over CaH_2 on the vacuum line with frequent degassing and stirring.

Tetrahydrofuran (Fluka) was fractionally distilled and stored over Na wires. When required, the THF was dried over CaH_2 on the vacuum line and degassed and then distilled onto a liquid sodium-potassium alloy; trace amount of α -methylstyrene was also distilled into the flask. Complete removal of air and water was signified by the appearance of a characteristic red color due to oligomeric α -methylstyryl anions. The solvent was distilled from this flask when required.

Of the tetraphenylboron salts, NaBPh_4 (British Drug Houses) was dried in a vacuum oven at 50°C before use. KBPh_4 was prepared by adding an equivalent amount of KCl to an aqueous solution of NaBPh_4 . The relatively insoluble precipitate of KBPh_4 was filtered, washed, and recrystallized twice from aqueous acetone and dried at 50°C under vacuum.

Na and K mirrors were obtained in glass ampoules with break-seals by distilling the metals under high vacuum.

The dilatometer assembly is shown in Figure 1. The dilatometer is composed of a number of small tubes A, of 5 mm ID, connected to a mixing

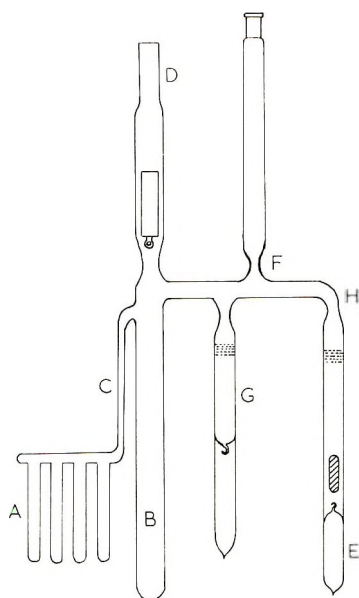


Fig. 1. Dilatometer assembly.

chamber B by a constant bore tube C of 2.5 mm ID. Also attached to B was a quartz optical cell D with a quartz spacer to give path lengths of 0.1 cm and 0.01 cm. E was an ampoule of metal mirror, and G was for attachment to another ampoule of metal mirror.

The required amount of tetraphenylboron salt was weighed and introduced into B. The dilatometer assembly was evacuated on the vacuum line. The required amounts of α -methylstyrene and THF were distilled into B, and the assembly was sealed at F. Ampoule E was opened, and the solution was allowed to come into contact with the metal mirror. The concentration of the living ends, [LE], could be controlled by the time of contact of the solution with the metal mirror. When the required concentration was reached (gauged visually from the intensity of the red color of the solution), the ampoule E was sealed off at the constriction H with the solution in B cooled in liquid air.

For both Na^+ and K^+ systems, the amounts of monomer and solvent used were such as to give an initial monomer concentration of 1.5M, except for one preparation of the reaction solution in the Na^+ series where the monomer concentration was 3M.

To follow the kinetics of polymerization, the dilatometer assembly was immersed in a thermostat bath controlled at $\pm 0.05^\circ\text{C}$. The contraction of the solution in A with time was followed with a cathetometer focussed on C.

The living end concentration was determined spectrophotometrically with a Hilger Uvispek instrument before and after each kinetic run. The measurements were made relative to air and a blank reading was ob-

tained at the end of the experiment after allowing the living ends to react with the atmosphere. The path lengths of the cell were determined from optical density measurements on alkaline potassium chromate solutions by using the extinction coefficient of Haupt.⁴

For kinetic measurements at another temperature the same solution can be used. It was only necessary to warm the solution to room temperature again, allow depolymerization to go to completion, check the optical density, and repeat the procedure. The solutions of living end were stable.

For a higher concentration of living ends, another ampoule of metal mirror was joined to G and the break-seals on G and on the metal mirror ampoule were crushed after evacuating the space between the two break-seals.

RESULTS

The reaction-time curves obtained dilatometrically were all analyzed by plotting $\log (h_t - h_\infty)$ against time, where h_t and h_∞ were the dilatometer readings at time t and infinite time, respectively. These plots were in general good straight-line plots, thus confirming that the propagation reaction is a first-order reaction with respect to the monomer.

The living end concentrations [LE] were calculated from the optical densities by using extinction coefficients⁵ of 1.59×10^4 l./mole-cm and 1.54×10^4 l./mole-cm at the absorption maximum 340 $m\mu$ for poly- α -methylstyryl sodium and poly- α -methylstyryl potassium, respectively.

For both Na^+ and K^+ systems, the pseudo first-order rate constants, k_1 , were accurately proportional to [LE] when the appropriate tetraphenylboron salt was added. The second-order rate constants, $k_{(\pm)} = k_1/[\text{LE}]$, were then the rate constants for ion-pair propagation and were calculated from the slopes of the k_1 against [LE] plots. The ion-pair rate constants at different temperatures are summarized in Table I and plotted in the Arrhenius form in Figure 2. For the Na^+ system the tetraphenylboron salt was sufficiently soluble to allow its concentration to be varied from $2 \times 10^{-2}M$ to $5 \times 10^{-2}M$. A change of salt concentration by a factor

TABLE I
Apparent Ion-Pair Rate Constants $k_{(\pm)}$ at Various Temperatures

Temperature, °C	$k_{(\pm)}$, l./mole sec	
	Na^+	K^+
-30	0.520	0.065
-20	0.520	0.096
-10	0.525	0.123
0	0.480	0.168
5	0.425	0.230
10	0.390	0.244

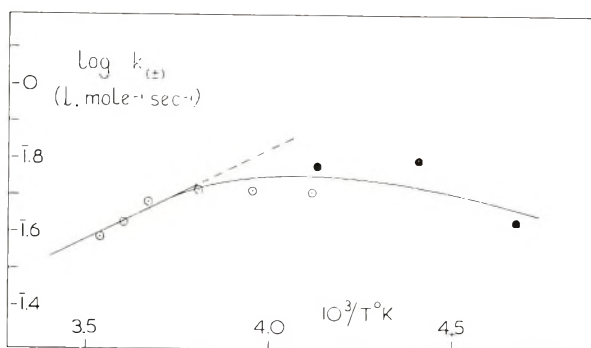


Fig. 2. Arrhenius plot for polymerization of α -methylstyrene in THF by ion-pairs with Na^+ as cation: (\circ) our values; (\bullet) Dainton's values.

of 2.5 had no effect on $k_{(\pm)}$. This confirmed that ion-pair dissociation was completely suppressed. For the K^+ system, as KBPh_4 was only sparingly soluble in THF, the reaction solution was saturated with KBPh_4 and it was found that at $[\text{LE}]$ lower than $\approx 8 \times 10^{-3}M$, the suppression of free-ion formation was complete.

DISCUSSION

The Arrhenius plot for the Na^+ - α -methylstyrene-THF system was a curve in the temperature range -30 to $+10^\circ\text{C}$, in contrast to the linear Arrhenius plots obtained for α -methylstyrene polymerizations in dioxane¹ and in tetrahydropyran⁷ (THP) with alkali metal as cations. By approximating the portion of the curve between -10 to $+10^\circ\text{C}$ to a straight line, the negative activation energy was estimated to be -2 kcal/mole (Fig. 2). The observation of a negative activation energy is in agreement with the prediction of Barnikol and Schulz² mentioned earlier and with Dainton and his co-worker's interpretation¹ of their results in terms of propagation by two types of ion-pairs: contact and solvent-separated ion-pairs.

When both contact and solvent-separated ion-pairs participate in the propagation, the ion-pair rate constant is given by

$$k_{(\pm)} = x_s k_s + x_c k_c \quad (1)$$

where x_s and x_c are, respectively, the fractions of solvent-separated and contact ion-pairs, so that $x_s + x_c = 1$ and the apparent activation energy $E_{(\pm)}$ is given by³

$$E_{(\pm)} = \frac{k_c E_c + k_s K_i (E_s + \Delta H_i)}{k_c + k_s K_i} - \frac{K_i}{1 + K_i} \Delta H_i \quad (2)$$

Equation (2) may be rearranged to

$$\frac{\Delta H_i}{1 + K_i} \left(1 - \frac{k_c}{k_s} \right) = - \left(\frac{k_c E_c - k_c E_{(\pm)}}{k_s K_i} \right) + (E_{(\pm)} - E_s) \quad (2a)$$

where E_c is the activation energy of propagation by contact ion-pairs; the meaning of k_s , k_c , E_s , K_i and ΔH_i has been explained earlier. Szwarc et al.,⁶ in their study of the anionic polymerization of the system Na^+ -styrene-THF, deduced that E_s is nearly the same as $E_{(-)}$, the activation energy for propagation by free ions. For our present system, we assume E_s to be equal to $E_{(-)}$ which is known⁷ to be about 7 kcal/mole. This assumption has support in the recent experimental findings of Hirota et al.,⁸ who studied the ESR spectra of sodium naphthalene ion-pairs and the kinetics of its electron transfer reactions with naphthalene. They concluded that the activation energy for the reaction of solvent-separated ion-pairs was very close to that of free ions. Substituting $E_{(\pm)} = -2$ kcal/mole and $E_s = 7$ kcal/mole in eq. (2a) we have

$$\frac{\Delta H_i}{1 + K_i} \left(1 - \frac{k_c}{k_s} \right) = - \left(\frac{k_c E_c + 2k_c}{k_s K_i} \right) - 9 \quad (3)$$

Since $k_s > k_c$, the term in parentheses on the left-hand side of eq. (3) will be positive and less than unity and the term in parentheses on the right-hand side of eq. (3) is also positive, hence $\Delta H \leq -9$ kcal/mole. If $k_s K_i \gg k_c$ and K_i is small which is to be expected in the range -10 to 10°C , then from eq. (3), $\Delta H_i = -9$ kcal/mole. In making the assumption $k_s K_i \gg k_c$, we may be guided by our knowledge of the Na^+ -styrene system. In this system, the activation energies of contact ion-pairs in THF and in dioxane are similar,⁹ and the values of k_c in the two solvents are, respectively,¹⁰ 13 and 6.5 l./mole-sec at 25°C . It is therefore reasonable to infer that k_c in THF may be higher than that in dioxane by not more than 5 times. In the Na^+ - α -methylstyrene system, at 0°C , $k_c = 0.0028$ l./mole-sec in dioxane;¹⁰ by analogy with the Na^+ -styrene system, k_c in THF at 0°C may be expected to be ≤ 0.014 l./mole-sec. We have found that at 0°C , $k_{(\pm)} = 0.48$ l./mole-sec, and as K_i is small at this temperature, x_c approaches unity and $x_s = K_i/1+K_i \approx K_i$, therefore from eq. (1), it may be seen that $k_s K_i$ is at least 35 times higher than k_c .

Dainton et al.¹ argued that since $E_c = 8$ kcal/mole for the Na^+ -styrene-THF system and $E_c = 12$ kcal/mole for the Na^+ - α -methylstyrene/dioxane system,¹⁰ reasonable values to assume for E_c for the Na^+ - α -methylstyrene-THF system would be 8-12 kcal/mole. They used $E_c = 9$ kcal/mole for their calculations of k_c and k_s at -31 and -59°C . For convenience of comparison with their results, we shall also use $E_c = 9$ kcal/mole for our calculations; it can be shown that the use of values other than 9 in the range 8-12 kcal/mole will have little effect on our conclusions. At 10°C , $k_{(\pm)}$ was found to be 0.39 l./mole-sec which may be considered to be the upper limit of k_c at this temperature. Applying the Arrhenius equation, we have

$$\log A_c \leq \log 0.39 + [9 \times 10^3 / (2.303R \times 283)]$$

With this value of $\log A_c$, we estimated the values of k_c at -31 and 59°C to be ≤ 0.026 l./mole-sec and ≤ 0.002 l./mole-sec, respectively. These

rather small values of k_c indicated that the contribution of contact ion-pairs to $k_{(\pm)}$ at -31 and -59°C , which were 0.61 and 0.42 l./mole-sec respectively,¹ were small. Therefore eq. (1) may be reduced to

$$k_{(\pm)} = x_s k_s \quad (1a)$$

for the temperature range -59 to -31°C .

On taking E_s as 7 kcal/mole and ΔH_i as -9 kcal/mole, the fraction of solvent-separated ion-pairs at -31 and -59°C may be estimated. Let K_1 and K_2 be the values of K_i at -31 and -59°C respectively. We have

$$\log K_2 - \log K_1 = \frac{9 \times 10^3}{2.303R} \left(\frac{1}{214} - \frac{1}{242} \right)$$

$$K_2/K_1 = 11.4$$

Let x_1 and x_2 be the values of x_s at -31 and -59°C respectively. Applying eq. (1a) and the Arrhenius equation, we have

$$\log \frac{0.61}{x_1} - \log \frac{0.42}{x_2} = \frac{-7 \times 10^3}{2.303R} \left(\frac{1}{242} - \frac{1}{214} \right)$$

$$x_2/x_1 = 4.57$$

Since $x_2 = K_2/(1 + K_2)$ and $x_1 = K_1/(1 + K_1)$, we have

$$K_1 = 0.17$$

$$K_2 = 1.92$$

$$x_1 = 0.15$$

$$x_2 = 0.66$$

At -31°C , $k_s = k_{(\pm)}/x_s = 4.2$ l./mole-sec, and similarly at -59°C , $k_s = 0.64$ l./mole-sec.

Our values of k_c and k_s are considerably lower than those obtained by Dainton et al.¹ This discrepancy arises mainly out of their use of their values of 0.05 and 0.25 for x_s at -31 and -59°C respectively which were estimated from spectrophotometric data. These values may be in error as they would give a ΔH_i value of -6.8 kcal/mole which, as can be seen in eq. (2), would imply the absence of a negative activation energy and contradict the results of the present investigation.

It must be emphasized that our values of x_1 , x_2 , k_s , and k_c obtained above depend on the values assumed for E_s and E_c and the value of ΔH_i ; if $\Delta H_i < -9$ kcal/mole, the values of x_1 and x_2 would be larger, and k_s would be smaller than those we have calculated. However it served to show the consequences of making these assumptions, which in our opinion, are reasonable and to give an indication of the magnitude of k_s which is about $1/12$ of $k_{(-)}$.

Szwarc et al.⁶ reported that for the Na^+ -styrene-THF system, a negative activation energy of -1.5 kcal/mole was observed. At -70°C , the fraction of solvent-separated ion-pairs was about 0.3, and they esti-

mated $\Delta H_i(C \rightleftharpoons S)$ to be -7.5 kcal/mole. For the Na^+ - α -methylstyrene-THF system, we have estimated $E_{(\pm)} = -2$ kcal/mole, $\Delta H_i = -9$ kcal/mole, and the fraction of solvent-separated ion-pairs at -59°C as 0.66. Therefore, it appears that in THF, poly- α -methylstyryl sodium has a higher tendency than polystyryl sodium to form solvent-separated ion-pairs. The decrease of $E_{(\pm)}$ with increase in cation size for the styrene-THP or -dioxane systems¹⁰ and the reverse trend for α -methylstyrene-THP systems³ seem to point to the same conclusion. This higher tendency may be attributed to the larger anion with a higher degree of charge delocalization in the poly- α -methylstyryl ion-pair and the steric effect of its methyl group; both these factors favor the formation of solvent-separated

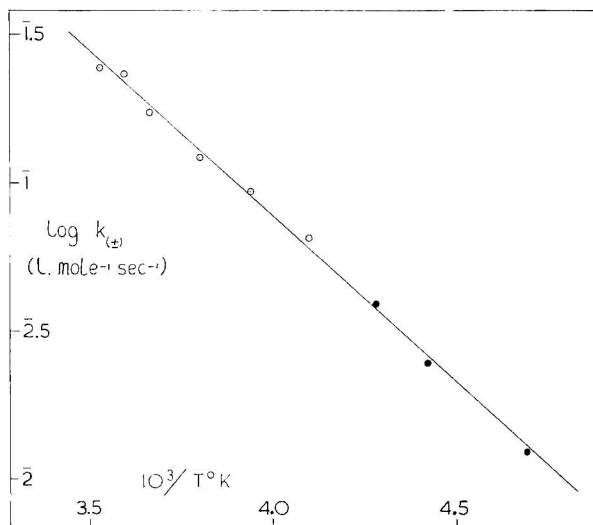


Fig. 3. Arrhenius plot for polymerization of α -methylstyrene in THF by ion-pairs with K^+ as cation: (○) our values; (●) Dainton's values.

ion-pairs. An example of this steric effect was reported by Roberts and Szwarc¹¹ for the sodium salt of the monoradical ion of tetraphenylethylene in THF.

For the K^+ - α -methylstyrene-THF system, no negative activation energy was observed by us in the temperature range -30°C to 10°C . In fact, the $k_{(\pm)}$ values obtained by us at -30°C to $+10^\circ\text{C}$ and those by Dainton et al. at -60°C to -40°C fit very well into a straight line when they were all plotted in the same Arrhenius plot (Fig. 3). From this plot, an activation energy of 5.2 kcal/mole and $\log A = 3.4$ (l./mole-sec) were obtained. It appears that for the α -methylstyrene-THF system, the activation energy of ion-pair propagation increases with the increase of cation size, a trend which was also observed in the α -methylstyrene-THP system. This trend may be explained in terms of propagation by two types of ion-pair and has been fully discussed by Dainton et al.³

Monomer concentration seems to have hardly any effect on the $k_{(\pm)}$ values obtained. Although the monomer concentration used by us was about five times that used by Dainton ($1.5M/0.3M$) in the K^+ system, a good straight line was obtained when our results and theirs were plotted in the same Arrhenius plot. We have also carried out a kinetic run with a monomer concentration of $3M$ instead of $1.5M$ in the Na^+ system. There was hardly any effect of monomer concentration on the rate constants obtained in this monomer concentration range. This is in agreement with the findings of Szwarc et al.¹²

We are grateful to Professor K. J. Ivin for communicating his results to us in advance of publication.

References

1. F. S. Dainton, G. A. Harpell, and K. J. Ivin, *Europ. Polym. J.*, **5**, 395 (1969).
2. W. K. R. Barnikol and G. V. Schulz, *Z. Physik. Chem. (Frankfurt)*, **47**, 89 (1965).
3. F. S. Dainton, K. M. Hui, and K. J. Ivin, *Europ. Polym. J.*, **5**, 387 (1969).
4. G. W. Haupt, *J. Opt. Soc. Amer.*, **42**, 441 (1952).
5. J. Comyn and K. J. Ivin, *Europ. Polym. J.*, **5**, 395 (1969).
6. T. Shimomura, K. J. Tölle, J. Smid, and M. Szwarc, *J. Amer. Chem. Soc.*, **89**, 796 (1967).
7. J. Comyn, F. S. Dainton, G. A. Harpell, K. M. Hui, and K. J. Ivin, *J. Polym. Sci. B*, **5**, 965 (1967).
8. N. Hirota, R. Carraway, and W. Schook, *J. Amer. Chem. Soc.*, **90**, 3611 (1968).
9. L. Böhm, W. K. R. Barnikol, and G. V. Schulz, *Makromol. Chem.*, **110**, 222 (1967).
10. F. S. Dainton, G. C. East, G. A. Harpell, N. R. Hurworth, K. J. Ivin, R. T. LaFlair, and (in part) R. H. Pallen and K. M. Hui, *Makromol. Chem.*, **89**, 257 (1965).
11. R. C. Roberts and M. Szwarc, *J. Amer. Chem. Soc.*, **87**, 5542 (1965).
12. T. Shimomura, J. Smid, and M. Szwarc, *Makromol. Chem.*, **108**, 288 (1967).

Received April 4, 1969

Monomer-Isomerization Polymerization. V. Effects of Transition Metal Compounds on Monomer-Isomerization Polymerizations of Butene-2 and Pentene-2

TAKAYUKI OTSU, AKIHIKO SHIMIZU, and MINORU IMOTO,
*Department of Applied Chemistry, Faculty of Engineering,
Osaka City University, Sumiyoshi-ku, Osaka, Japan*

Synopsis

In order to clarify the correlation between polymerization and monomer isomerization in the monomer-isomerization polymerization of β -olefins, the effects of some transition metal compounds which have been known to catalyze olefin isomerizations on the polymerizations of butene-2 and pentene-2 with $\text{Al}(\text{C}_2\text{H}_5)_3\text{-TiCl}_3$ or $\text{Al}(\text{C}_2\text{H}_5)_3\text{-VCl}_3$ catalyst have been investigated. It was found that some transition metal compounds such as acetylacetonates of Fe(III), Co(II), and Cr(III) or nickel dimethylglyoxime remarkably accelerate these polymerizations with $\text{Al}(\text{C}_2\text{H}_5)_3\text{-TiCl}_3$ catalyst at 80°C. All the polymers from butene-2 were high molecular weight polybutene-1. With $\text{Al}(\text{C}_2\text{H}_5)_3\text{-VCl}_3$ catalyst, which polymerizes α -olefins but does not catalyze polymerization of β -olefins, no monomer-isomerization polymerizations of butene-2 and pentene-2 were observed. When Fe(III) acetylacetonate was added to this catalyst system, however, polymerization occurred. These results strongly indicate that two independent active centers for the olefin isomerization and the polymerization of α -olefins were necessary for the monomer-isomerization polymerizations of β -olefins.

INTRODUCTION

In the previous papers,¹⁻⁴ it was reported that some β -olefins such as butene-2, pentene-2 and hexene-2 could polymerize in the presence of Natta catalyst with isomerization of monomer preceding polymerization to give high molecular weight polymers having the recurring unit of the corresponding α -olefins. It was also assumed that, in these monomer-isomerization polymerizations,⁴ there were two independent active centers: one responsible for the isomerization of monomer from β -olefin to α -olefin and the other for the polymerization of α -olefin.³

If these assumptions are correct, the addition of certain isomerization catalysts which do not catalyze the α -olefin polymerizations could be expected to accelerate the monomer-isomerization polymerization of β -olefins with the $\text{Al}(\text{C}_2\text{H}_5)_3\text{-TiCl}_3$ catalyst. On the other hand, the $\text{Al}(\text{C}_2\text{H}_5)_3\text{-VCl}_3$ catalyst, which catalyzes α -olefin polymerizations but not olefin isomerizations, may be able to induce the monomer-isomerization polymerization of

β -olefins if an additional isomerization catalyst is introduced. The present paper describes the effects of some transition metal compounds on the monomer-isomerization polymerizations of butene-2 and pentene-2 with $\text{Al}(\text{C}_2\text{H}_5)_3\text{-TiCl}_3$ and $\text{Al}(\text{C}_2\text{H}_5)_3\text{-VCl}_3$ catalysts.

In general, transition metal compounds of groups VI and VIII of the periodic table have been known as olefin isomerization catalysts. Of such compounds, for example, some metal carbonyls (group VIII),⁵⁻¹¹ metal oxides (groups VI and VIII),^{12,13} Rancy metals (group VIII),^{14,15} metal halides (groups VI and VIII),¹⁶⁻¹⁹ and coordinated metal complexes (groups VI and VIII)^{16,18,20} have been cited in the literature.

EXPERIMENTAL

Materials

Butene-1, *trans*-butene-2, and pentene-1 and -2 (Matheson Co.) were used after purification as described in the previous papers.^{3,4} Purities determined by gas chromatography were 97.9, 99.4, 99.9, and 99.2%, respectively; the pentene-2 consisted of 62.9% *cis* and 37.1% *trans* isomers.

Triethylaluminum (Ethyl Corp.), titanium trichloride, and vanadium trichloride (Stauffer Chem. Co.) were used without further purification. Nickel dimethylglyoxime [$\text{Ni}(\text{DMG})_2$] was prepared by reacting nickel acetate with dimethylglyoxime in hot ethyl alcohol. The other transition metal compounds used were commercially available reagents without purification. Solvents and other reagents were also used after ordinary purification.

Polymerization Procedure

Polymerizations were carried out in a sealed glass tube with shaking in a thermostat at 80°C for a given time. The charging of the required amounts of reagents into the tubes and the isolation of the resulting polymers from the reaction mixture were performed by methods described in the previous paper.³

The composition of the unreacted monomers after polymerization was determined by gas chromatography, by use of a benzyl ether column in a stream of hydrogen (30 ml/min) at 20°C.

Characterization of the Polymers

The structure of the resulting polymers was checked by infrared spectroscopy, and the isotacticity of the polybutene-1 was determined from the weight of hot diethyl ether-insoluble polymer.³ The intrinsic viscosity of the polymers was determined by viscosity measurement of dilute tetralin solutions at 135°C with an Ubbelohde viscometer.

RESULTS AND DISCUSSION

Effects of Transition Metal Compounds on the Polymerizations
by $\text{Al}(\text{C}_2\text{H}_5)_3\text{-TiCl}_3$ Catalyst

The effects of various transition metal compounds on the monomer-isomerization polymerization of *trans*-butene-2 with the Natta catalyst are shown in Table I, in which the results obtained with some binary catalyst systems of $\text{Al}(\text{C}_2\text{H}_5)_3$ and Fe or Ni compounds are also indicated.

TABLE I
Effects of Transition Metal Compounds (MeX) on the Monomer-Isomerization
Polymerization of *trans*-Butene-2 with $\text{Al}(\text{C}_2\text{H}_5)_3\text{-TiCl}_3$ Catalyst^a

MeX	Me/Ti molar ratio	Time, hr	Yield, %	Rate, %/hr	Et ₂ O-insoluble polymer		Composition in unreacted butenes, % ^b		
					%	[η], dl/g	Butene- 1	<i>trans</i> - Butene- 2	<i>cis</i> - Butene- 2
None	0	28	18.5	0.66	66.5	1.2	2.9	64.8	32.3
RhCl ₃	0.46	28	11.4	0.41	—	—	1.7	75.5	22.8
PdCl ₂	0.82	28	6.9	0.25	—	—	2.7	72.5	24.8
CrCl ₃	0.44	28	14.4	0.51	—	—	2.7	72.5	24.8
FeCl ₃	0.35	28	17.6	0.63	—	2.0	2.6	74.7	22.7
NiCl ₂	0.65	17	32.4	1.9	52.5	2.1	3.8	68.9	27.3
CoCl ₂	0.58	28	18.1	0.65	—	1.1	2.0	72.1	25.9
NiS	2.1	12	3.8	0.32	—	—	2.2	79.7	18.1
Ni(DMG)	0.62	5	27.5	5.5	66.2	2.1	4.4	68.1	27.5
Ni(acac) ₂	0.48	26	0.8	0.02	—	—	5.4	73.4	21.2
Fe(acac) ₃	0.43	5	18.6	3.7	79.5	2.2	3.2	72.6	24.2
Cr(acac) ₃	0.57	8	23.9	3.0	74.0	1.6	3.3	70.4	26.3
Co(acac) ₃	0.53	8	16.7	2.1	78.9	2.2	6.2	64.0	29.8
Fe(acac) ₃ ^c	0	25	0	0	—	—	6.1	65.7	28.2
Ni(acac) ₂ ^c	0	25	0	0	—	—	5.4	72.0	22.6
Ni(DMG) ₂ ^c	0	25	0	0	—	—	2.1	96.0	1.9

^a Al/Ti = 3.0; 80°C; [butene-2] = 6.0 mole/l.; [TiCl₃] = 50 mmole/l.; in *n*-heptane.

^b Determined by gas chromatography. In all cases, ~0.7% butane was also produced.

^c Polymerized with $\text{Al}(\text{C}_2\text{H}_5)_3\text{-MeX}$ catalysts (Al/Me = 3.0).

As is clearly shown, the $\text{Al}(\text{C}_2\text{H}_5)_3\text{-Fe(III)}$ acetylacetonate [$\text{Fe}(\text{acac})_3$], $\text{Ni}(\text{acac})_2$, or $\text{Ni}(\text{DMG})_2$ systems catalyze the isomerization of butene-2 but do not induce polymerization. In the presence of TiCl_3 , however, the above systems could initiate polymerization to polybutene-1. The addition of NiCl_2 , $\text{Fe}(\text{acac})_3$, $\text{Cr}(\text{acac})_3$, or $\text{Ni}(\text{DMG})_2$ to the $\text{Al}(\text{C}_2\text{H}_5)_3\text{-TiCl}_3$ catalyst was found to accelerate the polymerization of butene-2 with $\text{Al}(\text{C}_2\text{H}_5)_3\text{-TiCl}_3$ catalyst alone. It was noted that the acetylacetonates of Fe(III), Co(II), and Cr(III) and $\text{Ni}(\text{DMG})_2$ showed a remarkable accelerating effect, and the rates were faster, about three to eight times, than that by $\text{Al}(\text{C}_2\text{H}_5)_3\text{-TiCl}_3$ catalyst.

Although metal chlorides other than NiCl_2 , and Ni sulfide or acetylacetonate had almost no effect on the isomerization of *trans*-butene-2, these compounds retarded the polymerization. This seemed to destroy the active center for the polymerization of butene-1, not that for the isomerization.

All the polymers were confirmed to be polybutene-1 by infrared spectra.¹ As compared with the polymer obtained by $\text{Al}(\text{C}_2\text{H}_5)_3\text{-TiCl}_3$, the isotacticities of the polymers obtained in the presence of these metal compounds, except NiCl_2 , were not very different, but their intrinsic viscosities were higher.

Table II shows the effect of the Fe/Ti molar ratios in the $\text{Al}(\text{C}_2\text{H}_5)_3\text{-TiCl}_3\text{-Fe}(\text{acac})_3$ catalyst at constant TiCl_3 and $\text{Fe}(\text{acac})_3$ on the polymerization of butene-2 at 80°C. Table II indicates that the isomerization

TABLE II
Effects of Fe/Ti Molar Ratio on the Monomer-Isomerization Polymerization of *trans*-Butene-2 with $\text{Al}(\text{C}_2\text{H}_5)_3\text{-TiCl}_3\text{-Fe}(\text{acac})_3$ Catalyst^a

Fe/Ti molar ratio	Yield, %	Composition in unreacted butenes, %			
		Butane	Butene-1	<i>trans</i> - Butene-2	<i>cis</i> - Butene-2
0.4	18.6 ^b	0.7	3.1	72.0	24.2
1.0	Trace	0.5	4.5	79.3	15.7
2.4	0	0.6	3.3	89.6	6.5
7.0	0	0.5	1.9	93.3	4.3

^a $\text{Al}/(\text{Ti} + \text{Fe}) = 3.0$; 80°C; 8 hr; [butene-2] = 6.0 mole/l.; [$\text{TiCl}_3 + \text{Fe}(\text{acac})_3$] = 75 mmole/l.; in *n*-heptane.

^b Polymerized for 5 hr.

of butene-2 and hence the polymerization of butene-1 were retarded with increasing Fe/Ti ratios. At Fe/Ti ratios above 0.43, no polymerization was observed. These results might also suggest that separate active centers for isomerization and polymerization are necessary for monomer-isomerization polymerizations of β -olefins by a coordinated anionic mechanism.

Effects of $\text{Fe}(\text{acac})_3$ on the Polymerizations by $\text{Al}(\text{C}_2\text{H}_5)_3\text{-VCl}_3$ Catalyst

Table III shows the effect of $\text{Fe}(\text{acac})_3$ on the polymerization and isomerization of butene-2 and pentene-2 with $\text{Al}(\text{C}_2\text{H}_5)_3\text{-VCl}_3$ catalyst at 80°C. As a comparison, the results of polymerizations of butene-1 and pentene-1 are also indicated in this table.

Table III shows that the $\text{Al}(\text{C}_2\text{H}_5)_3\text{-Fe}(\text{acac})_3$ system did not induce the polymerizations of these β -olefins, but the compositions of the unreacted monomers reached an equilibrium mixture. On the other hand, the $\text{Al}(\text{C}_2\text{H}_5)_3\text{-VCl}_3$ system initiated the polymerizations of these α -olefins but did not induce polymerization or monomer isomerization of these β -olefins. However, the combined system $\text{Al}(\text{C}_2\text{H}_5)_3\text{-VCl}_3\text{-Fe}(\text{acac})_3$ was found to induce both polymerization and isomerization of these β -olefins. These observations also indicate that two different active centers for isomerization and polymerization are needed in the monomer-isomerization polymerizations of these β -olefins.

The infrared spectra of the polymers obtained from *trans*-butene-2 and pentene-2 with $\text{Al}(\text{C}_2\text{H}_5)_3\text{-VCl}_3\text{-Fe}(\text{acac})_3$ catalyst are shown in Figures 1

TABLE III
Effects of $\text{Fe}(\text{acac})_3$ on the Polymerizations of Butenes and Pentenes
with $\text{Al}(\text{C}_2\text{H}_5)_3\text{-VCl}_3$ Catalysts^a

Olefins	Fe/V molar ratio	Time, hr	Yield, %	[η], dl/g	Composition in unreacted olefins, % ^b			
					Alkane	α - Olefin	<i>trans</i> - Olefin	<i>cis</i> - Olefin
Butene-1	0	0.17	15.3	2.1	0.0	99.6	0.4	0.0
<i>trans</i> -Butene-2	0	28	0	—	0.5	1.0	95.0	3.5
"	0.81	25	0	—	0.6	6.1	65.1	28.2
"	0.55	28	3.7	1.0	0.5	5.3	72.8	21.4
Pentene-1 ^c	0	0.25	39.0	2.5	0.0	100.0	0.0	0.0
Pentene-2	0	28	0	—	0.0	1.0	38.7	60.3
"	0.50	28	0	—	0.3	4.5	73.4	21.8
"	0.47	28	5.8	1.0	0.4	4.4	71.8	23.4
Equimolar mixture of <i>trans</i> -butene-2 and pentene-2	0.55	28	6.5	—	0.7 ^d 0.4 ^e	5.7 ^d 4.4 ^e	66.6 ^d 72.0 ^e	27.0 ^d 23.2 ^e

^a Al/V = 3.0; 80°C; [butene] = 6.0 mole/l.; [pentene] = 4.0 mole/l.; [VCl_3] = 50 mmole/l.; in *n*-heptane.

^b Calculated concentrations of α -, β -*trans*- and β -*cis*-olefins in the equilibrium mixture are, respectively, 5.1, 72.4, and 22.5% for butene, and 3.1, 63.9, and 33.0% for pentene.

^c Al/V = 2.0.

^d Indicates isomer distributions in butenes.

^e Indicates isomer distributions in pentenes.

and 2, respectively; spectra of polymers obtained from butene-1 and pentene-1 with $\text{Al}(\text{C}_2\text{H}_5)_3\text{-VCl}_3$ catalyst are also indicated. The polymers obtained from both α - or β -olefins showed completely identical spectra. Thus the spectra from butene-1 or -2 and pentene-1 or -2 showed characteristic bands due to ethyl and *n*-propyl groups at 766 and 736 cm^{-1} , respectively.^{1,2} This result strongly indicated that these β -olefins isomerized to the respective α -olefins, and then polymerized as α -olefins through a coordinated anionic mechanism (monomer-isomerization polymerization).

The results of a copolymerization of an equimolar mixture of *trans*-butene-2 and pentene-2 are also shown in Table III. The isomer distribu-

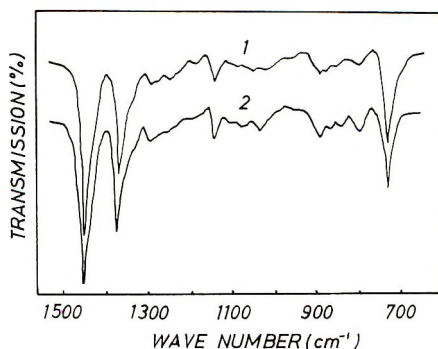


Fig. 1. Infrared spectra of the polymers (film); (1) obtained from butene-1 with $\text{Al}(\text{C}_2\text{H}_5)_3\text{-VCl}_3$ catalyst; (2) obtained from *trans*-butene-2 with $\text{Al}(\text{C}_2\text{H}_5)_3\text{-VCl}_3\text{-Fe}(\text{acac})_3$ catalyst.

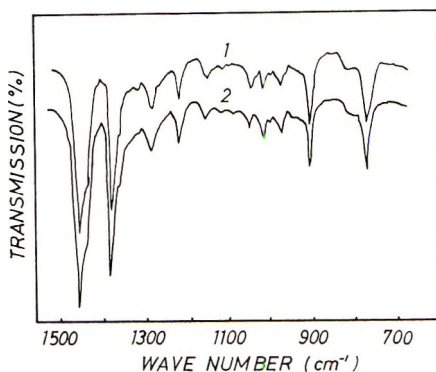


Fig. 2. Infrared spectra of the polymers (film): (1) obtained from pentene-1 with $\text{Al}(\text{C}_2\text{H}_5)_3\text{-VCl}_3$ catalyst (2) obtained from pentene-2 with $\text{Al}(\text{C}_2\text{H}_5)_3\text{-VCl}_3\text{-Fe}(\text{acac})_3$ catalyst.

tions in the unreacted monomers recovered after polymerization were close to those of the equilibrium mixture (see Table III) for both monomers, and the resulting polymer was confirmed to be a copolymer of butene-1 and pentene-1. Detailed results were described in the previous paper.⁴

Table IV shows the effects of Fe/V molar ratios on the monomer-isomerization of butene-2 with $\text{Al}(\text{C}_2\text{H}_5)_3\text{-VCl}_3\text{-Fe}(\text{acac})_3$ at a constant molar

TABLE IV
Effects of Fe/V Molar Ratios on the Monomer-Isomerization Polymerization of *trans*-Butene-2 with $\text{Al}(\text{C}_2\text{H}_5)_3\text{-VCl}_3\text{-Fe}(\text{acac})_3$ Catalyst^a

Fe/V molar ratio	Yield, %	Compositions in unreacted butenes, %			
		Butane	Butene-1	<i>trans</i> - Butene-2	<i>cis</i> - Butene-2
0.5	3.0	0.8	4.9	67.6	26.7
1.1	5.1	0.7	5.4	68.3	25.6
2.2	7.7	0.8	5.4	65.4	28.4
7.0	0.1	0.6	5.9	61.5	26.3

^a $\text{Al}/(\text{V} + \text{Fe}) = 3.0$; 80°C ; 25 hr.; [butene] = 6.0 mole/l.; $[\text{VCl}_3 + \text{Fe}(\text{acac})_3] = 75$ mmole/l.; in *n*-heptane.

ratio of $\text{Al}/(\text{V} + \text{Fe})$ of 3.0 at 80°C . From this table, the polymer yield was found to show a maximum at $\text{Fe}/\text{V} = 2.2$, indicating that the relative numbers of the active centers for isomerization and polymerization are also important.

References

1. A. Shimizu, T. Otsu, and M. Imoto, *J. Polym. Sci. B*, **3**, 449 (1965).
2. A. Shimizu, T. Otsu, and M. Imoto, *J. Polym. Sci. B*, **3**, 1031 (1965).
3. T. Otsu, A. Shimizu, and M. Imoto, *J. Polym. Sci. A-1*, **4**, 1579 (1966).
4. T. Otsu, A. Shimizu, K. Itakura, and M. Imoto, *Makromol. Chem.*, **123**, 289 (1969).

5. P. Asinger and O. Berg, *Ber.*, **88**, 445 (1955).
6. H. W. Sternberg, R. Markby, and L. Wender, *J. Amer. Chem. Soc.*, **78**, 5704 (1956); *ibid.*, **79**, 6116 (1957).
7. I. Wender, S. Metlin, S. Ergun, H. W. Sternberg, and H. Greenfield, *J. Amer. Chem. Soc.*, **78**, 5401 (1956).
8. R. F. Heck and D. Breslow, *J. Amer. Chem. Soc.*, **83**, 4023 (1961).
9. M. Orchin and G. L. Karapinaka, *J. Org. Chem.*, **26**, 4187 (1961).
10. T. A. Manuel, *J. Org. Chem.*, **27**, 3941 (1962).
11. M. Johnson, *J. Amer. Chem. Soc.*, **85**, 4859 (1963).
12. Ya. T. Eidus, *Izvl. Akad. Nauk*, **1959**, 2195; *Chem. Abstr.*, **54**, 10822 (1960).
13. Ya. R. Levina and F. F. Tzurikov, *Zh. Obshch. Khim. (USSR)*, **4**, 1254 (1934); *ibid.*, **7**, 747 (1937).
14. V. H. Dibeler and T. I. Taylor, *J. Chem. Phys.*, **16**, 1008 (1948).
15. Y. Amamiya, *Catalyst (Japan)*, **2**, 1 (1960).
16. J. F. Harrod and A. J. Chalk, *J. Amer. Chem. Soc.*, **86**, 1776 (1964).
17. R. E. Reinhart and R. W. Fuest, *Chem. Eng. News*, **43**, No. 7, 40 (Feb. 15, 1965).
18. A. Shimizu, T. Otsu, K. Itakura, and M. Imoto, unpublished results.
19. M. Iwamoto and S. Yukuchi, *Bull. Chem. Soc. Japan*, **40**, 159 (1967).
20. E. L. Erasova, B. A. Krentsel, N. A. Pokatilo, and A. V. Topchiev, *Vysokomol. Soedin.*, **4**, 1796 (1962).

Received January 31, 1969

Revised April 14, 1969

Monomer-Isomerization Polymerization. VI.

Isomerizations of Butene-2 with TiCl_3 or $\text{Al}(\text{C}_2\text{H}_5)_3\text{-TiCl}_3$ Catalyst

AKIHIKO SHIMIZU, KEISUKE ITAKURA,
TAKAYUKI OTSU, and MINORU IMOTO

*Department of Applied Chemistry, Faculty of Engineering,
Osaka City University, Sumiyoshi-ku, Osaka, Japan*

Synopsis

A study of the isomerization of butene-2 with TiCl_3 or $\text{Al}(\text{C}_2\text{H}_5)_3\text{-TiCl}_3$ catalyst in *n*-heptane has been investigated at 60–80°C to elucidate further the mechanism of monomer-isomerization polymerization. It was found that positional and geometrical isomerizations in the presence of these catalysts occurred concurrently with activation energies of 14–16 kcal/mole. The presence of $\text{Al}(\text{C}_2\text{H}_5)_3$ with TiCl_3 catalyst could accelerate the initial rates of these isomerizations and initiate the monomer-isomerization polymerization of butene-2. From the results obtained, it was concluded that the isomerization of butene-2 proceeds via an intermediate σ -complex between the transition metal hydride and butene isomers.

INTRODUCTION

In the monomer-isomerization polymerizations of β -olefins by a coordinated anionic mechanism, isomerization to the respective α -olefins prior to the polymerization is necessary. Thus the catalyst system must contain two independent active centers for olefin isomerization and polymerization of the isomerized α -olefins.^{1–4} These assumptions have been confirmed in a recent paper⁴ by the remarkable accelerating effect of added isomerization catalysts to the monomer-isomerization polymerizations of butene-2 and pentene-2 with $\text{Al}(\text{C}_2\text{H}_5)_3\text{-TiCl}_3$ or $\text{Al}(\text{C}_2\text{H}_5)_3\text{-VCl}_3$ catalyst.

Olefin isomerizations can be classified into geometrical, positional, and skeletal isomerizations. Only the former two isomerizations have been known to occur in the presence of some transition metal compounds at temperatures below 100°C. In these polymerizations, the positional isomerization from β -olefin to α -olefin is important, and its mechanism is also related to monomer-isomerization polymerizations. The present paper describes results of isomerization of butene-2 in the presence of TiCl_3 or $\text{Al}(\text{C}_2\text{H}_5)_3\text{-TiCl}_3$ catalyst at 60–80°C.

Two alternative mechanisms for olefin isomerization in the presence of transition metal compounds have been presented: σ -complex formation^{5,6}

and π -allyl complex formation.⁷ The former mechanism was supported by us³ and Schindler,⁸ and the latter one by Iwamoto et al.⁹ for isomerization during the polymerization of butene-2. Marvel and Rogers¹⁰ suggested that the isomerization from octadecene-1 to octadecene-2 and -3 occurs through a six-membered transition state during the polymerization of octadecene-1 with the Ziegler catalyst.

EXPERIMENTAL

Materials

The *trans*- or *cis*-butene-2 (Matheson Co.) was dried over calcium hydride, followed by fractional distillation. Purities determined by gas chromatography, in which a benzyl ether column was used in a stream of hydrogen (30 ml/min) at 30°C, were 99.3 or 97.9 and 99.2%, respectively.

Triethylaluminum (Ethyl Corp.) and titanium trichloride (Stauffer Chem.) were used without further purification.

n-Heptane was purified by washing with concentrated sulfuric acid, followed by drying over metallic sodium and distillation. Other solvents and precipitants were used after purification by conventional methods.

Isomerization Procedure

Isomerizations were carried out in sealed glass tubes according to the procedure described previously.³ After isomerization the tube was opened and the unreacted butenes were collected to analyze their compositions by gas chromatography as mentioned above. The contents of the tube were then poured into a large amount of isopropyl alcohol containing concentrated hydrochloric acid to precipitate the polymer produced.

RESULTS

Isomerizations by TiCl_3 Catalyst

The results of the isomerization of *trans*-butene-2 at 60, 70, and 80°C are summarized in Table I, and the changes in isomer distribution of butenes isomerized with reaction time are shown in Figures 1, 2, and 3, respectively. From Table I and Figures 1-3 it is clear that positional and geometrical isomerizations proceed concurrently, and that their rates increase with increasing TiCl_3 concentration and with the reaction temperature.

Figure 4 shows the Arrhenius plots of the initial rates of both positional (*trans*-butene-2 \rightarrow butene-1) and geometrical (*trans*-butene-2 \rightarrow *cis*-butene-2) isomerizations determined from the initial slopes in the appearances of butene-1 and *cis*-butene-2, respectively. The apparent activation energies obtained are summarized in Table II.

TABLE I
Results of Isomerization of *trans*-Butene-2 by TiCl_3 Catalyst in *n*-Heptane^a

Temp, °C	Time, hr	Composition of butenes recovered after reaction, %			
		Butane	Butene-1	<i>cis</i> - Butene-2	<i>trans</i> - Butene-2
60	0	0.4	0.1	1.6	97.9
	20	0.4	0.4	3.0	96.2
	30	0.3	0.4	3.7	95.6
	50	0.4	0.6	4.5	94.5
	70	0	0.4	0.1	1.6
70	20	0.4	0.5	3.2	95.9
	30	0.4	1.2	5.6	92.8
	40	0.4	1.2	5.3	93.1
	50	0.4	1.6	7.5	90.5
	80	0	0.4	0.1	1.6
80	10	0.4	0.6	2.6	96.4
	20	0.4	1.1	5.6	92.8
	30	0.5	1.3	6.1	92.1
	50	0.5	1.7	7.3	90.5
	80 ^b	0	0.3	0.0	0.4
80 ^b	2	0.3	0.1	0.5	99.1
	20	0.4	2.2	7.6	89.8
	52	0.6	3.9	15.6	79.9

^a $[\text{TiCl}_3] = 5.0 \times 10^{-2}$ mole/l. except as otherwise noted; [butene] = 6.0 mole/l.

^b $[\text{TiCl}_3] = 2.0 \times 10^{-1}$ mole/l.

TABLE II
Rate and Activation Energies of Isomerization of *trans*-Butene-2
by the Catalyst Systems Containing TiCl_3

Catalyst	Temp, °C	Positional isomerization (<i>trans</i> -butene-2 → butene-1)		Geometrical isomerization (<i>trans</i> → <i>cis</i>)	
		Initial rate, %/hr	Activation energy, kcal/mole	Initial rate, %/hr	Acti- vation energy, kcal/mole
TiCl_3	60	0.017	14	0.07	14
	70	0.020		0.12	
	80	0.054		0.22	
$\text{Al}(\text{C}_2\text{H}_5)_3$ - TiCl_3	60	0.1(0.13) ^a	14(22.5) ^a	0.3	16
	70	0.2		0.5	
	80	0.3(0.9) ^a		1.3	

^a Calculated on the basis of total amounts of butene-1 and polybutene-1 produced.

Isomerizations by $\text{Al}(\text{C}_2\text{H}_5)_3$ - TiCl_3 Catalyst

The results of isomerization of *trans*-butene-2 with $\text{Al}(\text{C}_2\text{H}_5)_3$ - TiCl_3 catalyst at 60, 70, and 80°C are shown in Table III. Comparison with the results with TiCl_3 alone (Table I) shows that positional and geometrical

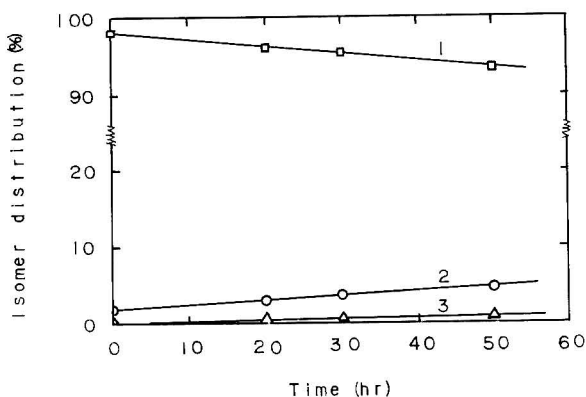


Fig. 1. Isomerization of *trans*-butene-2 with TiCl_3 catalyst at 60°C : (1) *trans*-butene-2; (2) *cis*-butene-2; (3) butene-1. $[\text{TiCl}_3] = 5.0 \times 10^{-2}$ mole/l.; [butene] = 6.0 mole/l.; in *n*-heptane.

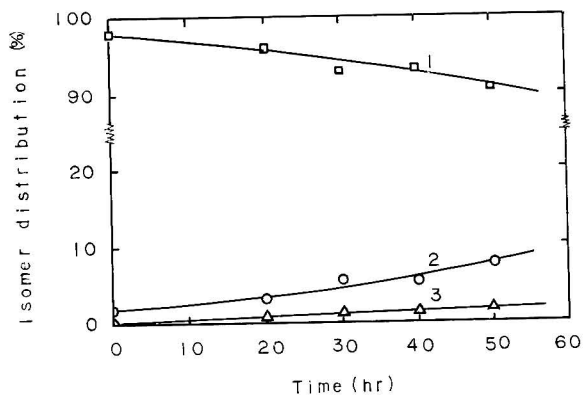


Fig. 2. Isomerization of *trans*-butene-2 with TiCl_3 catalyst at 70°C : (1) *trans*-butene-2; (2) *cis*-butene-2; (3) butene-1. $[\text{TiCl}_3] = 5.0 \times 10^{-2}$ mole/l.; [butene] = 6.0 mole/l.; in *n*-heptane.

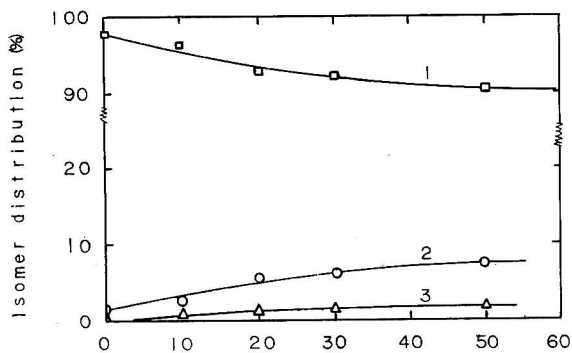


Fig. 3. Isomerization of *trans*-butene-2 with TiCl_3 catalyst at 80°C : (1) *trans*-butene-2; (2) *cis*-butene-2; (3) butene-1. $[\text{TiCl}_3] = 5.0 \times 10^{-2}$ mole/l.; [butene] = 6.0 mole/l.; in *n*-heptane.

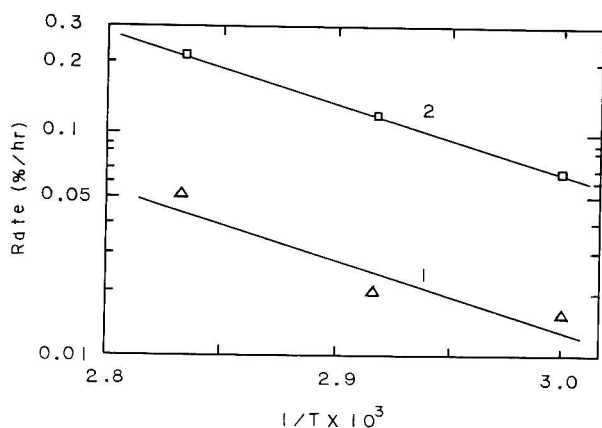


Fig. 4. Relationship between the rate and $1/T$ for the isomerization of *trans*-butene-2 with TiCl_3 catalyst: (1) positional isomerization; (2) geometrical isomerization.

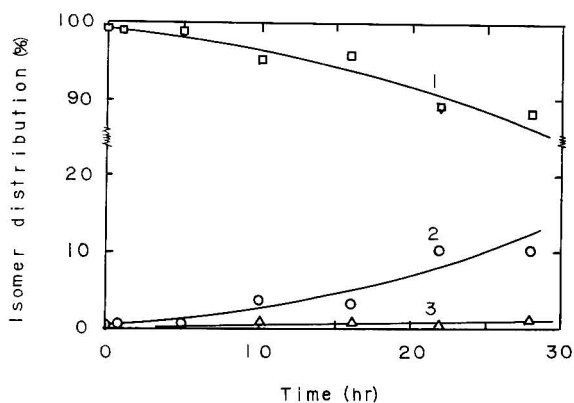


Fig. 5. Isomerization of *trans*-butene-2 with $\text{Al}(\text{C}_2\text{H}_5)_3\text{-TiCl}_3$ catalyst system at 60°C : (1) *trans*-butene-2; (2) *cis*-butene-2; (3) butene-1. $[\text{TiCl}_3] = 5.0 \times 10^{-2}$ mole/l.; $\text{Al/Ti} = 2.0$; $[\text{butene}] = 6.0$ mole/l., in *n*-heptane.

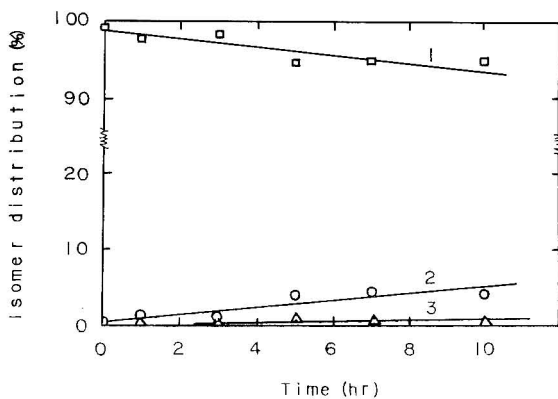


Fig. 6. Isomerization of *trans*-butene-2 with $\text{Al}(\text{C}_2\text{H}_5)_3\text{-TiCl}_3$ catalyst system at 70°C : (1) *trans*-butene-2; (2) *cis*-butene-2; (3) butene-1. $[\text{TiCl}_3] = 5.0 \times 10^{-2}$ mole/l.; $\text{Al/Ti} = 2.0$; $[\text{butene}] = 6.0$ mole/l.; in *n*-heptane.

TABLE III
Results of Isomerization of *trans*-Butene-2 by $\text{Al}(\text{C}_2\text{H}_5)_3\text{-TiCl}_3$
Catalyst ($\text{Al/Ti} = 2.0$) in *n*-Heptane^a

Temp, °C.	Time, hr	Yield of polymer, %	Composition of butenes recovered after reaction, %			
			Butane	Butene-1	<i>cis</i> - Butene-2	<i>trans</i> - Butene-2
60	0	—	0.3	0.0	0.4	99.3
	1	Trace	0.4	0.0	0.5	99.1
	5	Trace	0.4	0.0	0.6	99.0
	10	0.4	0.4	0.7	3.7	95.2
	16	0.0	0.4	0.6	3.1	95.9
	22	2.8	0.4	0.4	10.3	88.9
	28	2.4	0.5	1.1	10.0	88.4
70	0	—	0.3	0.0	0.4	99.3
	0.5	0	0.5	0.5	1.9	97.1
	0.8	0	0.4	0.0	2.6	97.0
	1	Trace	0.4	0.3	1.4	97.9
	3	Trace	0.4	0.2	1.1	98.3
	5	0.2	0.4	0.8	4.0	94.8
	7	0.3	0.4	0.4	4.3	94.9
	10	0.3	0.4	0.6	4.1	94.9
80	0	—	0.3	0.0	0.4	99.3
	0.1	0	0.4	0.6	0.8	98.2
	0.5	0	0.4	0.7	0.9	98.0
	1	Trace	0.4	0.6	1.1	97.9
	3	1.7	0.5	0.9	7.9	90.7
	5	3.1	0.5	1.5	9.8	88.2
	10	2.8	0.4	2.1	13.5	84.0
	16	4.9	0.5	2.2	17.0	80.3
22	6.2	0.6	2.3	18.9	78.2	

^a [Butene] = 6.0 mole/l.; $[\text{TiCl}_3] = 6.0 \times 10^{-2}$ mole/l. The catalyst was used after aging at 27°C for 1 hr.

TABLE IV
Results of Isomerization of *cis*-Butene-2 by $\text{Al}(\text{C}_2\text{H}_5)_3\text{-TiCl}_3$
Catalyst ($\text{Al/Ti} = 2.0$) in *n*-Heptane at 80°C^a

Time, hr	Conversion, %	Composition of butenes recovered after reaction, %			
		Butane	Butene-1	<i>cis</i> - Butene-2	<i>trans</i> - Butene-2
0	—	0.3	0.0	99.2	0.5
0.2	0	0.4	0.1	99.2	0.3
1	trace	0.4	0.1	98.6	0.9
3	trace	0.3	0.5	96.3	2.9
10	1.7	0.3	2.0	86.5	11.2
16	3.5	0.3	3.1	73.9	22.7
28	18.0	0.5	3.5	40.8	55.2

^a [Butene] = 6.0 mole/l, $[\text{TiCl}_3] = 5.0 \times 10^{-2}$ mole/l.

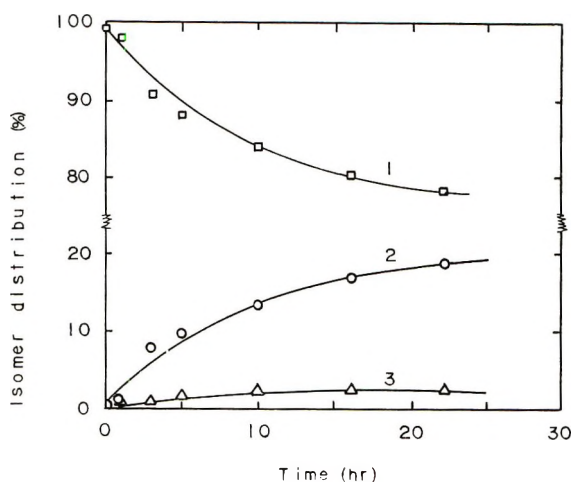


Fig. 7. Isomerization of *trans*-butene-2 with $\text{Al}(\text{C}_2\text{H}_5)_3\text{-TiCl}_3$ catalyst system at 80°C : (1) *trans*-butene-2; (2) *cis*-butene-2; (3) butene-1. $[\text{TiCl}_3] = 5.0 \times 10^{-2}$ mole/l.; $\text{Al/Ti} = 2.0$; $[\text{butene}] = 6.0$ mole/l.; in *n*-heptane.

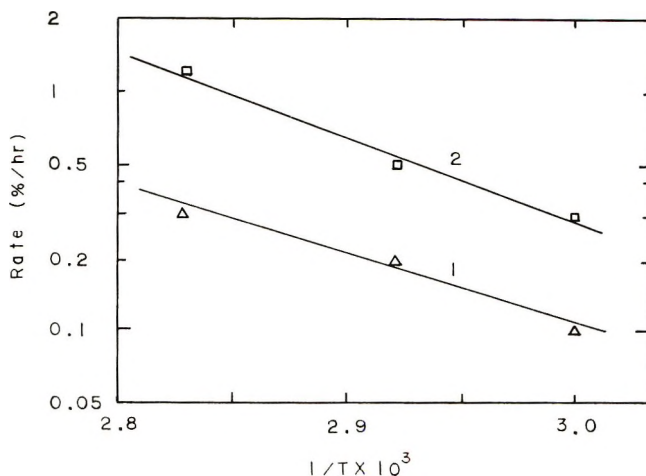


Fig. 8. Relationship between the rate and $1/T$ for the isomerization of *trans*-butene-2 with $\text{Al}(\text{C}_2\text{H}_5)_3\text{-TiCl}_3$ catalyst system: (1) positional isomerization; (2) geometrical isomerization.

isomerizations were accelerated in the presence of $\text{Al}(\text{C}_2\text{H}_5)_3$, and the yield of polybutene-1 increased as a function of time.

The plots of the concentrations of butene isomers and the reaction time at $60\text{--}80^\circ\text{C}$. are also shown in Figures 5-7. The initial rates of positional and geometrical isomerizations were determined as shown in Table II, from which the Arrhenius plots are also shown in Figure 8. The apparent activation energies obtained are also given in Table II.

In the positional isomerization, however, the part of butene-1 produced from isomerization was also consumed by polymerization. Accordingly,

the initial rates and the apparent activation energy were also calculated on the basis of the total yield of butene-1 and polybutene-1. The results are also shown in Table II.

As a comparison, the results of an isomerization started from *cis*-butene-2 in the presence of $\text{Al}(\text{C}_2\text{H}_5)_3\text{-TiCl}_3$ catalyst at 80°C are shown in Table IV.

DISCUSSION

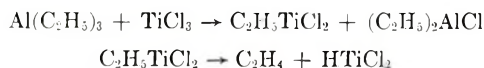
As can be seen from Table I, the concurrent isomerizations of *trans*-butene-2 to butene-1 and to *cis*-butene-2 took place without polymerization in the presence of TiCl_3 catalyst and the apparent activation energies for both isomerizations were identical (14 kcal/mole). The agreement of both the two activation energies might suggest that positional and geometrical isomerizations started from *trans*-butene-2 proceed via an identical intermediate.

In the presence of $(\text{C}_2\text{H}_5)_3\text{Al-TiCl}_3$ catalyst, the positional and geometrical isomerizations occurred simultaneously with polymerization (Table III), and these activation energies determined from the rate of appearance of butene-1 were 14–16 kcal/mole, in fairly good agreement with those in the presence of TiCl_3 alone. These results may suggest that the isomerizations of *trans*-butene-2 by the two catalysts occur by the same mechanism. However, the activation energy for positional isomerization, determined from the total yield of butene-1 and polybutene-1, were approximately obtained as 22.5 kcal/mole. This value may be considered to correspond to that for monomer-isomerization polymerization of *trans*-butene-2 as is seen from Table III.

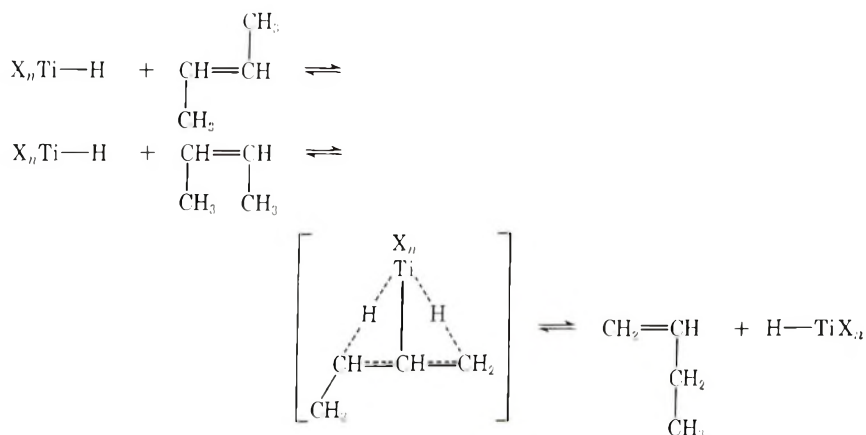
It was noted that the addition of $\text{Al}(\text{C}_2\text{H}_5)_3$ to TiCl_3 promoted the positional and geometrical isomerizations, i.e., $\text{Al}(\text{C}_2\text{H}_5)_3$ acted as a cocatalyst of these isomerizations and produced new active sites for the polymerization of butene-1.

As described above, if the isomerization of *trans*-butene-2 proceeds via a π -allyl complex or a six-membered transition state in which the initial catalyst system requires no hydride, only positional isomerization could be observed,^{5,7} and the geometrical isomerization from *trans*- to *cis*-butene-2 must proceed through an intermediate butene-1. This assumption was supported by Reinhart et al.⁷ from the fact that the concentration of butene-1 increased to about twice that of *cis*-butene-2 at the initial stage of the isomerization starting from *trans*-butene-2 in the presence of RhCl_3 or RuCl_3 in ethyl alcohol. The results in Tables I, III, and IV do not agree with the π -allyl complex mechanism.

On consideration of σ -complex formation mechanism for the present isomerization, the initial catalyst system must contain a hydride.^{5,6} One of these possibilities may be expected to be produced by an interaction of TiCl_3 with solvent or impurity. In the presence of $\text{Al}(\text{C}_2\text{H}_5)_3$, an intermediate titanium hydride may be formed through two ways: one is due to the presence of diethylaluminum hydride as an impurity in the $\text{Al}(\text{C}_2\text{H}_5)_3$ used, and the other is produced by the reaction of $\text{Al}(\text{C}_2\text{H}_5)_3$ with TiCl_3 .¹¹



Thus, if the catalysts used in this study contain a hydride, both positional and geometrical isomerizations of butenes may occur via a transition state.



A similar mechanism for butene isomerization with the Natta catalyst was proposed by Schindler.⁸

References

1. A. Shimizu, T. Otsu, and M. Imoto, *J. Polym. Sci. B*, **3**, 449 (1965).
2. A. Shimizu, T. Otsu, and M. Imoto, *J. Polym. Sci. B*, **3**, 1031 (1965).
3. T. Otsu, A. Shimizu, and M. Imoto, *J. Polym. Sci. A-1*, **4**, 1579 (1966).
4. T. Otsu, A. Shimizu, and M. Imoto, *J. Polym. Sci. A-1*, this issue.
5. T. A. Manuel, *J. Org. Chem.*, **27**, 3941 (1962).
6. G. L. Karapinka and M. Orchin, *J. Org. Chem.*, **26**, 4187 (1961).
7. R. E. Reinhart and R. W. Fuest, *Chem. Eng. News*, **43**, No. 7, **40** (Feb. 15, 1965).
8. A. Schindler, *Makromol. Chem.*, **90**, 284 (1966).
9. A. Iwamoto and S. Yuguchi, paper presented at the 13th Annual Meeting of Polymer Science of Japan, June 1964.
10. C. S. Marvel and J. R. Rogers, *J. Polym. Sci.*, **49**, 335 (1961).
11. M. Szwarc, *Fortschr. Hochpolym. Forsch.*, **2**, 275 (1960).

Received January 31, 1969

Revised April 14, 1969

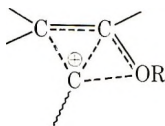
Cationic Polymerization of α,β -Disubstituted Olefins.

Part 12. Theoretical Consideration of the Reactivities of Vinyl Ethers and β -Substituted Vinyl Ethers

T. HIGASHIMURA, T. MASUDA, S. OKAMURA,
Department of Polymer Chemistry, and T. YONEZAWA,
Department of Hydrocarbon Chemistry, Kyoto University, Kyoto, Japan

Synopsis

To elucidate the propagation mechanism in the cationic polymerization of vinyl ethers and β -substituted vinyl ethers, the electron distribution in these monomers was computed by the extended Hückel method. Propylene and styrene derivatives were also studied in comparison with the vinyl ether derivatives. Attempts were made to explain the experimental results by various calculated reactivity indices. With the unsaturated hydrocarbons, the reactivity indices on the β -carbon parallel with the relative reactivity in the cationic polymerization or oligomerization. This agreement suggests that the transition state for the rate-determining step of the propagation reaction is represented by a model in which the carbonium ion interacts with the β -carbon of a monomer. On the other hand, the effect of β -alkyl or alkoxy groups on the reactivity of vinyl ethers could not be explained by the model in which the carbonium ion interacts with an olefinic carbon or an ether oxygen, or both with two atoms. The following model was proposed on the basis of the electronic stabilization energy due to the de-



localization from the occupied orbital of a monomer to the vacant orbital of a carbonium ion. This model can explain reasonably the relative reactivity of vinyl ethers and β -substituted vinyl ethers observed in the cationic copolymerization catalyzed by $\text{BF}_3 \cdot \text{O}(\text{C}_2\text{H}_5)_2$.

INTRODUCTION

In radical polymerization, α,β -disubstituted olefins are reluctant to polymerize because of the steric hindrance between the β -substituent in a growing polymer end and that in an incoming monomer, except in the case of cyclic compounds such as vinylene carbonate and maleimide. With a cationic catalyst, however, styrene and vinyl ether derivatives carrying the β -methyl group produced a high polymer. These results suggest that

the spatial position of the β -methyl group in the transition state of the propagation step in cationic polymerization is different from that in radical polymerization.¹

In cationic polymerization, the introduction of a β -methyl group has been found to reduce the reactivity of styrene derivatives^{1,2} but to increase the reactivity of vinyl ethers.³⁻⁵ For the reason of the opposing effects of the β -methyl group on the reactivity of styrene and vinyl ether derivatives, two possibilities should be considered; (1) the effect of β -methyl group on the electron distribution in monomer depends on the kind of monomer; (2) the conformation of transition state in the propagation reaction changes with the kind of monomer.

In the present work, to elucidate the rate-determining step in the propagation reaction, the electron distribution of vinyl ether derivatives, unsaturated hydrocarbons and related carbonium ions was calculated by the extended Hückel method,⁶ because the simple Hückel method leaves some ambiguities in the parametrization for alkyl groups and in the study on the reactivity of geometric isomers. The validity of the calculated value of the π -electron distribution has been confirmed in the previous paper⁷ by the chemical shifts in the C-13 NMR spectrum of the β -carbon. By using the value of the electron distribution in a monomer, several reactivity indices were calculated by the same treatment as in the simple Hückel method. A possible reaction mechanism is proposed on the basis of comparisons of the reactivity indices with the experimental results.

CALCULATION OF ELECTRON DISTRIBUTION

Method of Calculation

A molecular orbital is given as a linear combination of valence atomic orbitals on all atoms in a molecule.⁶ In this paper, the following values were used for the Coulomb integrals; H (1s), -13.60 eV; C (2s), -21.43 eV; C (2p), -11.42 eV; O (2s), -35.30 eV; O (2p), -15.45 eV. The resonance integral H_{ij} was approximated by eq. (1):

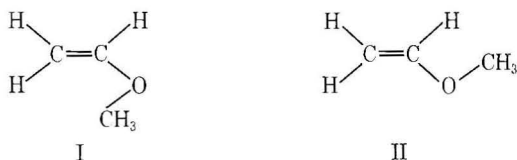
$$H_{ij} = 0.5 K (H_{ii} + H_{jj}) S_{ij} \quad (1)$$

with $K = 1.75$, where H_{ii} and H_{jj} are the Coulomb integrals, and S_{ij} is the overlap integral which was calculated by using Slater atomic orbitals.

The geometric structure of vinyl ether derivatives was described by the bond distance and the bond angle as following; saturated C—H, 1.09 Å; unsaturated C—H, 1.08 Å, C—C, 1.54 Å; C=H, 1.35 Å, saturated C—O, 1.427 Å; unsaturated C—O, 1.42 Å; the tetrahedral angle 109°28' for a saturated carbon, the trigonal angle 120° for an unsaturated carbon; and 107° for ether oxygen \angle COC. The bond distance and the bond angle used for unsaturated hydrocarbons were the same as those for vinyl ether derivatives except for unsaturated C—H; 1.07 Å, C=C, 1.34 Å; C—C in aromatics, 1.39 Å; and unsaturated C—C₆H₅ (aromatics), 1.47 Å. For calculations on a carbonium ion, the bond distance between C⁺ and an adjacent

carbon atom was assumed to be 1.54 Å; other values were the same as those for the corresponding monomer molecule. Although the calculation was based on approximate values of bond distance and bond angle, the relative electron distribution and the relative reactivity indices may deserve discussion.

The electron distribution in vinyl ethers and their derivatives was computed for the conformation in which a hydrogen atom of a methyl group eclipses the olefinic double bond as well as the unsaturated hydrocarbons. Problems arise with the conformation of the methyl vinyl ether. The presence of rotational isomers around the C—O bond were observed by the infrared spectrum of methyl vinyl ether. Owen et al.⁹ reported that methyl vinyl ether existed predominantly in the *s-cis* form (I) in gas phase, and the *s-trans* form (II) was stabilized in polar solvents at room temperature. Also, Mikawa et al.¹⁰ confirmed the existence of rotational isomers in *cis*- β -chlorovinyl methyl ether.



Although the *s-cis* form has been found to predominate in methyl vinyl ether, the *s-cis* form seems unstable because of steric interaction between an alkoxy group and a β -hydrogen, in particular, when an alkyl group becomes bulkier and branched. Therefore, to simplify the calculation, only the *s-trans* form was considered in this paper for all vinyl ether derivatives, including methyl vinyl ether.

For the computation of the electron distribution in unsaturated hydrocarbons, the conformation in which the hydrogen atom of a methyl group eclipses the olefinic double bond was assumed according to Hoffmann's result.⁶

Results of Calculations

Table I shows the atomic population (M_x) on the olefinic carbons and the ether oxygen. M_x is defined by eq. (2) and corresponds to the total electron density,

$$M_x = \sum_r^x N_r \quad (2)$$

where N_r is the atomic orbital population given by eq. (3), and C_r^j and C_s^j are the coefficients of the r th and s th atomic orbitals in the j th molecular orbitals.

$$N_r = 2 \sum_j^{\text{occ}} \sum_s C_r^j C_s^j S_{rs} \quad (3)$$

TABLE I
Atomic Population and Atomic Orbital Population of Vinyl Ethers and β -Substituted Vinyl Ethers

Monomer	Atomic population			Atomic orbital population of π -orbital			Atomic orbital population of highest occupied level in π -orbital		
	C_β	C_α	O	C_β	C_α	O	C_β	C_α	O
β α $CH_2=CHOCH_3$	4.3838	3.5410	6.9690	1.1312	0.9200	1.9438	0.5331	0.3385	0.1150
<i>cis</i> - $CH_3CH=CHOCH_3$	4.1546	3.6688	6.9718	1.0426	1.0389	1.9493	0.4060	0.4033	0.0851
<i>trans</i> - $CH_3CH=CHOCH_3$	4.1548	3.6674	6.9745	1.0409	1.0370	1.9515	0.4005	0.3970	0.0911
<i>cis</i> - $C_2H_5CH=CHOCH_3$	4.1739	3.6672	6.9718	1.0437	1.0384	1.9492	0.3667	0.3860	0.0762
<i>trans</i> - $C_2H_5CH=CHOCH_3$	4.1738	3.6657	6.9747	1.0420	1.0363	1.9515	0.3609	0.3778	0.0829
<i>cis</i> - $CH_3OCH=CHOCH_3$	3.6683	3.6683	6.9721	1.0422	1.0422	1.9525	0.3385	0.3985	0.0952
<i>trans</i> - $CH_3OCH=CHOCH_3$	3.6714	3.6714	6.9665	1.0419	1.0419	1.9327	0.3975	0.3975	0.0961
$CH_2=CHOCC_2H_5$	4.3841	3.5394	6.9776	1.1316	0.9197	1.9438	0.5160	0.3255	0.1262

TABLE II
 Atomic Population and Atomic Orbital Population of Unsaturated Hydrocarbons

Monomer	Atomic population		Atomic orbital population of π -orbital		Atomic orbital population of highest occupied level in π -orbital	
	C $_{\beta}$	C $_{\alpha}$	C $_{\beta}$	C $_{\alpha}$	C $_{\beta}$	C $_{\alpha}$
β α CH ₂ =CHCH ₃	4.3807	4.0210	1.1277	0.9197	0.5389	0.3451
<i>cis</i> -CH ₃ CH=CHCH ₃	4.1533	4.1533	1.0433	1.0433	0.4209	0.4209
<i>trans</i> -CH ₃ CH=CHCH ₃	4.1489	4.1489	1.0390	1.0390	0.4017	0.4017
CH ₂ =CH(CH ₃) ₂	4.4880	3.8263	1.2264	0.8563	0.5880	0.2839
CH ₂ =CHC ₆ H ₅	4.3255	4.0751	1.0545	0.9598	0.2878	0.0983
<i>trans</i> -CH ₃ CH=CHC ₆ H ₅	4.0804	4.1958	0.9509	1.0692	0.2656	0.1917

When M_x is larger than 1, 4, and 6 for hydrogen, carbon, and oxygen atoms, respectively, the atom is more electron-rich than the neutral atom.

For the styrene and propylene derivatives, M_x values on the olefinic carbons are shown in Table II. In the unsaturated hydrocarbons as well as the vinyl ether derivatives, M_x on the β -carbon decreased and M_x on the α -carbon increased with on introducing an electron-donating group on the β -carbon.

It is very difficult to confirm the reliability of values shown in Tables I and II, because we have no direct method to measure the electron density. However, as reported in the previous paper,⁷ the values of the atomic orbital population in the π -orbital were closely correlated with the chemical shift of the C-13 NMR spectrum of the olefinic β -carbon. Since the C-13 NMR spectrum undergoes an upfield shift with increasing π -electron density,^{11,12} the calculations for the vinyl ether derivatives prove to be reasonable for the prediction of the electron distribution. Also, in the aliphatic unsaturated hydrocarbons, a downfield shift of the C-13 NMR spectrum of the olefinic β -carbon and an upfield shift of the olefinic α -carbon resulted on introduction of an alkyl group on the olefinic β -carbon.¹³ This fact also supported the validity of the calculated electron distribution for propylene derivatives. Although there have been no reports on the C-13 NMR spectrum of styrene derivatives, the calculated values would be reasonable in analogy with the vinyl ether and the propylene derivatives.

REACTIVITY INDICES

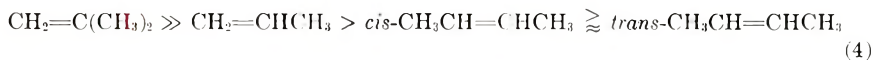
By using the calculated value of the electron distribution, reactivity indices for an electrophilic reaction were calculated by a procedure similar to the simple Hückel method.

Electrostatic Method

The carbonium ion will attack the atom with the largest electron density in the cationic polymerization where the electrophilic addition reaction to

a monomer takes place. Therefore, the reactivity of monomer may be estimated from the values of the atomic population (M_r) shown in Tables I and II. However, since the polymerization is caused by the interaction of an electrophilic reagent with the π -electron of a monomer, the monomer reactivity estimated from the atomic orbital population of the π -orbital should be more suitable for predicting the monomer reactivity than that from the atomic population. Tables I and II also show the values of the atomic orbital population of the π -orbital. As shown in Tables I and II the values of the atomic orbital population show the same tendency as the values of the atomic population.

In general, the relative reactivities of unsaturated hydrocarbons in the cationic polymerization or oligomerization tend to decrease in the following order:^{1,2,14}



Either the values of the atomic population or the values of atomic orbital population in π -orbital coincided with the order of the relative reactivities of monomers shown in (4) and (5). Although the values of the atomic population and the atomic orbital population on the β -carbon were in agreement with the order of reactivities of styrene and β -methylstyrene, the atomic population on the α -carbon of β -methylstyrene was larger than that of the β -carbon as shown in Table II, which predicts the α -carbon atom undergoes electrophilic attack. Experimentally, attack by an electrophilic reagent on the β -carbon was observed.¹⁵ This discrepancy could be explained by the frontier electron density¹⁶ as described below.

On the other hand, in the vinyl ether derivatives, there was no correlation between the atomic population or the atomic orbital population and the relative reactivity of monomers.

Frontier Electron Method

The reactivity of an electrophilic reagent may be discussed more reasonably on the basis of the partial atomic orbital population of the highest occupied level in the molecular orbitals than on the basis of the atomic population or the atomic orbital population. As shown in the last column of Tables I and II, the value of the partial atomic orbital population in the highest occupied level is in agreement with the experimental results for the unsaturated hydrocarbons and shows that the carbonium ion will attack the β -carbon even in β -methylstyrene. Nevertheless, the relative reactivity of the vinyl ether derivatives is not satisfactorily explained by the value of the partial atomic orbital population of the highest occupied level.

Total Electron Energy

The total electron energy of a monomer or a carbonium ion is given by eq. (6), where ϵ_i is the energy of the i th molecular orbital. Table III shows

TABLE III
 Total Electron Energy

Monomer	Total electron energy, eV		
	Monomer	Carbonium ion	$E_C^+ - E_M^a$
$\text{CH}_2=\text{CHOCH}_3$	-450.380	-559.106	-108.726
<i>cis</i> - $\text{CH}_3\text{CH}=\text{CHOCH}_3$	-554.734	-662.965	-108.231
<i>trans</i> - $\text{CH}_3\text{CH}=\text{CHOCH}_3$	-554.745	-662.965	-108.220
<i>cis</i> - $\text{C}_2\text{H}_5\text{CH}=\text{CHOCH}_3$	-659.031	—	—
<i>trans</i> - $\text{C}_2\text{H}_5\text{CH}=\text{CHOCH}_3$	-659.041	—	—
<i>cis</i> - $\text{CH}_3\text{OCH}=\text{CHOCH}_3$	-689.726	—	—
<i>trans</i> - $\text{CH}_3\text{OCH}=\text{CHOCH}_3$	-689.669	—	—
$\text{CH}_2=\text{CHOC}_2\text{H}_5$	-554.926	-663.770	-108.845
$\text{CH}_2=\text{CHCH}_3$	-315.362	-424.222	-108.860
<i>cis</i> - $\text{CH}_3\text{CH}=\text{CHCH}_3$	-419.661	-528.244	-108.582
<i>trans</i> - $\text{CH}_3\text{CH}=\text{CHCH}_3$	-419.805	-528.244	-108.439
$\text{CH}_2=\text{C}(\text{CH}_3)_2$	-419.865	-528.979	-109.113
$\text{CH}_2=\text{CHC}_6\text{H}_5$	-703.028	—	—
<i>trans</i> - $\text{CH}_3\text{CH}=\text{CHC}_6\text{H}_5$	-807.479	—	—

⁺
^a Total electron energy of CH_3 group; planar type -110.001 eV; tetrahedral type, -108.984 eV.

the total electron energy of monomers and their related carbonium ion

$$E = 2 \sum_i^{\text{occ}} \epsilon_i \quad (6)$$

assuming a structure with a methyl group on the β -carbon for simplicity. For example, structure III was proposed for a carbonium ion produced from *trans*-methyl propenyl ether. As the carbonium ion (IV) formed from *cis*-isomer should be very unstable, the structure of the carbonium ion (III) was assumed also for the *cis*-methyl propenyl ether carbonium ion.



The difference between the total electron energy of a carbonium ion and that of monomer ($E_C^+ - E_M$) corresponds to the heat of a reaction, because the sum of E_M and the electron energy of the methyl carbonium ion corresponds to the total electron energy of the initial system, and E_C^+ to that of the reaction product, respectively. If the same reaction mechanism applies to each monomer, the value of ($E_C^+ - E_M$) may serve as an index of the activation energy. On introducing a methyl group onto the β -carbon of an olefinic double bond, the difference $E_C^+ - E_M$ is reduced by 0.4 eV to 0.5 eV, as shown in the last column of Table III. The results of calculation were in agreement with the experimental results for unsaturated hydrocarbons but not for the vinyl ether derivatives.

TABLE IV
Superdelocalizability (S_r^E) and Delocalization Energy for Complex Formation (ΔE) of Vinyl Ethers and β -Substituted Vinyl Ethers.

Monomer	$S_r^E \times 10^3, \text{eV}^{-1}$			$\Delta E \times 10^3, \gamma/\text{eV}$				
	C_β	C_α	0	$C_\beta + C_\alpha$	$C_\beta + 0$	$C_\alpha + 0$	$C_\alpha + C_\beta + 0$	
$\text{CH}_2=\text{CHOCCH}_3$	3.6089	2.6501	6.5115	12.2004	7.5585	9.2771	16.2655	
<i>cis</i> - $\text{CH}_3\text{CH}=\text{CHOCCH}_3$	3.2931	3.2575	6.5512	12.7360	7.2791	9.5797	16.4935	
<i>trans</i> - $\text{CH}_3\text{CH}=\text{CHOCCH}_3$	3.2934	3.2583	6.5801	12.7504	7.3139	9.5279	16.4655	
<i>cis</i> - $\text{C}_2\text{H}_5\text{CH}=\text{CHOCCH}_3$	3.2953	3.2599	6.5588	12.8001	7.2911	9.5833	16.4869	
<i>trans</i> - $\text{C}_2\text{H}_5\text{CH}=\text{CHOCCH}_3$	3.2952	3.2545	6.5797	12.7411	7.1774	9.5298	16.4595	
<i>cis</i> - $\text{CH}_3\text{OCH}=\text{C}(\text{H})\text{OCCH}_3$	3.2310	3.2310	6.5272	12.5289	9.4186	9.4186	—	
<i>trans</i> - $\text{CH}_3\text{OCH}=\text{C}(\text{H})\text{OCCH}_3$	3.2302	3.2302	6.5855	12.5303	9.5006	9.5006	16.2883	
$\text{CH}_2=\text{CHOC}_2\text{H}_5$	3.6106	2.6484	6.5122	12.2010	7.5711	9.2670	16.3681	

Superdelocalizability

The stabilization energy due to the hyperconjugation of π -electrons in the transition state is approximately proportional to the superdelocalizability.¹⁷ Here, the superdelocalizability for the electrophilic reaction in the extended Hückel method, S_r^E , is tentatively given in eq. (7), where C_r^j is the coefficient of the r th $p\pi$ -atomic orbital in the j th π -molecular orbital.

$$S_r^E = 2 \sum_j^{\text{occ}} (C_r^j)^2 / -\epsilon_j \quad (7)$$

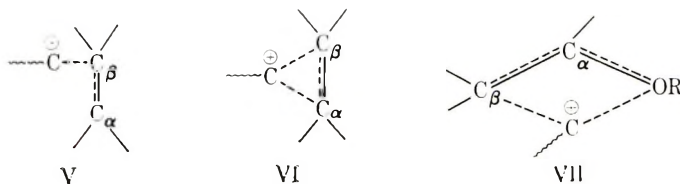
The calculated values of S_r^E are summarized in Tables IV and V for vinyl ether derivatives and unsaturated hydrocarbons, respectively. According to the definition of eq. (7), the position with a large S_r^E in a monomer is attacked by a carbonium ion, and a molecular consisting of atoms having a larger S_r^E value is more reactive than one having atoms with a small S_r^E value. As shown in Tables IV and V, S_r^E can explain the reactivity of the unsaturated hydrocarbons, but not the vinyl ether derivatives. This situation has been met with other reactivity indices.

TABLE V
Superdelocalizability (S_r^E) and Delocalization Energy for
Complex Formation (ΔE) of Unsaturated Hydrocarbons

Monomer	$S_r^E \times 10^3, \text{ eV}^{-1}$		$\Delta E \times 10^2,$
	C_β	C_α	γ/eV
$\text{CH}_2=\text{CHCH}_3$	3.5913	2.6549	12.2261
<i>cis</i> - $\text{CH}_3\text{CH}=\text{CHCH}_3$	3.2806	3.2806	12.7335
<i>trans</i> - $\text{CH}_3\text{CH}=\text{CHCH}_3$	3.2601	3.2601	12.7135
$\text{CH}_2=\text{C}(\text{CH}_3)_2$	4.0873	2.3964	12.4095
$\text{CH}_2=\text{CHC}_6\text{H}_5$	3.3514	2.6986	11.6351
<i>trans</i> - $\text{CH}_3\text{CH}=\text{CHC}_6\text{H}_5$	2.9633	3.2556	11.9209

Stabilization Energy due to Delocalization

S_r^E represents the delocalization energy acquired in the interaction of a carbonium ion with one atom in a monomer as shown in structure V. The alternatives, however, can be considered as a model for the interaction between a carbonium ion and a monomer, for example, the structure VI, in which a carbonium ion forms a complex with two olefinic carbon atoms,⁴ or the structure VII, in which a carbonium ion interacts with the β -carbon and the ether oxygen.⁸



The π electronic stabilization energy (ΔE) accompanying the delocalization (a complex formation) from the occupied orbital of the r th, s th atoms and so on to the vacant orbital of the carbonium ion is approximately given by eq. (8),¹⁸ where γ is the resonance integral between the electron acceptor and donor and is assumed for simplicity to be constant for any type of interactions. ΔE values are summarized in Tables IV and V, where the

$$\Delta E = \sum_j^{\text{occ}} [2(C_r^j + C_s^j + \dots)^2 / -\epsilon_j] \gamma \quad (8)$$

atoms indicated on the second top row are those assumed to have interaction with carbonium ion. ΔE values shown in the $(C_\alpha + C_\beta)$ column do not explain the reactivity order of unsaturated hydrocarbons, whereas those in the $(C_\alpha + C_\beta + O)$ column describe well the reactivity of vinyl ether derivatives. The latter will be discussed in more detail in the next section.

DISCUSSION

With the unsaturated hydrocarbons, a satisfactory parallel was found between the relative reactivity in the cationic polymerization and the various reactivity indices on the β -carbon of a monomer. However, ΔE - $(C_\alpha + C_\beta)$ did not explain the relative reactivity of monomers. These results suggest that the transition state for the rate-determining step in the propagation reaction is depicted by the structure V, in which the carbonium ion interacts with the β -carbon of the monomer, but not by the structure VI, in which the carbonium ion forms a complex with the α - and β -carbons.

On the other hand, in the vinyl ether derivative, the introduction of an electron-donating group on the β -carbon did not decrease the reactivity of vinyl ethers except for a monomer with a bulky α - and/or β -substituent. Table VI shows the relative reactivity of vinyl ether derivatives obtained in the copolymerization catalyzed by $\text{BF}_3 \cdot \text{O}(\text{C}_2\text{H}_5)_2$ at low temperatures.¹⁹ Considering the interaction of a carbonium ion only with the β -carbon in a monomer, the reactivity indices showed that the introduction of a β -substituent decreased the reactivity of the vinyl ether derivatives as well as of the unsaturated hydrocarbons. Therefore, the transition state in the propagation reaction of the vinyl ether derivatives could not be explained by the model V. Also, S_r^E values with respect to the α -carbon or the ether oxygen did not explain the relative reactivity of the vinyl ether derivatives as shown in Table VI.

Therefore, we should discuss structures by which the carbonium ion interacts with two or three atoms in a monomer to explain the relative reactivity of the vinyl ether derivatives. For structure VI, in which the carbonium ion reacts with the α - and β -carbons, $\Delta E(C_\alpha + C_\beta)$ could not explain the increase of the reactivity on introducing the β -methoxyl group and the reactivity difference between methyl and ethyl vinyl ethers. In structure VII proposed by Ledwith et al.,⁸ $\Delta E(C_\beta + O)$ does not increase on introduction of the β -methyl group. Moreover, as the sign of the coefficient

TABLE VI
Comparison between Relative Reactivity and Superdelocalizability (S_r^E) or Delocalization Energy
for Complex Formation (ΔE) of Vinyl Ether Derivatives in Cationic Polymerization

	Methyl and ethyl vinyl ether (MVE and EVE)	MVE, methyl propenyl ether (MPE) and 1,2-dimethoxyethylene (DME)	MVE and methyl butenyl ether (MBE)
Experimental result ^a	MVE < EVE	$trans\text{-DME} \lesssim MVE \lesssim trans\text{-MPE} < cis\text{-MPE} < cis\text{-DME}$	$trans\text{-MBE} < MVE < cis\text{-MBE}$
S_r^E	MVE \lesssim EVE	$trans\text{-DME} \approx cis\text{-DME} < trans\text{-MPE} \approx cis\text{-MPE} < MVE$	$trans\text{-MBE} \approx cis\text{-MBE} < MVE$
C_β	EVE \lesssim MVE	$MVE < trans\text{-DME} \approx cis\text{-DME} < trans\text{-MPE} \lesssim cis\text{-MPE}$	$MVE < trans\text{-MBE} < cis\text{-MBE}$
C_α	MVE \approx EVE	$MVE < cis\text{-DME} < cis\text{-MPE} < trans\text{-MPE} < trans\text{-DME}$	$MVE < cis\text{-MBE} < trans\text{-MBE}$
O	MVE \approx EVE	$MVE < cis\text{-DME} \lesssim trans\text{-DME} < cis\text{-MPE} < trans\text{-MPE}$	$MVE < trans\text{-MBE} < cis\text{-MBE}$
ΔE	MVE < EVE	$cis\text{-MPE} < trans\text{-MPE} < MVE < cis\text{-DME} < trans\text{-DME}$	$trans\text{-MBE} < cis\text{-MBE} < MVE$
	EVE < MVE	$MVE < cis\text{-DME} < trans\text{-DME} < trans\text{-MPE} < cis\text{-MPE}$	$MVE < trans\text{-MBE} < cis\text{-MBE}$
	MVE < EVE	$MVE < trans\text{-DME} < trans\text{-MPE} < cis\text{-MPE} < cis\text{-DME}$	$MVE < trans\text{-MBE} < cis\text{-MBE}$

^a Catalyst, $BF_3 \cdot O(C_2H_5)_2$, polymerization temperature, $-78^\circ C$.¹⁷

of the highest occupied atomic orbital of olefinic carbons is different from that of ether oxygen, $\Delta E(C_\beta + O)$ is small and structure VII is not suitable as the model of the transition state. For the same reason, $\Delta E(C_\alpha + O)$ gave a small value. For this structure, the increase of the reactivity due to the introduction of a β -methoxyl group and the higher reactivity of ethyl vinyl ether compared to methyl vinyl ether could not be explained.

Structure VIII was proposed for the transition state to explain the relative reactivity of the vinyl ether derivatives.



As *cis*-1,2-dimethoxyethylene has two ether oxygen atoms on the same side of the olefinic double bond, structure IX was assumed for the transition state. Further studies are necessary for a direct comparison of $\Delta E(C_\alpha + C_\beta + O)$ with $\Delta E(C_\alpha + C_\beta + 2O)$, because the resonance integral might not be the same in VIII and IX. However, it is very likely that IX has a larger delocalization energy than VIII.

The value of $\Delta E(C_\alpha + C_\beta + O)$ showed good agreement with the relative reactivity of the vinyl ether derivatives in the cationic copolymerization as shown in Table VI. The lower reactivities of *trans*-methyl butenyl ether and *trans*-1,2-dimethoxyethylene compared to the calculated values may be due to the steric hindrance of the β -substituent. Therefore, VIII or IX is expected to represent the structure of the transition state in the propagation reaction in the cationic polymerization of the vinyl ether derivatives. This conclusion is also supported by the fact that steric hindrance of the β -substituent in the cationic polymerization of the vinyl ether derivatives is of minor importance.

References

1. C. G. Overberger, D. H. Tanner, and E. M. Pearce, *J. Amer. Chem. Soc.*, **80**, 4566 (1958).
2. A. Mizote, T. Tanaka, T. Higashimura, and S. Okamura, *J. Polym. Sci. A*, **3**, 2567 (1965).
3. A. Mizote, S. Kusudo, T. Higashimura, and S. Okamura, *J. Polym. Sci. A-1*, **5**, 1927 (1967).
4. T. Okuyama, T. Fueno, and J. Furukawa, *J. Polym. Sci. A-1*, **6**, 993, 1001 (1968).
5. T. Higashimura, S. Kusudo, Y. Ohsumi, and S. Okamura, *J. Polym. Sci. A-1*, **6**, 2511 (1968).
6. R. Hoffmann, *J. Chem. Phys.*, **39**, 1397 (1963).
7. T. Higashimura, S. Okamura, I. Morishima, and T. Yonezawa, *J. Polym. Sci. B*, **7**, 23 (1969).
8. A. Ledwith and H. J. Woods, *J. Chem. Soc. B*, **1966**, 753.
9. N. L. Owen and N. Sheppard, *Trans. Faraday Soc.*, **60**, 634 (1964).
10. Y. Mikawa, S. Morita, and S. Tsumakawa, *Bull. Chem. Soc. Japan*, **35**, 1109 (1962).

11. M. Karplus and J. A. Pople, *J. Chem. Phys.*, **38**, 2803 (1963).
12. G. E. Maciel, *J. Phys. Chem.*, **69**, 1947 (1965).
13. R. E. Friedel and H. L. Retcofsky, *J. Amer. Chem. Soc.*, **85**, 1300 (1963).
14. R. L. Meier, *J. Chem. Soc.*, **1950**, 3656.
15. M. J. S. Dewar and R. C. Fahey, *J. Amer. Chem. Soc.*, **85**, 3645 (1963).
16. K. Fukui, T. Yonezawa, and H. Shiugu, *J. Chem. Phys.*, **20**, 722 (1952); *ibid.*, **22**, 1433 (1954).
17. K. Fukui, T. Yonezawa, and C. Nagata, *Bull. Chem. Soc. Japan*, **27**, 423 (1954).
18. K. Fukui, A. Imamura, T. Yonezawa, and C. Nagata, *Bull. Chem. Soc. Japan*, **34**, 1076 (1961).
19. T. Higashimura, J. Masamoto, and S. Okamura, *Kobunshi Kagaku*, **25**, 702 (1968) and unpublished data.

Received February 4, 1969

Revised April 15, 1969

Radiation-Induced Solid-State Polymerization of Methacrylic Acid. I. Crystalline Transition of the Monomer

YOSHIRO SAKAI* and MACHIO IWASAKI, *Government Industrial Research Institute, Nagoya, Kita-ku, Nagoya, Japan*

Synopsis

The anomalous crystalline transition of methacrylic acid found by broad-line NMR measurements was studied in connection with the build-up and decay of trapped radicals. The build-up of radicals is smaller and the decay rate of the trapped radicals is faster in the low-temperature range (phase II), which gave the narrower maximum slope distance ΔH_{msl} of the NMR spectrum, than those in the higher temperature range (phase I), which gave the broader ΔH_{msl} . From these experiments it was concluded that in phase I the crystals have a more closely packed structure, resulting in a more rigid matrix for the trapped radicals than those in phase II. This interpretation is consistent with the temperature dependence of the ESR spectrum of the trapped propagating radicals previously reported. The existence of the crystalline transition was also confirmed by DSC measurements, and the effects of the crystallization conditions on the transition were investigated and were discussed with reference to the results of broad line NMR measurements.

INTRODUCTION

Many workers have studied the solid-state polymerization of vinyl monomers. Some of them have studied the effect of crystal structures on the mechanism of polymerization. It is known that the structure of monomer crystals influences the mechanism of their polymerization or their rate of polymerization. When a crystalline polymer is formed from a crystalline monomer, it is a matter of course that the structure of monomer crystals affects the polymerization mechanism. On the other hand, even in the case of monomers giving amorphous polymers, e.g., solid methacrylic acid,^{1,2} it has been observed that the structure of the monomer crystals affects the rate of polymerization and the rate of free-radical formation. Bamford et al.³ have observed the temperature dependence of the rate of radical formation during the ultraviolet irradiation in the solid state and have reported that the maximum relative concentration of trapped radicals was obtained at -5°C . In addition, the ESR spectrum exhibits a structure depending on the irradiation temperature. An ordinary 9-line spec-

* Present address: Department of Industrial Chemistry, Faculty of Technology, Ehime University, Bunkyo-cho, Matsuyama, Ehime, Japan.

trum was observed when monomer crystals were irradiated above -5°C , while a 13-line spectrum was obtained between -5 and -30°C . This 13-line spectrum has been interpreted in terms of the nonequivalence of the methylene hydrogen atoms caused by the slight distortion from the symmetrical conformation of the methylene group to the half-filled p -orbital. The 13-line spectrum of methacrylate radical was assigned by O'Donnell et al.⁴ to a conformation which has the nonequivalent methylene hydrogen atoms. Fischer⁵ also postulated nonequivalence of methylene hydrogen atoms in order to interpret the 16-line spectrum of methacrylate radicals formed in aqueous redox systems. Bamford et al.⁶ believed that, during the solid-state polymerization below -5°C , geometrical constraints within the crystals force the radicals to adopt this conformation, which is maintained at this temperature on account of the reduced mobility below -5°C . Recently they⁶ have studied this system with broad line NMR and found transitions around -10°C and $+3^{\circ}\text{C}$. The transition at -10°C was considered to be related to the difference in the ESR spectrum. It was also proposed that below -10°C imperfect regions are formed in the crystals which favor the asymmetrical conformation giving the 13-line spectrum.

In our previous work⁷ broad-line NMR measurements were carried out over a wider temperature range (-150°C to $+10^{\circ}\text{C}$) and an anomalous transition was found around -30°C . Contrary to the ordinary cases, the maximum slope distance ΔH_{msl} is smaller in the lower-temperature region (phase II) than in the higher-temperature region (phase I). The temperature dependence of the ESR spectrum was investigated in connection with this anomalous transition. It was found that a 9-line spectrum observed below the transition point changes reversibly into a 13-line spectrum around the transition point. The change of the spectrum was interpreted on the basis of a hindered oscillation model assuming a lower hindering potential barrier in phase II than that in phase I.

In the present paper, the build-up and decay of the trapped free radicals were studied in relation to the anomalous crystalline transition. All the experimental results are well interpreted by assuming phase II to be loosely packed resulting in a softer matrix for the trapped radicals than phase I.

EXPERIMENTAL

Methacrylic acid monomer was purified by the method of Bamford et al.² The broad-line NMR was recorded with a Japan Electron Optics broad-line NMR spectrometer in the temperature range of -150°C to $+16^{\circ}\text{C}$ at 30 Mcps. For the ESR measurements the samples were degassed by repeated freezing and melting in a vacuum. Methacrylic acid was then distilled into Spectrosil ESR sample tubes which were sealed off under a pressure of 10^{-5} mm Hg. The samples were crystallized by shock cooling in liquid nitrogen. Irradiation was carried out at a dose rate of 1.75×10^4 R/hr. A Japan Electron Optics Model 3BSX spectrometer was used for recording the ESR spectrum at 9.4 Gcps with 100 Kcps modulation at -196°C . DSC measurements were carried out with a Perkin-Elmer

Model DSC-1B differential scanning calorimeter using sealed aluminum pans designed for volatile samples. For the radical decay measurements, the samples irradiated at -196°C were annealed in a cryostat for 5 min at the test temperature and cooled again to -196°C for the ESR measurements. For the measurements of the change of the radical concentration with irradiation time (radical build-up) the samples were crystallized at -196°C and then irradiated at various temperatures in a low-temperature cryostat. The relative radical concentration was obtained by double integration of the first-derivative ESR spectrum by use of a Japan Electron Optics Model JR-5 spectrum computer.

RESULTS AND DISCUSSION

Broad-Line NMR

Sample A was crystallized at -196°C by cooling the liquid rapidly from $+20^{\circ}\text{C}$ (mp $+16^{\circ}\text{C}$). The broad-line NMR spectra were observed at temperatures ranging from -150°C to $+10^{\circ}\text{C}$. Some of the spectra are shown in Figure 1a. The maximum slope distances ΔH_{msl} plotted against

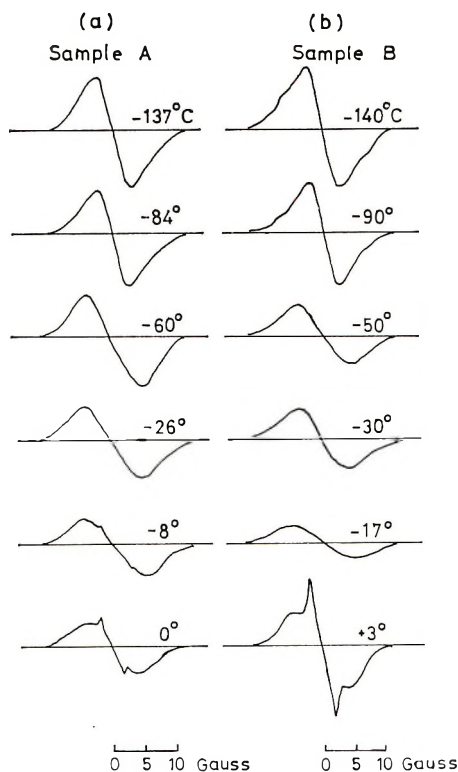


Fig. 1. Change with observation temperature of the broad-line NMR spectra of methacrylic acid: (a) sample cooled rapidly from liquid phase to -196°C ; (b) sample crystallized by keeping 1.5 hr at $+10^{\circ}\text{C}$ and cooling to -196°C .

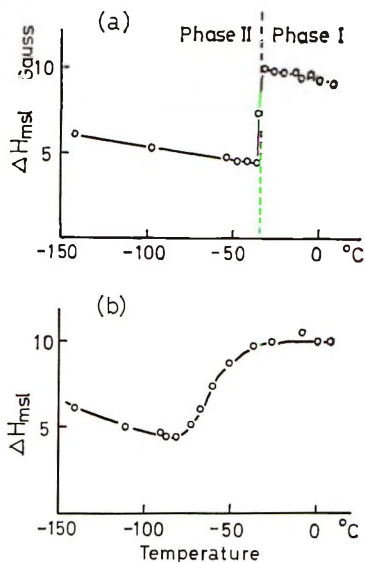


Fig. 2. Temperature dependence of ΔH_{msl} for methacrylic acid: (a) sample rapidly cooled to -196°C from the liquid phase; (b) sample crystallized by keeping 1.5 hr at $+10^{\circ}\text{C}$ and cooling to -196°C .

the temperature are shown in Figure 2a. ΔH_{msl} gradually decreased with increasing temperature from -196°C , but when the temperature reached ca. -30°C , ΔH_{msl} suddenly increased by about 5 gauss, followed by a gradual decrease up to around 0°C , at which temperature premelting started and a sharp component appeared overlapping the broad spectrum. In addition, this change took place reversibly when the sample was cooled very slowly around the transition point (e.g. $0.06^{\circ}\text{C}/\text{min}$ in our experiments), otherwise a sharp transition did not occur, as will be mentioned later in the case of sample B. This sudden change of ΔH_{msl} indicates the existence of a crystalline transition around -30°C . However, it should be noted that usually ΔH_{msl} of the broad line spectrum shows a sudden decrease in the high-temperature phase due to some motional effects. Contrary to the ordinary case, ΔH_{msl} is narrower in the low-temperature phase. This may mean that the dipolar interaction is stronger in phase I, possibly because the crystals are packed more closely than in phase II. However, another possibility should not be excluded, i.e., that some of the intermolecular $\text{H}\cdots\text{H}$ distances may become shorter due to the rearrangement of the molecules in the crystalline lattice. From this anomalous crystalline transition one may expect that the crystals in phase II act as a softer matrix for the trapped radicals than those in phase I.

In the study of the radiation-induced polymerization of methacrylic acid in the solid state, it was observed that the crystallization temperature affects the rate of polymerization. Monomer crystallized at $+10^{\circ}\text{C}$ (in-phase I) cooled to -196°C (in phase II) polymerized more rapidly than that crystallized by shock cooling to -196°C from the liquid phase. In

order to elucidate the effect of the crystallization conditions on the rate of polymerization, broad-line NMR measurements with samples crystallized under different conditions were carried out. Sample B was crystallized slowly at $+10^{\circ}\text{C}$ (phase I) for 1.5 hr and then rapidly cooled to -196°C . The broad-line NMR spectra obtained at several temperatures and the temperature dependence of ΔH_{msl} are shown in Figures 1*b* and 2*b*, respectively. As shown in Figure 2*b*, the change of ΔH_{msl} due to the crystalline transition started at a lower temperature (-80°C) than in the case of sample A but ended at the same temperature (-30°C). In the case of sample B rapidly cooled to -196°C (phase II) from $+10^{\circ}\text{C}$ (phase I), it is supposed that a small amount of crystals of phase I remained unchanged and admixed in crystals of phase II. Crystals of phase I may act as imperfections and lower the starting point of transition. As shown in Figure 2*b*, in the temperature range below the starting point of the transition, the spectrum has a weak shoulder due to the broad component of phase I. Since ΔH_{msl} of phase II is unusually small, phase II is considered to be more liquidlike and may have been achieved directly from the liquid phase in sample A without admixing the crystals of phase I. This may be the reason for the sharper transition in this case.

Odajima et al.⁸ have also observed the broad-line NMR spectrum of methacrylic acid, and reported a single-component spectrum with a ΔH_{msl} value of about 4 gauss which is almost constant in the temperature range of -196°C to $+10^{\circ}\text{C}$. However, in Figure 1 of their work⁸ one can see a weak shoulder having the ΔH_{msl} of 10 gauss at -196°C and -98°C , which is seemingly due to a small amount of crystals of phase I admixed in the crystals of phase II as observed in our experiment.

Bamford et al.⁶ have also studied the temperature dependence of the broad-line NMR spectra. They reported two transitions around -10°C and $+3^{\circ}\text{C}$ which we could not observe. These discrepancies may be due to differences of the crystallization or cooling conditions. For instance, according to the DSC measurements, to be discussed in the next section, the crystalline transition does not appear distinctly in slowly cooled samples.

Differential Scanning Calorimetry

Two samples were prepared. Sample 1 was crystallized by rapidly cooling to -196°C from the liquid phase. Sample 2 was cooled at rate of $0.625^{\circ}\text{C}/\text{min}$ from the liquid phase. DSC measurements were carried out by raising the temperature from -80°C to $+30^{\circ}\text{C}$ passing through the melting point. As shown in Figure 3, with sample 1 a sharp transition was observed around -15°C , while with sample 2 the transition occurred gradually over a wide range of temperature. The results of DSC measurements on samples 1 and 2 parallel the results of broad line NMR measurements on samples A and B. The above two different methods of observing the crystalline transition indicate that the appearance of the crystalline transition is greatly affected by the crystallization conditions and the thermal history of the crystals.

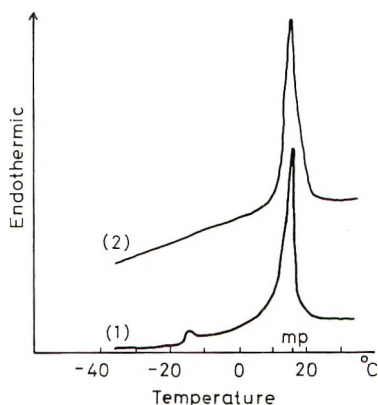


Fig. 3. DSC thermogram of methacrylic acid monomer: (1) sample rapidly cooled to -196°C from liquid phase; (2) sample cooled slowly from liquid phase at the rate of $0.625^{\circ}\text{C}/\text{min}$.

Radical Decay

The decay rate of the radical was expected to be different in the two crystalline phases. Therefore, the decay rate of the trapped radical was measured at several temperatures. The change of the relative radical concentration as a function of the annealing temperature is shown in Figure 4. As the annealing temperature increased from -196°C the radical concentration decreased gradually. Near -40°C the decay rate started to increase gradually to -30°C . Between -30°C and -10°C the decay rate became very slow. Above -10°C the radicals decayed very rapidly and completely disappeared around $+10^{\circ}\text{C}$. These results may be interpreted with the same postulates as made in the broad-line NMR experiments. Below -30°C (phase II) the crystals have a liquidlike structure and the trapped radicals decayed more easily than in phase I in the tem-

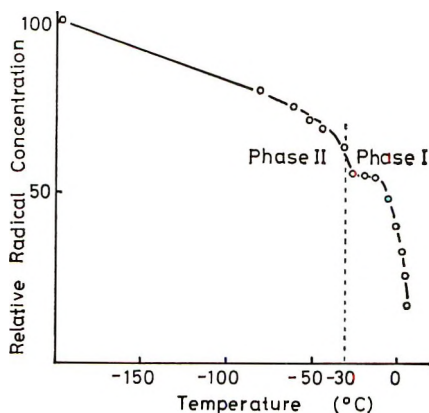


Fig. 4. Relative radical concentration vs. annealing temperature for methacrylic acid γ -irradiated at -196°C .

perature range between -30°C and -10°C . The increase of decay rate near the transition point is due to the molecular rearrangement which should accelerate the recombination of the trapped radicals. Above -10°C , as shown in NMR measurements, the premelting of the monomer crystals results in rapid decay of the radicals. Since it is known that the propagating radicals trapped in the polymer matrix are fairly stable,^{7,9} post-polymerization during the decay measurements produces some amount of polymers in which the decay rate is seriously affected. To judge from the results of the study of post-polymerization, however, the polymer yield during the radical decay measurements is less than 1%, which would little affect the decay of radicals.

Radical Build-Up

In Figure 5 the average rate of trapping of the radicals for the first few hours of irradiation is plotted against the irradiation temperature. There is a minimum below -30°C . This is clearly related to the fact that the decay rate below -30°C (in phase II) is faster than above -30°C , as shown in the previous section of radical decay. Near the transition point at -30°C the decay rate becomes very fast, and as a result the rate of trapping has a minimum at this temperature. On the other hand, between -30°C and -10°C the decay rate of radicals becomes slow, and as a result the concentration of radicals increases. According to the results of radical decay measurements, the radical concentration is expected to decrease

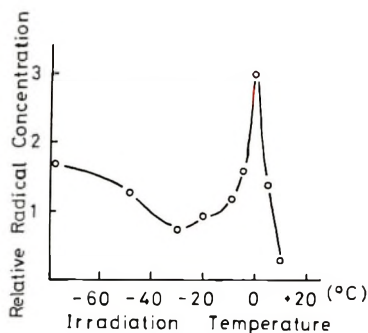


Fig. 5. Initial rate of radical trapping vs. irradiation temperatures for methacrylic acid.

above -10°C , as the decay rate increases again above -10°C . However, there appeared a maximum at 0°C in the build-up curve of the radicals. This disagreement with the results of radical decay may be interpreted as due to in-source polymerization near 0°C . At 0°C , 5% of polymer was formed on irradiation for 2 hr at a dose rate of 1.75×10^4 R/hr, while in the radical decay measurements the polymer content was less than 1%. The methacrylic acid radicals are much more stable in the polymer than in the crystalline monomer matrix. Consequently, at 0°C the radicals may become more stable in the case of radical build-up measure-

ments than in the case of radical decay measurements because of the difference of polymer content.

References

1. C. H. Bamford, A. D. Jenkins, and J. C. Ward, *J. Polym. Sci.*, **48**, 37 (1960).
2. C. H. Bamford, G. C. Eastmond, and J. C. Ward, *Proc. Roy. Soc. (London)*, **A271**, 357 (1963).
3. C. H. Bamford, G. C. Eastmond, and Y. Sakai, *Nature*, **200**, 1284 (1963).
4. J. H. O'Donnell, B. McGarvey, and H. Morawetz, *J. Amer. Chem. Soc.*, **86**, 2322 (1964).
5. H. Fischer, *Z. Naturforsch.*, **19a**, 866 (1964); *J. Polym. Sci. B*, **2**, 529 (1964).
6. C. H. Bamford, A. Bibby, and G. C. Eastmond, in *Macromolecular Chemistry, Prague, 1965* (*J. Polym. Sci. C*, **16**), O. Wichterle and B. Sedláček, Eds., Interscience, New York, 1967, p. 2417.
7. Y. Sakai and M. Iwasaki, *J. Polym. Sci. A-1*, in press.
8. A. Odajima, A. E. Woodward, and J. A. Sauer, *J. Polym. Sci.*, **55**, 181 (1961).
9. M. G. Ormerod and A. Charlesby, *Polymer*, **5**, 67 (1964).

Received February 26, 1969

Revised April 22, 1969

Thermal Decomposition Products of Poly(vinyl Alcohol)

YOSHIO TSUCHIYA and KIKUO SUMI, *Fire Section, Division of Building Research, National Research Council of Canada, Ottawa, Canada*

Synopsis

The thermal decomposition of poly(vinyl alcohol) is known to occur in two stages. In a study of first-stage decomposition, this polymer was pyrolyzed in vacuum at 240°C for 4 hr and the products were determined by using gas chromatography. The main products were water, aldehydes having the general formula $\text{HC}(\text{O})\text{-(CH=CH)}_n\text{CH}_3$, and

methyl ketones having the formula $\text{H}_3\text{C-C}(\text{O})\text{-(CH=CH)}_n\text{CH}_3$, where $n = 0, 1, 2, 3$, etc.

Mechanisms for the formation of these carbonyl compounds are discussed.

INTRODUCTION

The thermal decomposition of poly(vinyl alcohol) occurs in two stages.¹ The first stage, which begins at about 200°C, is mainly dehydration, accompanied by the formation of some volatile products; the residue is predominantly macromolecules having polyene structure. The published data on the volatile thermal decomposition products of this polymer are not only very limited, but are also conflicting. Yamaguchi and Amagasa² analyzed the products of the first-stage decomposition by chemical methods and found acetaldehyde, crotonaldehyde, benzaldehyde, and acetophenone. Kaesche-Krischer and Heinrich³ found formaldehyde, acetaldehyde, and acrolein. Ettre and Varadi⁴ used a pyrolysis-gas chromatographic technique and reported that the main organic products formed at a pyrolysis temperature of 500°C were acetaldehyde and acetic acid. They also found smaller amounts of ethanol, methyl acetate, and some hydrocarbons. At this temperature both stages of decomposition must have occurred. In second-stage decomposition of poly(vinyl alcohol), the macromolecules having polyene structure are degraded to produce carbon and hydrocarbons. Gilbert and Kipling⁵ analyzed the gases formed in the second-stage decomposition of vinyl polymers.

The authors of this paper are primarily interested in first-stage decomposition. The only important agreement in the data presented by others²⁻⁴ was the finding that acetaldehyde is one of the major products. The pur-

pose of the present investigation is to obtain more reliable information about the thermal decomposition products of poly(vinyl alcohol) by using the latest techniques in gas chromatography. The experimental data will be used to discuss the mechanism of thermal decomposition of poly(vinyl alcohol).

EXPERIMENTAL

Material

A commercial grade of poly(vinyl alcohol) (>99% hydrolysis) was dried at 80°C under vacuum for 48 hr, prior to pyrolysis. The molecular weight of the polymer was found to be about 130000 by a viscosity method.

Thermal Decomposition

The apparatus for the thermal decomposition of poly(vinyl alcohol) was similar to that used for a previous study.⁶ A sample weighing 1 g was placed in a Pyrex tube connected to a liquid nitrogen trap and a vacuum pump. After the system was evacuated to 1×10^{-4} mm Hg, the vacuum line to the pump was closed and the sample was heated at 240°C for 4 hr. Most of the volatile decomposition products were collected in a liquid nitrogen trap. When the liquid nitrogen was removed, the condensates in the trap separated into two layers: a water layer and an oil layer. The fraction volatile at room temperature was transferred from the trap into a gas sampling bottle of known volume. The three fractions were analyzed separately, and the combined amounts of each component were obtained.

The pyrolysis tube containing the solid residue was evacuated again, and the residue pyrolyzed at 450°C for 4 hr. The products from the second-stage decomposition were analyzed in the same way as those from the first-stage decomposition.

Analysis

The chromatographic conditions that were used to analyze the decomposition products are presented in Table I. The identification of the peaks was carried out as follows: (a) comparison of retention times with those of known compounds by use of three different columns; (b) collection of products that yield certain peaks by preparative gas chromatography, followed by chemical methods of identification; (c) determination of carbon structure of products by catalytic hydrogenation.⁷ For quantitative analysis, the areas under each peak were measured, and approximate substance correction factors were applied.⁸

RESULTS AND DISCUSSION

The results of the products from the first-stage decomposition of poly(vinyl alcohol) are presented in Figure 1. The quantitative data are represented by line charts, plotted against the retention indices. The reten-

TABLE I
Gas Chromatographic Conditions

No.	Type of column	Stationary phase	Carrier gas			Detector	Temperature	Purpose
			Type	Pressure, psi	Flow rate, ml/min			
1	Support coated open tubular, 100 ft, 0.02 in. ID	Carbowax 20 M	Helium	5	Flame ionization	Isothermal at several temperatures between 60 and 240°C	Identification of components; quantitative analysis	
2	Open tubular, 150 ft, 0.01 in. ID	Didecyl phthalate	Helium	10	Flame ionization	Isothermal at several temperatures between 25 and 150°C	Identification of components	
3	Packed 2 m, 1/4 in. OD	Tetraethylene glycol dimethyl ether (Perkin-Elmer column F)	Helium	20	Thermal conductivity	25, 80°C	Identification of oxygenated compounds	
4	Support coated open tubular, 100 ft, 0.02 in. ID	Squalane	Helium	5	Flame ionization	0, 50, 100°C	Identification of hydrocarbons	
5	Packed, 6 ft, 1/4 in. OD	60-80 mesh silica gel deactivated with 4% silicone oil DC-200	Helium	20	Flame ionization	Programmed 10°C/min from 60 to 200°C	Identification of C ₁ -C ₄ hydrocarbons	
6	Preparative, 10 ft, 3/8 in. OD	8% Carbowax 1540 on 60-80 mesh Chromosorb P	Helium	20	Thermal conductivity	80, 120°C	Trapping major peaks	
7	Catalytic hydrogenation sorb) 1/4 in. O.D. in series with support coated (squalane) open tubular, 100 ft, 0.02 in. ID	(1% Pd on Chromosorb)	Hydrogen	10	Flame ionization	Catalytic tube: 250°C Squalane: 0 and 50°C	Determination of chemical structure	

tion index of each component was determined by using *n*-alkanes as standards at gas chromatographic condition 1.

The major peaks, A_0 , A_1 , A_2 , and A_3 of Figure 1, are spaced uniformly on the retention index scale, suggesting that they belong to the same homologous series. The first three were identified as acetaldehyde, crotonaldehyde, and 2,4-hexadiene-1-al by comparing their retention indices with

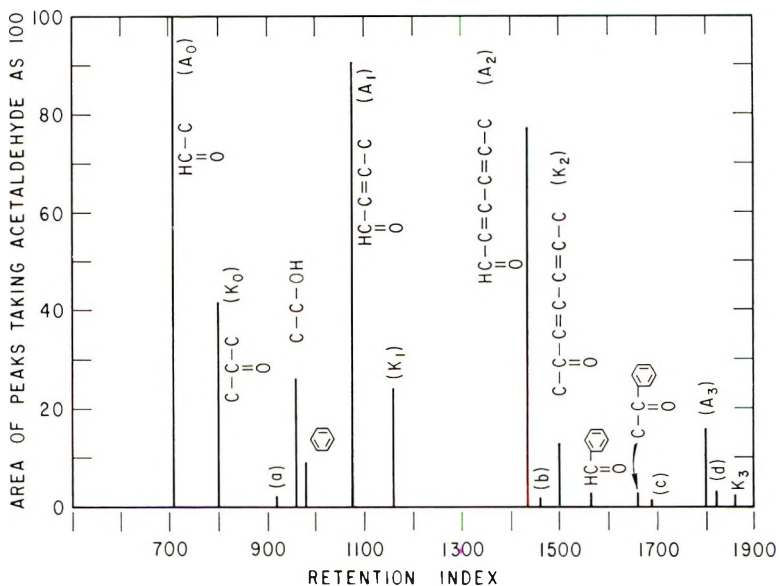
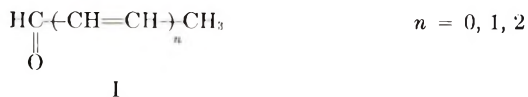


Fig. 1. First-stage decomposition products of poly(vinyl alcohol). Area of peaks vs. retention index.

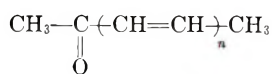
those of known compounds and by the determination of melting points of 2,4-dinitrophenylhydrazones of the three products. The general formula of these compounds is I:



Peak A_3 is believed to be due to 2,4,6-octatriene-1-al, the next compound in the same series. This suggestion is supported by the fact that *n*-heptane was obtained on catalytic hydrogenation of this product.

Peaks K_0 , K_1 , K_2 , and K_3 are also uniformly spaced and thus appear to be due to another homologous series. The first peak, K_0 , was due to acetone. The second peak, K_1 , which yielded a positive iodoform test and produced pentane by catalytic hydrogenation, was believed to be due to 3-pentene-2-one. Although 2-pentanol and 2-pentanone should yield the same results on these two tests, their retention indices are different. The third peak, K_2 , was identified as 3,5-heptadiene-2-one by comparing the re-

tention time with that from a synthesized sample.⁹ The general formula for this homologous series is II:



II

TABLE II
Thermal Decomposition Products of Poly(vinyl Alcohol)
(240°C, 4 hr)

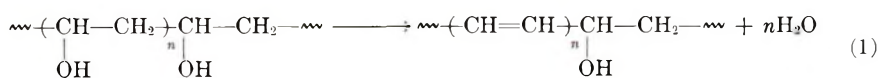
Product	Wt.-% of original polymer
Water	33.4
Carbon monoxide	0.12
Carbon dioxide	0.18
Hydrocarbons C ₁ -C ₃	0.01
Acetaldehyde	1.17
Acetone	0.38
Peak a	0.025
Ethanol	0.29
Benzene	0.06
Crotonaldehyde	0.76
K ₁ (3-pentene-2-one)	0.19
2,4-hexadiene-1-al	0.55
Peak b	0.014
3,5-Heptadiene-2-one	0.099
Benzaldehyde	0.022
Acetophenone	0.021
Peak c	0.017
A ₃ (2,4,6-octatriene-1-al)	0.11
Peak d	0.026
K ₃ (3,5,7-nonatriene-2-one)	0.020

TABLE III
Decomposition Products of Poly(vinyl Alcohol)
(Material Balance, in Weight Percentage of Original Polymer)

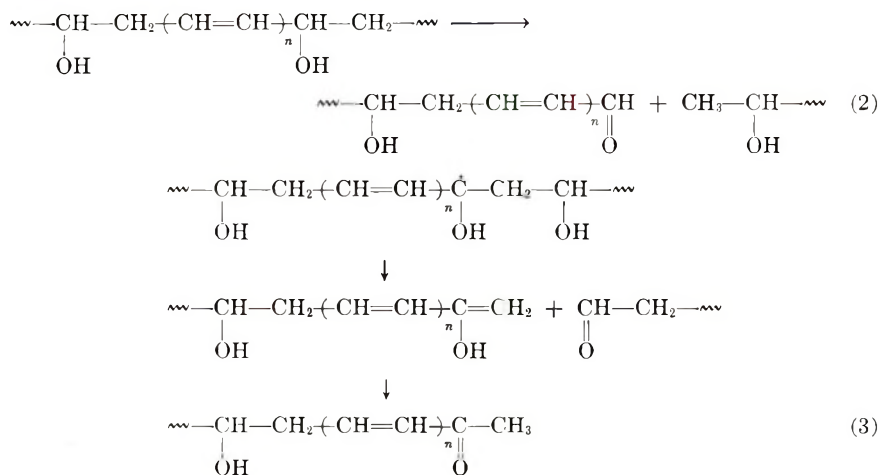
		1st stage (240°C, 4 hr)		2nd stage (450°C, 4 hr)		
Volatiles 47.9	Water layer	Water	33.4	Water layer	0.60	
		Org. Compds.	1.56			
	Oil layer	Org. Compds. Analyzed	1.19	Volatiles 27.7	Oil layer	22.30
		Not analyzed	4.99			
	Gas	0.92		Gas	2.46	
	Loss	5.81		Loss	2.34	
Residue				Residue		
52.1				24.4		

The decomposition products reported by others²⁻⁴ but not found in the present investigation were formaldehyde, acrolein, methyl acetate, and acetic acid. The difference in polymer samples could account for the discrepancy in the production of acetic acid, because poly(vinyl alcohol) samples are known to contain different amounts of acetyl groups.

The experimental data on the thermal decomposition products of poly(vinyl alcohol) are presented in Table II, and the data on material balance in Table III. The main decomposition products of the first stage were water and carbonyl compounds. The distribution of oxygen compounds in the products, based on 100 monomer units in the original polymer, was: water, 86.4 mole; aldehydes, 1.9 mole; ketones, 0.5 mole; other, 0.7 mole. Water is formed by a mechanism similar to that forming hydrogen chloride from poly(vinyl chloride) and acetic acid from poly(vinyl acetate), leaving a residue having conjugated polyene structure [eq (1)].



Scission of some of the C-C bonds results in the formation of the carbonyl ends. Aldehyde and methyl ketone end formation are expected to proceed as shown in eqs. (2) and (3), respectively.

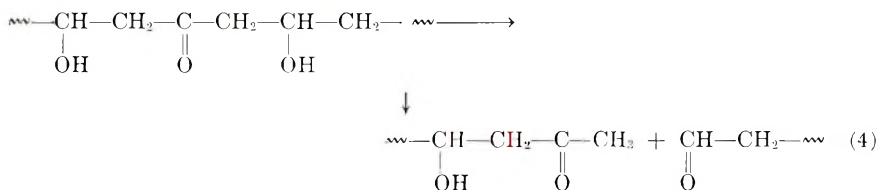


The formation of acetaldehyde, crotonaldehyde, 2,4-hexadiene-1-al, and 2,4,6-octatriene-1-al is plausible from the aldehyde ends, and the formation of acetone, 3-pentene-2-one, and 3,5-heptadiene-2-one is expected from the methyl ketone ends.

Considerably more aldehydes than ketones were found in the products. This difference was predictable from these reactions, because the aldehyde ends can be formed by both reactions (2) and (3), whereas the ketone ends are formed by the latter reaction only.

Yamaguchi and Amagasa¹⁰ predicted the formation of the series of aldehydes and ketones (found in the present study) from the mechanisms of

decomposition that they proposed. They suggested that the methyl ketone ends are formed from the carbonyl groups that are present in the original polymer [eq (4)].



The present authors suggest that the transfer of a hydrogen atom from a tertiary carbon followed by a decomposition reaction (3) could also account for the formation of methyl ketone ends.

A large portion of the oil layer was not analyzed (as noted in Table III), because most of these products were not sufficiently volatile for the gas chromatographic conditions used. The conversion of the carbonyl compounds in the oil layer to 2,4-dinitrophenylhydrazones resulted in a large yield, indicating that the carbonyl compounds represented a large portion of this layer.

The volatile decomposition products of the second stage were mainly hydrocarbons; series of *n*-alkanes, *n*-alkenes, and aromatic hydrocarbons were found. The second-stage pyrolysis products of poly(vinyl chloride) and poly(vinyl acetate) were also determined for comparison with those from poly(vinyl alcohol). The similarity in both the qualitative and quantitative data of the products from the three polymers indicates that the same mechanism applies to the second-stage decomposition of each of the three vinyl polymers.

CONCLUSION

Analysis by gas chromatography showed that the first-stage thermal decomposition products of poly(vinyl alcohol) are mainly composed of water, aldehydes having the general formula $\text{CH}(\text{CH}=\text{CH})_n\text{CH}_3$ and methyl

ketones having the formula $\text{CH}_3-\text{C}(\text{CH}=\text{CH})_n\text{CH}_3$, where $n =$

0, 1, 2, 3, etc. According to the mechanisms proposed in this study, dehydration is accompanied by some scission of the polymer chain, resulting in the formation of aldehyde ends by one type of reaction and of both aldehyde and methyl ketone ends by another type. These mechanisms explain the formation of these carbonyl compounds.

This paper is a contribution from the Division of Building Research, National Research Council of Canada, and is published with the approval of the Director of the Division.

References

1. J. B. Gilbert, J. J. Kipling, B. McEnaney and J. N. Sherwood, **3**, 1 (1962).
2. T. Yamaguchi and M. Amagasa, *Kobunshi Kagaku*, **18**, 645 (1961).
3. B. Kaesche-Krischer and H. J. Heinrich, *Z. Physik. Chem. (Frankfurt)*, **23**, 292 (1960).
4. K. Ettore and P. F. Varadi, *Anal. Chem.*, **35**, 69 (1963).
5. J. B. Gilbert and J. J. Kipling, *Fuel*, **41**, 249 (1962).
6. Y. Tsuchiya and K. Sumi, *J. Polym. Sci. A-1*, **7**, 813 (1969).
7. M. Beroza, *Anal. Chem.*, **34**, 1801 (1962).
8. R. Kaiser, *Chromatographie in der Gasphase. III*, Bibliographisches Institut, Mannheim, 1962, p. 136.
9. L. K. Evans and A. G. Gillam, *J. Chem. Soc.*, **1945**, 432.
10. T. Yamaguchi and M. Amagasa, *Kobunshi Kagaku*, **18**, 653 (1961).

Received May 5, 1969

Radiation-Induced Polymerization of Styrene in the Presence of *n*-Dibutyl Disulfide

L. A. MILLER* and V. STANNETT,† *Camille Dreyfus Laboratory,
Research Triangle Institute, Research Triangle Park,
North Carolina 27709*

Synopsis

The γ -radiation-induced polymerization of pure styrene and styrene-*n*-dibutyl disulfide mixtures has been studied at a number of temperatures and dose rates. Up to 0.04 Mrad/hr the rates were proportional to the square root of the dose rate. By measuring the rates at a number of disulfide concentrations and at three different dose rates, the relative rates of radical formation were determined by kinetic analysis. Considerable energy transfer from the styrene to the disulfide was found. The relative contributions of energy transfer and radical formation were separated by using the kinetic scheme of Nikitina and Bagdasaryan. Values of 8.5 and 3.1 were found for the relative rates of radical production and energy transfer, respectively. This leads to a *G* (radical) value of 3.1 for *n*-dibutyl disulfide. With azobisisobutyronitrile as the initiator, the chain transfer constant to the disulfide was determined at 55°C. Finally, the sulfur content of a number of the polymers were determined, an average of two sulfur atoms per polymer chain was found. In general, the rate of polymerization was found to increase in the presence of dibutyl disulfide.

INTRODUCTION

During a rather extensive study on the radiation-induced grafting of vinyl monomers to wool the possible site of initiation on the keratin molecules became of obvious interest.^{1,2} Electron spin resonance studies on irradiated wool indicates that sulfur radicals are probably involved, from the cleavage of the disulfide links. Little work has been published on the radiolysis of disulfides but the studies which have been made indicate that such links are rather sensitive to radiation. Since wool contains a large number of disulfide groups, about one for every eleven amino acid units, the role of such groups in radiation grafting becomes of great interest. In addition it has been shown that the grafted side chains are very short compared with comparable grafting condition with other fibers such as cellulose. The evidence indicates that chain transfer of the growing radical

* Present address: Division of Isotopes Development, U.S. Atomic Energy Commission, Washington, D. C. 20545. This work was performed while a member of staff of the Western Regional Research Laboratory U.S.D.A. Albany, California 94710.

† Present address: Department of Chemical Engineering, North Carolina State University, Raleigh, North Carolina 27607.

to the wool itself is involved.² Again, there have been very few studies on the role of disulfides in radical polymerization reactions. The present study tries to rectify these gaps in our knowledge of the part that disulfides play in the radiation polymerization of vinyl monomers both as initiators and as chain transfer agents. Styrene was chosen as the model monomer and *n*-dibutyl disulfide as the model disulfide.

EXPERIMENTAL

Styrene (Matheson, Coleman and Bell Co.) was routinely purified and stored in the following manner. The monomer was cold-distilled under high vacuum onto calcium hydride by utilizing a manifold fitted with Delmar-Urry joints and Viton O-rings; a conventional vacuum rack was utilized for the degassing and purification of monomer. The styrene was stored in the receiving flask containing the calcium hydride at ca. 0°C.

The di-*n*-butyl disulfide, as received, contained numerous impurities (approximately 5% by volume) and had to be repeatedly distilled from a spinning band fractional distillation column. In this way, all but one of the impurities (which amounted to ca. 0.7% of the total volume) was removed. This impurity, *sec*-butyl-*n*-butyl disulfide, should not greatly alter the results described later which are attributed to di-*n*-butyl disulfide. The purity of the sample was determined by gas-liquid chromatography (GLC) by use of an FM Model 300 with a 6-ft column of 5% silicon nitrile on acid washed Chromasorb P.

In order to eliminate, as best as possible, the presence of sensitizing materials in the styrene, the following procedure was carried out. The monomer stored over calcium hydride was cold-distilled under high vacuum into a 250-ml flask with a breakseal side arm. This flask was sealed off and irradiated to approximately 10% conversion. A train of four intermediate-size tubes (40–50 ml) with breakseal side arms on a glass manifold was then joined to the side arm of the pre-irradiated flask. The manifold with tubes was degassed and flamed, and after rupturing the breakseal the monomer was cold-distilled into the four tubes. These tubes were sealed off and stored in the dark at 15°C until used. When the dilatometers or ampoules were used in the studies on pure styrene, they were sealed to a manifold with one of the intermediate size tubes attached by the way of the breakseal side arm. Then degassing, flaming, and cold distillation of monomer into the dilatometer or ampoule was performed as just described for filling the intermediate size tubes. The dilatometers or ampoules were sealed off (at 10^{-6} torr) and stored at liquid nitrogen temperature in the dark until used (generally, very shortly after distillation).

For the polymerizations of styrene carried out in the presence of the di-*n*-butyl disulfide two techniques were used. One was to prepare mixtures of the disulfide with freshly distilled styrene (pre-irradiated) then add this to a side-arm reservoir. After thorough degassing by freeze-thaw cycles using liquid nitrogen as the coolant, the reservoir was inverted. The

solution then flowed into the dilatometer where it is solidified by cooling with liquid nitrogen then sealed off while open to the vacuum system at 10^{-5} – 10^{-6} torr.

The other technique was to simply inject the solution of styrene–disulfide into the dilatometer with a hypodermic syringe then to degas in the dilatometer by the same freeze-thaw method.

The α -irradiations were carried out in a 1500-Ci ^{60}Co source. This consisted of a room irradiation facility with remote control for raising and lowering of the ^{60}Co out of and into, respectively, a heavily shielded receptacle, such that when the γ -source is down one may enter the irradiation area for placement of samples. This type of facility permits a wide range of dose rates by varying the distance of the sample from the source. It also allows wide variation in temperature with very close control depending upon the type of thermostatted unit involved.

With rapid flow of the cooling or heating liquid through 2.5×45 cm glass jackets and utilizing for temperature control a Brinkman-Laude (NBS-X) constant temperature bath, as many as six jackets holding six dilatometers or ampoules could be controlled to $\pm 0.02^\circ\text{C}$.

For the runs at 0°C , a Formatemp Jr. was utilized for temperature control.

TABLE I
Molecular Weights of Radiation-Produced Polystyrene

Sample	Disulfide, %	Dose rate, Mrad/hr	Number-average molecular weight	
			From viscosity ^a	By osmometry
SDS3-3	5	0.005	194 800	188 500
SDS4-4	10	0.0025	216 300	200 700
PS3-4	0	0.005	299 700	289 300
PS3-4	0	0.0025	486 000	477 000

^a Calculated from the equation:³ $\bar{M}_n = 167\,000 [\eta]^{1.37}$.

Dose rates were determined by Fricke dosimetry experiments using the $G(\text{Fe}^{+++})$ value of 15.6. The log of the dose rate was linear with the log of the distance from the source and the log–log plot was used as a reference for setting up experiments at predetermined dose rates. This plot was periodically corrected for decay of the ^{60}Co .

Viscosities were determined with the use of toluene as solvent in a 30°C bath. The viscometers were modified Ubbelohde instruments of the suspended-level dilution type of approximately 140 sec solvent time, and hence kinetic corrections were not made. The viscometers had an internal fritted disk which protected the solution brought into the calibrated reservoir from extraneous matter. In all cases the extrapolation to zero concentration was done from five separate concentration values (i.e., four dilutions).

As a check on the relationship of Mayo et al.³ for converting intrinsic viscosities to number-average molecular weight, a random sampling of the radiation-produced polystyrene from both pure styrene and styrene-disulfide polymerizations was checked on a high speed automatic osmometer. The results are presented in Table I and show good agreement between the two methods. The sulfur content of the polystyrenes was determined by neutron activation analysis by Gulf-General Atomic, Incorporated, San Diego, California.

RESULTS

Pure Styrene

Meaningful comparisons need reliable data acquired for pure styrene under conditions identical to those used with the disulfide experiments. Some anomalous results which have appeared,⁴ such as the low activation energy values in the 0–40°C temperature range and the deviation from the inverse square-root relationship of molecular weight to dose rate prompted the experimental effort which has taken place and the discussion of it that follows. By using the dilatometric method, γ -radiation-initiated polymerizations of pure styrene were conducted at a number of dose rates between 625 and 200000 rad/hr and at various temperatures between 0 and 55°C. Typical conversion curves are presented in Figure 1. In most cases the plots departed from linearity to a small extent after about 8% conversion. At higher dose rates and temperatures, linearity was preserved to much higher conversions. The reasons for the small deviations from linearity are not known and the initial rates were always taken as the correct ones. The dependence of the initial rates on the dose rate is shown in Figure 2 in the form of log-log plots for low temperatures. The rates of 40 and 55°C were corrected for the measured thermal polymerizations by using the equation $R_{\text{rad}} = (R_{\text{tot}}^2 - R_{\text{th}}^2)^{1/2}$, where R_{rad} , R_{tot} , and R_{th} are the radiation-initiated, total, and thermal rates, respectively. This equation can be readily derived from conventional polymerization kinetics. The slopes of the plots are all found to be 0.46, close to the one-half order expected theoretically. The corresponding molecular weight data are shown in Figure 3. Again, slopes of close to 0.5 were obtained. However, at 40 and 55°C and at the lower dose rates the molecular weights leveled off towards the thermal values of about one million. No attempts were made to correct the molecular weight data from the contributions from the thermal polymer.

The data obtained at different temperatures is presented in Figures 4 and 5 as Arrhenius plots of the rates and molecular weights, respectively. The rate data were corrected for the thermal rate contributions. The activation energies for the rates and molecular weights were found to be 5.9 and 6.4 kcal/mole, respectively, in good agreement with each other and also the literature.

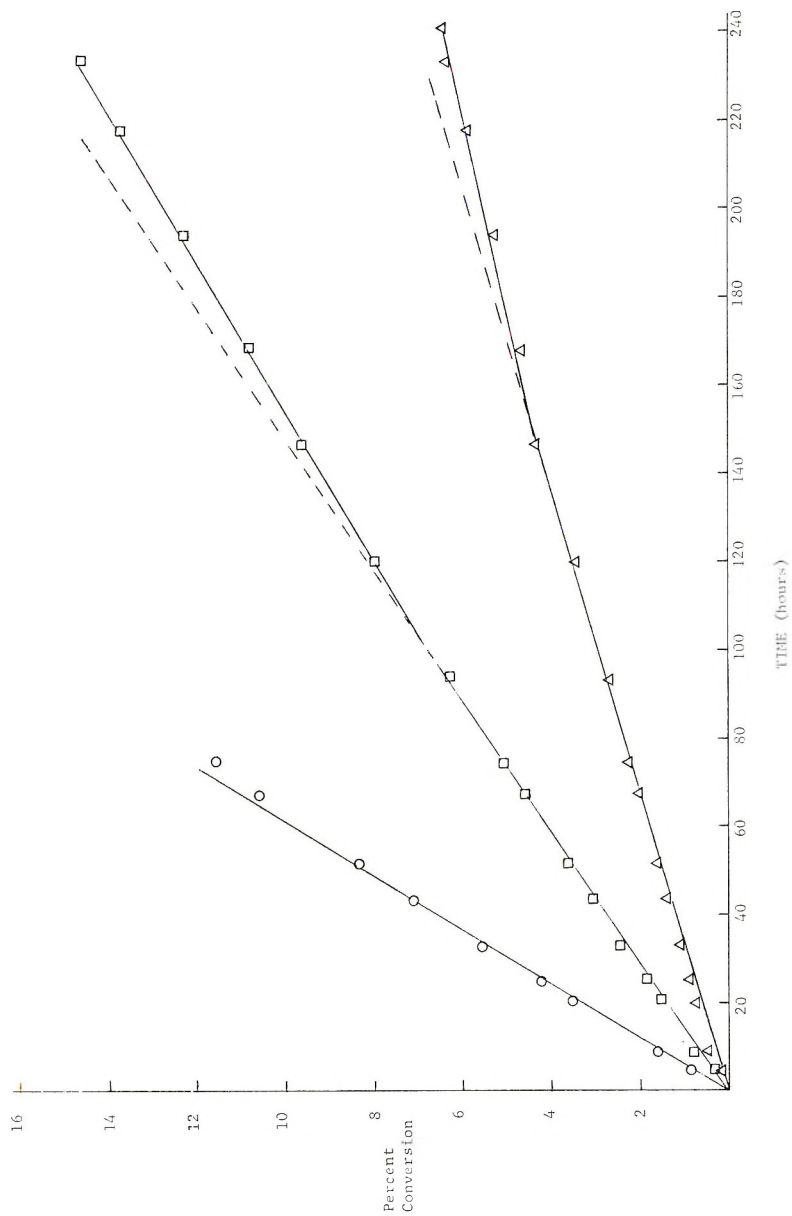


Fig. 1. Conversion curves for the radiation-initiated polymerization of pure styrene at 25°C: (O) 40 000 rad/hr; (□) 5 000 rad/hr; (Δ) 625 rad/hr.

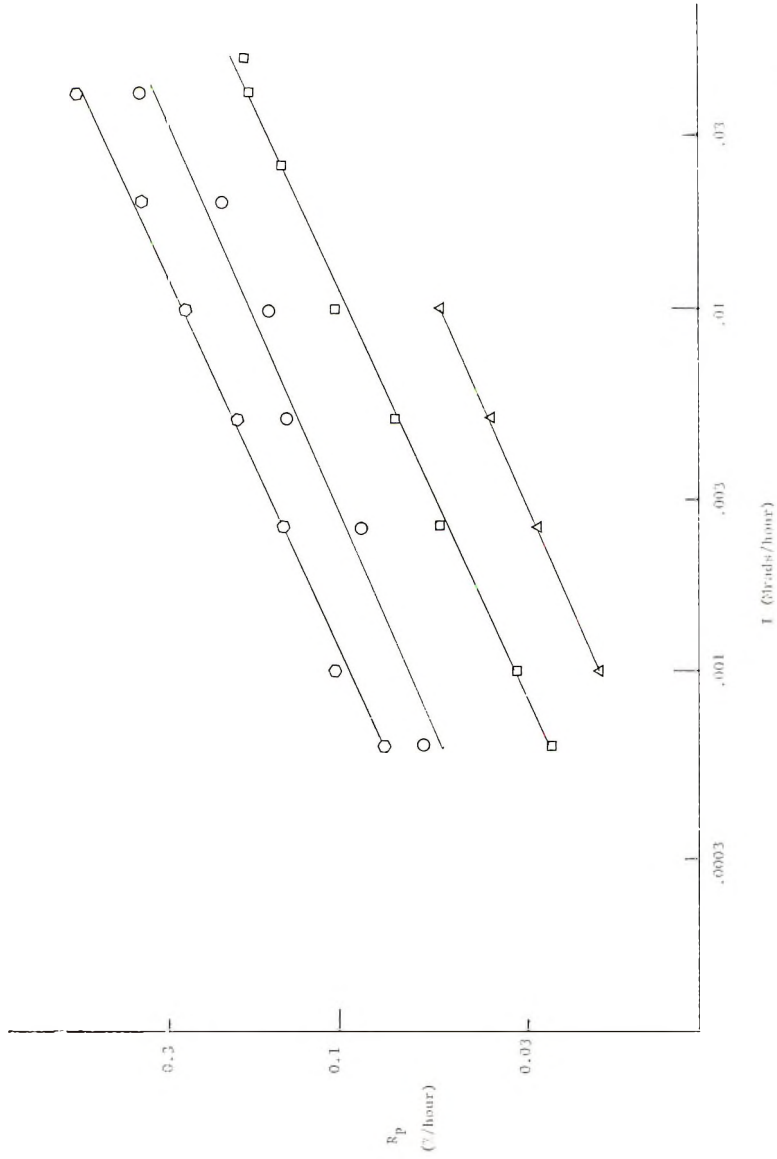


Fig. 2. Dependence on rate of polymerization on dose rate for pure styrene: (O) 55°C; (□) 40°C; (Δ) 10°C.

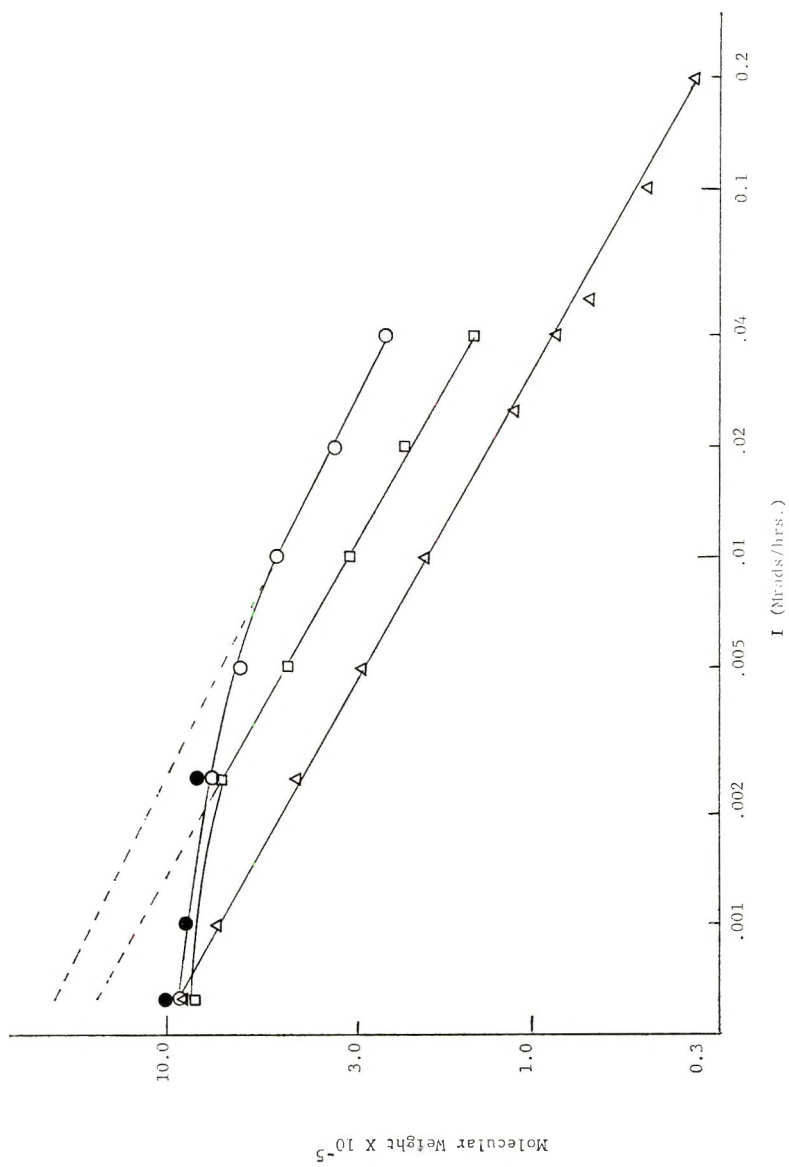


Fig. 3. Dependence of molecular weight on dose rate for pure styrene: (O) 55°C; (□) 40°C; (Δ) 25°C.

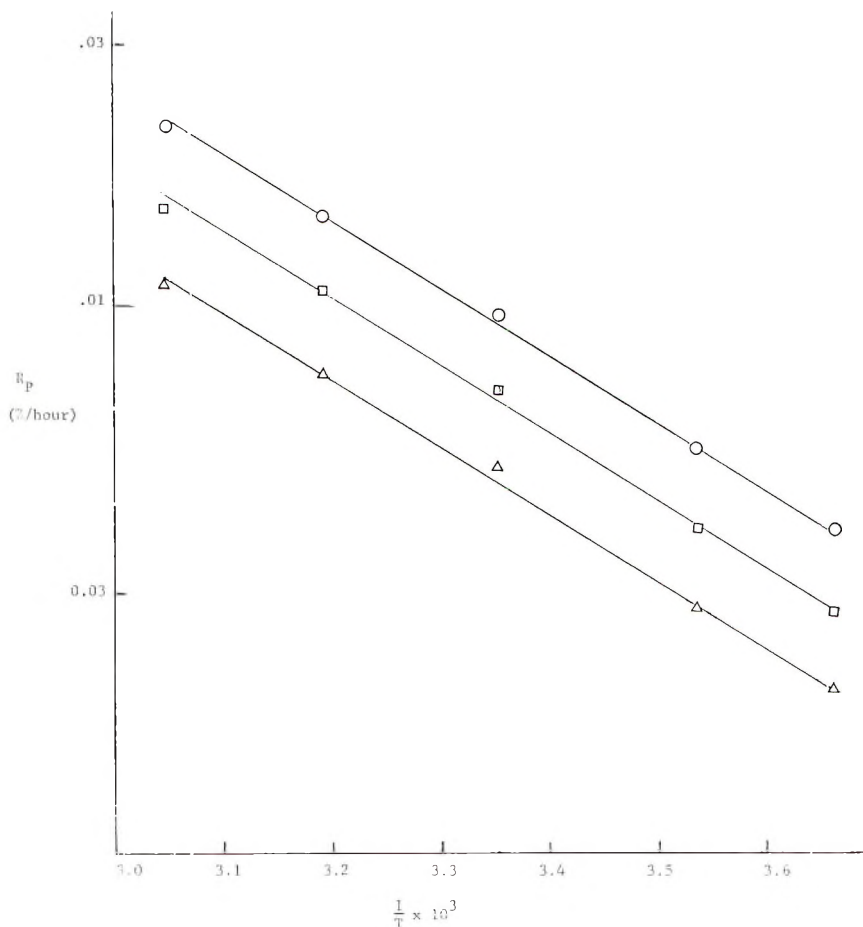


Fig. 4. Dependence of rate of polymerization on temperature for pure styrene: (○) 10000 rad/hr; (□) 5000 rad/hr; (△) 2500 rad/hr.

In summary, it can be stated that no unusual features were found with the radiation-induced polymerization of pure styrene, and normal polymerization kinetics were observed. The rates of polymerization obeyed the normal one-half order on the dose rate up to the highest dose rate used of 55.5 rad/sec.

Polymerization in the Presence of *n*-Dibutyl Disulfide

In principle the *n*-dibutyl disulfide will play the following two roles in the polymerization reaction: (a) it will participate as a chain transfer agent; (b) it will participate in the initiation process due to the initiating radicals produced by the radiolysis of the disulfide. The magnitude of both effects were determined quantitatively from a study of the polymerization reaction kinetics.

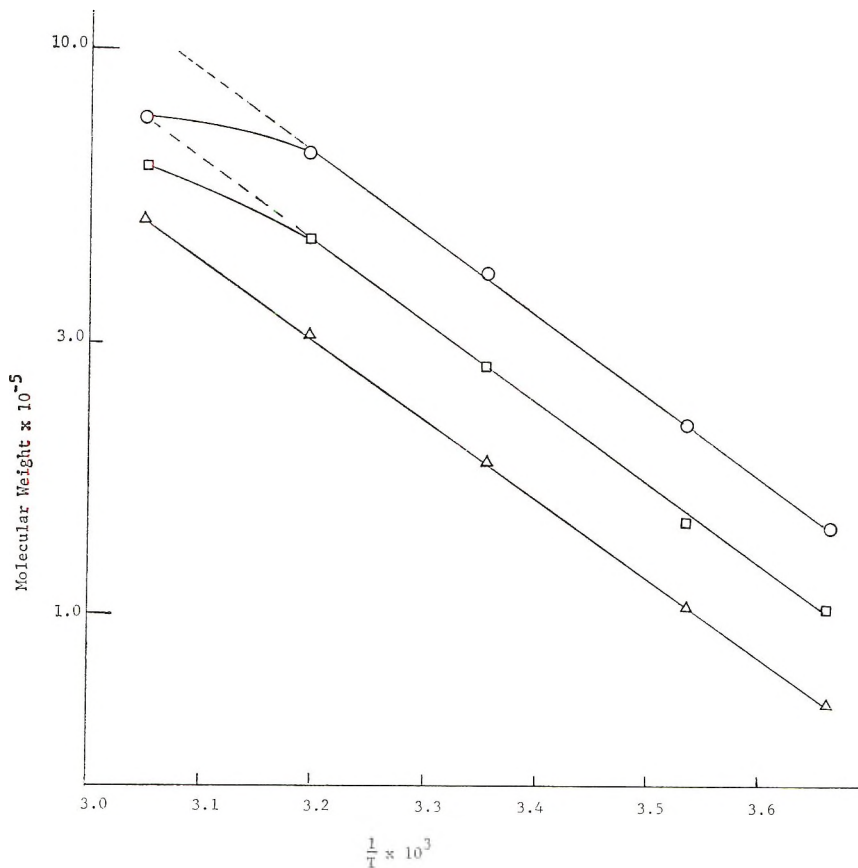


Fig. 5. Dependence of molecular weight on temperature for pure styrene: (O) 2500 rad/hr; (□) 5000 rad/hr; (Δ) 10000 rad/hr.

Chain-Transfer Constant of *n*-Dibutyl Disulfide. To avoid the complications due to the participation of the disulfide in the radiation-initiated polymerization it was decided to use chemical initiation. Azobisisobutyronitrile was chosen as the initiator since its decomposition rate is known to be insensitive to most solvents. The actual polymerization rates were kept essentially constant by maintaining a constant ratio of monomer concentration to the square root of the catalyst concentration as shown in Table II. The conversions were all kept to below 10% and the conversion and molecular weights determined as before. The experimental data is summarized in Table II. The molecular weight data are shown plotted in the form developed by Mayo⁵ in Figure 6. A clear linear relationship was obtained, and from the slope the chain transfer constant was found to be 1.54×10^{-3} at 55°C. This value, together with others reported in the literature⁶⁻¹⁰ for other temperatures is plotted as an Arrhenius plot in Figure 7. Extrapolation leads to a value of the chain transfer constant at 25°C of $0.79 \pm 0.07 \times 10^{-3}$. The activation energy of the chain transfer con-

TABLE II
Determination of Chain-Transfer Constant for Di-*n*-butyl disulfide 55°C^a

Styrene, %	[M], mole/l.	[ABIN], g/100 ml	Time, hr	Conversion, % polymer	R_p , %/hr	\bar{M}_n (calcd $[\eta]$)	Rate ^b $\sqrt{C[M]}$
100	8.66	0.25	3	5.9	1.97	121000	4.5×10^{-5}
80	6.93	0.16	4.17	6.99	1.68	88500	4.7×10^{-6}
60	5.20	0.09	5	6.19	1.24	67100	4.6×10^{-6}
40	3.46	0.04	10	7.34	0.73	42900	4.2×10^{-6}
20	1.73	0.01	28	8.94	0.32	20700	3.7×10^{-6}

^a Di-*n*-butyl disulfide purified by repeated distillations contained approximately 0.7% *n*-butyl-*sec*-butyl disulfide.

^b Rate expressed in mole/l-sec.

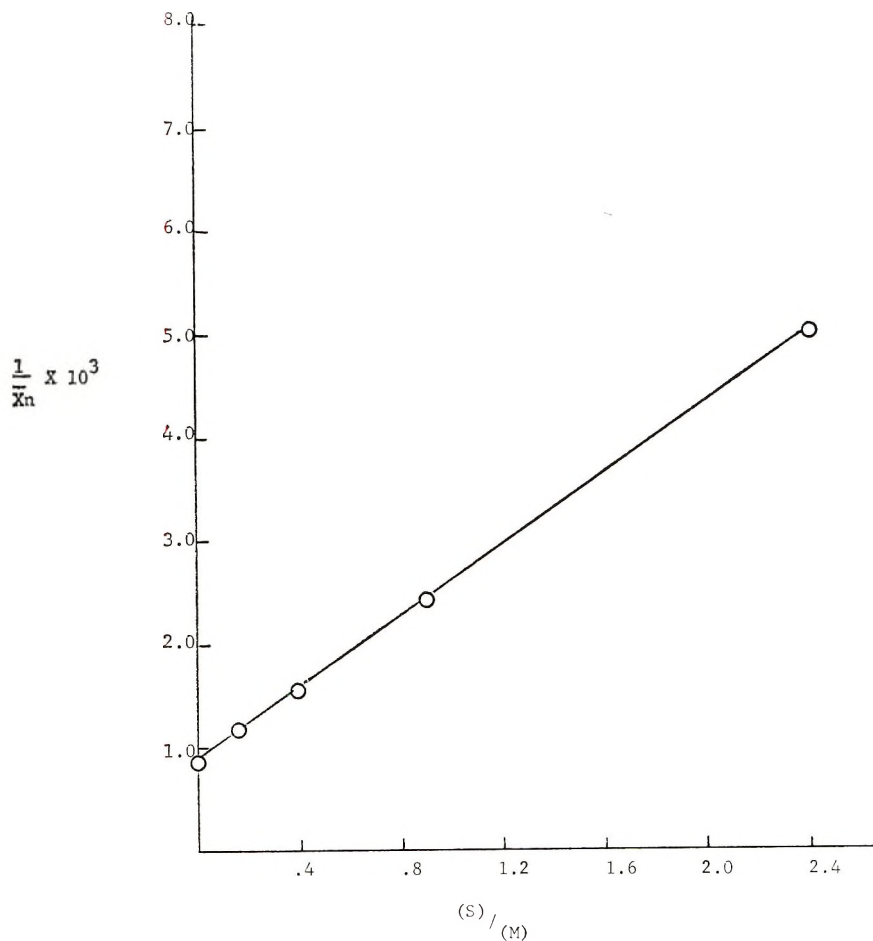


Fig. 6. Dependence of molecular weight on the *n*-dibutyl disulfide concentration at 55°C initiated with azobisisobutyronitrile.

stant was found to be 7.3 kcal/mole. An excellent discussion of the mechanism of chain transfer with disulfides has been presented by Pryor⁶ and by Pryor and Pickering.⁷

Effect of *n*-Dibutyl Disulfide on the Initiation Process. A number of radiation-induced polymerizations were conducted with mixtures of disulfide and styrene. Three different dose rates were used, good linear plots were obtained, and the initial rates were taken from the slopes. The actual rates at 25°C at three different dose rates and at a number of disulfide concentrations are all brought together in Table III. The rates were found to be proportional to the square roots of the dose rates, and good agreement was found between the three dose rate studies as can be seen from the relative rate data presented in Table III.

Chapiro¹¹ has discussed in detail the kinetics of radiation-induced homogeneous radical polymerization. In particular it was shown that, when the

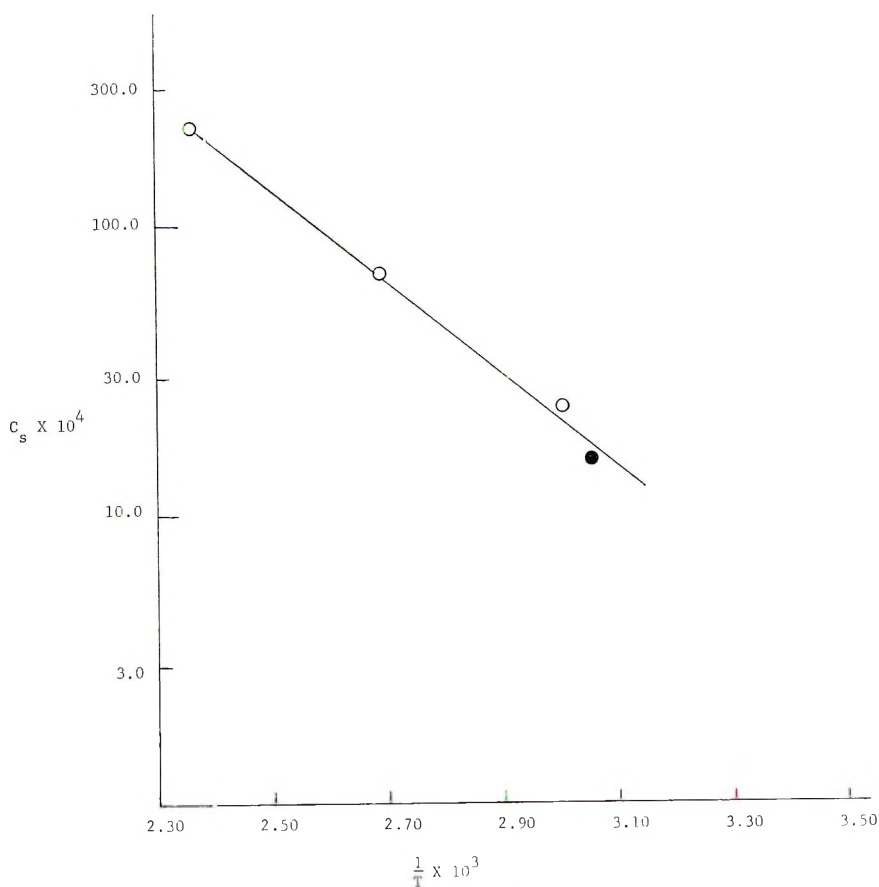


Fig. 7. Temperature dependence of the chain-transfer constant of *n*-dibutyl disulfide and styrene.

TABLE III
Rate Data For Radiation-Induced Polymerization of Styrene
at 25°C in the Presence of *n*-Dibutyl Disulfide

Di-sulfide, %	Mole fraction monomer	C/C_0 at various dose rates ^a			Mean C/C_0	Cal- culated ϕ_{rel}
		0.0025 Mrad/hr	0.005 Mrad/hr	0.010 Mrad/hr		
0	1.00	—	—	—	1.00	—
5	0.969	1.57	1.47	1.46	1.50	44.0
10	0.937	1.59	1.50	1.45	1.51	23.8
20	0.869	1.74	1.63	1.61	1.66	16.6
40	0.703	2.16	2.25	2.26	2.22	17.3
60	0.532	2.22	2.25	2.30	2.26	13.6
80	0.297	1.92	1.74	1.93	1.87	6.9

^a C_0 values were 0.049, 0.070, and 0.094%/hr for 0.0025, 0.005, and 0.010 Mrad/hr, respectively.

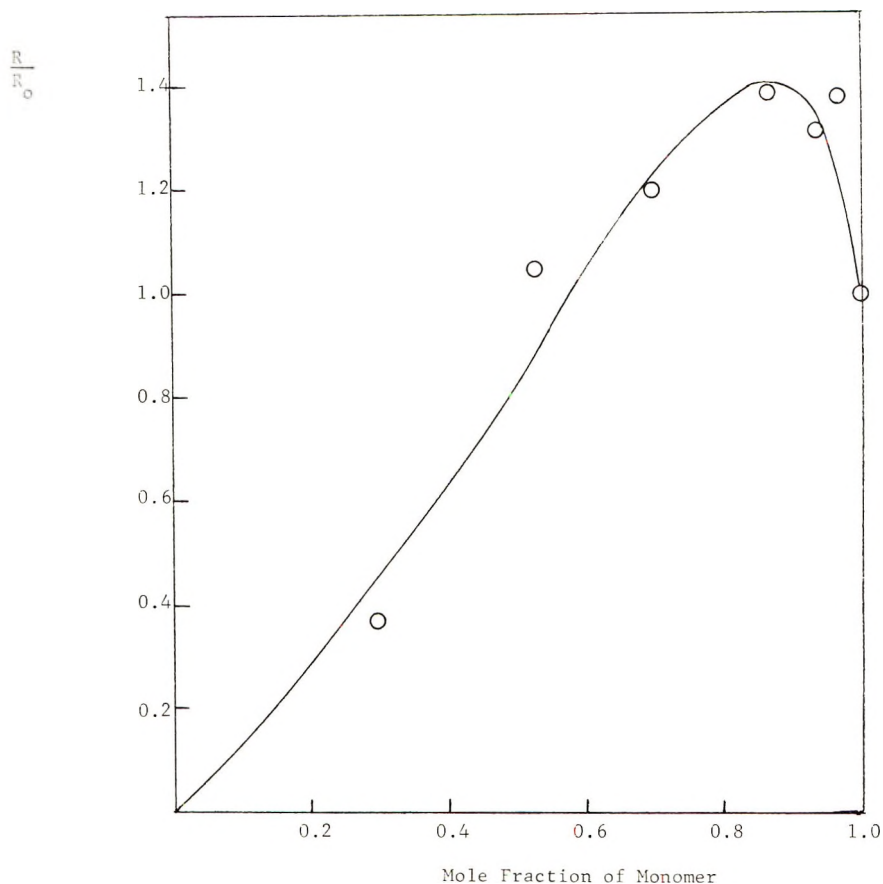


Fig. 8. Relative rates of radiation initiation polymerization versus mole fraction of *n*-dibutyl disulfide at 25°C: (—)Nikitina and Bagdasaryan eq. (4) with the values of $\phi_{rel} = 8.5$ and $P_{rel} = 3.1$.

The data presented in Table III have been converted to rates and used to calculate the values of P_{rel} and ϕ_{rel} by using a computer technique, further details of which are given in the appendix. The closest fit to the data was found to be with the values of $\phi_{rel} = 8.5$ at $P_{rel} = 3.1$. The theoretical plot of R/R_0 versus the mole fraction of monomer using these values is presented in Figure 8, together with the experimental values. Although there is some scatter, the points are reasonably close to the theoretical line, with a maximum difference of less than 20%. It is interesting that the computer technique used clearly showed that only one set of ϕ_{rel} and P_{rel} values fitted the data with the range 0–30.0 and 0–45.0 for each parameter, respectively. On correcting the ϕ_{rel} values for the differences in density, molar volumes, and electron density of the disulfide and the monomer and by using the generally acceptable value of 0.7 for the $G(\text{radical})$ for styrene, a value of 3.1 was obtained for $G(\text{radical})$ for dibutyl disulfide. Values for $G(\text{radicals})$ have been reported for a number

TABLE IV
Sulfur Content of Polymers Prepared by the γ -Induced Polymerization of Styrene-Di-*n*-butyl Disulfide Solutions at 25°C.

Sample number	Disulfide in monomer-disulfide, %	Dose rate, Mrad/hr	Total dose, Mrad	Polymer, %	S content in polymer, % ^a	\bar{M}_n ^b	Mean sulfur atoms per chain
SDS4-2	10	0.01	1.68	25	0.0477 \pm 0.011	114700	1.71
SDS7-3	40	0.01	1.97	39.5	0.132 \pm 0.003	47900	1.98
SDS10-1	40	0.01	1.39	25.5	0.125 \pm 0.005	50200	1.96
SDS10-4	40	0.0025	1.02	21.5	0.0775 \pm 0.0024	85100	2.06
SDS11-7	80	0.005	1.04	24.0	0.394 \pm 0.013	13600	1.67
SDS11-8	80	0.0025	0.52	17.0	0.320 \pm 0.015	17800	1.78

^a Determined by neutron activation analysis (Gulf General Atomic, Inc.).

^b Determined by viscosity measurements.

of disulfides using DPPH in toluene and in benzene.^{13,14} $G(\text{radical})$ values ranged from 2.0 for dibenzyl disulfide to 2.2 for diphenyl and di-*p*-tolyl disulfides in toluene.¹³ In benzene solution, the values obtained were 3.0 and 2.8 for diphenyl and dibenzyl disulfides, respectively, and 0.6 for both diethyl and dioctyl disulfides.¹⁴ These values are unexpectedly low and were determined by using the DPPH method; no explanation can be offered as to why lower results were obtained compared with the present study. It was shown that considerable energy transfer took place from the aromatic solvent to the disulfide in the case of the diaryl disulfides.^{13,14} The low values for the two dialkyl disulfides was attributed to less energy transfer. The reported values are all lower but of a similar order of magnitude to the value found in the present work for dibutyl disulfide, as is also the low but integral P_{rel} value for energy transfer from the styrene to the disulfide.

The combination of the increased initiation rate resulting from the radiolysis of the disulfide plus the chain transfer results in polymers with many sulfide endgroups. A number of polymers were analyzed for sulfur by using neutron activation analysis. Their number-average molecular weights were estimated from their intrinsic viscosities. The results are summarized in Table IV. It can be seen that an average of about two sulfur atoms per chain was present within the experimental error. This means that most of the polymer chains were initiated by sulfide radicals and terminated by chain transfer to the *n*-dibutyl disulfide under the conditions used. In general, the rate of polymerization was found to increase in the presence of dibutyl disulfide.

APPENDIX

Estimate of the Parameters

The conventional method used to estimate the parameters of non-linear equations is to select some objective function of the residuals. The objective function is then minimized either analytically or numerically. The parameters corresponding to the minimum in the objective function are selected as the best estimators of the population parameters.

The class of objective functions most generally used are:

$$R = \sum_{i=1}^n W_i (|y_i - f(x_i)|)^\alpha$$

where y_i is the observed value, $f(x_i)$ is the value predicted by model, W_i are weighting factors, and α is an exponential weighting factor. When $W_1 = W_2 = W_3 = \dots = W_n$ and $\sum_{i=1}^n W_i = 1$ and $\alpha = 2$, R is simply the overall residual sum of squares, designated as RSS. The minimization of RSS corresponds to the least square criterion for parameter estimation. The least-squares objective function is probably the most commonly used

for the reason that if the data is normally distributed about the model then the parameters corresponding to the minimum RSS are also maximum likelihood estimators.

The Bagdasaryan equation¹² [eq. (2)] contains the two parameters ϕ_{rel} and P_{rel} which are to be estimated from experimentally determined R/R_0 as a function of m .

Thus, there are two parameters to be estimated and in such a case one deals with an RSS surface in the two parameter space, P_{rel} and ϕ_{rel} .

There are a number of mathematical strategies to obtain the parameters of the minimum RSS, but all of these methods rely on the assumption that the RSS surface is unimodal, that is, only one minimum exists in a specified space. In order to inquire whether the estimated parameter is unique, i.e., the surface is unimodal, the safest approach is to examine this surface.

This surface for the region $0 < P_{rel} < 45$ and $0 < \phi_{rel} < 30$ was examined. For the global minimum in RSS, the corresponding parameters were found to be $P_{rel} = 3.1$ and $\phi_{rel} = 8.5$. There is a ridge at a higher RSS which corresponds to a much higher RSS than the global minimum. Thus, it seems that in the investigated space a unique solution exists.

The values of R/R_0 and various values of the mole fraction of monomer were calculated using these values of ϕ_{rel} and P_{rel} . These are presented as the solid line in Figure 8, together with the experimental points. There is no way of determining whether the differences are randomly distributed or not. In view of this lack of information no judgment as to the source of the differences can be made at this time. Further details of the mathematical technique may be found elsewhere.^{15,16}

We would like to thank Mr. Andrew Klein for devising and carrying out the computer calculations described in the appendix. Also, we would like to thank the Camille and Henry Dreyfus Foundation for their partial support of this work and the Western Regional Research Laboratory of the U.S. Department of Agriculture for their support of the senior author.

References

1. V. Stannett, K. Araki, J. A. Gervasi, and S. W. McLeskey, *J. Polym. Sci. A*, **3**, 3763 (1965).
2. D. Campbell, J. L. Williams, and V. Stannett, *Advan. in Chem. Ser.*, **66**, 221 (1967).
3. F. R. Mayo, R. A. Gregg, and M. S. Matheson, *J. Amer. Chem. Soc.*, **73**, 1691 (1951).
4. S. Srinivassan, C. J. Phalangas, and J. Silverman, paper presented at I.U.P.A.C. Symposium on Macromolecular Chemistry, Prague, 1965, Abstract A112.
5. F. R. Mayo, *J. Amer. Chem. Soc.*, **65**, 2324 (1943).
6. W. A. Pryor, *Mechanism of Sulfur Reactions*, McGraw-Hill, New York, 1962, pp. 46-57.
7. W. A. Pryor and T. L. Pickering, *J. Amer. Chem. Soc.*, **84**, 2705 (1962).
8. A. V. Tobolsky and B. Baysal, *J. Amer. Chem. Soc.*, **75**, 1757 (1953).
9. V. A. Dinsburg and A. A. Vansheidt, *Zh. Obshch. Khim.*, **24**, 840 (1954).
10. J. Brandrup and E. H. Immergut, Eds., *Polymer Handbook*, Interscience, New York, 1966, II, p. 129.

11. A. Chapiro, *Radiation Chemistry of Polymeric Systems*, Interscience, New York, 1962.
12. T. Nikitina and K. S. Bagdasaryan, *Sbornik Rabot po Radiatsionnoi Khimii*, Academy of Sciences, Moscow, 1955, p. 183; see also ref. 11, pp. 266-269.
13. W. Ando, K. Sugimoto, and S. Oae, *Bull. Chem. Soc. Japan*, **37**, 357 (1964).
14. V. A. Krongauz and K. S. Bagdasaryan, *Dokl. Akad. Nauk SSSR*, **132**, 1136 (1960).
15. E. M. L. Beale, *J. Roy. Statist. Soc.*, **B22**, 41 (1960).
16. D. J. Hudson, *Statistics Lectures II*, C. E. R. N., 64-18, C. E. R. N., Geneva, 1964.

Received April 4, 1969

Revised May 12, 1969

Radiation-Induced Solid-State Polymerization of Methacrylic Acid. II. In-Source Polymerization

YOSHIRO SAKAI, *Department of Industrial Chemistry, Ehime University, Bunkyo-cho, Matsuyama, Ehime, Japan*

Synopsis

The in-source polymerization of methacrylic acid in the solid state with γ -rays was studied. The conversion rates at various temperatures were obtained as well as the radical concentrations by the measurements of ESR spectrum. The rate of polymerization was found to be proportional to $I^{0.65}$ at 0°C. The results could be interpreted on the basis of the assumption that the rate of propagation is proportional to the concentration of the propagating radical, of the monomer, and of the polymer. The addition of water to the monomer seems to accelerate the polymerization reaction. The change of the line shape of the propagating radical during polymerization was interpreted in terms of the change of the matrix which surrounds the propagating radical.

INTRODUCTION

Many workers have studied the mechanism of solid-state polymerization, and various kinetic schemes have been proposed. Morawetz and Rubin¹ studied the tacticity of the polymer formed by solid-state polymerization of methacrylic acid with γ -rays, while Bamford et al.² carried out the solid-state polymerization of methacrylic acid with ultraviolet light. They also observed the effect of pressure on the polymerization of crystalline methacrylic acid and have found the inhibiting or retarding effect of pressure on the polymerization with ultraviolet light.³ In addition, they studied^{4,5} the propagating radical of methacrylic acid by the measurement of the ESR spectrum in connection with the study of solid-state polymerization. We found⁶ a crystalline transition around -30°C with broad-line NMR and differential scanning calorimetry measurements, and the change with observation temperature of the ESR spectrum and the behavior of methacrylic acid radicals were well explained by reference to this transition.

EXPERIMENTAL

Methacrylic acid was dried with sodium sulfate anhydride and then with pure benzene by azeotroping and distilled at reduced pressure ($50^{\circ}\text{C}/7$ mm Hg), the distillation being performed in the presence of ferrous sulfate and copper powder. For the in-source polymerization, 5 g portions of purified methacrylic acid in ampoules of 5 cm diameter were degassed by repeated

melting and freezing under vacuum. The degassed samples were then sealed at a pressure of 10^{-4} mm Hg. Irradiation was carried out with 3 Kci ^{60}Co γ -ray source. The dose rate was 1.85×10^4 R/hr. The samples were irradiated in the low temperature cryostat which allowed control of temperature between $+10$ and $-60^\circ \pm 0.5^\circ\text{C}$. After the irradiation, the samples were cooled down to -78°C and the unreacted monomer was dissolved into cold ether at -78°C . The undissolved poly(methacrylic acid) was filtered, dried, and weighed. Viscosity was measured in methanol solution.

For the ESR spectrum measurements, the purified and degassed methacrylic acid was distilled into a Spectrosil sample tube (5 mm diameter) and sealed under vacuum. The irradiation was carried out under the same conditions as used for polymerization. After the irradiation the sample was rapidly cooled down to -196°C at which temperature the ESR spectra were also observed. A Japan Electron Optics Model 3BSX spectrometer was used for recording the spectra at 9.4 Geps with 100 keps modulation. The relative radical concentration was calculated by double integration of the first-derivative ESR spectrum using a Japan Electron Optics Model JR-5 spectrum computer.

RESULTS

Effect of Irradiation Temperature

Irradiation was carried out at various temperatures for the polycrystalline methacrylic acid crystallized by shock cooling to -196°C from the liquid phase. A plot of weight per cent conversion versus time is shown in Figure 1. Irradiation at -78°C for 24 hr at an intensity of 2.1×10^4

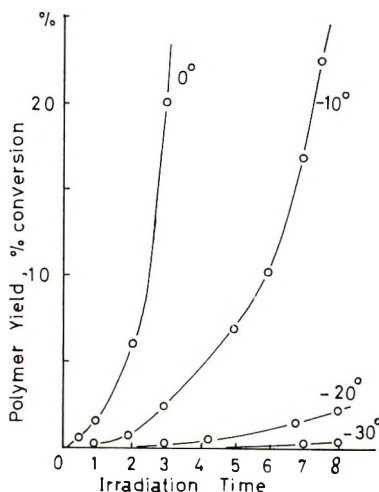


Fig. 1. Polymer yield vs. time for solid-state polymerization of methacrylic acid with γ -rays. Dose rate, 3×10^4 R/hr.

R/hr yielded no polymer, although these irradiated samples occlude the active centers which can initiate the post-polymerization at the elevated temperatures. The rate of polymerization seems to be accelerated. In

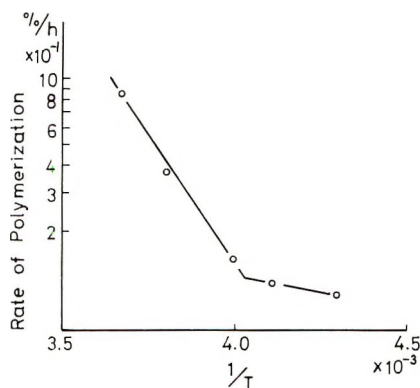


Fig. 2. Initial rate of conversion vs. reciprocal of absolute temperature for solid-state polymerization of methacrylic acid.

Figure 2 the initial rate of polymerization is plotted against the reciprocal of the absolute temperature. The slope of the straight line suddenly changes around -30°C . The activation energies were calculated from this Arrhenius plot to be 2.9 ± 0.2 kcal/mole above -30°C and 0.4 ± 0.1 kcal/mole below -30°C .

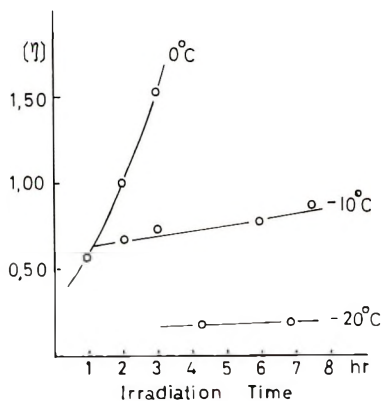


Fig. 3. Intrinsic viscosity vs. irradiation time for solid-state polymerization of methacrylic acid.

Figure 3 shows a plot of intrinsic viscosity versus irradiation time at various temperatures at the dose rate of 6.3×10^4 R/hr. The viscosity is shown to be independent of irradiation dose below -10°C . The intrinsic viscosity increases with irradiation temperature.

Effect of Irradiation Intensity

Polymerization was carried out at various irradiation intensities. The results are shown in Figure 4. In Figure 5, the logarithm of initial rate of polymerization is plotted against the logarithm of dose rate. The slope of the line in Figure 5 shows that the rate of polymerization is proportional to $I^{0.65}$ at 0°C .

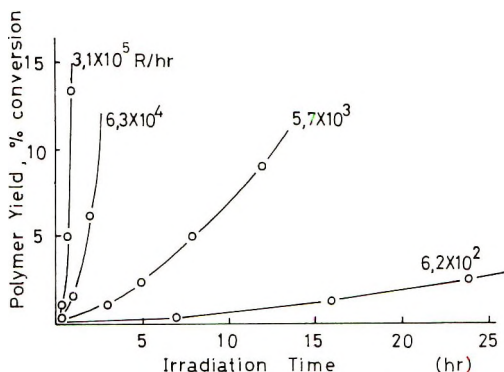


Fig. 4. Polymer yield vs. irradiation time at various dose rates at -5°C .

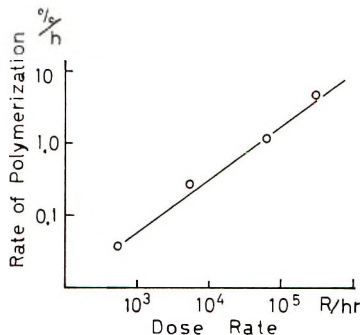


Fig. 5. Plot of logarithm of rate of polymerization vs. logarithm of dose rate at -5°C .

Addition of Water

It is known that a small amount of water in methacrylic acid monomer acts as a retarder in the case of liquid-phase polymerization. However, in the solid-state polymerization, the effect of water is quite different from that in the liquid-state polymerization.

The mixtures of methacrylic acid and water were rapidly cooled to -78°C from the liquid phase and then irradiated at -5°C . The per cent conversion for the first hour of polymerization was obtained for samples having various mixing ratios and the results are shown in Figure 6. The initial rate of polymerization increases with increasing content of water, while the intrinsic viscosity increases with increasing water content up to

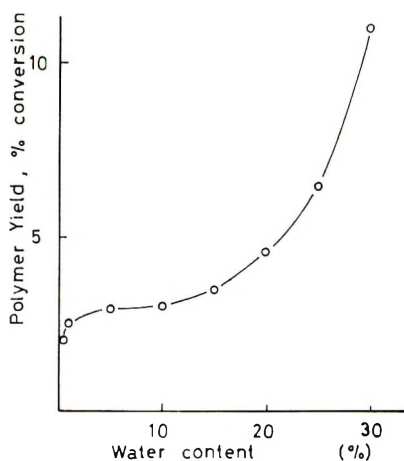


Fig. 6. Polymer yield for the first hour of polymerization vs. water content for the solid-state polymerization of methacrylic acid-water mixtures. Polymerization was carried out at -5°C ; dose rate, 6.3×10^4 R/hr.

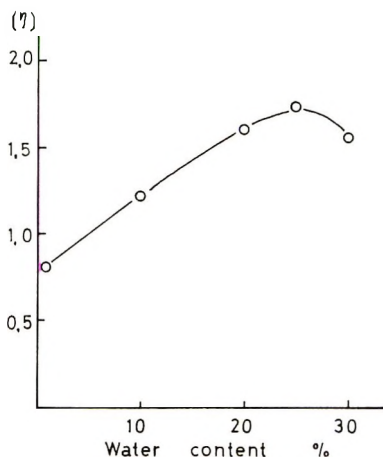


Fig. 7. Intrinsic viscosity of poly(methacrylic acid) formed in the solid-state polymerization of methacrylic acid-water mixtures.

20% water content and then decreases at higher water content, as shown in Figure 7.

Change of Radical Concentration during Polymerization

The crystalline methacrylic acid samples irradiated at various temperatures were rapidly cooled to -196°C , and their ESR spectra were recorded at that temperature. The relative radical concentration was obtained by double integration of the first ESR spectrum by use of a computer. The change of the relative radical concentration with irradiation time is shown in Figure 8. The radical concentration increases linearly with irra-

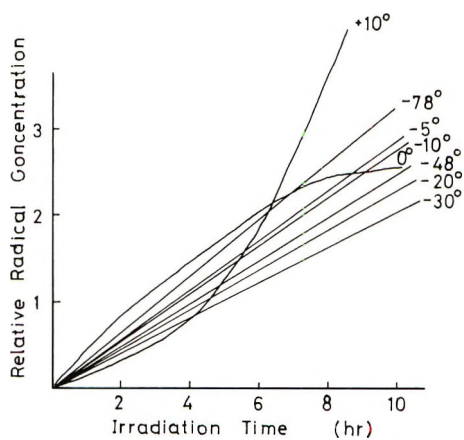


Fig. 8. Radical build-up at various temperatures.

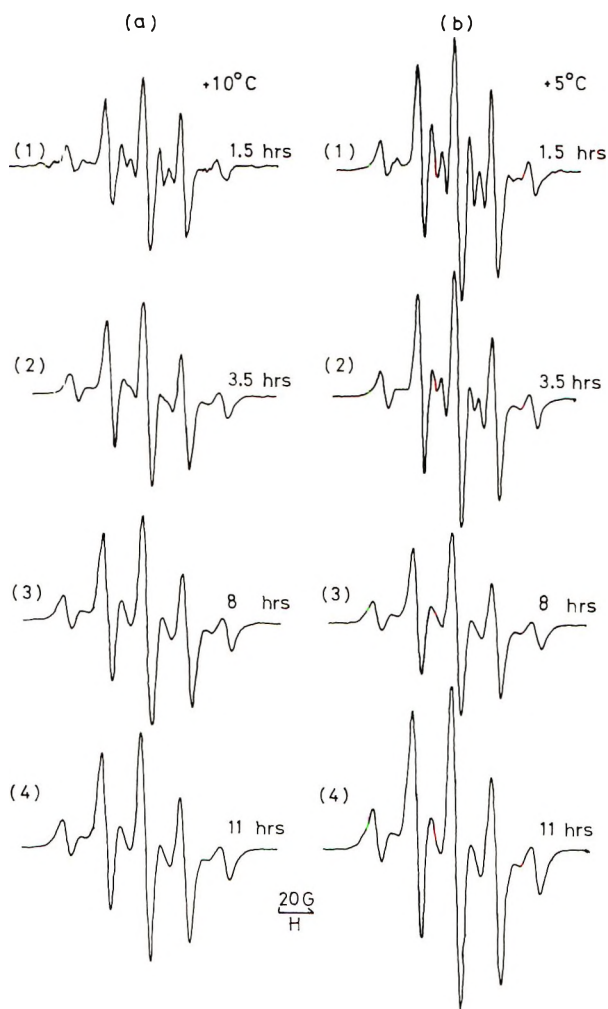


Fig. 9. (continued)

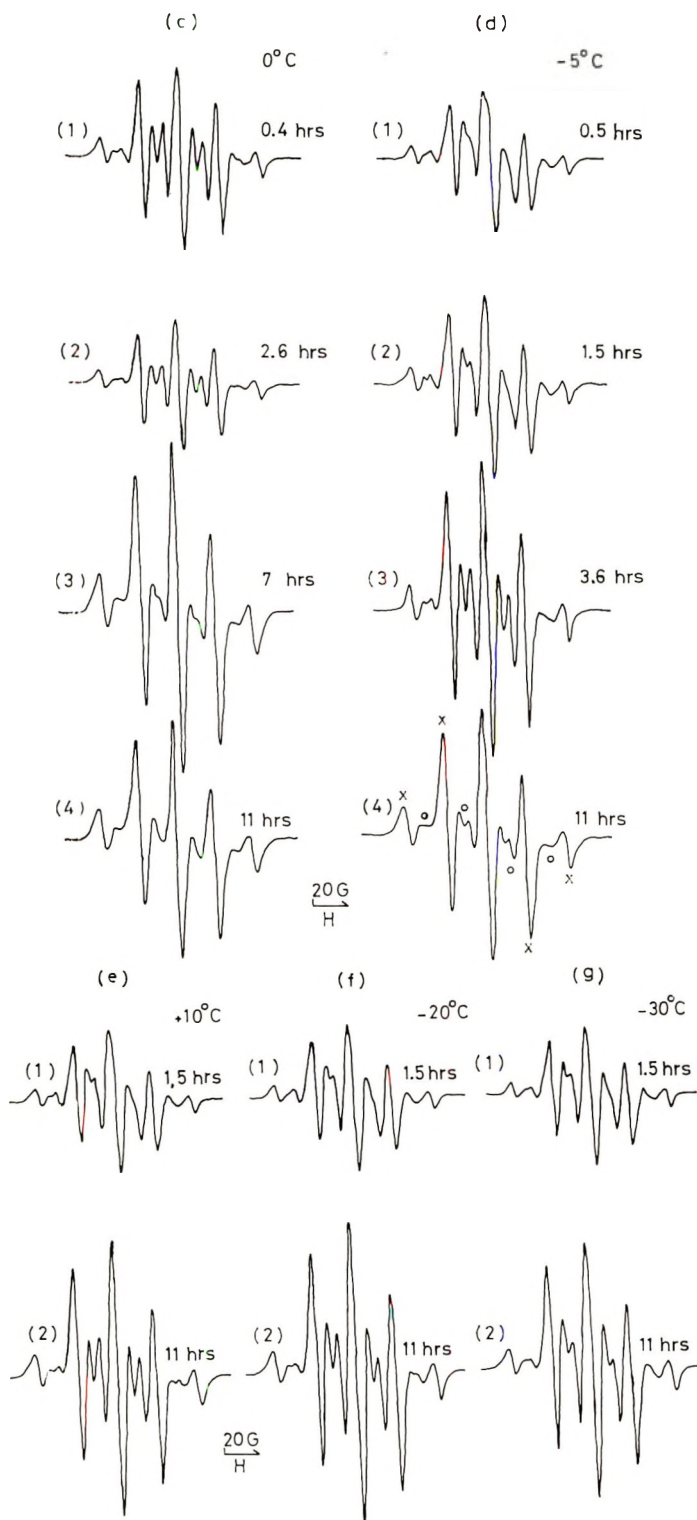


Fig. 9. Change of ESR spectrum with irradiation time at various temperatures: (a) 10°C; (b) 5°C; (c) 0°C; (d) -5°C; (e) -10°C; (f) -20°C; (g) -30°C.

diation time below -5°C , but the trapping rate of the radicals seems to be accelerated with increasing irradiation dose at $+10^{\circ}\text{C}$.

Change of ESR Spectrum during Polymerization

The ESR spectra of crystalline methacrylic acid irradiated at various temperatures were recorded at -196°C . The observed spectra are shown in Figure 9. Above 0°C for the low-dose irradiation, a 13-line spectrum was obtained, while as the irradiation dosage increases, the spectrum changes into 9-line spectrum (Fig. 9a, 9b, and 9c). On the other hand, at -5°C the results are a little different. For the low-dose irradiation some of the lines are unresolved and appeared as the shoulders because of the broad-line width. The line width becomes narrower after 3.6 hr irradiation and a 13-line spectrum appears. For prolonged irradiation, the so-called 4-line component (the lines marked \circ in Fig. 9d, spectrum 4 become weak compared with the so-called 5-line component marked \times in Fig. 9d, spectrum 4). As shown in Figure 9e, 9f, and 9g, when the samples were irradiated at lower temperatures, the intensity of the so-called 4-line component did not become so weak even after 11 hr irradiation as in the case of the samples irradiated above 0°C .

DISCUSSION

Effect of the Crystalline Transition on the Rate of Polymerization

A study of the broad-line NMR and differential scanning calorimetry of crystalline methacrylic acid⁶ indicated that there is a transition point around -30°C and that the crystals above the transition point (phase I) have a more closely packed structure than those below the transition (phase II), which is contrary to the usual case. This conclusion was also confirmed by the observation of the behavior of the trapped radicals in these two phases such as radical build-up and decay measurements. The details of the crystalline transition were described in the previous report.⁶ The results shown in Figure 2 can be explained in terms of the difference in rigidity of the crystals between the two phases. The discontinuity in the linear $1/T$ versus rate plot at -25°C is attributable to this transition. It seems reasonable to assume that the difference of activation energy between two crystalline phases is due to the difference of the arrangement of the molecule, as the different crystalline phases must have different molecular arrangement. Hardy et al.⁷ observed a similar effect of the crystalline transition on the rate of polymerization of solid cetyl methacrylate. According to their results, there is a transition at -16°C , and a marked change of the rate of polymerization was observed at that transition point. This change of the rate of polymerization was explained as due to both changes in the structure of the solid and in the mechanism of polymerization.

Kinetics of Solid-State Polymerization of Methacrylic Acid

Various polymerization mechanisms have been reported for the radiation-induced polymerization of solid monomers. Lipscomb et al.⁸ reported a mechanism that the polymerization reaction of solid methyl methacrylate is proportional to the polymer concentration [P]

$$d[P]/dt = kI^{\alpha}[P]$$

where I is dose rate. On the other hand, Hardy et al.⁹ studied the mechanism of solid-state polymerization of *N*-vinylsuccinimide and proposed other kinetics. They said that the accelerated character of polymerization curves is the overall result of radical accumulation and the autocatalytic effect of polymer. Thus the rate of polymerization is proportional to the momentary concentrations of free radicals [\dot{R}], of the monomer and of the polymer

$$-d[M]/dt = k_p[\dot{R}][M]([M_0] - [M] + a_0)$$

where $[M_0]$ and $[M]$ are the initial concentration and the momentary concentration of the monomer, respectively, and k_p is the rate constant of the chain growth reaction. In both postulations cited above, the chain termination was neglected.

In the case of methacrylic acid, however, chain termination seems not to be negligible, according to the study of the decay of trapped radicals by ESR measurements. The results of ESR measurements have shown that the decay rates are appreciable above -10°C . Although there is some controversy as to whether the radicals observed by ESR measurements are the real propagating species or not, the results of post-polymerization have also shown that termination reactions occur during polymerization. The details will be discussed in Part III of this series.¹⁰ It was observed from ESR measurements and post-polymerization that the decay rate of radicals in the solid monomer matrix is proportional to the momentary concentration of the radicals in the temperature range below 0°C . Besides, the results of radical build-up measurements as shown in Figure 8, indicate that different kinetics must be applied to the polymerization below -10°C , at 0°C and $+10^{\circ}\text{C}$.

Below -10°C . In Figure 8 it is shown that the rate of radical accumulation is constant below -10°C , so that

$$d[R]/dt = K \quad (1)$$

where $[R]$ is radical concentration and K is constant. When the rate of polymerization is assumed to be proportional to the concentration of the radical, of the monomer and of the polymer, then

$$-d[M]/dt = k_p[R][M]([M_0] - [M] + c) \quad (2)$$

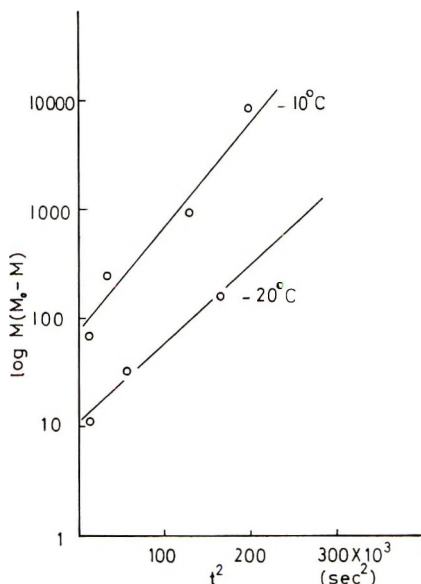


Fig. 10. Logarithm of the product of concentration of the monomer and the polymer vs. the square of irradiation time.

where $[M]$ and $[M_0]$ are the momentary and initial concentrations of the monomer, respectively, and c is a constant. From eqs. (1) and (2), eq. (3) is obtained:

$$1/([M_0] + c) \ln c[M_0]/\{[M]_0 - [M] + c\} = 1/2Kk_p t^2 \quad (3)$$

Then a plot of $\log [M]([M_0] - [M])$ versus t^2 should give a straight line, assuming c is negligibly small. Such a plot, as given in Figure 10 for various temperatures, shows that the relationship (3) holds below -10°C .

At 0°C . As is shown in Figure 8 the rate of accumulation of the trapped radicals is not constant at 0°C . Consequently eq. (4) should be used in place of eq. (1).

$$d[\dot{R}]/dt = R_i - k_t[\dot{R}] \quad (4)$$

where R_i is the rate of formation of the radical and K_t is the decay constant. From eqs. (2) and (4) the relationship (5)

$$\begin{aligned} 1/([M_0] + c) \ln c[M_0]/\{[M]([M_0] - [M] + c)\} \\ = -k_p R_i/k_t(-e^{-k_t t}/k_t - t - 1/k_t) \end{aligned} \quad (5)$$

is obtained. Equation (5) means that a plot of $\log [M]([M_0] - [M])$ versus $e^{-k_t t}/k_t + t$ should give a straight line if c is extremely small compared with $[M]$. Such a plot is given in Figure 11, assuming k_t is $1.86 \times 10^{-4} \text{ sec}^{-1}$ according to the results of post-polymerization measurements.

At $+10^\circ\text{C}$. At $+10^\circ\text{C}$ the kinetics is more complicated because the rate of accumulation of the radicals seems to be accelerated by the presence

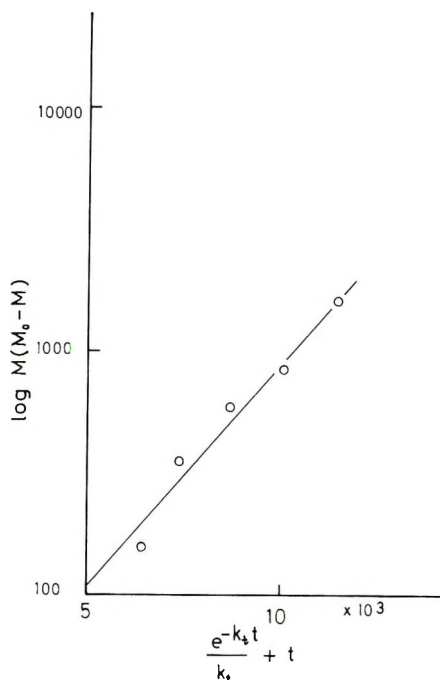


Fig. 11. Logarithm of the product of concentration of the monomer and the polymer vs. $e^{-k_d t}/k_t + t$.

of polymer in the system. Thus the rate of radical accumulation is expressed as

$$d[R]/dt = R_i - k_t[R^2][M]/[M_0] \quad (6)$$

where R_i is assumed to be constant and the radicals decay by second-order kinetics by reference to the radical decay measurements. However, the overall rate of polymerization is too complicated to be expressed in a simple equation.

Effect of Addition of Water

The study of the effect of water admixed in the solid monomer gives important information of the mechanism of solid-state polymerization of methacrylic acid. According to the differential scanning calorimetry measurements, methacrylic acid and water do not form an eutectic mixture. They seem to crystallize separately. As the percentage of water in the monomer increases, both the polymer yield and the intrinsic viscosity increase up to 20% water content, as shown in Figures 6 and 7. This would mean that polymerization occurs initially on the surface or the defect of the crystals and the admixed water has the effect of increasing the number of such active sites. In this case, the number of propagating chains increases. In addition, the rate of propagation changes because the increase

in disorder of the matrix which surrounds the propagating radicals may favor the addition of monomer to the propagating radicals in the case of methacrylic acid. As a result of this, the polymer yield and molecular weight increase when water is added to the monomer. On the other hand, when the water content is more than 20%, the chain transfer reaction may

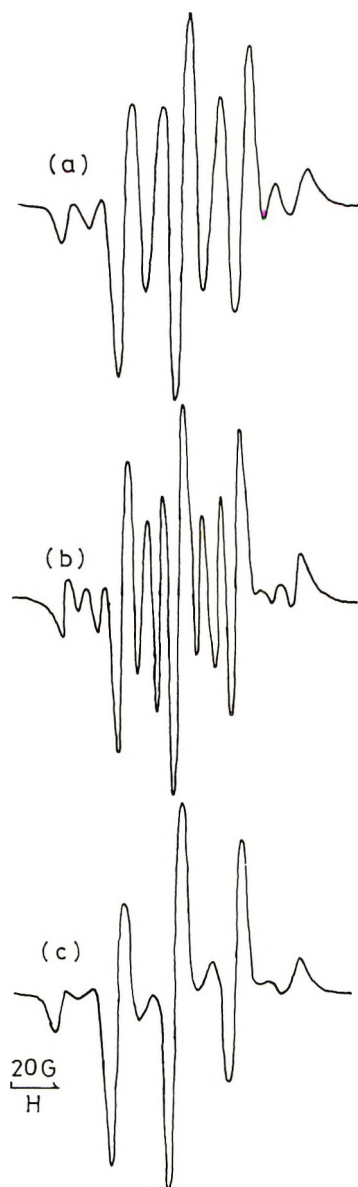
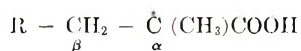


Fig. 12. ESR spectra of (a) the radicals trapped in methacrylic acid crystals at -160°C (in phase II) and (b) at -24°C (in phase I); (c) the radicals trapped in poly(methacrylic acid) (at $+25^{\circ}\text{C}$).

become significant, resulting in a decrease in the average molecular weight, whereas the number of initiating sites is much increased, yielding more polymer than in the case of lower water content.

ESR Spectrum of Propagating Radical

It has been shown by many workers that free radicals trapped in irradiated crystalline methacrylic acid have the same structure as those trapped in poly(methacrylic acid) when irradiated with ionizing radiation. They have been shown to be the propagating radical, $R-CH_2-\dot{C}(CH_3)COOH$, but the lifetime and the ESR spectrum of this radical are different, depending on the matrix which surrounds the radicals. The radicals trapped in the poly(methacrylic acid) are fairly stable even at room temperature, while the radicals trapped in the crystalline methacrylic acid monomer are stable only at low temperatures and cannot be observed near the melting point ($+16^\circ C$). Typical ESR spectra of methacrylic acid radicals trapped in the monomer matrix and in the polymer matrix are shown in Figure 12. The ESR spectrum of the radicals in the monomer matrix changes with observation temperature and they have a 9-line ($5 + 4$ line) structure in phase II (below the transition point) (Fig. 12*a*), while a 13-line ($5 + 8$ line) spectrum is observed in phase I (above the transition) (Fig. 12*b*). On the other hand, the ESR spectrum of the radicals formed in poly(methacrylic acid) shows little temperature dependence and has a 9-line structure (Fig. 12*c*). In addition, it should be noted that the intensity of the so-called 4-line component is much weaker in the case of poly(methacrylic acid) radicals than that in the case of radicals trapped in the monomer. It has been shown that the radicals in the monomer matrix have an asymmetrical conformation, that is to say, the two β -protons of the propagating radical



have unequal coupling constants, giving the conformational angle of the half-filled p -orbital to the C—H bond as 55° and 65° , respectively. The change in the ESR spectrum with temperature was interpreted in terms of the exchange of the two β -protons due to the hindered oscillation around the $C_\alpha - C_\beta$ bond.¹¹ On the other hand, the ESR spectrum of the poly(methacrylic acid) radical was interpreted by introducing the concept of the distribution of the conformational angle in the irregular polymer matrix.¹² The 9-line spectrum having a weak 4-line component was well simulated if a Gaussian distribution was assumed around the most probable conformation, which is the same as that of the propagating radical trapped in the monomer matrix.

Consequently, the difference in the intensity of the 4-line component between the spectra of monomer and polymer is the cause of the change of the ESR spectrum during the polymerization of crystalline methacrylic acid. The change of the ESR spectrum of methacrylic acid radical with the conversion of the monomer into the polymer is shown in Figure 9. As

shown in Figure 9a the 4-line component (in this case actually each line of the 4-line component is split into a doublet) becomes weak as the polymerization proceeds, because the matrix which surrounds the free radicals changes into polymer-rich matrix. On the other hand, at low temperature the degree of conversion into polymer is so small that the intensity of the 4-line component remains unchanged, as shown in Figures 9e, 9f, 9g. Bowden et al.¹³ studied the ESR spectrum of γ -irradiated barium dihydrate at various annealing temperatures and obtained various spectra. These spectra were all attributed to the methacrylate propagating radical $\text{RCH}_2\dot{\text{C}}(\text{CH}_3)\text{COO}^-$ and were considered to result from different conformations of the β -methylene carbon-hydrogen bonds. These conformations were believed to depend on the length of the radical chain, the temperature, and the environment. In the present case of methacrylic acid, the environment of the radical is considered to be the most significant factor which determines the line shape of ESR spectrum.

The author wishes to thank Dr. M. Iwasaki of Government Industrial Research Institute Nagoya for his helpful advice.

References

1. H. Morawetz and I. D. Rubin, *J. Polym. Sci.*, **57**, 687 (1962).
2. C. H. Bamford, A. D. Jenkins, and J. C. Ward, *J. Polym. Sci.*, **48**, 37 (1960).
3. C. H. Bamford, G. C. Eastmond, and J. C. Ward, *Proc. Roy. Soc. (London)*, **A271**, 357 (1963).
4. C. H. Bamford, G. C. Eastmond, and Y. Sakai, *Nature*, **200**, 1284 (1963).
5. C. H. Bamford, A. Bibby, and G. C. Eastmond, in *Macromolecular Chemistry, Prague, 1965* (*J. Polym. Sci. C*, **16**), O. Wichterle and B. Sedláček, Eds., Interscience, New York, 1967, p. 2417.
6. Y. Sakai and M. Iwasaki, paper presented at 16th Symposium on Macromolecular Chemistry, Japan, 1967; *J. Polym. Sci. A-1*, in press.
7. Gy. Hardy, K. Nyitray, G. Kovacs, and N. Fedorova, *Acta Chim. Hung.*, **43**, 121 (1965).
8. N. T. Lipscomb and E. C. Weber, *J. Polym. Sci. A-1*, **5**, 779 (1967).
9. Gy. Hardy, J. Varga, G. Nagy, F. Cser, and J. Erő, in *Macromolecular Chemistry, Prague, 1965* (*J. Polym. Sci. C*, **16**), O. Wichterle and B. Sedláček, Eds., Interscience, New York, 1967, p. 2583.
10. Y. Sakai, *J. Polym. Sci. A-1*, this issue.
11. Y. Sakai and M. Iwasaki, *J. Polym. Sci. A-1*, in press.
12. M. Iwasaki and Y. Sakai, *J. Polym. Sci. A-1*, in press.
13. M. J. Bowden and J. H. O'Donnell, *J. Phys. Chem.*, **72**, 1577 (1968).

Received April 10, 1969

Revised May 19, 1969

Radiation-Induced Solid-State Polymerization of Methacrylic Acid. III. Post-Polymerization

YOSHIRO SAKAI, *Department of Industrial Chemistry, Ehime University, Bunkyo-cho, Matsuyama, Ehime, Japan*

Synopsis

The post-polymerization of methacrylic acid in the solid state was studied. The decay of the trapped radicals was also observed by ESR measurements. The decay of trapped radicals is a first-order reaction below 0°C but a second-order reaction at +10°C. The results of the post-polymerization were compared with the results of radical decay measurements. A kinetic scheme was proposed for the post-polymerization of methacrylic acid. The effect of conditions of monomer crystallization on the polymer yield was also investigated. Fine crystals gave a greater limiting conversion than large crystals. The addition of water to the monomer increased the polymer yield. The change in the ESR spectrum during post-polymerization was interpreted in terms of the change in the matrix which surrounds the propagating radicals.

INTRODUCTION

In the preceding reports,¹⁻³ the ESR spectrum of propagating radicals of methacrylic acid, the crystalline transition of methacrylic acid, and the in-source polymerization in the solid state were investigated. The temperature dependence of the line shape of the ESR spectrum, the behavior of trapped radicals such as radical decay and build-up were well explained by reference to the difference in rigidity of the two phases of crystals. A crystalline transition was found to exist around -30°C by measurements of the broad-line NMR and differential scanning calorimetry. In the study of in-source polymerization, a discontinuity in the Arrhenius plot of the rate of conversion appeared at this transition point. It was found that in the in-source polymerization between 0°C and -20°C the rate of polymerization is proportional to the concentrations of propagating radical, monomer, and polymer. In the present paper, the post-polymerization of methacrylic acid in the solid state was investigated in connection with the behavior of the trapped radicals.

EXPERIMENTAL

The irradiation was carried out with γ -rays from a Co⁶⁰ source at a dose rate of 3×10^4 R/hr at -78°C. The purification of methacrylic acid and the degassing procedure are identical to that reported previously.¹ The samples were crystallized by shock cooling to -196°C from +20°C

(liquid) and were irradiated at -78°C . After the irradiation they were kept at elevated temperatures in a thermostat to polymerize for a given time and then rapidly cooled to -78°C . The polymer was isolated by dissolving the unreacted monomer in cold ether (-78°C). The amount of polymer produced was determined gravimetrically.

The samples for the ESR measurements were sealed in Spectrosil tubes under vacuum. ESR spectra were recorded by using a Japan Electron Optics Model 3BSX at 9.4 Gcps with 100 keps modulation. The relative radical concentration was obtained by double integration of the first-derivative ESR spectra with the use of a Japan Electron Optics Model JR-5 spectrum computer.

RESULTS AND DISCUSSION

Decay of the Trapped Radicals and Post-Polymerization

The samples irradiated at -78°C were annealed at various temperatures for a given time and then rapidly cooled to -196°C , at which temperature ESR spectra were recorded. The calculation of relative radical concentration was carried out simultaneously by use of a computer. Figure 1 shows the decay of the trapped radicals at various temperatures. Good first-order rate plots were obtained below 0°C as shown in Figure 2, but at 10°C the radicals decay by a second-order reaction, as shown in Figure 3.

In Figures 4 and 5 the per cent conversion is plotted against polymerization time in minutes at various temperatures in the range $+10$ to -20°C

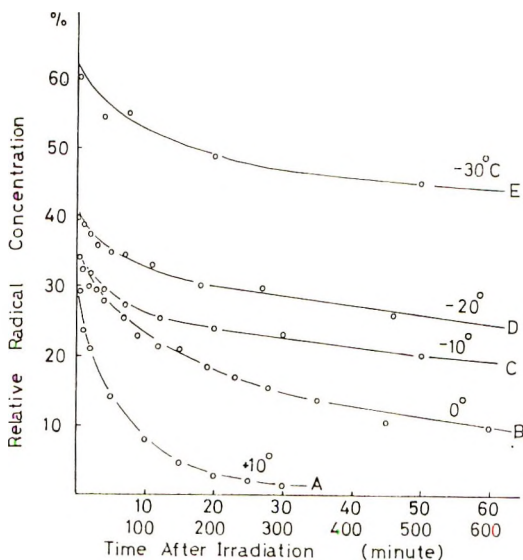


Fig. 1. Decay of trapped radicals. The upper scale of the abscissa is for curves A, B, and C; the lower scale is for curves D and E. The radical concentration immediately after the irradiation was taken as 100%. The irradiation dose was 3×10^5 R at -78°C .

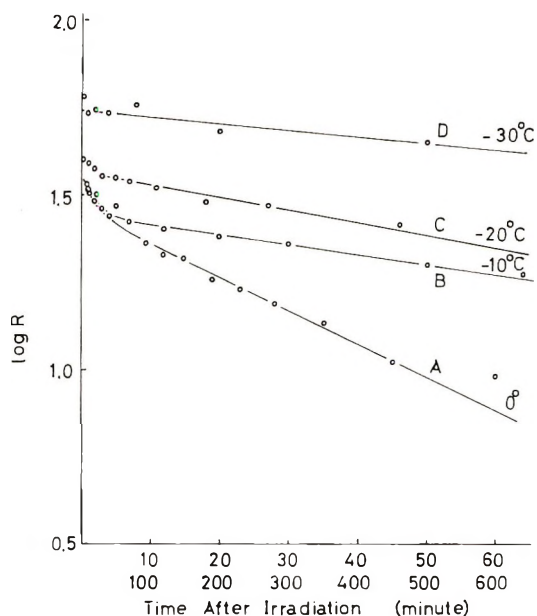


Fig. 2. Logarithm of relative radical concentration vs. annealing time. The upper scale of the abscissa is for curves *A* and *B*; the lower scale is for curves *C* and *D*.

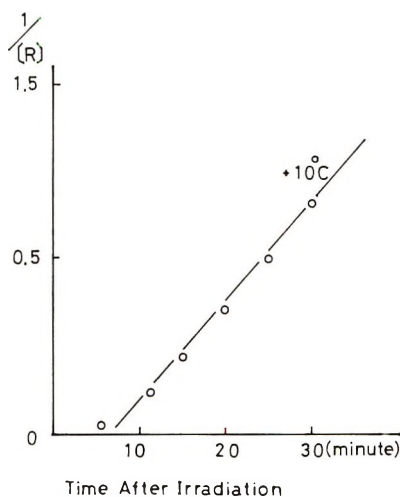


Fig. 3. Reciprocal of relative radical concentration vs. annealing time at $+10^{\circ}\text{C}$.

and at pre-irradiation doses of 2.3×10^4 to $3.2 \times 10^5\text{R}$. These figures show that limiting conversions exist in the post-polymerization of methacrylic acid in the solid state. The intrinsic viscosity was found to be independent of the irradiation dose. As the termination reaction proceeds by a first-order reaction, it seems reasonable that the intrinsic viscosity is independent of the irradiation dose if the density of the initiation sites is not so high that the propagating chains interact with each other.

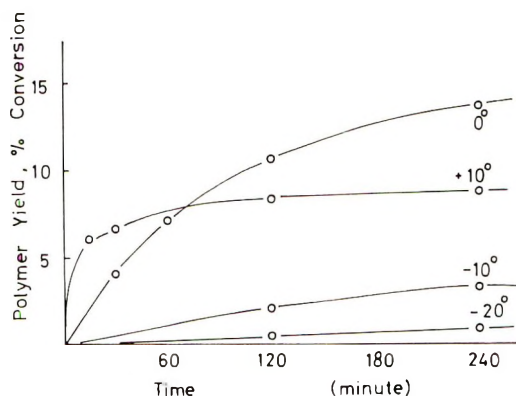


Fig. 4. Polymer yield vs. time for post-polymerization at various temperatures. The irradiation dose was $9.6 \times 10^5 R$.

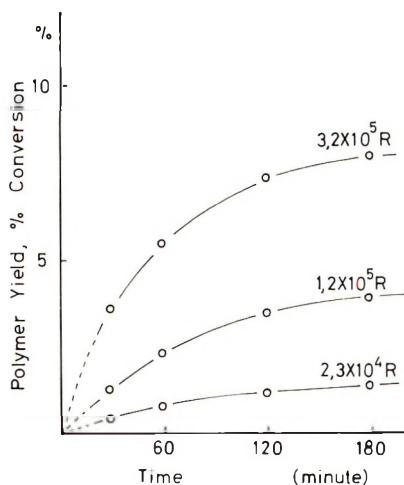


Fig. 5. Polymer yield vs. time for post-polymerization at $0^\circ C$ at various pre-irradiation doses.

There have been reported various kinetics of solid-state polymerization. Parrish and his co-workers⁴ observed the post-polymerization of γ -irradiated 2-vinylnaphthalene in the solid state. They assumed the existence of a limiting conversion and suggested the equation:

$$-d(a - x)/dt = k_p[M^*](a - x) \quad (1)$$

where a is the limiting conversion of the monomer, x is the amount of monomer converted into polymer, and $[M^*]$ is the concentration of the active species. On integrating eq. (1), eq. (2) is obtained:

$$\ln a/(a - x) = k_p[M^*]t \quad (2)$$

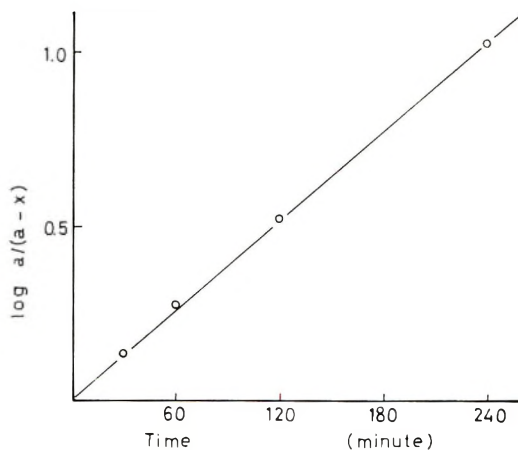


Fig. 6. Plot of $\log a/(a-x)$ vs. polymerization time. a is the limiting conversion, taken as 15% in this case, and x is the degree of conversion at time t .

Under the conditions of irradiation of methacrylic acid used, the limiting conversion must be 15%. Although in Figure 5 the limiting conversions can be expected to be higher than 15% for higher irradiation doses, the experimental results showed that this limiting value of 15% can be expected even at higher dose, e.g. 14.4% of conversion was obtained for the 180 min polymerization at a pre-irradiation dose of 6×10^6 . In Figure 6 $\log a/(a-x)$ is plotted against time for the data at 0°C. The straight line in Figure 6 shows that eq. (1) also holds in the case of the methacrylic acid. However, measurements of ESR of the trapped radicals, as shown in Figures 2 and 3, show that the radicals decay by a first-order reaction below 0°C and by a second-order reaction at +10°C; the decay constants were evaluated as $1.12 \times 10^{-2} \text{ min}^{-1}$ at 0°C. Consequently, the relation for the radical decay reaction should be added to the above relation, that is, below 0°C

$$-d[M^*]/dt = k_t[M^*] \quad (3)$$

and at +10°C

$$-d[M^*]/dt = k_t[M^*]^2 \quad (4)$$

From eqs. (2) and (3), eq. (5) is obtained:

$$\ln a/(a-x) = [M_0^*]k_p/k_t(1 - e^{-k_t t}) \quad (5)$$

where $[M_0^*]$ is the initial radical concentration. If relations (2) and (3) hold below 0°C, a straight line should be obtained when $\log a/(a-x)$ is plotted against $1 - e^{-k_t t}$. Such a plot for the measurements at 0°C is given in Figure 7. The curve deviated markedly from linearity when k_t is taken as $1.12 \times 10^{-2} \text{ min}^{-1}$ according to the results of radical decay measurements. In order to obtain a straight line, as shown by the dotted line in Figure 7, k_t must have a value of $1 \times 10^{-3} \text{ min}^{-1}$, that is about one

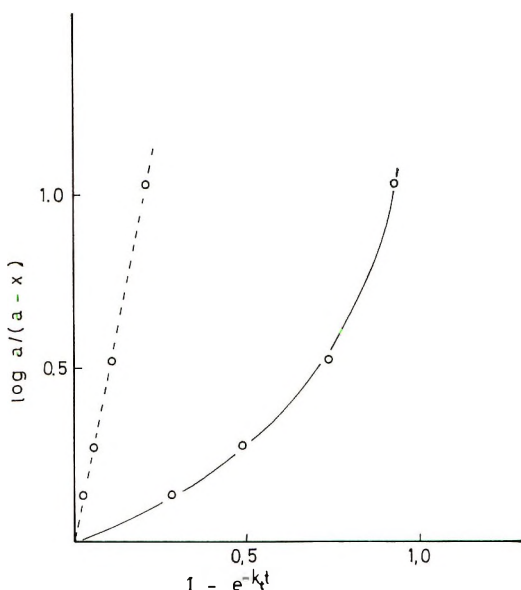


Fig. 7. Plot of $\log a/(a-x)$ against $1 - e^{-k_t t}$. a is the limiting conversion, that is, 15% in this case, and x is the degree of conversion at time t . k_t is the rate constant of radicals decay reaction.

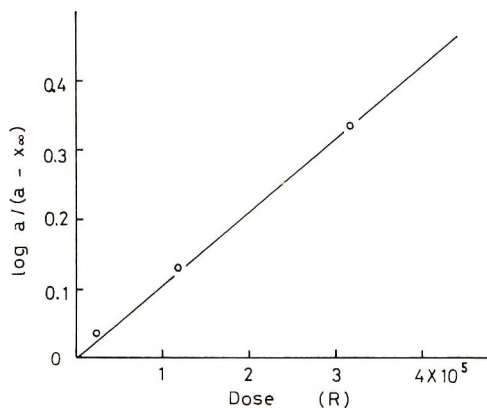


Fig. 8. Plot of $\log a/(a-x_{\infty})$ at $t \rightarrow \infty$ against irradiation intensity. a is 15%, x is the limiting conversion at each dose rate.

tenth of the decay constant given by ESR measurements. The reason for this discrepancy may be that ESR measurements may give values for the decay of all the radicals, regardless of the size of the propagating radicals. By the gravimetric method, however, relatively short chains are omitted. Because the k_t is small, the termination reaction can be neglected in the post-polymerization of solid methacrylic acid as shown in eq. (2). That is the reason why a straight line is obtained in Figure 6 despite neglect of the termination reaction.

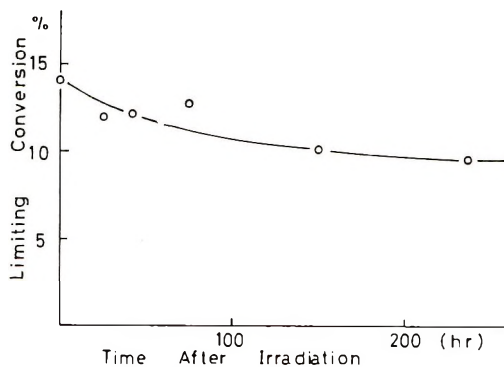


Fig. 9. Decay of active species which initiate the post-polymerization.

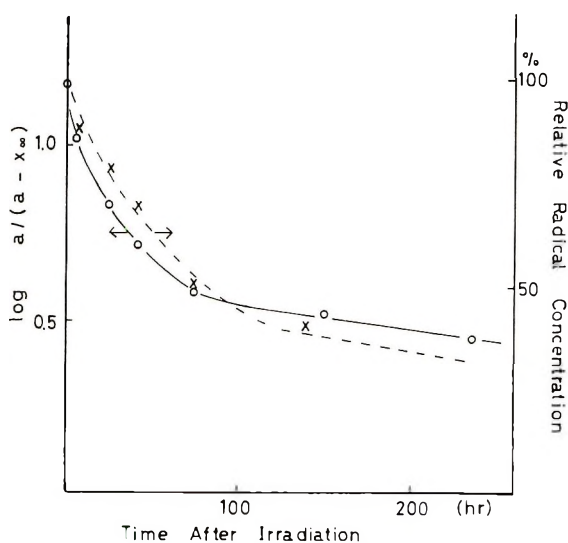


Fig. 10. Plot of $\log a/(a - x_{\infty})$ vs. time after irradiation. A comparison of the decay curve of the trapped radicals calculated from the data of post-polymerization (—) with those (---) obtained by ESR measurements.

From eq. (5) the limiting conversion for a given pre-irradiation dose can be calculated, assuming that the initial radical concentration $[M_0^*]$ is proportional to the pre-irradiation dose, that is when $t \rightarrow \infty$, eq. (5) becomes

$$\ln a/(a - x_{\infty}) = [M_0^*]k_p/k_t \quad (6)$$

where x_{∞} is the limiting conversion for a given pre-irradiation dose. In Figure 8, $\log a/(a - x_{\infty})$ is plotted against the pre-irradiation dose and a linear relationship is observed. This linear relationship given in Figure 8 indicates that eq. (6) holds at 0°C . As it was proved in Figure 8 that the initial radical concentration $[M_0^*]$ is proportional to $\ln a/(a - x_{\infty})$, it is possible to estimate $[M_0^*]$ from the limiting conversion x_{∞} , which means

TABLE I
Effect of Crystallization Temperature of the Monomer

	Crystallized at +13°C	Crystallized at -196°C
limiting conversion, %	12.8	3.7
$[\eta]$, dl/g	4.12	3.29
Relative radical concentration immediately after irradiation (<i>a</i>)	100	89
Relative radical concentration after annealing at -78°C (<i>b</i>)	82	73
Ratio <i>b</i> / <i>a</i>	0.82	0.82

that the change of the concentration of the trapped radicals can be given by the measurements of limiting conversions as well as by ESR measurements. Comparison of the results by these two methods must be of interest. Several samples irradiated at -78°C with the same dose were stored at -78°C . The samples were post-polymerized at 0°C after various storage times, and the limiting conversion was obtained at each storage time. The results were plotted in Figure 9. From the data in Figure 9 $\log a/(a - x_{\infty})$, which is proportional to the initial radical concentration, was calculated and is plotted against storage time in Figure 10. The decay curve obtained by ESR measurements is also plotted in the same figure by the dotted line. The decay curve of the trapped radicals obtained by the method of polymerization is in fair agreement with that obtained by ESR measurements.

It is known that the crystallization conditions of monomers affect the rate of polymerization in the solid state. Two different crystalline samples were prepared. The one crystallized at $+13^{\circ}\text{C}$ (mp $+16^{\circ}\text{C}$) gave a greater limiting conversion than that crystallized at -196°C . The former sample consists of larger crystals than the latter. The limiting conversions, the intrinsic viscosity, and the relative radical concentration obtained by ESR measurements are summarized in Table I. These results

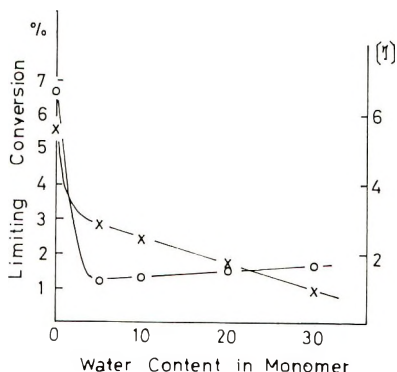


Fig. 11. Effect of addition of water on limiting conversion and intrinsic viscosity of poly(methacrylic acid): (O) limiting conversion; (X) intrinsic viscosity.

suggest that most of the termination reaction occurs at the surface or the defects of the crystals because the smaller crystals prepared at -196°C , which have a greater surface area and more defects than the crystals prepared at $+13^{\circ}\text{C}$, gave the lower limiting conversion and viscosity.

The effect of additives in the methacrylic acid crystals may also give some information on the mechanism of post-polymerization. The methacrylic acid samples containing various amounts of water were crystallized at -196°C and irradiated at -78°C . The irradiated mixed crystals were polymerized at -10°C . Figure 11 shows that the limiting conversion and the intrinsic viscosity are markedly decreased by the addition of water in methacrylic acid. It is attributable to the enhanced termination of propagating radicals due to the chain transfer to water. However, another possibility should not be excluded, that is the effect of added water on the concentration of trapped radicals. Several samples containing various amounts of water were irradiated at -78°C and their relative radical concentration were obtained by ESR measurements at -196°C . The results are shown in Table II. It is indicated that the concentration of trapped radicals is independent of the water content.

TABLE II
Effect of Addition of Water on the Concentration of the Trapped Radicals

Water in the monomer, %	Relative radical concentration
0	1.00
10	1.24
20	1.20
30	1.24

Change of ESR Spectrum during Post-Polymerization

It was reported in a previous paper¹ that the ESR spectrum of crystalline methacrylic acid changes with observations temperature because the line shape of the spectrum depends on the matrix which surrounds the radicals. It was also observed that the crystalline form of the matrix close to the propagating radicals remains unchanged when the sample was rapidly cooled down to -196°C passing through the transition point. As a result the ESR spectrum of the sample which was rapidly cooled down to -196°C from an elevated temperature was observed at -196°C and it was the same as that observed at the elevated temperature. Consequently the effect of the surrounding matrix at a given temperature on the trapped radicals can be observed when the samples are rapidly cooled down to -196°C from the given temperature. Crystalline methacrylic acid irradiated at -196°C was kept at an elevated temperature for 5 min and then rapidly cooled down to -196°C , at which temperature the ESR spectrum was recorded. The procedure was then repeated at a higher annealing temperature. The intensity of the ESR spectrum decreased as the annealing

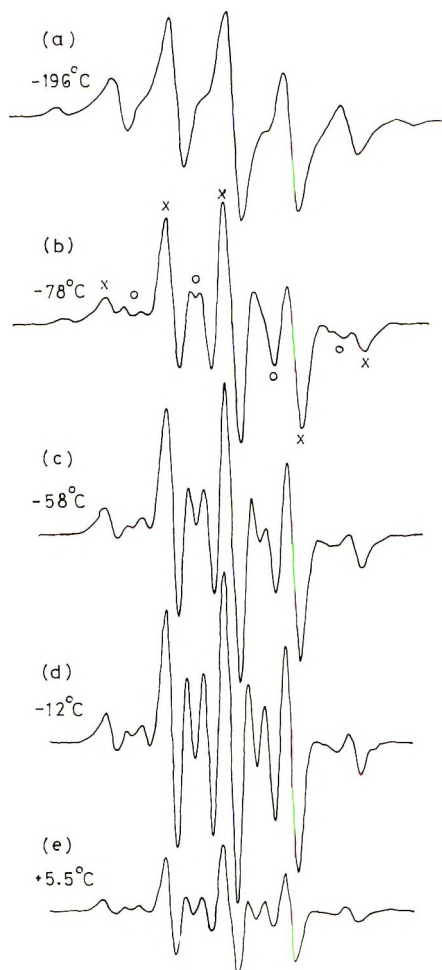


Fig. 12. Change of line shape of ESR spectrum in the course of radical decay.

temperature increased; in addition, the line shape of the spectrum changed, depending on the crystalline forms and the polymer content in the methacrylic acid crystals. The ESR spectra are shown in Figure 12. At first, immediately after the irradiation at -196°C , a 7-line spectrum was observed as shown in Figure 12a; this was assigned to the monomer radical $\text{CH}_3-\dot{\text{C}}(\text{CH}_3)\text{COOH}$. But when the methacrylic acid was annealed at -78°C , the spectrum changed into a 9-line spectrum which is attributable to the propagating radical $\text{R}-\text{CH}_2-\dot{\text{C}}(\text{CH}_3)\text{COOH}$ (Fig. 12b). As the annealing temperature was raised further, the 9-line spectrum changed into a 13-line spectrum. This change was interpreted in terms of the exchange of the two β -protons due to the hindered oscillation around the $\text{C}_\alpha-\text{C}_\beta$ bond of the propagating radical.¹ Above 0°C , post-polymerization proceeded to some extent, and the effect of the polymer which surrounds the

radicals appeared. It was reported⁵ that the intensity of the 4-line component of the ESR spectrum of the radicals formed in poly(methacrylic acid) is much weaker than that of the radicals trapped in methacrylic acid monomer crystals. In the case of the radicals trapped in poly(methacrylic acid) the so-called 4-line component (denoted by the circles, ○) in Figure 12b became weak due to some distribution of the conformation of the radicals. Consequently as the polymerization proceeded, the polymer content in the matrix which surrounds the radical increased, and as a result the intensity of the 4-line component decreased. The details of the intensity of the 4-line component of the ESR spectrum of methacrylic acid radicals trapped in the monomer crystals which contain the polymer were discussed in a previous report.³

The author wishes to thank Dr. M. Iwasaki of Government Industrial Research Institute Nagoya for his helpful advice.

References

1. Y. Sakai and M. Iwasaki, *J. Polym. Sci. A-1*, in press.
2. Y. Sakai and M. Iwasaki, paper presented at 16th Symposium on Macromolecular Chemistry of Japan, 1967; *J. Polym. Sci. A-1*, this issue.
3. Y. Sakai, *J. Polym. Sci. A-1*, this issue.
4. C. F. Parrish, W. A. Triner, and C. K. Burton, *J. Polym. Sci. A-1*, **5**, 2557 (1967).
5. M. Iwasaki and Y. Sakai, *J. Polym. Sci. A-1*, in press.

Received April 10, 1969

Revised May 19, 1969

Polymers Derived from 2,5-Diamino-*p*-benzoquinone-diimide and Related Compounds

J. SZITA and C. S. MARVEL, *Department of Chemistry, University of Arizona, Tucson, Arizona 85721*

Synopsis

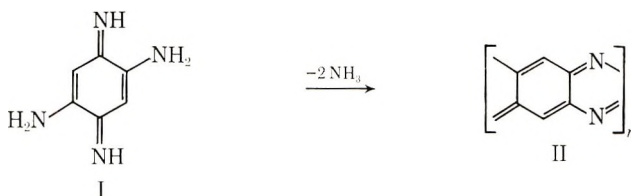
A number of new polymeric materials have been prepared by the self-condensation of 2,5-diamino-*p*-benzoquinonediimide and by its condensation with 2,5-diamino-*p*-benzoquinone, 2,5-dihydroxy-*p*-benzoquinone, and 2,5-dichloro-*p*-benzoquinone. Ladder polymers were expected, but in every case polymers with some open rings were obtained. 2,5-Diaminohydroquinone was condensed with 2,5-diamino-*p*-benzoquinonediimide and with 2,5-diamino-*p*-benzoquinone to produce heat stable polymers but the expected ladder structures were not obtained. Thermogravimetric analyses of the polymers in nitrogen all showed a weight loss at 100–150°C of 3–14% which was presumably due to loss of either chemically combined or absorbed water on the polymer and then only a 5% weight loss up to about 600°C with a final weight loss of 19% at 900°C.

INTRODUCTION

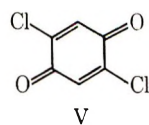
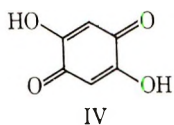
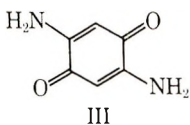
2,5-Diamino-*p*-quinonediimide (I) is a tetrafunctional molecule readily prepared pure by the method of Nietzki and Hagenbach¹ and as such it seemed a likely monomer to use in the synthesis of ladder structures which should show good thermal stability.

DISCUSSION

Self-condensation of the diimide by loss of the molecule of ammonia would be expected to yield a ladder polymer (II) with a low hydrogen content.

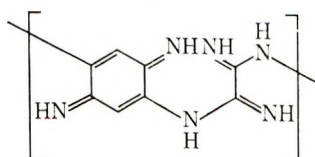


Similarly, condensation with 2,5-diamino-*p*-benzoquinone (III), 2,5-dihydroxy-*p*-benzoquinone (IV), and 2,5-dichloro-*p*-benzoquinone (V) could yield the same ladder polymers.



In actual practice it has been found that these reactions do not proceed completely to yield the desired products but a variety of partial ladder structures which have good thermal stability have been obtained.

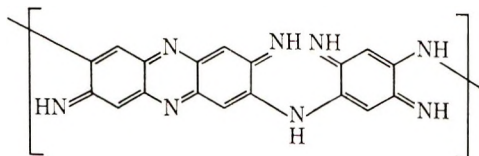
When the crude imide (I) or the hydrochloride was treated with polyphosphoric acid (PPA) first at room temperature, then at 60°C, and finally at 210°C, a black polymer was obtained after repeated purification by filtering, washing, and drying. Analyses showed it was not the expected ladder structure II but that it contained some oxygen which undoubtedly came from hydrolysis of some imide groups to carbonyl groups. The analytical and infrared data on this and other polymers prepared from the recrystallized free base under different conditions support the view that these polymers contain combinations of the recurring units VI-IX.



Polymer unit VI

with 2 =NH groups hydrolyzed to =O VI/1

with 3 =NH groups hydrolyzed to =O VI/2

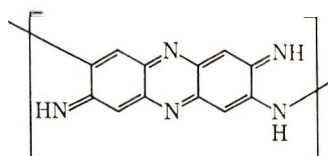


Polymer unit VII

with 1 =NH group hydrolyzed to =O VII/1

with 2 =NH groups hydrolyzed to =O VII/2

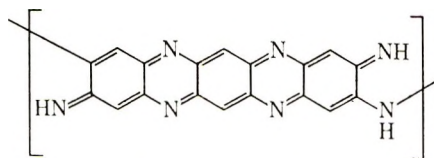
with 3 =NH groups hydrolyzed to =O VII/3



Polymer unit VIII

with 1 =NH group hydrolyzed to =O VIII/1

with 2 =NH groups hydrolyzed to =O VIII/2



Polymer unit IX

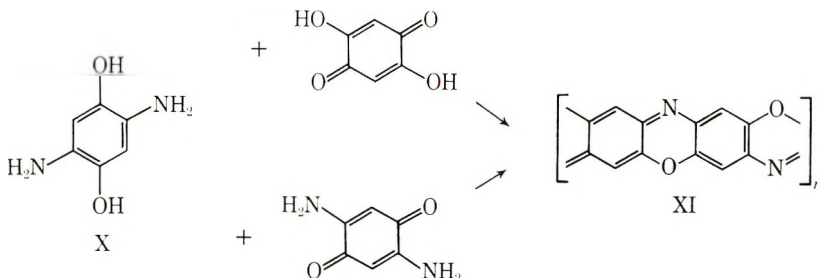
with 1 =NH group hydrolyzed to =O IX/1

with 2 =NH groups hydrolyzed to =O IX/2

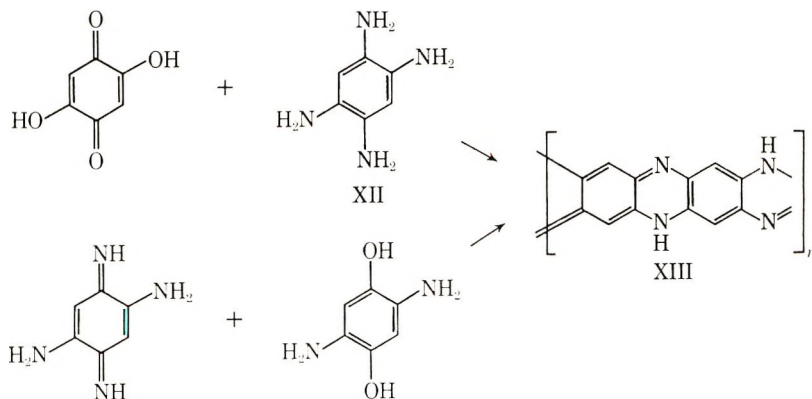
2,5-Diamino-*p*-benzoquinonediimide has also been condensed with 2,5-diamino-*p*-benzoquinone in PPA with 2,5-dihydroxy-*p*-benzoquinone in PPA and hexamethylphosphoramide (HMP) and with 2,5-dichloro-*p*-

benzoquinone in a mixture of dimethylacetamide (DMAc) and diethylaniline to yield partial ladder polymers which, on heating, further cyclized.

2,5-Diaminohydroquinone (X) was also used as a comonomer in some condensation reactions. Stille and Freeburger² have described the condensation of the hydroquinone and 2,5-dihydroxybenzoquinone, so we did not repeat that condensation. We expected to get the same polymer (XI) from 2,5-diamino-*p*-benzoquinone by cocondensation with the 2,5-diaminohydroquinone:



with 2,5-diamino-*p*-benzoquinonediimide and 2,5-diaminohydroquinone, it was expected that we would obtain the same polymer (XIII) which Stille and Mainen³ obtained from tetraaminobenzene (XII) and 2,5-dihydroxy-*p*-benzoquinone:



However, we did not obtain a complete ladder structure when we carried out our condensation in solution.

Thermogravimetric analyses on some of the samples, determined in nitrogen atmosphere at a heating rate of 3°C/min (180°C/hr) show that, in spite of the incomplete ring structure, the polymers exhibited good thermal stability. The weight loss of 3–14% between 50 and 150 is probably due to adsorbed moisture. Initial weight loss by chemical decomposition begins between 450 and 480°C, and the most thermostable polymers lost only about 5% of their weight at 600°C and 19% at 900°C. A typical TGA curve is shown in Figure 1.

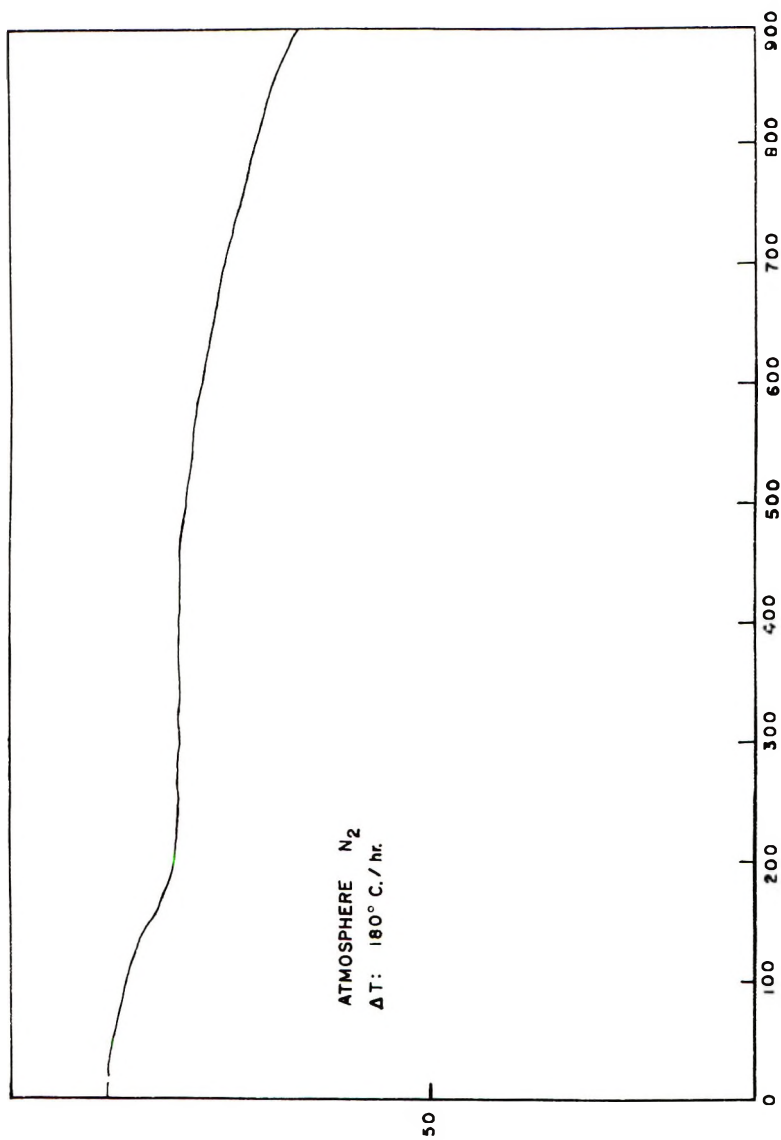


Fig. 1. TGA curve for polymer HP-2 prepared by self-condensation of 2,3-diamino-*p*-benzoquinonediimide.

EXPERIMENTAL

Monomers

Preparation of 2,5-Diamino-p-benzoquinonediimide

Hydrochloride. 1,2,4,5-Tetraaminobenzene tetrahydrochloride (5.7 g, 0.02 mole, from Burdick and Jackson) was dissolved ($\sim 50^\circ\text{C}$) in 25 ml of water, and the solution was filtered. A filtered solution of 31 g (0.05 mole) of iron trichloride hydrate ($\text{FeCl}_3 \cdot 6\text{H}_2\text{O}$) in 15 ml water was added dropwise under stirring at room temperature. In the next 30 min the temperature was kept between 45 and 50°C . The green-grey suspension was filtered after 3 hr at room temperature, and the precipitate washed with 2*N* hydrochloric acid and acetone and dried under reduced pressure at 55– 60°C . The yield was nearly quantitative (4.1 g). The green-brown product does not melt below 350°C .

ANAL. Calcd for $\text{C}_6\text{H}_{10}\text{N}_4\text{Cl}_2$: C, 34.50%; H, 4.82%; N, 26.81%. Found: C, 34.82%; H, 4.92%; N, 27.40%.

The HCl salt is easily soluble in water, soluble in hexamethylphosphoramide (HMP), partially soluble in hot dimethylformamide (DMF) and dimethylacetamide (DMAc), and insoluble in acetone, tetrahydrofuran and concentrated hydrochloric acid. It reacts (precipitation and decoloration) at higher temperatures in alcohols, dimethyl sulfoxide (DMSO), HMP, and PPA.

Free Base. 1,2,4,5-Tetraaminobenzene tetrahydrochloride (57.0 g, 0.2 mole) was oxidized as described above. The HCl salt obtained was dried for a while at 50°C under reduced pressure. The wet precipitate* was suspended in 400 ml concentrated sodium carbonate solution and stirred at room temperature for 3 hr. The dark grey-brown suspension turned light brown after 5–10 min and changed later to orange. The free base was filtered, washed several times with distilled water and acetone, and dried overnight at 60°C in a vacuum oven. The yield of the crude product was 23.6 g (86% from tetraaminobenzene). The light brown powder decomposed partially between 195 and 210°C .

ANAL. Calcd for $\text{C}_6\text{H}_8\text{N}_4$: C, 52.93%; H, 5.92%; N, 41.15%. Found: C, 53.30%; H, 5.91%; N, 41.72%.

A 7.0-g portion of the crude free base were recrystallized from 100 ml DMAc. The yield was 4.8 g. The orange-brown needles decomposed partially at 195– 210°C .

ANAL. Found: C, 52.93%; H, 5.79%; N, 41.08%.

The recrystallized free base was soluble in cold DMSO and in hot DMAc and DMF, partially soluble in methanol, ethanol, and HMPA, and not or only slightly soluble in water, tetrahydrofuran, acetone, acetonitrile, chloroform, and ether. The product reacted with dioxane at room temper-

* If the product is completely dried, the ion exchange takes more time.

ature and in DMSO, nitrobenzene, HMPA and PPA at higher temperature: pK_b values: 6.1 and 8.6.

Other Monomers

2,5-Diamino-*p*-benzoquinone and 2,5-diamino-*p*-hydroquinone dihydrochloride were prepared from 2,5-dihydroxy-*p*-benzoquinone by the known procedure.⁴

2,5-Dihydroxy-*p*-benzoquinone was obtained from Eastman Organic Chemicals and purified by recrystallization from absolute alcohol.

2,5-Dichloro-*p*-benzoquinone was purchased from Eastman Organic Chemicals and used as received.

Polymers

Self-Condensation of 2,5-Diamino (p)-benzoquinonediiimide

P-1. The hydrochloride of the diimide (3.5 g) was suspended in 50 g of polyphosphoric acid (82.5% P_2O_5) at room temperature under a nitrogen stream. After several minutes an intensive evolution of hydrogen chloride occurred. The product dissolved with a violet color. The mixture was heated for 1 hr at 60°C. During this time the HCl evolution slowed down. Afterwards the temperature was gradually raised to 200°C, and the mixture was kept at this temperature for 24 hr. The resulting dark green-black viscous reaction mixture was added portionwise to 1 liter of ammonium carbonate solution. The black precipitate was filtered, washed with diluted ammonium carbonate solution and distilled water, and then extracted with water for 4 days. The residue was dried at 70°C under reduced pressure. The yield of the black, H_2SO_4 -insoluble, powdery polymer was 2.7 g. Elemental analyses and infrared bands of this and of the following polymers are summarized in Table I.

P-2. The crude free base of the diimide (3.0 g) was suspended in 50 g of PPA. By heating, the brown suspension changed to a dark violet solution and at higher temperature this color turned to dark brown and green-black. The reaction mixture was stirred under nitrogen stream at 200°C for 24 hr and further treated as P-1. The yield of the dried black polymer was 2.4 g. It was insoluble in concentrated H_2SO_4 , CH_3SO_3H , and in organic solvents.

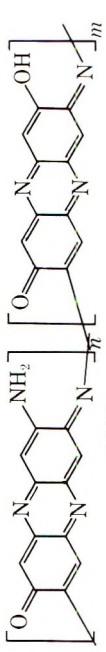
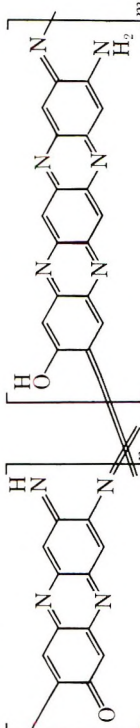
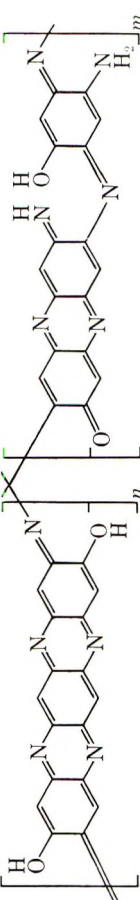
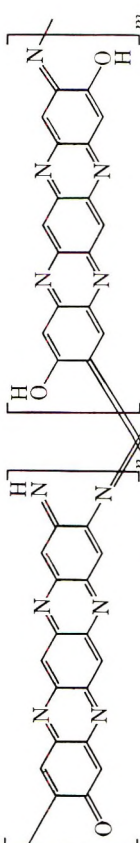
P-3. In a 100-ml three-necked flask equipped with a mechanical stirrer, two inlet tubes, and thermometer was suspended a 3-g portion of recrystallized diimide in 45 ml of PPA; this was stirred at room temperature under vacuum for 1 hr. In the next 45 min the temperature was increased to 200°C under N_2 atmosphere. After 3 hr the temperature was raised to 280°C for the last 30 min (in the last 10 min without vacuum and N_2). Afterwards the reaction mixture ceases to flow (became rubbery). It was precipitated in 1.5 liter water. After filtration the black polymer was suspended several times in concentrated ammonium carbonate solution and washed with 150 ml of distilled water. For purification, the product was

TABLE I
Analytical and Infrared Data of Polymers from 2,5-Diamino-*p*-Benzoquinonediimide Prepared by Self-Condensation

No.	Elemental analysis							Calculated for proposed polymer unit			Infrared cm ⁻¹
	C, %	H, %	N, %	O, %	P, %	Res., %	Formula	Type and ratio			
P-1	Found:	59.73	3.00	20.24	15.35	0.32	1.48	C ₂₃ H ₁₃ N ₃ O ₃	VI/1:VI/2 \cong 1:1	1600, 1430, 1200-1240	
	Calcd:	59.88	3.14	20.38	16.60	—	—				
P-2	Found:	63.27	3.25	25.20	7.00	0.32	1.28	C ₁₂ H ₆ N ₄ O	VIII/1	1600, 1430, 1200-1255	
	Calcd:	64.88	3.72	25.20	7.20	—	—				
P-3	Found:	61.28	2.84	23.25	11.86 ^a	0.2	0.79	C ₃₆ H ₁₆ N ₁₁ O ₃	VII/2:VII/3 \cong 1:1	1600, 1430, 1200-1250	
	Calcd:	62.99	2.79	22.47	11.65	—	—				
P-4	Found:	66.29	3.05	23.01	6.77 ^a	0.2	0.88	C ₃₆ H ₁₆ N ₁₁ O ₃	IX/1:VII/2 \cong 1:1	1500, 1425, 1200-1250	
	Calcd:	64.88	2.72	25.20	7.20	—	—				

^a Calculated as difference from 100%.

TABLE II
Analytical Data of Polymers from 2,5-Diamino-*p*-Benzoquinonediimide Prepared by Self-Condensation (after Heating)

No.	Elemental analysis				Assumed polymer unit	
	C, %	H, %	N, %	O, %		Res., %
HP-1 from P-1	Found:	64.45	2.14	22.33	9.47 ^a	1.61
	Calcd:	64.73	2.49	22.00	10.78	—
						
<p>Poly[(7-amino-3-oxo-2-phenaziny]l-8-(3<i>H</i>)-ylidene]nitrilo]copolymer with poly[(7-hydroxy-3-oxo-2-phenaziny]l-8-(3<i>H</i>)-ylidene]nitrilo]</p>						
HP-2 from P-2	Found:	64.51	2.55	25.42	6.23 ^a	1.29
	Calcd:	65.60	2.62	25.54	6.24	—
						
HP-3 from P-3	Found:	63.42	2.32	23.59	9.72 ^a	0.95
	Calcd:	64.75	2.56	23.10	9.59	—
						
HP-4 from P-4	Found:	66.38	2.24	23.85	6.58 ^a	0.68
	Calcd:	66.55	2.33	23.72	7.40	—
						

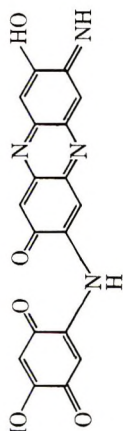
^a Calculated as difference from 100%.

TABLE III
Analytical and Infrared Data on Polymers from 2,5-Diamino-*p*-Benzoquinonediimide
Prepared by Cocondensation with *p*-Benzoquinone Derivatives

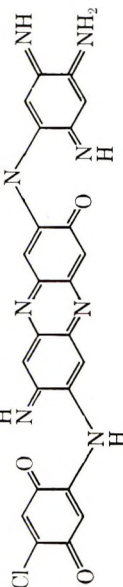
No.	Elemental analysis					Calculated for polymer unit			Infrared bands cm ⁻¹	
	C, %	H, %	N, %	O, %	Cl, %	Res., %	Formula	Type		Ratio
P-5	Found: 62.03	2.62	18.76	17.45	—	0.1	C ₂₄ H ₁₂ N ₆ O ₅	VI/2 and VIII/2	1:1	1610, 1400-1450, 1140-1250
HP-5 ^a	Calcd: 62.07 Found: 64.86	2.61 2.20	18.10 19.37	17.22 13.15	—	— 0.54	—	—	—	—
P-6	Calcd: 65.06 Found: 60.58	2.24 3.25	19.56 14.84	13.14 20.23	—	— 1.74	C ₆₆ H ₃₇ N ₁₇ O ₁₀	VIII/2 and IX/2	4:1	—
HP-6 ^a	Calcd: 59.80 Found: 64.24	2.84 2.68	16.26 14.47	21.20 16.66	—	— 1.95	C ₆₀ H ₃₄ N ₁₄ O ₁₆	Oligomer ^b and VI/2	3:2	1610, 1500, (1520), 1440, 1210-1260
P-8	Calcd: 62.50 Found: 58.37	2.45 3.86	17.00 22.35	18.05 9.90	—	— 0.30	C ₆₀ H ₂₈ N ₁₄ O ₁₃	Oligomer ^b and VI/2-H ₂ O	—	—
HP-8 ^a	Calcd: 57.78 Found: 63.87	3.03 2.75	22.45 24.31	9.63 7.61	7.11 1.26	— 0.19	C ₂₄ H ₁₅ N ₃ O ₃ Cl ^c	Oligomer ^c	—	1625, 1495, 1400, 1250, 1230-1250, 1010
	Calcd: 64.61	2.79	24.10	7.18	1.32	—	6(Oligomer ^c)- 5HCl-6H ₂ O	—	—	—

^a After heating.

^b Structure:



^c Structure:



extracted with water for 4 days. After drying in vacuum at 70–80°C, the yield was 2.5 g. The black polymer was slightly soluble in concentrated sulfuric acid and not soluble in other solvents.

P-4. A 3-g portion of diimide (recrystallized) was dissolved at room temperature in 50 ml of PPA under nitrogen atmosphere. The solution was heated at 170°C for 16 hr, at 190° for 3 hr, and then at 280°C for 3 hr under N₂ atmosphere. A highly viscous reaction mixture was obtained. Isolation and purification of the black polymer were as described for P-3. The yield was 2.6 g. This polymer was partially soluble in concentrated H₂SO₄ (9% soluble part).

Analytical data and infrared spectra showed that all of these polymers have uncyclized units. In order to get further ring closure they were heated under vacuum at elevated temperature. The temperature was raised in 3 hr stepwise to 350–360°C and maintained for 3 hr. Table II contains the analytical data for these heated polymers and the possible formulas which they may have. During the heating, elimination of water (and/or ammonia) took place, but no polymer with a completely ladder structure was obtained. They seem to be composed of short segments with ladder structures. Further heating of these products under strenuous conditions (5 hr at 420°C) resulted in only 1–2% lower oxygen content, which indicates that in none of these cases was complete ring closure achieved.

Condensation of 2,5-diamino-*p*-benzoquinonediimide with 2,5-diamino-*p*-benzoquinone

P-5. A mixture of 0.685 g (0.005 mole) of diimide (recrystallized) and 0.691 g (0.005 mole) of 2,5-diamino-*p*-benzoquinone was dissolved in 28 g. of PPA and the solution heated under nitrogen atmosphere. The temperature was raised to 190°C in 2 hr and kept for the next 4 hr at 195–200°C. The highly viscous solution (ceased to flow under 100°C.) was poured into 1 liter of water to yield a black precipitate. This was filtered, neutralized with diluted ammonium carbonate, washed several times with water and extracted with water for 4 days. After drying under reduced pressure at 70–80°C the yield was 1.1 g. The black polymer was slightly soluble in concentrated H₂SO₄ and insoluble in other solvents. Elemental analysis of the polymer and typical infrared bands are given in Table III.

Cocondensation of Diimide with 2,5-Dihydroxy-*p*-benzoquinone (DHB)

Method 1

P-6. A mixture of 0.685 g (0.005 mole) of diimide (recrystallized) and 0.70 g (0.005 mole) of DHB (recrystallized from alcohol), was dissolved in 25 g of PPA under vacuum at room temperature. The reaction mixture was heated (190°C) under N₂ atmosphere for 4 hr. The cooled highly viscous solution was added slowly to 1 liter of water. After filtration, the black precipitate was washed with 100 ml of water, three times with 100

ml of concentrated ammonium carbonate solution, and finally twice with 150 ml of water. The polymer was extracted with water for 5 days and dried under reduced pressure at 70–80°C (finally 110°C for 1 hr). The yield was 0.94 g. The air-dried polymer was completely soluble in concentrated H₂SO₄ before extraction and drying. After these procedures, it was only partially soluble (42%). The viscosity of the soluble part was very low; $\eta_{2inh} < 0.01$ (determined in concentrated H₂SO₄ at 30°C). Typical infrared bands and analytical data are shown in Table III.

Method 2

P-7. The same mixture of both reactants as described for P-6 (method 1) was dissolved in 25 ml of hexamethylphosphoramide and stirred for 66 hr at 180°C under nitrogen atmosphere. The cooled reaction mixture was added to 300 ml of chloroform to yield a dark-brown precipitate. (No precipitate in water.) The air-dried product was soluble in methanol and in water. After drying at 60°C, it was completely soluble only in concentrated H₂SO₄ and methanesulfonic acid, partially soluble in alkalis, and no longer soluble in methanol, water and in organic solvents (DMAc, HMP). The elemental analysis of the condensation products showed a high phosphorus and residue content (P = 8.91%; Res. 6.98%). Viscosity measurement in concentrated sulfuric acid (0.5 g/100 ml at 30°C) indicated a very low molecular weight ($\eta_{inh} < 0.01$). Typical infrared bands were found at 3030, 2780, 1620, 1520, 1470, and 1220–1260 cm⁻¹.

Condensation of Diimide with 2,5-Dichloro-*p*-benzoquinone

P-8. In a mixture of 20 ml of dimethylacetamide and 5 ml of diethylaniline were dissolved 0.685 g (0.005 mole) of diimide (recrystallized) and 0.890 g (0.005 mole) of 2,5-dichloro-*p*-benzoquinone. The reaction mixture was gradually heated to 160°C (4 hr) under nitrogen and kept for 24 hr. During the reaction a dark brown product precipitated (P-8). It was collected by filtration, washed with DMAc and water, and extracted with water for 5 days. From the filtrate a second product (P-8/a) was precipitated by benzene. The yields of P-8, P-8/a, and total polymer were 0.500, 0.245, and 0.745 g, respectively. P-8 was completely soluble in concentrated H₂SO₄ and CH₃SO₃H. η_{inh} was 0.10, as determined in concentrated H₂SO₄ at 30°C ($c = 0.5$ g/100 ml). The analytical and infrared data are shown in Table III.

ANAL. Found for P-8/a: C, 54.63%; H, 4.73%; N, 18.24%; O, 7.98%.

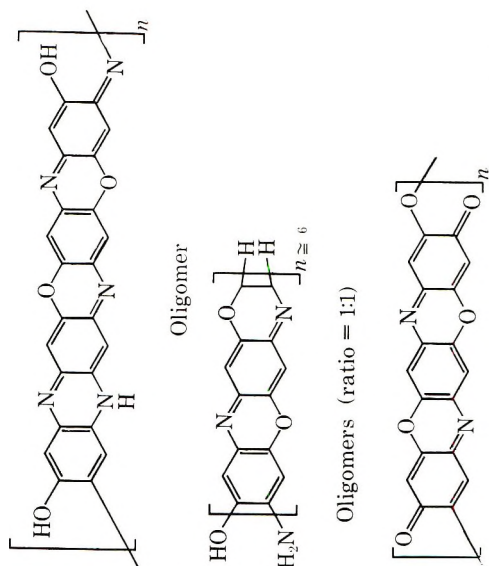
Cocondensation of Diimide with 2,5-Diamino-*p*-hydroquinone Dihydrochloride (DAH)

Method 1

P-10. A mixture of 0.685 g (0.005 mole) of diimide and 1.065 g (0.005 mole) DAH was dissolved in 25 ml of methanesulfonic acid in N₂ atmosphere. The temperature of the mixture was raised to 110°C and this

TABLE IV
 Analytical and Infrared Data of Polymers from 2,5-Diaminohydroquinone Dihydrochloride Prepared by Cocondensation with
p-Benzoquinone Derivatives

No.	Infrared bands, cm^{-1}	η_{inh}^a	Elemental analysis C, % H, % N, % O, % Res., %	Calculated formula	Assumed polymer unit
P-9	1600, 1445, 1240(1160)	0.15 ^e	Found: 62.54 3.01 22.52 10.25 1.04 Calcd: 64.16 3.36 21.81 10.67 —	$\text{C}_{24}\text{H}_{18}\text{N}_7\text{O}_3$	
HP-9 ^b	—	—	Found: 64.40 2.39 22.65 7.08 0.78 Calcd: 66.82 3.04 22.72 7.42 —	$\text{C}_{24}\text{H}_{13}\text{N}_7\text{O}_2$	
P-10	1600, 1450, 1215-1300, (1155)	0.20	Found: 62.67 2.70 16.40 18.42 0.41 Calcd: 63.85 2.90 15.53 17.72 —	$\text{C}_{24}\text{H}_{13}\text{N}_5\text{O}_3$	



HP-10 ^b	—	—	Found: 65.05 2.43 16.20 13.28 0.33 Calcd: 66.51 2.56 16.17 14.76 —	C ₂₄ H ₁₁ N ₅ O ₄
P-11	1615, 1425, (1375) 1225-1270	—	Found: 63.26 2.90 15.18 18.42 1.07 Calcd: 63.85 2.83 14.49 18.90 —	C ₃₆ H ₁₉ N ₇ O ₅
HP-11 ^b	—	—	Found: 66.87 2.18 14.96 16.37 0.96 Calcd: 67.30 2.28 14.22 16.20 —	C ₇₂ H ₃₉ N ₁₃ O ₁₃
P-12	1600, 1260- 1300 (1040), (1365)	0.05	Found: 60.44 2.72 7.66 28.36 — Calcd: 60.50 2.54 7.85 29.11 —	C ₁₈ H ₁₀ N ₂ O ₇ C ₁₈ H ₈ N ₂ O ₆
HP-12 ^b	—	—	Found: 66.12 2.08 8.71 22.17 0.92 Calcd: 65.48 1.83 8.49 24.20 —	C ₁₈ H ₆ N ₂ O ₅

^a Determined in conc. H₂SO₄ at 30°C.; c = 0.5 g./100 ml.

^b After heating.

^c Soluble part = 46%.

temperature was maintained for 5 hr. For the last 1 hr the solution was heated at 150°C and, after cooling, poured into 1 liter of distilled water. A black powder precipitated and was filtered, washed several times with concentrated ammonium carbonate solution and water, then extracted for 8 days with water. A considerable part of the product was dissolved with a dark violet color in the ammonium carbonate solution and in water during the washing and extraction. After precipitation and drying at 80°C, the product was completely soluble in concentrated H₂SO₄, partially soluble in methanesulfonic acid and alkali, and insoluble in organic solvents. The yield was 1.07 g; $\eta_{inh} = 0.20$ (determined in concentrated H₂SO₄ at 30°C, $c = 0.5$ g/100 ml). Typical infrared bands and analytical data of this and of the following polymers are shown in Table IV.

Method 2

P-9. In 28 g of PPA (82.5% P₂O₄) the same amount of diimide (re-crystallized) and DAH was dissolved as for P-10. The temperature of the mixture was raised to 190°C gradually (90°C, 120°C) during 3 hr and was kept at this temperature for the next 3 hr. The black polymer was isolated exactly as described for P-6. This polymer was, like P-10, partially dissolved during the purification procedure in ammonium carbonate solution and in water. After purification and drying, the black powder was partially soluble in concentrated H₂SO₄ (46%) and in methanesulfonic acid and insoluble in organic solvents. The yield was 0.96 g. Viscosity of the soluble part in concentrated H₂SO₄, $\eta_{inh} = 0.15$ (at 30°C).

Condensation of 2,5-Diamino-*p*-benzoquinone with 2,5-Diamino-*p*-hydroquinone Hydrochloride

Method 1

P-11. A mixture of 2,5-diamino-*p*-benzoquinone (0.691 g, 0.005 mole) and 2,5-diamino-*p*-hydroquinone hydrochloride (1.066 g, 0.005 mole) was suspended in 28 g PPA (82.5% P₂O₅) and heated slowly under nitrogen (2.5 hr) to 190°C. The dark-violet solution turned dark blue between 145 and 160°C, then dark green at 180°C. For the next 3 hr the temperature was kept at 200°C, then the reaction had to be stopped because reaction mixture ceased to flow. The black rubbery mass was put in 1 liter of water and, after standing overnight, the residue was collected by filtration, neutralized with ammonium carbonate solution, washed several times with water and extracted (H₂O) for 9 days. After drying *in vacuo* at 80°C, 1.052 g black polymer only slightly soluble in H₂SO₄, was obtained.

Method 2

P-12. The same mixture as described for method 1 was dissolved in 25 ml of methanesulfonic acid and the solution heated under nitrogen slowly (2 hr) to 140°C and maintained at this temperature for 2 hr. Then

the temperature was raised to 150°C and maintained for the next 20 hr. In the last 30 min the solution was heated to 165°. After cooling the reaction product was precipitated in 1 liter of water, washed several times with water, and dried *in vacuo* at 80°C. The dark-brown, powdery material was partially soluble in polar organic solvents (DMF, DMAc, DMSO), alkali, methanol, and completely soluble in concentrated H₂SO₄. The yield was 1.21 g; $\eta_{inh} = 0.05$ (in concentrated H₂SO₄ at 30°C $c = 0.5$ g/100 ml).

General Procedure for the Heating of Polymers with Uncyclized Units to Get a Ring Closure

In a glass tube 100–200 mg of the polymer was heated under vacuum (0.5–2 mm Hg). In the first hour the temperature was raised to 290–300°C, in the second hour to 340–350°C, and for the next 3 hr. was maintained at 350–360°C.

We are indebted to Dr. Kurt L. Loening, Chemical Abstracts Service, for the names of our polymers.

We are indebted to Dr. G. F. L. Ehlers, Air Force Materials Laboratory, Wright-Patterson Air Force Base, for thermogravimetric curve.

This work was supported by the Air Force Materials Laboratory, Research and Technology Division, Air Force Systems Command, Wright-Patterson Air Force Base, Ohio.

References

1. R. Nietzki and E. Hagenbach, *Ber.*, **20**, 328 (1887).
2. J. K. Stille and M. E. Freeburger, *J. Polym. Sci. A-1*, **6**, 161 (1965).
3. J. K. Stille and E. L. Mainen, *Macromolecules*, **1**, 36 (1968).
4. R. Wolf, M. Okada, and C. S. Marvel, *J. Polym. Sci. A-1*, **6**, 1503 (1968).

Received March 28, 1969

Revised May 20, 1969

Structure and Reactivity of α,β -Unsaturated Ethers.

VII. Electronic Effects of the β -Methyl Substitution on the Cationic Polymerizabilities of Alkyl Vinyl Ethers*

T. FUENO and T. OKUYAMA, *Faculty of Engineering Science, Osaka University, Toyonaka, Osaka, Japan*, and J. FURUKAWA, *Department of Synthetic Chemistry, Kyoto University, Kyoto, Japan*

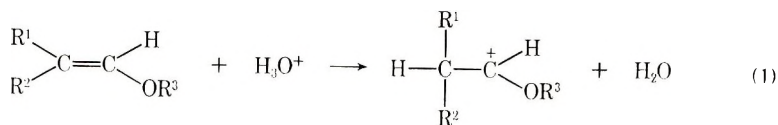
Synopsis

Reactivities of propenyl alkyl ethers toward various cationic agents are summarized, and the effects of a β -methyl group and geometrical isomerism are discussed on the basis of the extended Hückel molecular orbital theory. The reactions considered include cationic polymerization, acid-catalyzed hydrolysis, and silver-ion complexation. The effects of a β -methyl substitution on the reactivity of vinyl ether are different depending on the type of the reactions. The substitution enhances the reactivity of vinyl ether in homogeneous polymerization, whereas it reduces the reactivity in hydrolysis. This contrasting effect of a β -methyl group was found to be compatible with the results of the theoretical calculations of the electronic energy changes accompanying the formation of the relevant transition states. A π -complex-type transition state was concluded for the cationic polymerization. Several lines of experimental evidence in support of the conclusion are presented.

INTRODUCTION

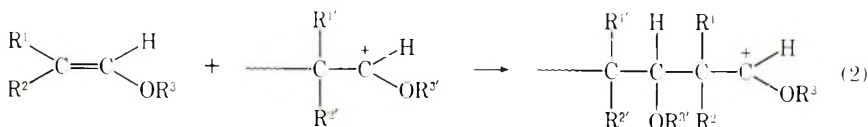
Structural factors influencing the reactivities of α,β -unsaturated ethers toward various cationic species have been the research subject of our continuing interest. The reactions treated so far include the acid-catalyzed hydrolysis,^{1,2} cationic polymerizations,³⁻⁶ and silver-ion complexation.⁷ In all these cases, primary reactions involve the attack of cationic species on the double bond of the ether (i.e., electrophilic additions) as shown in eqs. (1)-(3).

Acid-catalyzed hydrolysis:

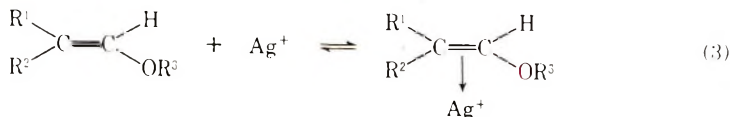


* Presented in part at the 16th Polymer Symposium in Japan, Fukuoka, October 1967.

Cationic polymerization:



Silver-ion complexation:



We have demonstrated previously that the ease of these reactions is sensibly influenced by the geometrical configuration of the ethers as well as the type of their alkyl substituents, and that these influences are apparently different depending on the nature of the attacking cations. For example, a β -methyl group reduces the reactivity of vinyl ethers toward both hydronium¹ and silver ions,⁷ while it enhances their reactivity toward carbonium ions.³

Clearly, the reaction rates are the direct reflection of the free energy difference between the initial and the transition states of the reacting systems. Therefore, any variation in relative reactivities of a series of compounds in different reactions must be ascribed to the difference in nature of the transition states of the individual reactions.

In the present paper, we will be primarily concerned with the electronic effects of the β -methyl group in the above-mentioned reactions of unsaturated ethers. Thus, in the first place, we will summarize the experimental results on the reactivities of both *cis*- and *trans*-propenyl ethyl ethers relative to vinyl ethyl ether, and the significance of these results will be briefly considered on a qualitative ground. Next, on the basis of the extended Hückel molecular orbital theory,⁹ attempts will be made to estimate the stabilities of the transition states of both hydrolysis and polymerization of these three ethers. Finally, in the light of both the experimental and theoretical implications, a model of the transition state will be suggested for the propagation step of the cationic copolymerization of unsaturated ethers.

Reactivities of Propenyl Ethyl Ether

Reactivities of *cis*- and *trans*-propenyl ethyl ether (PEE) relative to vinyl ethyl ether (VEE) are summarized in Table I for the reactions (1)–(3). It is seen from Table I that, in all the reactions investigated, the *cis* isomer is several times more reactive than the *trans*. In the homogeneous cationic polymerization (2a), a β -methyl group enhances the reactivity. On the contrary, in the acid-catalyzed hydrolysis (1), cationic polymerization by heterogeneous catalysis (2b), and the silver-ion complexation (3), the ether reactivity is reduced to a considerable extent by

the same group. Here, the reactivity toward the silver ions means the relative stabilities of the silver-ion complexes formed and is measured by the magnitudes of the equilibrium constants for the complex formation.

As has previously been described,⁷ steric effects of β -alkyl groups play an important role in determining the stabilities of the silver-ion complexes of alkenyl alkyl ethers. In the present instance of propenyl ether, an adverse steric effect of a β -methyl group must be a major factor acting to reduce the complex stability.

In the course of the cationic polymerization by heterogeneous catalysis of the aluminum sulfate-sulfuric acid complex (2b), coordination of monomers on the catalyst surface before or during the attack of the chain-end carbonium ion is considered to be an important process.³ In this coordination process of the polymerization, a steric effect of the substituent

TABLE I
Reactivities of Propenyl Ethyl Ether toward Various Cationic Reagents

No.	Reaction	Attacking agent	Temp, °C	Relative reactivity			Ref.
				<i>cis/trans</i>	<i>cis</i> /VEE ^a	<i>trans</i> /VEE ^a	
1	Hydrolysis	H ₃ O ⁺	25	2.93	0.39	0.12	1
2a	Cationic polymerization (homogeneous)	$\sim\text{CH}_2^+\text{CH}(\text{O}-i\text{-Bu})$	-78	2.43	3.99	1.64	4
2b ^b	Cationic polymerization (heterogeneous)	$\sim\text{CH}_2^+\text{CH}(\text{O}-i\text{-Bu})$	0	5.91	0.64	0.032	3
3	Argentation	Ag ⁺	20	5.80	0.47	0.080	7

^a Vinyl ethyl ether.

^b Reactivities of propenyl isobutyl ether relative to vinyl isobutyl ether.

should be operative in a manner similar to that in the silver-ion complexation. This might be a reason for the lower reactivity of the propenyl ethers in the polymerization (2b).

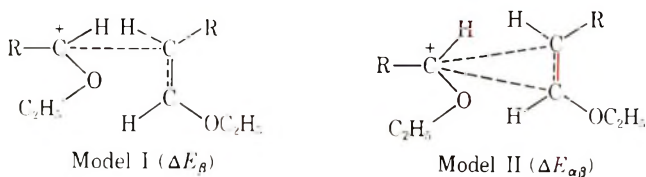
In contrast, it was concluded in previous papers that little steric effect of a β -methyl group is apparent both in the acid-catalyzed hydrolysis of vinyl alkyl ethers¹ and in their cationic polymerization in homogeneous media (2a).^{3,4} Thus, it remains to be settled why a β -methyl group enhances the reactivity of the ethers toward carbonium ions (polymerization) while it reduces their reactivity toward a hydronium ion (hydrolysis). Obviously, these contrasting reactivities toward the two sorts of electrophilic reagents cannot be explained concurrently in terms of the electronic structure of the ground state alone of the reactant ethers. This difference should necessarily be ascribed to the different nature of the transition states of the two reactions.

Models of the Transition States

When the steric effect is not important, the relative reactivities may be discussed in terms of the electronic energy changes that the reactants may experience on going from the ground to the transition state along the reaction coordinate. Such energy changes may be calculated by the molecular orbital (MO) method, if the geometry of the transition state is known.

For the acid-catalyzed hydrolysis of alkenyl ethers, the transition state is considered to be very close to the carbonium ion which is formed by the rate-determining protonation at the β -carbon atom.^{1,2} Consequently, to a first approximation, a carbonium ion can be assumed as a model of the transition state of the vinyl ether hydrolysis.

If, also in the cationic polymerization, the transition state were near the carbonium ion as Mizote et al.³ suggested, then the relative reactivities should be parallel to those in hydrolysis, in contradiction with the observed results. Although the carbonium ion may certainly be a useful extrapolation of the transition state of the cationic polymerizations, its carbonium-ion character⁵ seems not to be as great as that of the hydrolysis. Thus, it may be conceivable that the delocalized state such as model I or II, which has been considered as a transition state model for an electrophilic addition to olefins, can reasonably depict the activated complex of the present cationic polymerization.



Admittedly, the transition-state models (I and II) of polymerization must be crude ones in view of the generally known effects of catalysts and solvents on cationic polymerization. Perhaps, the role of the gegenions may be a factor that should not be ignored for precise understandings of the difference in behavior of any given set of monomers. However, because the principal purpose of the present treatments is to rather roughly demonstrate how the electronic contribution of a β -methyl group should influence the vinyl ether polymerizability, it is considered that such naive models as have been proposed may not be entirely impermissible simplifications. In other words, we may implicitly assume that, to a first approximation, the other various factors be identical for the three ethers in question. Adequacy of such an assumption may only be judged from its logical outcome and be assessed with these limitations in mind.

Calculations of the Transition-State Stabilities

In order to consider the effects of the β -methyl substitution on the electronic state of vinyl alkyl ether in both *cis* and *trans* positions, the σ -elec-

tronic system as well as the π -system should be dealt with. Obviously, the simple π -electron approximation is useless for this purpose. Thus, the extended Hückel MO method developed by Hoffmann⁹ was adopted for the calculations. In calculating the delocalization energies, however, only the π -part of the molecular wave functions of both the carbonium ions and the ethers were used, since π -electrons probably play a dominant role in the electron delocalization.

For the extended HMO calculations, the Coulomb integrals, H_{rr} , of atomic orbitals were chosen from the valence-state ionization potential data of neutral atoms compiled by Pritchard and Skinner.¹⁰ They were -13.60 (H1s), -21.43 (C2s), -11.42 (C2p), -35.30 (O2s), and -17.76

TABLE II
Bond Lengths Adopted for the Extended Hückel MO Calculations

Bond	Length, Å
C(sp^2)=C(sp^2)	1.34
C(sp^2)—C(sp^2)	1.50
C(sp^3)—C(sp^2)	1.54
C(sp^2)—O	1.45
C(sp^3)—O	1.48
C(sp^2)—H	1.08
C(sp^3)—H	1.09

TABLE III
Relative Reactivities and Calculated Energy Changes in the
Acid-catalyzed Hydrolysis and the Cationic Polymerization of RCH=CHOC₂H₅

R	Hydrolysis		Polymerization		
	Relative reactivity ^a	ΔE , eV	Relative reactivity ^b	ΔE_{β} , γ^2 /eV	$\Delta E_{\alpha\beta}$, γ^2 /eV
H	(1.00)	4.6596	(1.00)	0.3387	1.1443
<i>cis</i> -CH ₃	0.39	4.6339	3.99	0.3314	1.3505
<i>trans</i> -CH ₃	0.12	4.5153	1.64	0.3321	1.3448

^a Data of Okuyama et al.¹

^b Reactivities toward the vinyl isobutyl ether cation.⁴

(O2p) in units of eV. The parameter K for the estimation of the resonance integrals, $H_{rs} = (K/2)(H_{rr} + H_{ss})S_{rs}$, was taken as 1.75, according to the original proposal of Hoffmann.⁹ The overlap integrals were evaluated by the aid of the formula derived by Mulliken et al.¹¹ Since the geometry of each molecule has not yet been established, a reasonable one was postulated with usual bond lengths (given in Table II) and angles (tetrahedral sp^3 carbons and planar symmetrical sp^2 carbons), although the C—O—C bond angle was rather arbitrarily assumed to be tetrahedral. Shown in Figure 1 are the molecular geometries adopted here. All the numerical calculations were performed on the NEAC-2200/500 of the Osaka University Computation Center.

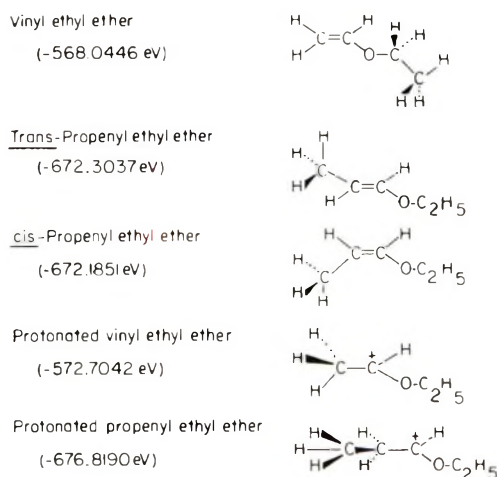


Fig. 1. Conformations of the ethers and the carbonium ions assumed in the extended HMO calculations. The conformations of the ethoxy groups have been assumed to be identical for all the species considered here. The numerical values in parentheses are the calculated total electronic energies.

The total electronic energies calculated for the relevant structures are given in Figure 1. Electronic energy changes, ΔE , on going from the ethers to the carbonium ions are shown in the third column of Table III. It may be noted that their magnitudes are roughly those of the C—H bond dissociation energies.

Atomic M_x and atomic-orbital populations N_r on the olefinic carbons of the ethers are given in Table IV. Here, the quantities are defined as

$$N_r = 2 \sum_j^{\text{occ}} \sum_s C_r^j C_s^j S_{rs} \quad (4)$$

and

$$M_x = \sum_r^{\text{on } x} N_r \quad (5)$$

where the symbols have their usual meanings. The summation in eq. (5) extends over all the valence-state atomic orbitals belonging to the atom X.

TABLE IV
Atomic Population (AP) and π -Atomic Orbital Population (π -AOP)^a
on the α - and β -Carbons of Vinyl and Propenyl Ethyl Ethers ($RCH=CHOC_2H_5$)

R	AP		π -AOP		π -AOP(HO) ^a	
	C_β	C_α	C_β	C_α	C_β	C_α
H	4.3811	3.4687	1.1076	0.9210	0.5455	0.4114
<i>cis</i> -CH ₃	4.1181	3.6179	1.0101	1.0608	0.3846	0.4689
<i>trans</i> -CH ₃	4.1423	3.6134	1.0094	1.0603	0.3831	0.4671

^a Highest occupied π -orbital.

The delocalization energies, ΔE_β and $\Delta E_{\alpha\beta}$, were calculated from the usual expressions derived by the second-order perturbation method:¹²

$$\Delta E_\beta = 2 \left\{ \sum_i^{\text{occ}} \sum_j^{\text{unocc}} - \sum_j^{\text{occ}} \sum_i^{\text{unocc}} \right\} \frac{(C_+^i)^2 (C_\beta^j)^2}{E_i - E_j} (-\gamma^2) \quad (6)$$

$$\Delta E_{\alpha\beta} = 2 \left\{ \sum_i^{\text{occ}} \sum_j^{\text{unocc}} - \sum_j^{\text{occ}} \sum_i^{\text{unocc}} \right\} \frac{(C_+^i)^2 (C_\alpha^j + C_\beta^j)^2}{E_i - E_j} (-\gamma^2) \quad (7)$$

where the subscripts +, α , and β refer to the $2p_z$ atomic orbitals of the charged carbon in the carbonium ion and of the α - and β -carbons in the parent ethers, respectively, and where γ is the resonance integral for the weak bonds formed by the electron delocalization. For the sake of simplicity, $\text{CH}_3^+\text{CH}(\text{OC}_2\text{H}_5)$ was assumed as an attacking carbonium ion. The results of calculations are given in the fifth and sixth columns of Table III.

Comparisons with Experiments

To begin with, it may be worthwhile to compare the total electronic energies calculated for the geometrical isomer pair of the propenyl ether. As can be seen from Figure 1, *trans*-propenyl ethyl ether is predicted to be more stable than its *cis* isomer. This prediction is in qualitative agreement with the observation regarding the relative thermochemical stabilities of the isomeric ethers, as reduced from the *cis-trans* isomerization equilibrium experiments.¹³ A similar agreement has already been noted by Hoffmann⁹ for the case of butene-2. Although the factors affecting the relative stabilities of geometrical isomer pairs are still beyond our comprehension, these agreements between theory and experiment may be taken as an implication that the electronic contribution to the isomer stabilities is in some cases more important than has hitherto been appreciated.

We now turn our attention to the reactivity problems.

In the first place, the electron population data given in Table IV suggest that the electrophilic reactivity at the β -carbon (C_β) atom of vinyl ethyl ether be reduced by the β -methyl substitution. In particular, the π -atomic orbital populations (π -AOP) on the C_β atom correctly predicts the reactivity order, vinyl (H) > *cis*-propenyl(*cis*-CH₃) > *trans*-propenyl(*trans*-CH₃), for the protonation reaction (i.e., the acid-catalyzed hydrolysis).

In this criterion based on the π -AOP, however, the protonation of both *cis*- and *trans*-PEE should occur at the C_α atom, where the calculated π -AOP is greater than at the C_β atom, a prediction which conflicts with observations. On the other hand, no such incompatibility is manifested in the calculated data of the total atomic populations (AP); in each compound studied, the AP for the C_β atom is far greater than that for the C_α atom. Yet, the AP cannot be accepted as a reactivity index either, because it erroneously predicts a higher reactivity of the *trans*-CH₃ derivative relative to the *cis*-CH₃ isomer.

These failures of the calculated electron population data in interpreting the reactivity may imply that the population data cannot be useful as an index for ionic reactivity in general cases. Admittedly, the method of calculations here employed may inherently be too crude to be used for the prediction of correct electron distributions, but more crucial is perhaps the criterion that the electron distribution is a primary factor governing general reactivities of compounds toward ionic species. Breakdown of this criterion has even been obvious at the very outset in view of the fact that the reactivity order of the three ethers varies with the change in the type of the reactions, as has repeatedly been pointed out in foregoing sections.

Alternatively, chemical intuitions suggest that, for the interpretation of any reactivity problem, direct evaluations of the transition state stabilities will be more general and reliable than will be the considerations of the electronic structures of the initial stages. In reality, Table III shows that the calculated values of the energy gains on protonation of the β -carbon, ΔE , decrease in the order: $H > cis\text{-CH}_3 > trans\text{-CH}_3$, in agreement with the reactivity order observed for the hydrolysis. This agreement between theory and experiment certainly lends support to the previous conclusion that the intermediate alkoxy-carbonium ions closely resemble the transition states of the acid-catalyzed hydrolysis of unsaturated ethers.¹

In the case of cationic polymerizations, the π -conjugative stabilization energies, ΔE_β and $\Delta E_{\alpha\beta}$, calculated for the respective transition state models I and II predict different orders of reactivity for the three ethers. Assumption of the model I has led to a prediction of the reactivity order completely opposite to that observed experimentally. On the contrary, the energies, $\Delta E_{\alpha\beta}$, for model II have correctly reproduced the relative polymerizability diminishing in the order: $cis\text{-CH}_3 > trans\text{-CH}_3 > H$. Thus, for the cationic polymerization of vinyl ethers, a π -complex-type transition state as depicted by model II appears to be more likely than model I which involves preferential attack of the carbonium ions on the β -carbon of the vinyl linkage.

Finally, a comment seems to be in order regarding the use of $\text{CH}_3^+\text{CH}(\text{OC}_2\text{H}_5)$ as a model species of the attacking chain end unit. The adoption of this model ion has simply been a matter of computational expedience, and is believed not to provide a faulty guide to considerations of the relative reactivities of the various ethers toward the vinyl ether end.⁴ However, we have noticed in separate experiments¹⁴ that the oxycarbonium ion $\text{CH}_3^+\text{CH}(\text{OC}_2\text{H}_5)$ prepared from the acetal and $\text{BF}_3 \cdot \text{OEt}_2$ undergoes addition to the three ethers in bulk at 0°C with the relative ease diminishing in the order: $cis\text{-CH}_3 > H > trans\text{-CH}_3$. Discrepancy of this reactivity order from that observed for polymerization may partly be ascribable to the difference in reaction temperature. At this juncture, therefore, it may be fair to state that model II will be valid for cationic polymerization of unsaturated ethers in homogeneous media at low temperatures.

DISCUSSION

As may be deduced from the theoretical calculations, the transition state of the cationic polymerization of vinyl ethers appears to be of the π -complex type. This would mean that the polymer chain ends should approach the monomer from above the center of its double bond and interact with both the α - and β -carbons, gradually forming a bond with the β -carbon of the monomer.

In contrast, in the acid-catalyzed hydrolysis, the primary attack of the protonium ions on the vinyl linkage takes place at its β -carbon exclusively.¹ This difference in mechanism between the two types of reactions appears to be compatible with our previous suggestion⁵ that the transition state of cationic polymerization of phenyl vinyl ether should have a carbonium ion character smaller than that of the acid-catalyzed hydrolysis of the same compound.

The enhancement of polymerizability of vinyl ethyl ether by the β -methyl substitution is no doubt a reflection of the electronic contribution of the methyl group to the activation process. The methyl group should perturb the electronic structure of the parent ether. As far as the electron distribution is concerned, this perturbation should act in the direction to oppose the polarization of the vinyl linkage originally effected by the partial migration of the oxygen lone pair electrons. As a result, the electron density on the α -carbon would be increased at a sacrifice of the density on the β -carbon atom. The situation is clearly discernible in the electron population data given in Table IV. The increased polymerizability of the β -methyl derivatives could thus most reasonably be understood by assuming the α -carbon atomic orbitals of monomers to participate in the monomer—cation interaction in the activation process. Equation (7) represents a formal π -electron approximation to the transition state stabilities due to such an interaction in the propagation step.

A piece of evidence in support of the above view may be provided from the result of our separate experiment¹⁵ on the reactivity of 1,2-diethoxyethylene, $C_2H_5OCH=CHOC_2H_5$. It was found that the *cis* diether possesses polymerizability about five times greater than that of vinyl ethyl ether, while its amenability to hydrolysis is only a few thousandths that of the reference ether. Only by invoking the transition state model II would this large increase in polymerizability of the diether be interpretable.

Further, we have recently found a more direct experimental indication¹⁵ in favor of the π -complex-type transition state. This has stemmed from the kinetic studies of the effects of ring substituents on the cationic copolymerizations between styryl ethyl ethers, $XC_6H_4CH=CHOC_2H_5$. In brief, the reaction constant $\rho \simeq -2$ for their copolymerization rates was found to be about the same in magnitude as the ρ values for those electrophilic additions (e.g., $\rho = -2.24$ for bromination¹⁶ and $\rho = -2.41$ for sulfenyl chloride addition¹⁷) of styrene derivatives which have been concluded to proceed via π -complex-type intermediates. In general, these

substituent effects are intermediate in magnitude between those in simple β -addition reactions (e.g., $\rho \simeq -1.0$ for the acid-catalyzed hydrolysis of styryl ethyl ethers¹⁵) and those in simple α -additions (e.g., $\rho = -4.6$ for the acid-catalyzed isomerization of *cis*-cinnamic acid¹⁸). Details of this phase of the problem will be published elsewhere.

In conclusion, both experimental and theoretical informations presently at our hand strongly suggest the validity of assuming the π -complex character for the transition state of the cationic polymerizations of α,β -unsaturated ethers.

This work is abstracted from the Doctoral dissertation of T. O., which was submitted to the Graduate School, Kyoto University, in 1968.

References

1. T. Okuyama, T. Fueno, H. Nakatsuji, and J. Furukawa, *J. Amer. Chem. Soc.*, **89**, 5826 (1967).
2. T. Fueno, I. Matsumura, T. Okuyama, and J. Furukawa, *Bull. Chem. Soc. Japan*, **41**, 818 (1968).
3. T. Okuyama, T. Fueno, and J. Furukawa, *J. Polym. Sci. A-1*, **6**, 993 (1968).
4. T. Okuyama, T. Fueno, J. Furukawa, and K. Uyeo, *J. Polym. Sci. A-1*, **6**, 1001 (1968).
5. T. Fueno, T. Okuyama, I. Matsumura, and J. Furukawa, *J. Polym. Sci. A-1*, **7**, 1447 (1969).
6. T. Okuyama, T. Fueno, and J. Furukawa, *J. Polym. Sci. A-1*, in press (Part VI).
7. T. Fueno, O. Kajimoto, T. Okuyama, and J. Furukawa, *Bull. Chem. Soc. Japan*, **41**, 785 (1968).
8. A. Mizote, S. Kusudo, T. Higashimura, and S. Okamura, *J. Polym. Sci. A-1*, **5**, 1727 (1967).
9. R. Hoffmann, *J. Chem. Phys.*, **39**, 1397 (1963).
10. H. O. Pritchard and H. A. Skinner, *Chem. Rev.*, **55**, 745 (1955).
11. R. S. Mulliken, C. A. Rieke, D. Orloff, and H. Orloff, *J. Chem. Phys.*, **17**, 1248 (1949).
12. M. J. S. Dewar, *J. Amer. Chem. Soc.*, **74**, 334 (1952).
13. T. Okuyama, T. Fueno, and J. Furukawa, *Tetrahedron*, in press.
14. T. Okuyama, T. Fueno, and J. Furukawa, *J. Polymer Sci. A-1*, in press.
15. T. Okuyama, N. Asami, and T. Fueno, to be published.
16. K. Yates and W. V. Wright, *Can. J. Chem.*, **45**, 167 (1967).
17. W. L. Orr and R. Kharasch, *J. Amer. Chem. Soc.*, **78**, 1201 (1956).
18. D. S. Noyce, P. A. King, S. A. Lane, and W. L. Reed, *J. Amer. Chem. Soc.*, **84**, 1638 (1962).

Received February 28, 1969

Revised May 20, 1969

Polymerization of Aromatic Amines with Ferric Chloride to Produce Thermally Stable Polymers

A. BINGHAM and BRYAN ELLIS, *Department of Glass Technology, The University, Sheffield S10 2TZ, England*

Synopsis

Simple aromatic amines have been polymerized by use of ferric chloride as a combined Friedel-Crafts catalyst and oxidant to yield polymers which are both thermally and oxidatively stable. Under certain reaction conditions a polydiphenylamine was prepared which was stable in air up to 465°C as shown by thermogravimetric analysis. This polymer has a softening point of ca. 80–100°C and is soluble in some organic solvents. Such a polydiphenylamine and other polymers with similar properties are regarded as useful for conversion to thermally stable Phillips-type resins by crosslinking with conventional difunctional agents.

INTRODUCTION

For organic polymers to have high thermal stability the presence of aromatic structures is a well established necessity.¹ For those structures which have intrinsically high thermal stability the effect of the linkage between aromatic rings has been estimated by Hamman² and Dale et al.^{3,4} They showed that the thermal stability decreased in the order benzene > phenyl-phenyl bond > aromatic ether > aromatic amine > phenoxy-silane and benzophenone > diphenylmethane. Chains of repeating units tend to be less stable than the model compounds, which only have a single linkage between aromatic rings.

Polymers of 2,6-disubstituted phenols have been found to produce thermally stable polyphenylene ethers, and these have been extensively studied.⁵⁻⁸ There has been some study of the polymers produced by direct coupling of aromatic rings. Kovacic⁹⁻¹⁶ has developed a method for coupling aromatic rings by the simultaneous use of a Friedel-Crafts catalyst and an oxidant, such as aluminum chloride and cupric chloride. Other catalysts, such as ferric chloride or molybdenum pentachloride, act with a dual role, being both a Friedel-Crafts catalyst and an oxidant.

Bilow and Miller¹⁷ have prepared fusible branched polyphenylenes using methods similar to those of Kovacic, but with reaction in the melt instead of in solution. These polymers were shown to have good thermal stability properties.

The object of the present work is to extend the method of Kovacic to produce thermally and oxidatively stable polyamines by use of simple

amines, such as diphenylamine, with ferric chloride as the combined catalyst and oxidant. These polymers should be both thermally stable and soluble in organic solvents, thus being useful for conversion to Phillips-type resins.¹⁸ Thus we have shown that these polyamine resins are capable of being crosslinked by reaction with *p*-xylylene dichloride or *p*-xylylene glycol dimethyl ether with stannic chloride as a Friedel-Crafts catalyst to produce a crosslinked resin, but this crosslinking will not be discussed here.

EXPERIMENTAL

General Method of Preparation of Polymers

Catalyst was added slowly to the amine solution with vigorous stirring, the rate of addition being controlled so as to keep the temperature below the preparation temperature (since the reaction is exothermic). The catalyst used was anhydrous grade, but no attempt was made rigorously to exclude water from the system, since Kovacic¹⁹ has shown that the presence of some water is essential for reaction to occur. Additional oxidant, if any, was added at this stage.

The mixture was heated to the preparation temperature with vigorous stirring. Reaction times were varied from 20 min to 8 hr and the reaction stopped by cooling in ice water. Crude solid product was filtered and freed from solvent by drying at 50°C. After grinding the solid it was repeatedly triturated with boiling 20% hydrochloric acid, with regrinding between each trituration where necessary, until the filtrate was colorless.

The product was freed from acid by washing with boiling distilled water until the washings gave a negative chloride test and dried at 80°C. To remove any unchanged monomer it was washed with solvent and dried at 80°C.

Thermogravimetric Analyses

These were performed on a Stanton thermobalance. The sample was heated in air at a rate of 4°C/min, and the initial sample weight was ca. 100 mg. The triggering temperature was taken to be the lowest temperature at which a weight loss of at least 1.5% in 10°C (2.5 min) occurred after correction of the thermogram for loss of low molecular weight materials (<5%).

Infrared Spectra

To measure the spectra of solid polymers the potassium bromide disk technique (polymer concentration ca. 1.5%), and a Grubb-Parsons Spectromaster (2–25 μ) were used.

To study oxidation, films of the polymer were cast from *N,N*-dimethylformamide (DMF) onto one side of a potassium bromide disk. To ensure total removal of solvent, these disks were held at ca. 60°C for 48 hr. The coated disks were placed into a small furnace, the temperature of which

could be raised to 300°C, with the coated side facing the incident beam. This method is similar to that of Conley,¹⁹ with a furnace of improved design.²⁰

RESULTS AND DISCUSSION

Preparation and General Properties

The results summarized in Tables I and II show that mild reaction conditions (low temperatures, short reaction times) are sufficient to give a good yield of polymer in the case of diphenylamine (DPA) (Table I) and triphenylamine (TPA) (Table II).

In converting benzene to *p*-polyphenyl with ferric chloride, Kovacic⁹ used high temperatures and longer reaction times and obtained a lower yield of polymer. The increased reactivity of the aromatic amines over benzene is due to activation of the aromatic nucleus by the amine nitrogen atom.²¹ The reactivity was low for the aliphatic amine polydibenzylamine (polymer 10), very little product being obtained.

The preparation temperature and reaction time in the polymerization of DPA critically affects the physical properties of the polymer (Table I). Thus in order to produce duplicate batches of exactly the same polymer it is necessary to control the reaction conditions to a high degree. All the reactions were exothermic.

It can be seen from Table I that the lower the preparation temperature, the higher the TGA triggering temperature. Polymers prepared at low temperatures are paler in color than those prepared at higher temperatures. This can be explained by postulating that a higher proportion of conjugated centers are formed at higher temperatures, these centers conferring a deep color to the polymer. It is possible that such conjugated centers contribute to thermal instability. With lower preparation temperatures the polymers have higher solubility and lower softening points, and hence low temperatures are preferred for the preparation of these materials.

The solvent used in the reaction affects the characteristics of the polymer produced. In the case of triphenylamine, reaction in benzene yielded a dark-red solid (polymer 6) which possessed high thermal stability, moderate solubility, and no softening point. Reaction in acetone, however, yielded a pale green solid (polymer 7) possessing a very low thermal stability, high solubility, and a very low softening point.

Complexes of aromatic ketones and ferric chloride have been isolated,²² but aliphatic ketone–ferric chloride complexes have not. However, it is possible that an acetone–ferric chloride complex exists in solution, and the ESR work of Lohmann et al.²³ does not conflict with this possibility. Such a complex would modify the catalytic activity of the ferric chloride to produce a polymer with a modified structure. The general structure of the polymer prepared in acetone solution is similar to that prepared in benzene (see infrared spectral data in Table III), but there must obviously be small

TABLE I

No.	Monomer Type	Mole	Cat- alyst (FeCl ₃) mole	Solvent (ben- zene) ml	Reaction conditions	Poly- mer yield, %	Appearance	Elemental analyses	Solubility	Triggering temp (TGA in air), °C	Soft- ening point, °C
1	DPA	0.1	0.1	97.5	80°C (reflux)/ 8 hr	33.7	Green powder, medium intensity	C, 83.7%; H, 5.8%; N, 6.7%; Cl, 2.45%	Sol. in DMF, part. sol. in 1,4-dioxane	350	None ^a
2	DPA	0.1	0.1	88.5	35°C/ 20 min	42.0	Green powder, very pale	C, 85.5%; H, 5.98%; N, 8.6%; Cl, 0.5%	Sol. in DMF, <i>o</i> -di- chlorobenzene, dichloroethane; mod. sol. in dioxane	465	~80°C ^b

3	DPA	0.5	0.5	265.5	40-45°C/ 30 min	60.0	Green powder, medium intensity	C, 82.1%; H, 5.44%; N, 5.5%; Cl, 3.46%	Sol. in DMF; fairly sol. in acetone; slightly sol. in dioxane, 1,2-dichloro- ethane	320	Part softens ~70- 80°C ^e
4	DPA	2.0	2.0	750	^d	42.0	Dark green powder	—	Sol. in DMF; sl. sol. in cold acetone; v. sl. sol. in dioxane	300	None ^a
5	DPA	0.2	0.2	300	33-34°C/ 25 min	65.0	Pale green- brown powder	—	Sol. in DMF; hot dioxane, hot acetone	320	^e

^a Decomposes as a solid.

^b Fully melted at 100-110°C.

^c This portion volatilizes; remainder does not soften.

^d Due to exotherm, temperature rose to 75°C; it was cooled to 40°C rapidly and allowed to cool to room temperature over 30 min.

^e Does not totally soften. Darkens in color at ca. 100°C, suggests part softens here; bulk decomposes without melting.

TABLE II

No.	Monomer ^a		Catalyst (FeCl ₃) mole	Solvent		Reaction conditions	Poly- mer yield, %	Appear- ance	Elemental analyses	Solubility	Triggering temp (TGA, in air) °C	Soft- ening point, °C
	Type	Mole		Type	Vol, ml							
6	TPA	0.0615	0.0815	Benzene	88.5	80°C (reflux)/ 1 hr	40.5	Deep red powder	C, 80.91%; H, 0.18%; N, 2.66%; Cl, 6.3%; res., 4.5%	Mod. sol. in 1,2-dichloro- ethane; v. sl. sol. in DMF	440	None ^b
7	TPA	0.0615	0.0815	Acetone	150	35°C/1 hr	86.5 ^c	Pale green powder	—	Sol. in DMF, acetone, benzene, CCl ₄ , CS ₂	180	40/45°C
8	Aniline	1.0	1.0	CCl ₄	200	^d	19.0 ^e	Black powder	—	Sol. in DMF; part. sol. in dichloro- ethane, dioxane	325	None ^b

9	PPD	0.25	0.125	Acetone	200	Cooled to 1.5°C; exothermed to 20°C, stirred 30 min; no heat supplied	13.0°	Black powder	—	Slightly sol. in hot DMF; insol. in cold DMF, hot acetone, dioxane	None ^f	None ^b
10	DBA	0.1	0.1	CCl ₄	150	Exothermed to 28°C; stirred for 30 min; no heat supplied	*	Light brown viscous gum	—	Sol. in DMF, dioxane	— ^h	< Room temp
11	DPE	0.2	0.2	Benzene	200	50°C/ 30 min; then 55°C/ 1 hr	27.0	Black powder	C, 80.95%; H, 3.77%; O, 15.28% (by dif- ference)	Sol. in hot DMF (brown soln); fairly sol. in acetone, dioxane (green- brown solns)	400	None ^b

^a Monomers: TPA = triphenylamine; PPD = *p*-phenylenediamine; DBA = dibenzylamine; DPE = diphenyl ether.

^b Decomposes as a solid.

^c Another product, a yellow solid, also obtained.

^d Exothermed violently; all solvent boiled off.

^e A large fraction of product was water-soluble.

^f Progressively degrades starting at low temperatures (< 100°C).

^g Very small amount of polymer. Complex of the amine and FeCl₃ (yellow crystals) was main product.

^h Insufficient material.

This dissolved during trituration.

detailed differences in structure which remain to be elucidated, these differences leading to low thermal stability.*

Poly-DPA (polymer 2) has the highest triggering temperature (465°C); poly-TPA (polymer 6) ranks second with 440°C , and third is the polymer of diphenyl ether (DPE) (polymer 11), with a triggering temperature of 400°C . These figures are considered to be quite promising on comparing them with data obtained from recently developed thermally stable polymers.²⁴⁻²⁶ The thermal stability of the polymer of *p*-phenylenediamine (PPD) (polymer 9) is extremely low probably due to it being prepared in acetone. Further discussion of the TGA results is given below.

Infrared Spectra and Structure

Typical infrared spectra of the poly DPA's are shown in Figures 1 (polymer 1, $2.5\text{--}3.5\ \mu$) and 2 (polymer 2, $6\text{--}15.5\ \mu$). A summary of the re-

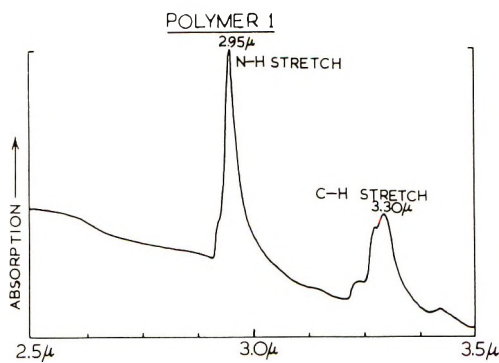


Fig. 1. Infrared spectrum of polymer 1 ($2.5\text{--}3.5\ \mu$)

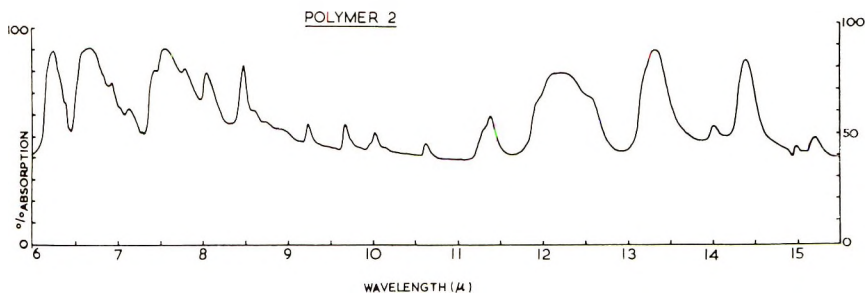


Fig. 2. Infrared spectrum of polymer 2 ($6.0\text{--}15.5\ \mu$)

sults for polymers 1-11 is given in Table III together with the general assignments discussed by Bellamy.²⁷

* The referee has suggested that, since the aromatic amine is activated, there may be some alkylation in the presence of acetone. It is not possible at present to confirm this, but alkylation alone would not account for all the differences in properties of polymers prepared in acetone.

TABLE III

No.	Polymer	Infrared Absorption, μ			
		N—H Stretch (2.86– 3.03 μ , m)	Aromatic C—H out-of-plane vibrations (10.5–15.5 μ)	N—H deformation (6.06–6.45 μ , vw)	C—N vibrations, aromatic (7.36–8.0 μ s)
1	Poly-DPA	One band, 2.95	11.43(m), 12.35(s) 13.38(s), 14.45(s)	6.45 vw	7.65 (s)
2	Poly-DPA	“	11.40(m), 12.22(s) 13.36(s), 14.40(s)	shoulder 6.40 (vw)	7.60 (s)
3	Poly-DPA	“	11.45(m), 12.35(s) 13.40(s), 14.45(s)	shoulder 6.45 (vw)	7.65 (s)
4	Poly-DPA	“	11.40(m), 12.40(s) 13.40(s), 14.45(s)	6.45 (vw)	7.65 (s)
5	Poly-DPA	“	11.40(m), 12.35(s) 13.40(s), 14.45(s)	6.45 (vw)	7.65 (s)
6	Poly-TPA	—	11.86(m), 12.35(s) 13.40(s), 14.48(s)	—	7.63 (s)
7	Poly-TPA	—	11.23(m), 12.25(s) 13.40(s), 14.45(s)	—	7.57(s), 7.64(s)
8	Poly-A	—	11.20(m), 12.15(s) 13.30(s), 14.45(s)	Obscured by skeletal vibrations	7.7 (s)
9	Poly-PPD	Broad doublet peaks, 3.0, 3.125	One peak, 12.10 (s)	Not well resolved probably obscured	7.7 (s)
10	Poly-DBA	One band, 2.93	Two peaks, 13.45(s), 14.30(s)	Not well resolved	8.3 (vw) (aliphatic C—N)
11	Poly-DPE	—	11.12(m), 11.56(m) 12.10(s), 13.37(s) 14.52(s)	—	—

In the 10.5–15.5 μ region, where absorption due to aromatic C-H out-of-plane vibrations occurs, polymers 1–8 and polymer 11 all have similar spectra, with only slight variation. The pattern shows monosubstitution and 1,2,4-trisubstitution,²⁸ which is to be expected with activating amine groups which are *ortho/para*-directing groups.²¹ Polymer 9 shows only one band at 12.10 μ which is characteristic of 1,4-disubstitution, polymer 10 showing two peaks at 13.45 and 14.30 μ which are characteristic of monosubstitution. In the case of polybenzyl, the infrared spectrum indicates the presence of predominantly monosubstituted aromatic rings,²⁰ and from the behavior of molecular models, it has been concluded that the probable maximum degree of substitution is 4, i.e., the ratio monosubstitution:tetrasubstitution is 4:1. However, since the monosubstituted aromatic rings have higher extinction coefficients than polysubstituted aromatics, the presence of higher degrees of substitution is often obscured.²⁰ This explanation of the predominance of the infrared absorption due to monosubstitution in aromatic polymers can be extended to polymer 10.

The N—H stretching mode (2.86–3.03 μ) is seen at 2.95 μ in the five DPA polymers (polymers 1–5) and at 2.93 μ in the DBA polymer (polymer 10). This shows that these polymers contain the secondary amine group, thus confirming that reaction has taken place by direct nuclear coupling and not via the amine groups. The PPD polymer (polymer 9) has a broad doublet having peaks at ca. 3.0 and 3.125 μ , showing the presence of primary amine groups, the two bands being the asymmetric and symmetric stretching vibrations of the —NH₂ group. The structure of polymer 9, prepared in acetone solution and having low thermal stability, poses a difficult problem, since the infrared spectrum indicates only 1,4-disubstitution and the presence of unreacted primary amine groups. Thus, the infrared method is not sufficiently sensitive. For instance, the 12.10 μ band indicative of disubstitution will have a higher extinction coefficient than those due to higher degrees of aromatic substitution.

The N—H deformation is seen as a very weak band or shoulder ca. 6.45 μ in the DPA polymers (polymers 1–5), again confirming that the —NH— group remains intact in the polymer. The C—N vibration in polymers 1–9 occurs between 7.6 and 7.7 μ as a strong band corresponding to that of an aromatic amine, while in the aliphatic DBA polymer (polymer 10), the C—N band is found at 8.3 μ .

In the 5–6 μ region where the aromatic C—H out-of-plane overtone and combination bands occur, nothing was resolved except in the case of polymer 7. In this polymer bands were observed at 5.20 μ (m), 5.43 μ (m), 5.63 μ (m) and 5.85 μ (m), which are characteristic of monosubstitution. There is, thus, a predominance of monosubstitution over trisubstitution in this polymer, and this is probably the case in all the polymers where mono- and trisubstitution occur.

The polymer of dibenzylamine (DBA) (polymer 10) has a weak band at 3.4 μ due to —CH₂— (in-phase H-vibrations) and poly-DPE (polymer 11) has a broad strong band between 8.1 and 8.3 μ which may be assigned to the C—O—C vibration of an aryl ether. No C—Cl stretching band [12.50–16.67 μ (s)] was observed in any of the spectra; thus the extent of nuclear chlorination is insufficient to give infrared absorption, which agrees qualitatively with the elemental analyses (Tables I and II).

The elemental analyses are consistent with nuclear coupling occurring but it is not possible to use the C/H atomic ratios to estimate the degree of polymerization, since with only eight diphenylamine units, the C/H ratio is 1.297 which is already approaching the limiting value of 1.33. Kovacic¹³ found a similar situation to exist with his *p*-polyphenyls. In general, the solvent (benzene) was not copolymerized, but in the case of polymer 3, some benzene must have been incorporated because the C/N ratio of 17.4 is significantly higher than for polymers 1 and 2, in which the C/N ratio is approximately that expected, i.e., 12.0. However, there was no significant difference between the infrared spectra of polymers 1, 2, and 3 despite this copolymerization in the case of polymer 3.

Thermal and Oxidative Degradation

Doyle²⁹ has extensively reviewed the subject of thermogravimetric analysis. Newkirk³⁰ has effectively assumed that all pyrolytic decompositions can be fitted by first-order kinetics with respect to weight loss. He has proposed the calculation of first-order rate coefficients at each of a number of temperatures on the continuous weight loss curve, followed by construction of the appropriate Arrhenius plot which is examined for linearity. Linearity over a wide range of conversion was taken by Newkirk to be evidence for a simple kinetic form for the rate determining reaction.

Smith³¹ has modified this procedure merely by applying it to each separate stage of a multistage reaction rather than to the whole of a complex weight versus temperature TGA curve.

The thermograms obtained were treated by Smith's method and a selection of these thermograms (polymers 2, 3, 6, 9, and 11) are given in Figure 3. In many cases the Arrhenius plots were linear, as for polymer 13 (Fig. 4). Calculated activation energies (E) are given in Table IV, and it can be seen that there is no obvious correlation between the triggering temperatures and these activation energies.

To avoid large extrapolations of the Arrhenius plots, the pre-exponential A factors were thus determined by plotting $T \log k$ versus T to give straight lines of slope $\log A$ as for polymer 4 (Fig. 5). These A factors are also given in Table IV and differ considerably, values ranging from 10 to $4.6 \times$

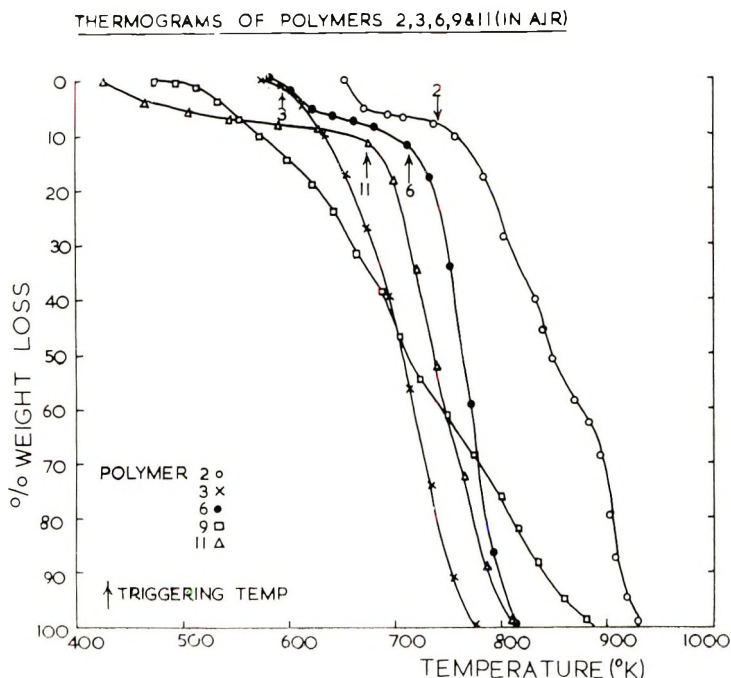


Fig. 3. Thermograms of polymers 2, 3, 6, 9, and 11 (in air).

TABLE IV
 Activation Energies and *A* Factors

No.	Polymer	Triggering temp, °C	Activation energy, kcal/mole		A factor, min ⁻¹	
			<i>E</i> _I	<i>E</i> _{II}	<i>A</i> _I	<i>A</i> _{II}
1	Poly-DPA	350	38.4	None	4.1×10^{11}	None
2	Poly-DPA	465	44.4 ^a	66.5	4.1×10^{11}	4.6×10^{16}
3 ^b	Poly-DPA	320	15.3 ^c	24.1 ^c	2.7×10^3	5.6×10^5
4	Poly-DPA	300	24.6	None	7.5×10^6	None
5	Poly-DPA	320	17.4	None	7.0×10^5	None
6	Poly-TPA	440	No straight line ^d	30.7	None	8.9×10^8
7	Poly-TPA	180	24.1 ^a	56.1 ^a	1.4×10^9	1.0×10^{13}
8	Poly-A	325	No straight line ^d	13.8	None	3.4×10^3
9	Poly-PPD	Progressively degrades	7.6 ^c	53.4 ^c	1.0×10^1	3.5×10^{15}
11 ^b	Poly-DPE	400	No straight line ^d	18.8 ^c	$E_{III} =$ None	$A_{III} =$
				37.6		1.0×10^{11}

^a TGA curve divided into two stages; each stage treated separately.

^b For polymers 3 and 11 the exact significance of the activation energies and *A* factors requires further analysis. The values given here would enable reconstruction of our Arrhenius plots and calculation of the first-order rate constants.

^c No break in TGA curve, but plot of $\log k$ vs $1/T$ over the whole temperature range gives two straight lines.

^d Slight weight loss which occurs before the triggering temperature.

10¹⁶. The higher values are in the expected range, but the lower ones are anomalous and will require further study.

Despite the common practice of reporting only *E*, it is obvious that as a parameter for characterizing the thermal stability of a polymer, *E* is inadequate, and that both *E* and *A* must be quoted.

The oxidative degradation of poly-DPA was studied by an infrared technique with the use of a thin film of polymer cast onto a potassium bromide disk as a sample. With polymer 2, spectra were recorded at 18.5, 200, and 300°C, using the same sample during the heating run. The sample was allowed 30 min to equilibrate at each temperature before recording the spectrum. At 200°C, a further measurement was made 105 min after the standard equilibration time. Apart from the expected general loss of resolution and intensities, all four spectra were almost identical. No new bands appeared on heating, and no existing ones were lost. However, there was a relative change in intensity of the three aromatic C—H out-of-plane bands at 12.30, 13.45, and 14.50 μ . At 18.5°C, $I_{13.45} > I_{12.30} = I_{14.50}$, but at 200°C and above, $I_{12.30} > I_{13.45} > I_{14.50}$. Sufficient data are not available at present to enable these intensity changes to be interpreted. The results as a whole

show that little or no oxidative degradation occurs up to 300°C with this type of polymer. It is of interest to note that with polybenzyl or with a Phillips-type resin, considerable oxidation would have taken place at this temperature due to the susceptibility of the —CH₂— group to oxidation.^{19,20}

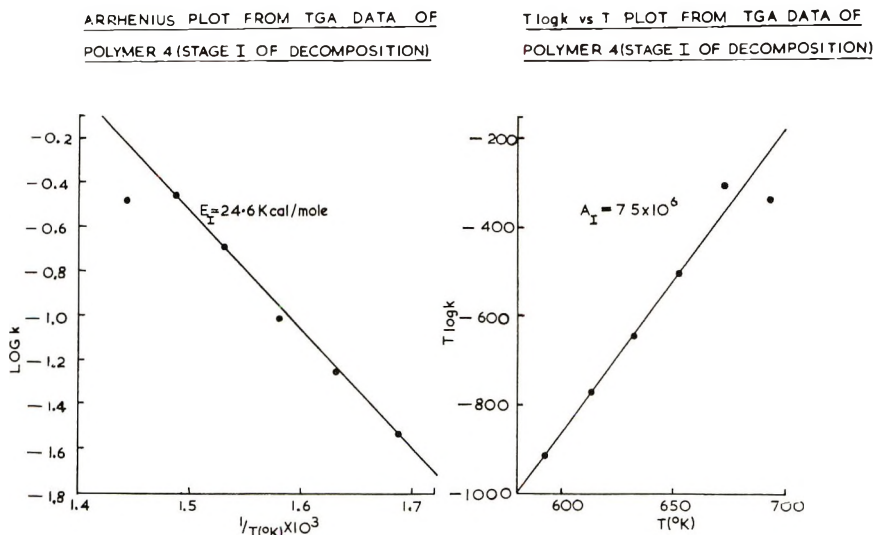
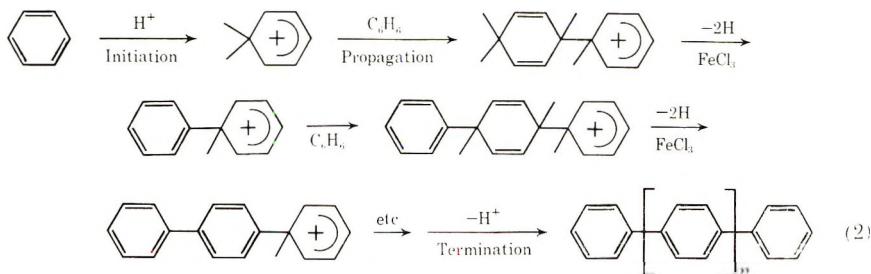
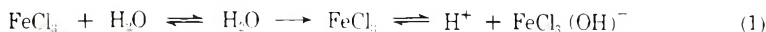


Fig. 4. Arrhenius plot from TGA data of polymer 4.
Fig. 5. Plot of $T \log k$ vs. T from TGA data of polymer 4.

Similar experiments were carried out on polymer 3 at 20, 100, and 220°C. In this case, the three spectra were identical, apart from the expected general loss in intensities, but the relative intensities of all the bands in a given spectrum were the same in all the spectra.

Reaction Mechanism

Kovacic has postulated an oxidative cationic mechanism for this type of reaction. For the polymerization of benzene with ferric chloride^{32,33} he postulates the mechanism of eqs. (1)–(2):



An alternative initiating species formed by one-electron reduction of FeCl_3 to yield a carbonium ion



has also been suggested.³³

Kovacic claims that an oxidant and a catalyst are required, since aluminum chloride alone is not effective, yet aluminum chloride–cupric chloride or aluminum chloride–nitrogen dioxide³⁴ are effective. He proposes that ferric chloride and molybdenum pentachloride perform a dual role of catalyst and oxidant. Kovacic has shown that some nonlinear products are also obtained due to formation of chromophoric polynuclear species.*

In the reactions investigated here, large amounts of catalyst are required for polymerization to take place (ca. 1 mole monomer: 1 mole catalyst) as was also found by Kovacic in similar systems. Since ferric chloride acts as both catalyst and oxidant, it follows that, as the reaction proceeds, ferric chloride will be reduced to ferrous chloride, thus reducing the amount of oxidant and possibly active catalyst present. These reactions of aromatic amines with ferric chloride do not seem to be affected by any possible complexing of the amines with the ferric ion. Compared with other Lewis acids, ferric chloride has quite a low affinity for forming complexes with amines. In the case of the aliphatic dibenzylamine, however, a yellow crystalline complex was obtained in addition to poly-DBA. We have also shown that the possibility of complex formation in solution between ferric chloride and acetone may account for polymerization in acetone, yielding polymers with a modified structure and low thermal stability.

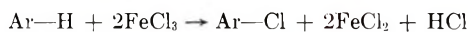
During the purification process, large amounts of 20% hydrochloric acid and distilled water were required to remove the residual catalyst. Since both ferric and ferrous chloride are soluble in these solvents and ferric chloride has a limited solubility in benzene (2% w/w),⁹ it would appear that polymerization must take place on the surface of the catalyst particles. Thus during the reaction, there is a gradual reduction in the area of active catalyst with the formation of an insoluble coating (the polymers are insoluble in benzene and water) and hence a large ratio of catalyst:monomer is required. Kovacic³⁷ agrees that these reactions in benzene are probably heterogeneous, however, since ferric chloride is soluble in acetone, and polymers are produced using this solvent, it is obvious that the reaction is homogeneous in this case.

According to Kovacic's mechanism, if an oxidant is supplied which is capable of aromatizing cyclohexadiene ring systems, then only small amounts of Friedel-Crafts catalyst should be necessary. Additional organic oxidants (dibenzoyl peroxide, chloranil, lead tetraacetate, and *n*-bromo-

* The referee has pointed out that *o*-polyphenylene linkages are formed from *o*-*p* directing aromatic monomers, e.g., halobenzenes³⁵ and toluene,³⁶ and by analogy may be present in the amine polymers.

succinimide) were introduced into the diphenylamine–ferric chloride–benzene system in the mole ratio diphenylamine:ferric chloride:additional oxidant = 10:1:1. There was only a small polymer yield using this diminished amount of ferric chloride together with these oxidants. Experiments with other Friedel-Crafts catalysts which do not have a lower oxidation state of reduced catalytic activity may help to resolve this question. Marvel³⁸ also investigated the use of organic oxidants for the aromatization of 1,3-cyclohexadienes but failed to obtain sufficiently high yields. Thus the mechanism of the dehydrogenation reactions involved is at present unknown. The recent review³⁹ of the mechanism of the Scholl reaction shows the paucity of information on this important reaction step.

Aromatic chlorination by ferric chloride is known to occur quite generally.^{40,43} Kovacic⁴¹ has stated that the reaction



proceeds, at least in the rate-determining step, by an electrophilic substitution mechanism, the overall effect of the reaction involving oxidation–reduction. He has since proposed a detailed mechanism for aromatic chlorination.⁴² The extent of nuclear chlorination in these polymers (0.5–6.3% in a temperature range of 35–80°C and a reaction time range of 0.5–8 hr) is greater than that obtained by Bilow and Miller¹⁷ (1–2.5% in a temperature range 100–160°C and reaction time range 2–24 hr). This is to be expected, since activation of the aromatic ring by the amine group renders the ring more susceptible to attack by electrophilic species. However, the extent of nuclear chlorination is lower than that of Kovacic's polymers (up to 19.7%), probably due to the more severe reaction conditions (temperatures up to 115°C and reaction times as long as 28 hr).

Finally, it should be noted that the reaction conditions affect the detailed structure of the polymers formed, the latter having widely differing thermal stabilities. However, with moderate polymerization temperatures, ferric chloride is a suitable combined catalyst and oxidant for the preparation of polymers of high thermal and oxidative stability from aromatic amines.

This work is part of an investigation of the properties of thermally stable polymers under Ministry of Technology contract No. PD/31/032.

We are grateful for the elemental analysis to Miss M. A. McKinnon of the Department of Chemistry and also to Dr. J. H. Sharp of the Department of Ceramics with Refractories Technology for use of the thermobalance.

“Crown Copyright,” reproduced with the permission of the Controller, Her Majesty's Stationary Office.

References

1. J. Idris Jones, *Repts. Progr. Appl. Chem.* **1965**, **621**, W. W. Wright and W. A. Lee, in *Progress in High Polymers*, Vol. 2, J. C. Robb and F. W. Peaker, Eds., Heywood, London, 1968, p. 189.
2. W. C. Hamman, WADC-TR 57-657, p. 158–171, Jan. 1958, ASTIA DOC. No. AD142285.
3. J. W. Dale, I. B. Johns, E. A. McElhill, and J. O. Smith, WADC-TR 59-427, p. 309–323, Jan. 1960, ASTIA DOC. No. AD234424.
4. J. W. Dale, E. A. McElhill, G. J. O'Neill, P. G. Scheurer, and G. R. Wilson, WADC-TR 59-95, Parts I, II and III 1961, ASTIA DOC. No. AD267980.

5. A. S. Hay, H. S. Blanchard, G. F. Endres, and J. W. Eustance, *J. Am. Chem. Soc.*, **81**, 6335, (1959).
6. A. S. Hay, *J. Polym. Sci.*, **58**, 581 (1962).
7. G. F. Endres and J. Kwiatak, *J. Polym. Sci.*, **58**, 593 (1962).
8. H. S. Blanchard, H. L. Finkbeiner, and G. A. Russell, *J. Polym. Sci.*, **58**, 469 (1962).
9. P. Kovacic and C.-S. Wu, *J. Polym. Sci.*, **47**, 45 (1960).
10. P. Kovacic, F. W. Koch, and C. E. Stephan, *J. Polym. Sci. A*, **2**, 1193 (1964).
11. P. Kovacic, *Friedel-Crafts and Related Reactions*, Vol. 4, G. Olah, Ed., Interscience, New York, 1964, Chap. 48.
12. P. Kovacic and R. M. Lange, *J. Org. Chem.*, **28**, 968 (1963).
13. P. Kovacic and A. Kyriakis, *J. Amer. Chem. Soc.*, **85**, 454 (1963).
14. P. Kovacic and J. Oziomek, *J. Org. Chem.*, **29**, 100 (1964).
15. P. Kovacic and R. M. Lange, *J. Org. Chem.*, **29**, 2416 (1964).
16. P. Kovacic and F. W. Koch, *J. Org. Chem.*, **30**, 3176 (1965).
17. N. Bilow and L. J. Miller, *J. Macromol. Sci. (Chem.)*, **A1**, 183 (1967).
18. L. N. Phillips, *Trans. Plastics. Inst.*, **32**, 298 (1964).
19. R. T. Conley, *J. Appl. Polym. Sci.*, **9**, 1107 (1965).
20. B. Ellis and P. G. White, Ministry of Technology Report, 1966-67, Contract No. PD/31/032.
21. P. Sykes, *A Guidebook to Mechanism in Organic Chemistry*, Longmans, London, 1962, p. 107.
22. B. P. Susz and P. Chalandon, *Helv. Chim. Acta*, **41**, 1332 (1958).
23. W. Lohman C. F. Fowler, W. H. Parkins, and J. L. Sanders, *Nature*, **209**, 908 (1966).
24. R. L. Van Deusen, O. K. Goins, and A. J. Sicree, *J. Polym. Sci. A-1*, **6**, 1777 (1968).
25. T. Shono, M. Hachihama, and K. Shiara, *J. Polym. Sci. B*, **5**, 1001 (1967).
26. J. Preston and R. W. Smith, *J. Polym. Sci. E*, **4**, 1033 (1966).
27. L. J. Bellamy, *The Infra-Red Spectra of Complex Molecules*, 2nd Ed., Methuen, London, 1964.
28. H. A. Szymanski, *Theory and Practice of Infra-Red Spectroscopy*, Plenum Press, New York, 1964, p. 276.
29. C. D. Doyle, in *Techniques and Methods of Polymer Evaluation*, P. E. Slade and L. T. Jenkins, Eds., Edward Arnold, London, 1966, p. 113.
30. A. E. Newkirk, *Anal. Chem.*, **32**, 1558 (1960).
31. D. A. Smith, *Trans. Inst. Rubber Ind.*, **39**, No. 6, 245 (1963).
32. P. Kovacic and A. Kyriakis, *Tetrahedron Letters*, **1962**, 467.
33. P. Kovacic and F. W. Koch, *J. Org. Chem.*, **28**, 1864, (1963).
34. P. Kovacic and R. J. Hopper, *J. Polym. Sci. A-1*, **4**, 1445 (1966).
35. P. Kovacic, J. T. Uchic, and L.-C. Hsu, *J. Polym. Sci. A-1*, **5**, 945 (1967).
36. P. Kovacic and J. S. Ramsey, unpublished work.
37. P. Kovacic, private communication.
38. C. S. Marvel and G. E. Hartzell, *J. Amer. Chem. Soc.*, **81**, 448 (1959).
39. A. T. Balaban and C. D. Nenitzescu, in *Friedel-Crafts and Reactions* Vol. 2, Part 2, G. Olah, Ed., Interscience, New York, 1964, Chap. 23.
40. V. Thomas, *C. R. Acad. Sci. (Paris)*, **126**, 1211 (1898); *ibid.*, **127**, 184 (1898); *ibid.*, **128**, 1576 (1899); *Bull. Soc. Chim. [3]*, **21**, 286 (1899).
41. P. Kovacic and N. C. Brace, *J. Amer. Chem. Soc.*, **76**, 5491 (1954).
42. P. Kovacic, C. Wu, and R. W. Stewart, *J. Amer. Chem. Soc.*, **82**, 1917 (1960).
43. M. Dangyan, *J. Gen. Chem. U. S. S. R.*, **8**, 1780 (1938).

Received March 12, 1969

Revised May 22, 1969

Reaction of Poly(vinyl Chloride) with Magnesium and Grignard Reagents

YUJI MINOURA, *Research Institute for Atomic Energy, Osaka City University, Osaka, Japan*, and HISASHI HIRONAKA, TOSHIYUKI KASABO, and YUKIO UENO, *Kyowa Rubber Industry Co., Ltd., Osaka, Japan*

Synopsis

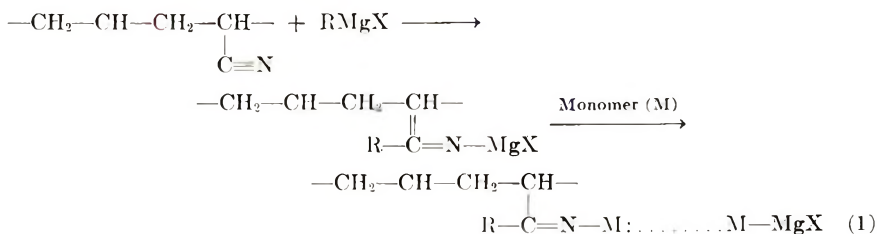
Reaction of poly(vinyl chloride) with magnesium under various conditions was attempted, but poly(vinyl chloride) did not react with magnesium. The reactions of poly(vinyl chloride) with benzylmagnesium chloride and allylmagnesium chloride as Grignard reagents were carried out in tetrahydrofuran at reflux temperature. It was found that the chlorine atoms in the poly(vinyl chloride) were replaced by benzyl and allyl groups by the coupling reaction, and a small amount of Grignard reagent of poly(vinyl chloride) was formed by the magnesium-halogen exchange reaction. The extent of the substitution increased with increasing reaction time and concentration of the Grignard reagent.

INTRODUCTION

The reactions of poly(vinyl chloride) with alkali metals,¹ organometallic reagents² such as *n*-butyllithium, sodium naphthalene and living polymers^{3,4}, and zinc^{5,6} have been reported.

It is also known that magnesium reacts with halides to give a Grignard reagent of the RMgX type, and this reagent reacts with various functional groups.

Greber and Egle⁷ reported that the reaction of dimethylsilylmethylmagnesium chloride with styrene-acrylonitrile copolymer yields a macromolecular polymerization initiator which permits the graft polymerization of 4-vinylpyridine, acrylonitrile, and methyl methacrylate [eq. (1)].



Beckerbauer and Baumgarten⁸ investigated the reactions of styrene-*p*-cyanostyrene copolymer with methylmagnesium chloride and *n*-butylmagnesium chloride.

However, no reports have been published on the reactions of polymers with magnesium and Grignard reagent. In a previous paper,⁹ the reaction of polyepichlorohydrin, which has a primary chlorine atom, with magnesium was discussed; it was found that although the Grignard reagent of polyepichlorohydrin was formed, the Grignard reagent reacted immediately with another chloromethyl group. Furthermore, the reactions of polyepichlorohydrin with benzylmagnesium chloride and allylmagnesium chloride were carried out, and it was found that chlorine atom in the polymer was substituted with benzyl and allyl groups.

In the present study, the reactions of poly(vinyl chloride), which has secondary chlorine atoms, with magnesium and Grignard reagents were investigated.

EXPERIMENTAL

Materials

A commercially available poly(vinyl chloride) (PVC) having a degree of polymerization of 1050 was dissolved in tetrahydrofuran (THF), after treating with hot acetone. The solution was poured into methanol. After reprecipitation and vacuum drying, the PVC was completely dried by standing over phosphorus pentoxide for a week.

THF, benzyl chloride, allyl chloride, magnesium, and other reagents were purified as described earlier.⁹

Reaction Procedure

The reactions were carried out according to the procedure described previously.⁹

Infrared Spectra

The infrared absorption spectra of thin films of the polymers cast from THF solution were obtained by using a Japan Spectroscopic Co., Ltd. spectrometer.

Intrinsic Viscosity

The intrinsic viscosity was measured in THF at 30°C by using an Ubbelohde viscometer.

Measurements of Chlorine Content and Unsaturation

The chlorine content was determined by the Schöniger method.¹⁰ The degree of unsaturation was determined according to the method of Rosenmund.¹¹

Measurements of Tensile Strength and Elongation

The tensile strength and elongation of specimens of polymers cast from THF solution on mercury were determined at 20°C by use of a tensile test machine of the Schopper type at the rate of extension of 300 mm/min.

RESULTS AND DISCUSSION

Reaction of PVC with Magnesium

PVC (0.625 g, 0.01 mole), magnesium (0.24 g, 0.01 mole), and 30 ml of THF were placed into a 100-ml reaction flask, and PVC was dissolved in THF under stirring and flushing with nitrogen. After the PVC was completely dissolved, a small amount of iodine was added to the mixture as a reaction initiator. The reaction was carried out at THF reflux temperature for 40 hr. Determinations of the Grignard reagent of PVC were attempted at suitable time intervals according to the method of Gilman and Schulz,¹² but the Grignard reagent was not detected over the reaction period. On the other hand, carbonation of the reaction mixture was carried out by the method described below. The infrared spectrum of the carbonation product agreed well with that of PVC, and the absorption band due to the carboxyl group was not observed. After 40 hr of the reaction, the reaction mixture of PVC and magnesium in THF was filtered, and the solution was poured into methanol. After reprecipitation and vacuum drying, the chlorine content and the infrared spectrum of the product were measured, but both chlorine content and the spectrum were almost the same as those of PVC.

Moreover, the reaction of PVC with magnesium was carried out under similar conditions in the presence of trimethylchlorosilane (0.05 mole, trimethylchlorosilane/PVC = 5.0), which does not react with magnesium but reacts with Grignard reagent above. The infrared spectrum of the product did not show the band at 850 cm^{-1} assigned to the trimethylsilyl group.

Furthermore, although the reactions were carried out under various conditions using hexamethylphosphoramide as solvent instead of THF and 1,2-ethylene dibromide as initiator instead of iodine, results to support the formation of Grignard reagent of PVC were not obtained.

It has been shown in the previous paper⁹ that polyepichlorohydrin, which has primary chlorine atoms, underwent dechlorination through the formation of Grignard reagent in the reaction with magnesium. On the other hand, it was found that PVC, which has secondary chlorine atoms, did not react with magnesium. The reason for this is thought to be the fact that the reactivity of secondary chlorine atoms is lower than that of primary chlorine atoms.

Reaction of PVC with Benzylmagnesium Chloride

It is well known that the Grignard reagent is sensitive to certain functional groups ($-\text{Cl}$, >C=O , $-\text{C}\equiv\text{N}$ etc.). Thus the reactions of this reagent with compounds having various functional groups have been widely investigated. In the previous paper,⁹ the reactions of polyepichlorohydrin with some Grignard reagents were discussed.

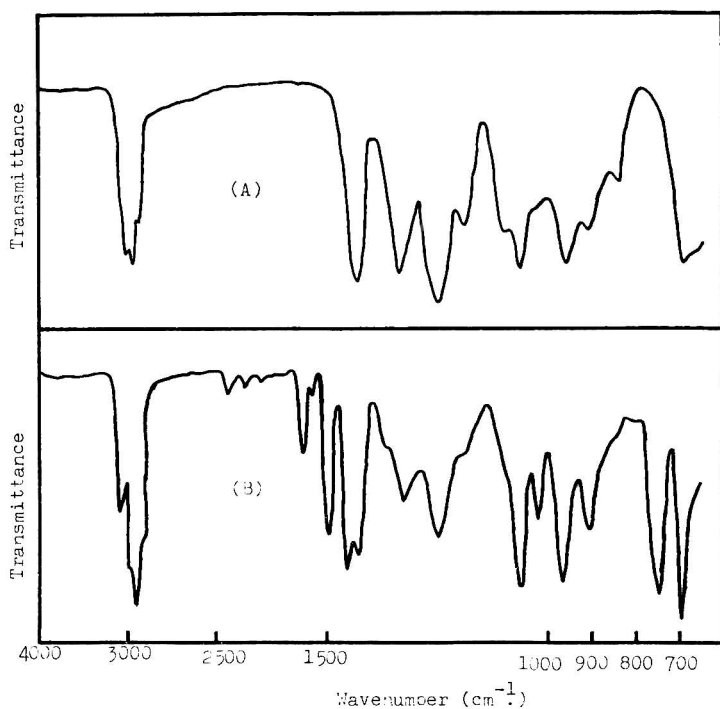
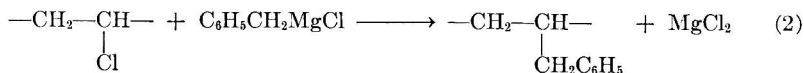


Fig. 1. Infrared spectra of (A) PVC and (B) reaction product of PVC with BzMgCl . In 50 ml THF; reflux temperature; 10 hr., PVC = 0.01 mole; $\text{BzMgCl/PVC} = 7.0$.

In this study, PVC (0.01 mole) was reacted with benzylmagnesium chloride (BzMgCl , 0.07 mole) in THF (50 ml) at reflux temperature. The infrared spectra of PVC and the product obtained after reaction for 10 hr are shown in Figure 1.

The spectrum of the product (Fig. 1B) showed new absorption bands at 3060, 1603, and 1500 cm^{-1} characteristic of the benzene ring which were not observed in the spectrum of PVC (Fig. 1A). In the range of 2000–1700 cm^{-1} , bands due to the monosubstituted benzene ring were observed. The intensity of these absorption bands increased with the increasing reaction time. These results indicated that the chlorine atom in PVC was replaced by a benzyl group by a coupling reaction as shown in eq (2).



The relationship between the chlorine content of the product and the reaction time is shown in Figure 2.

The chlorine content of the product decreased with increasing reaction time; that is, the extent of the substitution appears to increase with increasing reaction time. No coloration was observed in any of the products. Only one product which was obtained after a reaction period of 20 hr was insoluble in solvents such as THF and dimethylformamide.

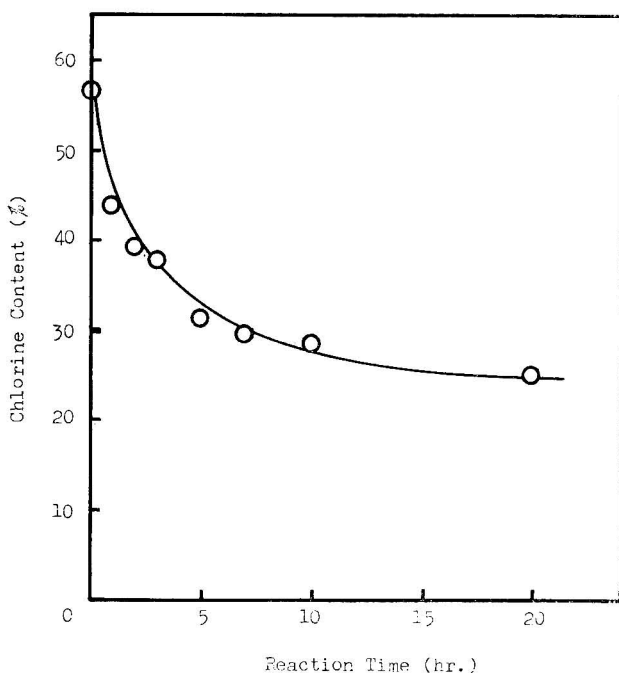
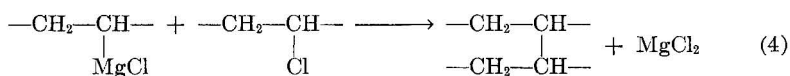
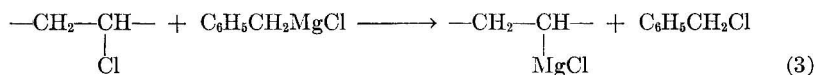
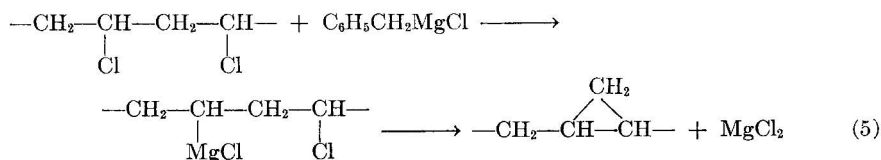


Fig. 2. Relationship between chlorine content of product and reaction time. PVC = 0.01 mole; BzMgCl/PVC = 7.0; THF, 50 ml; reflux temperature.

It has been shown by Reeve and Fine¹³ that magnesium-halogen exchange reaction occurs readily between *n*-butylmagnesium compounds and 1,1,1-trichloropropylene oxide. Therefore, it may be considered that the crosslinking results from the coupling reaction between Grignard reagent of PVC, which is formed by the exchange reaction between PVC and Bz-MgCl, with another PVC [eqs. (3) and (4)]:



On the other hand, if the Grignard reagent of PVC was formed, the formation of a propane ring might be possible in the intramolecular coupling reaction of the Grignard reagent with an adjacent chlorine atom [eq. (5)].



However, the formation of the cyclopropane ring was not confirmed from the infrared spectrum of the product, since the band at 1025 cm^{-1} assigned

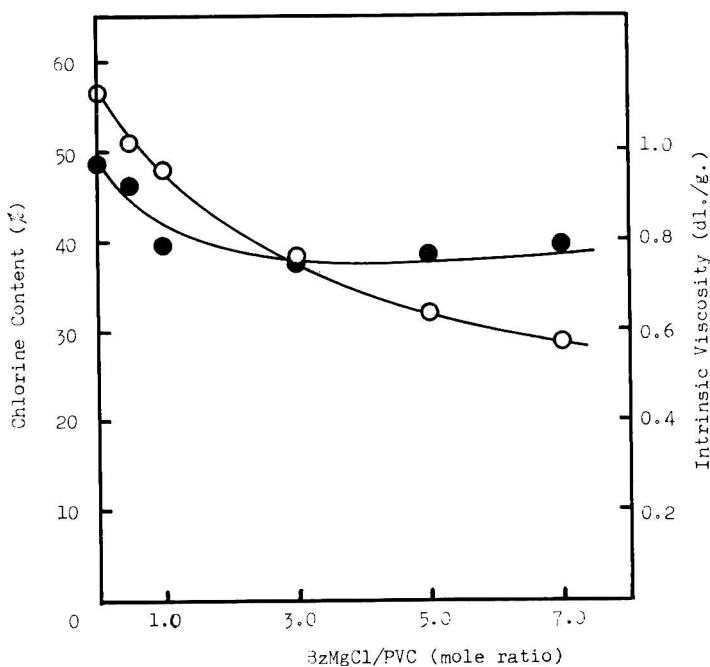


Fig. 3. Relationships between (○) chlorine content and (●) intrinsic viscosity of product and BzMgCl concentration. PVC = 0.01 mole; THF, 50 ml; reflux temperature; 10 hr.

to the cyclopropane ring overlapped the characteristic band of benzene ring.

In order to determine the relationship between the chlorine content and the intrinsic viscosity of the products and BzMgCl concentration, PVC

TABLE I
Composition of the Product^a

BzMgCl/PVC (mole ratio)	Composition			Analysis					
	I, mole- %	II, mole- %	III, mole- %	Found			Calcd from Composition		
				C, %	H, %	Cl, %	C, %	H, %	Cl, %
0 (PVC)	100	—	—	—	—	56.16	38.43	4.84	56.73
0.5	96.5	1.3	2.2	39.33	5.05	54.27	40.22	5.05	54.75
1.0	88.2	4.2	7.6	44.51	5.48	49.14	44.51	5.48	50.01
3.0	74.1	19.9	6.0	51.99	5.98	41.51	52.01	5.96	42.03
5.0	54.5	37.8	7.7	62.34	6.72	31.91	62.34	6.72	30.94
7.0	49.2	42.7	8.1	65.16	6.93	28.74	65.16	6.93	27.91

^a Reaction conditions; PVC, 0.01 mole; THF, 50 ml; reflux temperature; 10 hr.

TABLE II
Tensile Strength and Elongation of the Product^a

BzMgCl/PVC (mole ratio)	Extent of substitution, %	Tensile strength, kg/cm ²	Elongation, %
0	0 (PVC)	420	10
1.0	4.2	300	80
3.0	19.9	173	215
7.0	42.7	75	260

^a Reaction conditions: PVC, 0.01 mole; THF, 50 ml; reflux temperature; 10 hr.

was reacted in various concentrations of BzMgCl under similar conditions for 10 hr. The results are shown in Figure 3.

The chlorine content of the product decreased with increasing BzMgCl concentration. This result suggests that the extent of substitution increases with increasing BzMgCl concentration. Table I shows the composition of the products, calculated from the carbon and hydrogen content assuming the formation of cyclopropane rings.

It was proved from this result that the extent of the substitution increased with increasing BzMgCl concentration. On the other hand, the intrinsic viscosity of the product decreased with increasing BzMgCl concentration, i.e., increasing extent of substitution, as shown in Figure 3.

The tensile strength and elongation of some of the products obtained were measured. As shown in Table II, the tensile strength decreased and the elongation increased with increasing extent of substitution.

These results indicate that benzyl group introduced into PVC acts as a plasticizer. No coloration of the products was observed. Color changes in the products were observed on heating at 150°C for 5 hr. in air. The extent of the color change increased with increasing extent of substitution, and the color change for the products obtained when the molar ratio BzMgCl/PVC was 0.5 and 1.0, was less than that for PVC. This result suggests that a reactive C-Cl bond in PVC is replaced first with the benzyl group.

Thermogravimetric analyses of the products and PVC were carried out under nitrogen. It was found that decomposition of these polymers began at about 100°C; the rates of weight loss were almost the same; that is, there was no difference between the products and PVC.

Reaction of PVC with Allylmagnesium Chloride

The introduction of a reactive functional group such as a vinyl group into PVC without coloration is interesting. In this study, to introduce unsaturation, the reactions of PVC with AllylMgCl were carried out in THF under similar conditions to those described above.

The infrared spectrum of the product is shown in Figure 4.

Absorption bands at 3100, 1650, 990, and 915 cm⁻¹ assigned to the vinyl group appeared, and also a new band at 1025 cm⁻¹, which was not observed

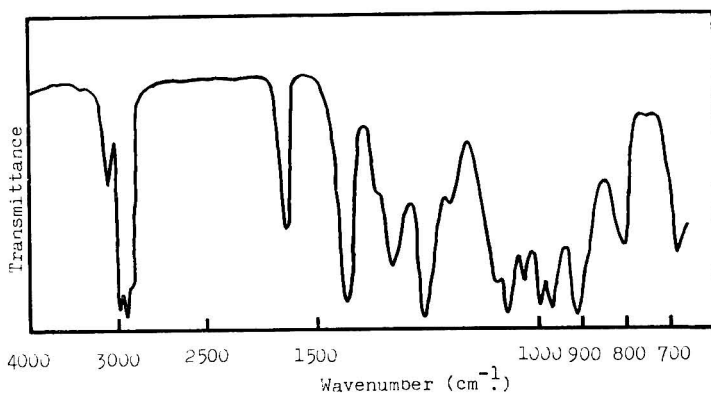


Fig. 4. Infrared spectrum of reaction product of PVC with AllylMgCl. In 50 ml. THF; reflux temperature; 10 hr; PVC = 0.01 mole, AllylMgCl/PVC = 7.0.

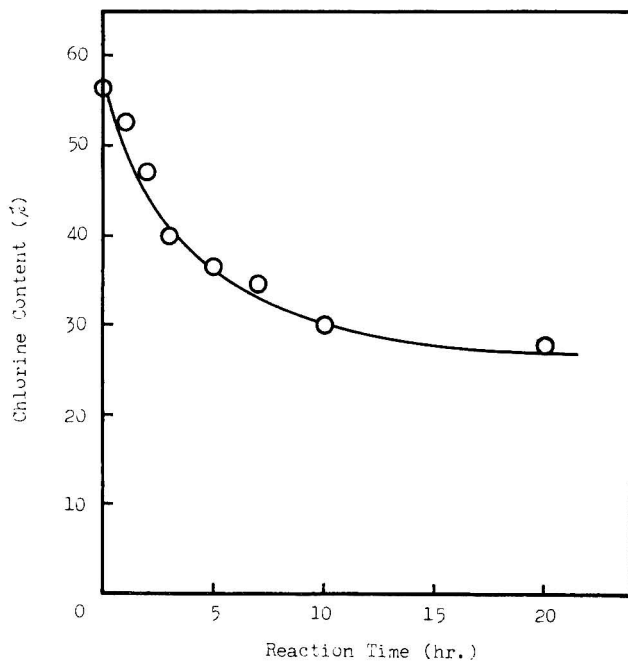


Fig. 5. Relationship between chlorine content of product and reaction time. PVC = 0.01 mole; AllylMgCl/PVC = 7.0; THF, 50 ml.; reflux temperature.

in allyl group or PVC. This band may be derived from the cyclopropane ring, which was formed by the intramolecular coupling reaction of the Grignard reagent of PVC as described above.

Figure 5 shows the relationship between the chlorine content of the products and the reaction time.

The chlorine content of the products decreased with increasing reaction time, and only one product, which was obtained after the reaction period of 20 hr was insoluble in THF.

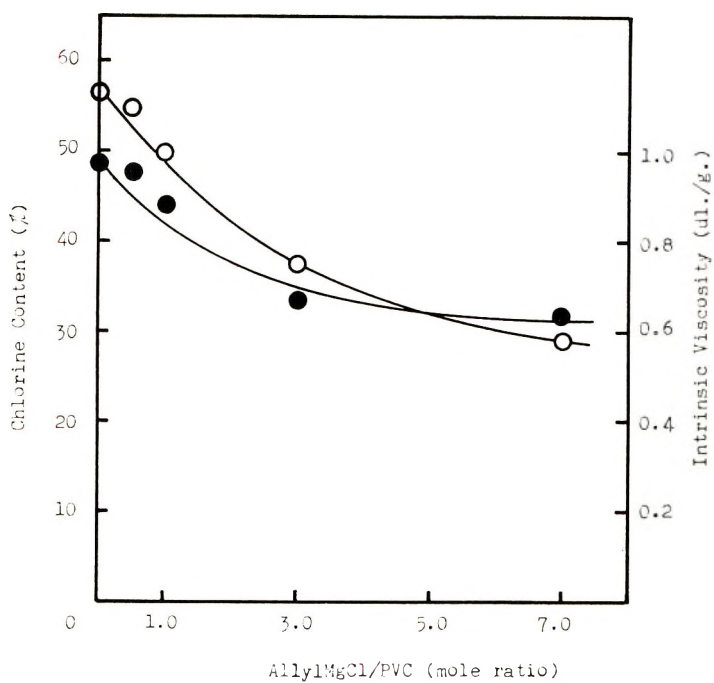


Fig. 6. Relationships between (O) chlorine content and (●) intrinsic viscosity of product and AllylMgCl concentration. PVC = 0.01 mole; THF, 50 ml; reflux temperature; 10 hr.

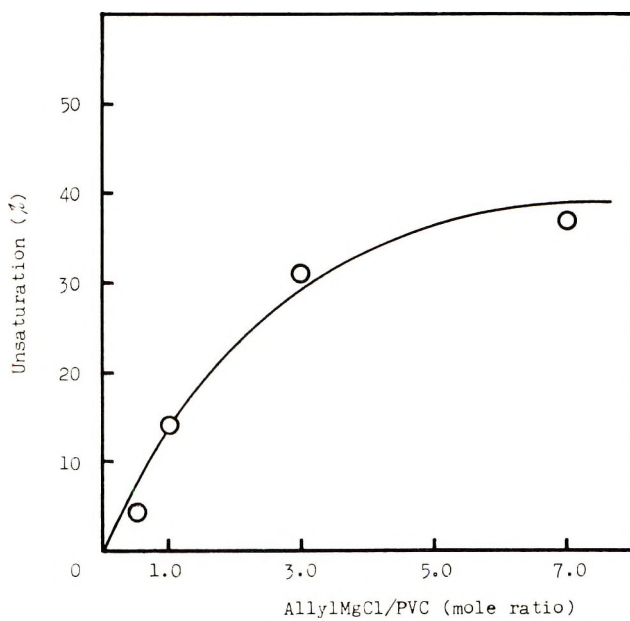


Fig. 7. Unsaturation of product. PVC = 0.01 mole; THF, 50 ml; reflux temperature; 10 hr.

The relationships between the chlorine content and intrinsic viscosity of the products and AllylMgCl concentration are shown in Figure 6.

The chlorine content and intrinsic viscosity of the product decreased with increasing AllylMgCl concentration. On the other hand, the unsaturation in the product increased with increasing AllylMgCl concentration, as shown in Figure 7.

It was found from these results that the extent of the substitution increased and the intrinsic viscosity decreased with increasing AllylMgCl concentration.

The products obtained were white solids which were soluble in THF. These products crosslinked on standing at room temperature for over a week, and the crosslinking was accelerated by application of moderate heat, but coloration did not occur.

Carbonation of a Mixture of PVC and AllylMgCl in THF

It was pointed out in the reaction of PVC with Grignard reagents that the Grignard reagent of PVC was formed by the magnesium-halogen exchange reaction followed by the intermolecular and intramolecular coupling reactions to give crosslinking and cyclopropane rings, respectively. Therefore, the carbonation reaction was applied to the reaction mixture of PVC

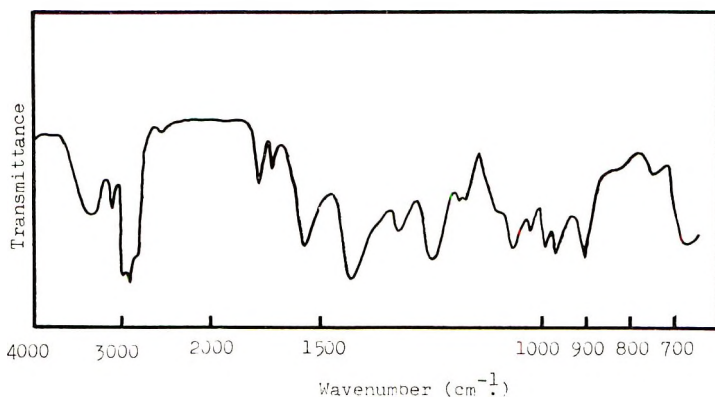
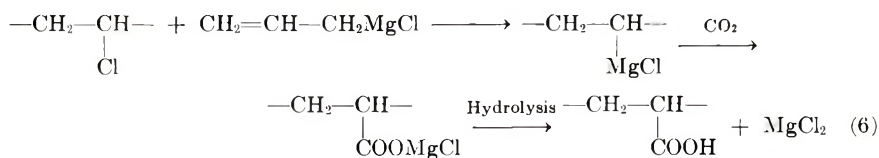


Fig. 8. Infrared spectrum of carbonation product from reaction of PVC and AllylMgCl in THF. Reaction time, 5 hr; PVC = 0.01 mole; AllylMgCl/PVC = 7.0; THF, 50 ml; reflux temperature.

and AllylMgCl in THF to confirm the formation of the Grignard reagent of PVC. The reaction mixture, after 5 hr reaction, was poured into a Dry Ice-THF slurry and then hydrolyzed in the usual way. The infrared spectrum of the carbonation product is shown in Figure 8.

The spectrum showed new absorption bands at 1780 and 1725 cm^{-1} assigned to the carbonyl group and bands at 3400-3100 cm^{-1} assigned to the hydroxyl group, which were not observed in the spectrum of the reaction

products of PVC with AllylMgCl (Fig. 4). This result indicates that a carboxyl group is introduced into PVC as indicated in eq. (6).



It was confirmed that in the reaction of PVC and Grignard reagent, the Grignard reagent of PVC was formed by the magnesium-halogen exchange reaction, and this was followed by intermolecular and intramolecular coupling to give crosslinking and a cyclopropane ring, respectively.

References

1. S. Kambara, I. Shinohara, and H. Tsuchida, *Kogyo Kagaku Zasshi*, **66**, 1404 (1963).
2. Y. Minoura and K. Shiina, *J. Polym. Sci. A-1*, **4**, 1069 (1966).
3. Y. Gallot, P. Rempp, and J. Parrod, *J. Polym. Sci. B*, **1**, 329 (1963).
4. Y. Minoura, H. Hironaka, T. Kasabo, and Y. Ueno, *J. Polym. Sci. A-1*, **6**, 2773 (1968).
5. C. S. Marvel, J. H. Sample, and M. G. Roy, *J. Amer. Chem. Soc.*, **61**, 3241 (1939).
6. K. Takemoto and Y. Mizohata, *Kogyo Kagaku Zasshi*, **63**, 347 (1960).
7. G. Greber and G. Egle, *Makromol. Chem.*, **62**, 196 (1963).
8. C. R. Beckerbauer and H. E. Baumgarten, *J. Polym. Sci. A*, **2**, 503 (1964).
9. Y. Minoura, H. Hironaka, T. Kasabo, and Y. Ueno, *J. Polym. Sci.*, in press.
10. W. Schöniger, *Mikrochim. Acta*, **1955**, 123 (1955).
11. K. W. Rosenmund, *Angew. Chem.*, **37**, 58 (1924).
12. H. Gilman and F. Schulze, *J. Amer. Chem. Soc.*, **47**, 2002 (1925).
13. W. Reeve and L. W. Fine, *J. Amer. Chem. Soc.*, **86**, 880 (1964).

Received April 21, 1969

Revised June 4, 1969

NOTES

Irradiation Popcorn Polymers

We wish to report results on the radiation stability of popcorn polymers which show a remarkable difference between the behavior of seed material and material proliferated in a monovinyl compound.¹

The seed material was obtained by polymerizing styrene-divinylbenzene feed under optimum popcorn-forming conditions. The proliferation (popcorn growth) was carried out in pure styrene. In the nonproliferated material, therefore, a certain concentration of chemical crosslinks corresponding to the divinylbenzene content of the feed is present, whereas in the proliferated material the concentration of primary crosslinks is reduced according to the degree of proliferation, to $^{1/12-1/30}$ of the original value. Both materials are characterized by their benzene uptake (by swelling and by sorption into the porous structure) and by their nearly identical micro-optical anisotropy.¹

In most experiments the specimens were irradiated to a total gamma dose of 2.5×10^7 rad at a dose rate of $3.2-3.3 \times 10^6$ rad/hr in an inert atmosphere with the use of a 10-ke ⁶⁰Co source.

Three nonproliferated specimens (0.35% *p*-divinylbenzene) of different porosity were irradiated. The differences in porosity were obtained by polymerization of identical feeds in vessels of different size and shape, the polymer with the lowest porosity being obtained in the most narrow tube. The benzene uptake before and after irradiation was as shown in Table I.

TABLE I
Irradiation of Styrene-*p*-divinylbenzene-Popcorn Polymers

Sample	Benzene uptake, g/g	
	Before irradiation	After irradiation
1	4.58	4.38
2	1.05	1.18
3	0.82	0.72

The differences among the three samples are a measure of differences in porosity. The irradiation produced no visible change of the micro-optical anisotropy of the polymers. Thus irradiation has only a very small influence on the properties of the samples. This is in agreement with the known radiation stability of the normal crosslinked and non-crosslinked polystyrene shown in Table II.

The known crosslinking *G* value for polystyrene is 0.04, so that a dose of 25 Mrad would increase the crosslink density by one per 10^4 styrene unit; this would be negligible compared with the concentrations of divinylbenzene used.

Entirely different effects are observed in the irradiation of the proliferated popcorn polymer samples. The irradiated specimens in the dry state maintain their micro-optical anisotropy but in contact with benzene they swell, become optically isotropic, and then dissolve, either partially or completely, depending on the sample and the irradiation dose. Typical results are shown in Table III for a popcorn polymer containing originally 0.5 mole-% *p*-divinylbenzene and proliferated in styrene to 12 times its original weight. Following irradiation over a broad dose range specimens were contacted with benzene for 24 hr at room temperature.

It may be noted that the benzene uptake, compared with the initial mass of proliferated polymer is almost unaltered.

Also proliferated popcorn polymers (12 times its original weight) with a benzene uptake of only 1.9 g/g were found to be almost completely soluble in benzene and gave an optically isotropic gel after an irradiation dose of 25 Mrad.

These results show that crosslinks responsible for the limited swelling of proliferated popcorn polymers do not have the same stability against irradiation as the divinylbenzene crosslinks in the nonproliferated material. This fact supports the entanglement

TABLE II
Irradiation of Polystyrene^a

	[η], ml/g		Benzene uptake, g/g		Notes
	Before irradiation	After irradiation	Before irradiation	After irradiation	
Noncrosslinked polystyrene	77.1	79.2			
Crosslinked polystyrene					
Styrene- <i>p</i> -divinylbenzene (4%)			1.38	1.40	True swelling
Styrene-divinylbenzene (Tech 19%)			0.09	0.08	True swelling
Styrene-divinylbenzene (Tech 19%), macroporous			0.64	0.66	Swelling + porous

^a Dose = 25 Mrad.

TABLE III
Irradiation of a Proliferated Popcorn Polymer

Dose Mrad	Sol fraction, %	Benzene uptake, g/g	
		Gel fraction	Initial weight
0	0	4.5	4.5
5	21	5.6	4.4
25	46	9.9	5.3
120	97	200	6.0

concept of popcorn polymer structure developed in earlier papers.¹ For the first time we have a means or method to differentiate experimentally between proliferated and non-proliferated styrene-divinylbenzene popcorn polymers.

Other popcorn polymer systems have been found to behave differently. The micro-optical anisotropy of a non-proliferated methylmethacrylate-glycol dimethacrylate (2 mole-%) popcorn polymer completely disappears under identical irradiation conditions to a dose of 25 Mrad. This is to be expected, since poly(methyl methacrylate) is known to undergo scission under radiation.

Reference

1. J. W. Breitenbach, in *Advances in Macromolecular Chemistry*, Vol. 1, W. M. Pasika, Ed., Academic Press, New York, 1968.

J. W. BREITENBACH
H. SULEK

Institut für Physikalische Chemie
Universität Wien
Vienna, Austria

A. CHARLESBY
P. J. FYDELOR

J. J. Thomson Laboratory
Royal Military College of Science
Shrivenham, Swindon, Wilts, England

Received March 21, 1969
Revised June 3, 1969

**Endgroup Studies of Peroxodisulfate-Initiated Vinyl
Polymerization: Re-Examination of the Proposed
Mechanism of Initiation in Acid Solution**

It has been reported by Ghosh et al.¹ that when potassium peroxodisulfate is used as initiator for vinyl polymerization, the ratio of sulfate to hydroxyl groups on the polymer varies with the acidity of the polymerization medium. This ratio is reported greater than one in basic to neutral polymerization media and found to decrease sharply to less than one in acidic media. The experimental results attribute this to a rapid decline in the proportion of sulfate endgroups on the polymer with the increase in acidity.* In the case of basic to neutral media, the results of the endgroup studies are explained by capture of the sulfate radical-ions and hydroxyl radicals, resulting from the thermal decomposition of the peroxodisulfate ions; however, in the case of acidic polymerization media, the results are not so readily explained. To account for the hydroxyl radical being the major initiating species in acid solution. Ghosh et al. have proposed that the sulfate radical-ions react rapidly with hydroxonium ions:



It is the purpose of this communication to re-examine the initiation of polymerization in acid solution.

On the basis of a detailed study, Ilakola³ has shown that in dilute acid solution, the overall decomposition of potassium peroxodisulfate is equal to the sum of the separate decompositions of the peroxodisulfate and hydrogen peroxodisulfate ions. Each species is found to decompose at its own rate and by a separate mechanism. The rate equation being:

$$-d[\text{K}_2\text{S}_2\text{O}_8]/dt = k_1[\text{S}_2\text{O}_8^{2-}] + k_2[\text{HS}_2\text{O}_8^-]$$

where k_1 and k_2 are the rate coefficients for the decomposition of the peroxodisulfate and hydrogen peroxodisulfate ions, respectively. If K_2 is the acidity constant for the hydrogen peroxodisulfate ion, and

$$[\text{S}_2\text{O}_8^{2-}]_{\text{total}} = [\text{S}_2\text{O}_8^{2-}] + [\text{HS}_2\text{O}_8^-]$$

then

$$-d[\text{K}_2\text{S}_2\text{O}_8]/dt = k[\text{S}_2\text{O}_8^{2-}]_{\text{total}}$$

where

$$k = (k_1K_2 + k_2[\text{H}_3\text{O}^+])/(K_2 + [\text{H}_3\text{O}^+])$$

Many workers^{4,5} have investigated the thermal decomposition of the peroxodisulfate ion (commonly termed the spontaneous or uncatalyzed decomposition) and although there is no definite agreement as to the exact mechanism, the results of most studies are readily explained by the simple mechanism of Bartlett and Cotman:⁶



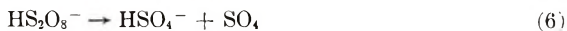
where reaction (2) is the rate-determining step.

* Acid hydrolysis of polymer sulfate in the polymerization systems, as computed from the rate data of Kurz,² appears to be quite insignificant.

As stated above, the results of the endgroup studies in basic to neutral media are quite compatible with such a mechanism.

The mechanism of the decomposition of the hydrogen peroxodisulfate ion has not been fully elucidated, although the kinetics of its decomposition have been investigated in detail.^{3,7}

Kolthoff and Miller⁷ have proposed the reaction scheme (5)–(7) for the decomposition of potassium peroxodisulfate in acid solution

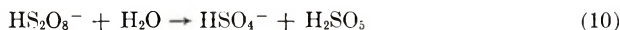


and suggest eq. (8) in strong acid solution.



It should be pointed out that there is no conclusive evidence for the existence of sulfur tetroxide in the decomposition system. Indeed, Lunenok-Burmakina and Potemskaya⁸ have shown that the oxygen evolved during the acid decomposition (and derived from the peroxodisulfate) is made up exclusively of peroxide oxygen, and hence reactions (6)–(8) that imply cleavage of the peroxide bond, appear to be quite incompatible with the experimental observations.

It is known from decomposition studies at higher acidities than employed in the polymerization systems, that peroxomonosulfuric acid (Caro's acid) is formed during the decomposition and that this undergoes hydrolysis to sulfuric acid and hydrogen peroxide.^{7,9} Such considerations have led House⁴ to formulate the scheme of eqs. (9)–(11) for the decomposition in acid solution:



It should be noted that at the acid concentration of the polymerization system, the contribution of the hydrogen peroxodisulfate ion decomposition to the total decomposition is several times that of the peroxodisulfate ion.* Since it has been shown that the decomposition of the hydrogen peroxodisulfate ion does not proceed by a free-radical mechanism,¹⁰ the concentration of sulfate radical-ions available for reaction with hydroxonium ions as in reaction (1) is considerably reduced, particularly when the additional removal of sulfate radical-ions by addition to monomer is considered.

Also, the rapid removal of sulfate radical-ions in acid media [by reaction (1) or any other] seems very doubtful since when sulfate radical-ions are generated by γ -irradiation of deaerated 5.4 *M* sulfuric acid glass at 77°K, there is no evidence for their ($\text{SO}_4^{\cdot -}$) disappearance.†

* The polymerization system in question is: $1.85 \times 10^{-2}M$ $\text{K}_2\text{S}_2\text{O}_8$, 0.1*M* HCl, and $9.4 \times 10^{-2}M$ methyl methacrylate at 30°C. Using the reported values of k_1 , k , and $K_2/[\text{H}_3\text{O}^+]$ for the decomposition of 0.05*M*, 0.1*M*, and 0.2*M* $\text{K}_2\text{S}_2\text{O}_8$ in 0.04*M* KHSO_4 at 25°C and 35°C and extrapolating to 0.02*M* $\text{K}_2\text{S}_2\text{O}_8$ (cf. $1.85 \times 10^{-2}M$ $\text{K}_2\text{S}_2\text{O}_8$ in the polymerization recipe) one may compute both the concentration *C* of hydrogen peroxodisulfate expressed as a percentage of the total peroxodisulfate, and its per cent contribution *R* to the overall decomposition. Although the values so computed are only approximate, they serve to demonstrate the significant contribution of the hydrogen peroxodisulfate to the overall decomposition. It is found that, in the system of 0.02*M* $\text{K}_2\text{S}_2\text{O}_8$ and 0.04*M* KHSO_4 , *C* is not less than 18–25% (at 35–25°C) and *R* is not less than 65–74% (at 35–25°C). At the higher acidity used in the polymerization recipe, both *C* and *R* are expected to be higher than computed here.

† The author is indebted to Professor F. S. Dainton for raising this point.^{11,12}

The sulfate radical-ion-hydroxyl radical interconversion has been reviewed by Wilmarth and Haim.⁵ These authors emphasize that the experimental evidence (from a study of the hydrogenation of the peroxodisulfate ion) strongly supports the view that the rate of the sulfate radical-ion-hydroxyl radical interconversion increases with increasing alkalinity. This implies that sulfate radical-ions react with hydroxyl ions



in a parallel reaction path to their oxidation of water [reaction (3)].

Hayon and McGarvey¹³ and Dogliotti and Hayon¹⁴ have studied the production of sulfate radical-ions by flash photolysis of sulfate and peroxodisulfate ions in aqueous solutions. The experimental results confirm the stability of $\text{SO}_4^{\cdot-}$ in acid solution and the view that the sulfate radical-ion-hydroxyl radical interconversion increases with pH. In the pH range of 9.8–10.4, the sulfate radical-ions disappear rapidly with a pseudo-first order, dependent on hydroxyl ion concentration; their disappearance is complete above a pH of 10.8.

It is rather difficult to entertain the validity of a rapid reaction (1) in the light of this recent experimental evidence to the contrary.

Peroxodisulfate decomposition studies at high acidities ($>2M$), may tempt one to postulate that the role of initiator may also be shared by hydrogen peroxide [formed according to eqs. (9)–(11) above] which by its decomposition (catalyzed by trace metal ion contamination) produces hydroxyl radicals which then initiate polymerization.¹⁵ In acid solution, the concentration of free-radicals (sulfate radical-ion and hydroxyl) from the decomposition of the potassium peroxodisulfate is significantly reduced. The increase in hydroxyl radical concentration from hydrogen peroxide decomposition would result in a predominance of hydroxyl radicals over sulfate radical-ions. Such a mechanism of initiation may be quite feasible at high acidities; however it does not account for the polymerization studies in question, since hydrogen peroxide is not detected at the acidities of the polymerization systems.¹⁶

With our present, rather incomplete, understanding of the decomposition of potassium peroxodisulfate in dilute acid solution, it is not apparent what the initiation mechanism is under such conditions.

I am pleased to express my thanks to Professor F. S. Dainton and Professor S. R. Palit who kindly read and commented on the original manuscript.

References

1. P. Ghosh, S. C. Chada, A. R. Mukherjee, and S. R. Palit, *J. Polym. Sci. A*, **2**, 4433 (1964).
2. J. L. Kurz, *J. Phys. Chem.*, **66**, 2239 (1962).
3. E. Hakoila, *Ann. Univ. Turku*, **A66**, 55 (1963).
4. D. A. House, *Chem. Rev.*, **62**, 185 (1962).
5. W. K. Wilmarth and A. Haim, in *Peroxide Reaction Mechanisms*, J. O. Edwards, Ed., Interscience, New York, 1962, p. 175.
6. P. D. Bartlett and J. D. Cotman, Jr., *J. Amer. Chem. Soc.*, **71**, 1419 (1949).
7. I. M. Kolthoff and I. K. Miller, *J. Amer. Chem. Soc.*, **73**, 3055 (1951).
8. V. A. Lunenok-Burmakina and A. P. Potemskaya, *Ukr. Khim. Zh.*, **30**, 1262 (1964).
9. E. I. Denisov, *Zh. Priklad. Khim.*, **13**, 596 (1940).
10. C. E. H. Bawn and D. Margerison, *Trans. Faraday Soc.*, **51**, 925 (1935).
11. D. M. Brown and F. S. Dainton, *Trans. Faraday Soc.*, **62**, 1139 (1966).
12. A. Treimin in *Radical Ions*, E. T. Kaiser and L. Kevan, Eds., Interscience, New York, 1966, p. 525.
13. E. Hayon and J. J. McGarvey, *J. Phys. Chem.*, **71**, 1472 (1967).
14. L. Dogliotti and E. Hayon, *J. Phys. Chem.*, **71**, 2511 (1967).

15. R. G. R. Bacon, *Quart. Rev.*, **9**, 287 (1955).
16. Y. K. Gupta, *J. Indian Chem. Soc.*, **37**, 755 (1960).

Department of Physical Chemistry
University of Sydney
Sydney, N. S. W., Australia

Received February 18, 1969

Revised July 16, 1969

EDWARD P. CREMATY

BOOK REVIEWS

Man-Made Fibers: Science and Technology. Volume I. H. F. Mark, S. M. Atlas, and E. Cernia, Eds., Interscience, New York, 1967. xi + 432 pp. \$17.50.

My original copy of this book was lost in the mails, so this review is unavoidably late. There is one advantage of the delay, however. I have been able to check my opinion with that of a colleague, who is a spinning expert. He was initially disappointed because he found so few new leads to problems that had been facing him. On reflection, however, he realized that, to quote, "But, to be fair, I think that we must admit that very little is known about the subjects that aren't treated adequately in the book, in spite of the incredible size of the fiber industry and the large expenditure on research and development." This book, then, is not so much for the specialist as it is for those who hope to become specialists, or those like myself, who never expect to spin fibers, but need to know a good deal about the field.

The two chapters by A. Ziabicki, on fundamentals of spinning, were very interesting to me. I particularly liked the discussion of tensile viscosity and of the factors limiting the amount of draw-down during spinning. I wondered whether more emphasis shouldn't be paid to the amount of stored elastic energy in the spinning melt or dope, rather than the main relaxation time, particularly when dealing with fiber breakage and fluctuations of diameter. (My colleague doubts the validity of my contention.)

The chapter on dry-spinning, by J. Corbiere, is more restricted in scope. The emphasis is on practical matters, and primarily on cellulose acetate.

Chapters on transition phenomena, by K. Ueberreiter, and chain folding, by A. Peterlin, are very good. However, so little is known about fiber problems in these fields that much of the treatment applies to polymers in general, rather than specifically to fibers. What I particularly missed throughout the book were thorough discussions of the effects of melt orientation and of solvents on crystallization. I also did not note a complete treatment of the effects of temperature and of solvents on fiber drawing.

The chapter on morphology, by O. and I. Szabolis, is even less definite. Many details are presented, but useful generalizations are rare.

"Conjugate Fibers," by E. M. Hicks, E. A. Tippetts, J. V. Hewett and R. H. Brand differs from the rest of the book, in that a very specialized topic is discussed. The treatment is good.

I must now warn the reader that two of the chapters are very inadequate. The first, by two of the editors, is far too short to serve as a proper introduction to structural principles of fiber-forming polymers. Almost every statement made is subject to so many qualifications that very misleading impressions can be created. For example, it is stated that addition polymerization is more versatile than condensation polymerization because the breadth of the distribution can be varied from very narrow to very wide. In the first place, the statement isn't generally true. Interfacial polymerization leads to a wide distribution and all that limits one with other condensation polymers is the ability to make the high molecular weight component of a blend. It is exceedingly difficult to secure a narrow distribution with Ziegler catalysts, and unusual with other systems. In the second place, there are no hints as to the beneficial or adverse effects of a wide or narrow distribution. This discussion is not given elsewhere in the book, so this would have been an excellent place to round out the picture.

The chapter on wet-spinning is so deficient that the editors recommend other treatments of the subject.

All in all, I feel that the effect of the editors to assemble discussions from European authors has been successful. Only one translation was poor.

A final judgment must await completion of the other two volumes. Also, we must remember that the editors have not attempted to replace the works of Rowland Hill and others, but rather to bring the story up to date. Nevertheless, I am sorry to report that I didn't learn very much about the special problems involved in the development of new polymers for fibers, or about the relative virtues of various methods of spinning, when the polymer is at hand.

H. M. Spurlin

Hercules Inc.
Research Center
Wilmington, Delaware 19899

Man-Made Fibers: Science and Technology, Volume III. H. F. Mark, S. M. Atlas, E. Cernia, Eds., Wiley, New York, 1968. xi + 706. \$27.00.

Having treated generally the subject of processing of polymers into fibers in Volume I of this series, and the Cellulosic and Polyamide fibers in Volume II, the editors of Volume III in this series have apparently chosen to complete their treatise on the Science and Technology of man-made fibers. Accordingly, this volume contains chapters on Polyesters and Copolyesters, Acrylic and Modacrylics, plus individual chapters on fibers from Polyvinyl Alcohol, Polyvinylidene Chloride, Polyvinyl Chloride, Linear Polyolefins, segmented Polyurethanes, Glass, "Elementoorganic Polymers" and Metals. In addition, there are chapters on the general principles of dyeing and finishing and the testing of man-made fibers.

Since the bulk of the technology in the field of man-made fibers has been developed in industrial laboratories; and, further, since the industry is highly competitive, a great deal of what is known and what is commonly practiced is not now available for publication. Therefore, with few exceptions, the subjects are treated with varying degrees of superficiality. Perhaps the worst example of this is the eighteen-page chapter on Polyethylene Terephthalate. On the other hand, the sections on Acrylic and Modacrylic fibers are particularly well-done and a very creditable job has been done on the section on Copolyesters.

In the context of the paucity of authoritative information in the field of man-made fibers technology, this volume, taken with the earlier two volumes, does a creditable job in surveying the field and making available references to published information in the literature.

R. F. Heitmiller

Beaunit Fibers Technical Center
Post Office Box 12234
Research Triangle Park, N. C. 27709

Review of Volume IX Encyclopedia of Polymer Science and Technology. Interscience Publishers a division of John Wiley & Sons, Inc., New York. 860 pp. \$50.00. Herman F. Mark, Norman G. Gaylord, and Norbert M. Bikales, Eds.

Volume IX of the *Encyclopedia of Polymer Science and Technology* continues to maintain the excellent quality of the previous members of the series. The subject matter represents a great deal of work on the part of the editors and authors, and promises to be of great value for research purposes in the macromolecular area.

This volume is very informative and will be very useful as a reference. The breadth of coverage will be very beneficial for use by workers entering a field in which they have little experience, as well as a reference for experts.

Again, the editors and authors should be congratulated for their excellent presentation of the material which is valuable and beneficial as well as interesting.

C. G. Overberger

University of Michigan
Department of Chemistry
Ann Arbor, Michigan 48104

Carbanions Living Polymers and Electron Transfer Processes—M. Szwarc, Wiley, New York, 1968. 695 pp. \$27.50.

Although ionic initiation phenomena have played an important role in early observations and studies of addition polymerization involving unsaturated organic molecules, it happened that the initiation of these processes by *free radicals* became prevalent from the point of view of basic investigations and practical application. As a consequence, the science and technique of radical initiation addition polymerization grew to be a large body of fundamental information and commercial products. The next step was the clear recognition of the initiating and propagation capacity of *organic cations* and the evolution of the growing science and technology. Articles were published, patents issued and several commercial products became available on the basis of this development.

It was only through the dramatic events which followed the pioneering efforts of Ziegler and Natta and through the brilliant contributions of Dr. Szwarc that *anionic* initiation and propagation reached an equally important scientific and practical level in comparison with the two other mechanisms.

This volume provides the proof for this statement. It deals with all aspects of anionic initiation propagation, chain transfer and termination and focuses appropriately the readers' attention on the spectacular phenomena of living polymers which is particularly characteristic for anionic polymerization processes.

As is fitting for the first comprehensive treatment in a new wide field of activity, the presentation is elaborate in the description of experimental procedures, in the mathematical formulation of the ideas and in the correlation to other similar phenomena. Nevertheless, the text makes good reading and has, everywhere, a refreshing atmosphere of constructive criticism and authenticity.

A careful study of the book shows that this was a very difficult volume to write, and convinces the reader that it will be most helpful for him in his efforts to develop new ideas, experiments and products.

H. Mark

Polytechnic Institute of Brooklyn
333 Jay Street
Brooklyn, New York 11201

ERRATUM

Method for Computing the Specific Rate of Hydrolysis of Glucosidic Bonds in Some Trisaccharides

By ALEXANDER MILLER

*Research Laboratory, Australian Paper Manufacturers
Limited, Melbourne, Australia*

article in *J. Polymer Sci. A-1*, **6**, 2415 (1968)

Figure 1 and Figure 2 have been transposed.

The captions for these figures are incorrect.

The caption for Figure 1 should read: Kinetic
Reaction Scheme of Hydrolysis of Isomaltotriitol.

The caption for Figure 2 should read: Rate Plot According to Eq. (5).